The Active Template Approach to Mechanically Interlocked Nanocarbons

By

James H. May

A dissertation accepted and approved in partial fulfillment of the
requirements for the degree of
Doctor of Philosophy
In Chemistry

Dissertation Committee:

Darren W. Johnson, Chair

Ramesh Jasti, Advisor

Micheal M. Haley, Core Member

Jayson Paulose, Outside Member

University of Oregon

Fall 2023

DISSERTATION ABSTRACT

James H. May

Doctor of Philosophy in Chemistry

Title: The Active Template Approach to Mechanically Interlocked Nanocarbons

Graphitic carbon nanomaterials hold tremendous promise for a variety of applications. The realization of this potential, however, has been hampered by the lack of synthetic methods by which we can prepare such materials in a selective manner. On the other hand, through organic synthesis we can construct small molecule analogues of these materials, a.k.a. molecular nanocarbons, in which the structure and composition can be precisely controlled. In doing so, we uncover the fundamental properties associated with these materials at the molecular size regime and begin to fill the gap between molecular and material properties. Furthermore, with organic synthesis we can begin to create nanocarbon structures with exotic topologies that do naturally occur in extended materials. In doing so, the structural landscape available to explore is limited only by the creativity of the pursuer and the synthetic methods available to them. With this in mind, the incorporation of molecular nanocarbons into mechanically interlocked architectures represents an exciting yet underexplored venture in the context of carbon nanoscience. In this dissertation I describe the development of active-metal template methods to incorporate [*n*]cycloparaphenylenes ([*n*]CPPs) into mechanically interlocked molecules (MIMs).

Chapter I provides an overview of the synthetic methods that have been developed for the synthesis of MIMs and [*n*]CPPs, ending with recent examples from the literature in which these methods are merged. Chapter II describes an active metal template approach to the synthesis of mechanically interlocked cycloparaphenylenes via copper catalyzed sp^3-sp^3 cross-coupling reactions. Chapter III describes an alternative active metal template approach, improving on the work presented in Chapter II, based on a copper catalyzed azide-alkyne cycloaddition reaction. The chapters include previously published and unpublished co-authored material.

AKNOWLEDGEMENTS

First, I would like to extend my deepest thanks to my Ph.D. advisor, Ramesh Jasti, for his unwavering support throughout my tenure at the University of Oregon. On no occasion was I ever dissuaded from pursuing my interests, and I will always be grateful for the freedom afforded to me during my Ph.D. I would like to thank the entire Jasti research group, including all current members and alumni. Special thanks to Dr. Jeff Van Raden for his mentorship in my early years, for laying the foreground for my research, and for his inspiring work ethic and dedication. Special thanks to Julia Fehr and Tavis Price. We have gone through all of this together and their friendship and companionship has been invaluable. Thank you to my committee members Darren Johnson, Mike Haley, and Jayson Paulose for their support and feedback. Thank you to the NSF-GRFP for funding much of my research. The financial support eased a great deal of stress and I believe it made my advisor happy to not pay me for a few years. A huge thank you to the Chemistry and Biochemistry staff – particularly Janet Macha, Christi Mabinuori, Kathy Noakes, and Helen Durany who I interacted with most— whose help was never taken for granted. Finally, thank you to my family to whom I owe it all. To my parents Paul S. May and Mary T. Berry whose love and support has meant everything to me. To my brother and best friend Paul B. May and his family Elizabeth May, Raymond P. May, and of course the baby Robert J. May. Welcome to the world Robert.

TABLE OF CONTENTS

LIST OF FIGURES

Figure/Caption Page

CHAPTER I

MERGING THE FIELDS OF CARBON NANOSCIENCE AND MECHANICALY INTERLOCKED STRUCTURES

Chapter **I** was written by myself and edited by Professor Ramesh Jasti.

Chapter **II** is based on published work in *Nature Chemistry*. The manuscript was written by myself with editorial assistance from Professor Ramesh Jasti. Experimental work included in this chapter was carried out by me. Dr. Lev N. Zakharov provided crystal structure analysis discussed in the manuscript.

Chapter **III** is based on unpublished work and was written by me with editorial assistance from Professor Ramesh Jasti. The experimental work was carried out by myself or with assistance from Jacob Lorenz under my direction. Dr. Lev N. Zakharov provided crystal structure analysis of compounds discussed in this chapter.

I.I Introduction.

A primary objective in synthetic chemistry is total control over the structure and composition of molecules and materials such that their properties may be tailored for specific applications. One of the more impressive displays of synthetic control in contemporary chemistry are molecules (materials) with interwoven components that trace topologically non-trivial structures such as catenanes, rotaxanes and knots. For many years these so-called mechanically interlocked molecules (MIMs) have inspired chemists owing to the aesthetic nature of their structures coupled with the shear challenge associated with their rational synthesis. However, with the evolution of template directed syntheses that allow for the high-fidelity formation of mechanical bonds, MIMs have transcended from the realm of synthetic curiosity into myriad fields

of application driven research such as chemical sensing,[1] catalysis,[2] soft materials,[3] and the generation of artificial molecular machinery[4] (as recognized by the 2016 Nobel Prize in Chemistry). The utility of MIMs can largely be attributed to the unique dynamic characteristics of molecules that are not covalently linked but entangled with one another owing to mutual mechanical entrapment. This is significant as it allows for the relative motions of the molecular components to be controlled and manipulated to a degree that would be difficult or impossible to achieve with purely covalent bonding, or traditional supramolecular systems in which entropy and Brownian motion must be conquered to assemble molecular components into well-defined architectures. Despite tremendous progress since their initial syntheses, genuine applications of MIMs remain elusive, and many barriers still exist before such molecular devices can become practically useful. As such, a major objective is to develop new synthetic strategies to overcome the limitations that prevent new molecular architectures from being realized. This thesis outlines my efforts to merge the fields of carbon nanoscience and MIMs in search of unusual properties that may arise from nanocarbons of novel topologies.

Graphitic carbon nanomaterials hold tremendous promise for applications across many fields of science and technology.[5] The broad scope of applications for these materials is largely correlated with their profound structure-function relationships, illustrated by the distinct sets of properties observed within, and between families of graphitic carbon allotropes. For example, graphene, a two-dimensional material constituting a hexagonal array of sp^2 carbon atoms, is a zero-gap semiconductor. When this same material is rolled into a cylindrical topology—as with carbon nanotubes—the resulting material can be either metallic or semiconducting, depending on the chiral axis of the "roll" and the diameter of the tube. While this strong structure-function dependency potentially provides a powerful platform wherein electronic properties may be tailored

via seemingly small structural perturbations, the precise synthesis of carbon nanomaterials of specific identity remains challenging. As such, significant interest has manifested for the synthesis of molecular analogues of these materials whose structure and composition may be meticulously controlled via bottom-up synthetic strategies. Notable among these so-called *molecular nanocarbons* are the [*n*]cycloparaphenylenes ([*n*]CPPs) and related oligoparaphenylene-derived 'nanohoop'/'nanobelt' macrocycles, which represent molecular substructures of carbon nanotubes. Since the synthesis of the first [*n*]CPPs in 2008,[6] nanohoops have been the focus of many research efforts owing to their unique radial conjugation and accompanying size-dependent optoelectronic characteristics. More recently, researchers have begun to develop methods to integrate nanohoops into mechanically interlocked architectures (e.g., rotaxanes, catenanes, and knots) providing an opportunity to interrogate the effects of topological manipulation on the properties of these molecular nanocarbons.[7–18]

In this chapter I will provide a brief history of MIMs synthesis, specifically focusing on those methods that have been shown to be useful for incorporating nanohoops into mechanically interlocked systems. Afterward, I will provide an overview of the various methods that have been developed for the synthesis of carbon nanohoops and their incorporation into mechanically interlocked structures. In chapter **1.2**, I will discuss the syntheses of the first mechanically interlocked structures, specifically to highlight the difficulties associated with their preparation via the synthetic methods available at the time. Next in chapter **1.3** I will discuss the advent of metal-ion templated reactions that have provided a general strategy to synthesize MIMs. In chapter **1.4** I will provide several examples in which non-covalent interactions – separate from metal-ligand interactions – which have proven to be powerful in MIM synthesis. I will then transition into the synthesis of [n]cycloparaphenylene macrocycles in chapter **1.5** and, finally in chapter **1.6** I will

provide recent examples from the literature in which the methods discussed in chapter **1.3-1.4** have been adapted to integrate cycloparaphenylenes and related conjugated nanohoop macrocycles into mechanically interlocked structures.

I.2 The history of MIMs synthesis.

The first synthesis of a mechanically interlocked molecule was reported in 1960 by Edel Wasserman at Bell laboratories.[19] Wasserman's approach was based on the sodium-mediated acyloin condensation of diester **I.2** in a melt of deuterated cyclo-hydrocarbon **I.3** with xylenes as a co-solvent (Figure I.1). The principle of this approach is that the macrocyclization of **I.2**, when conducted in the presence of the pre-formed macrocycle **I.3** should result in a statistically appreciable quantity of the catenated molecule **I.1**.

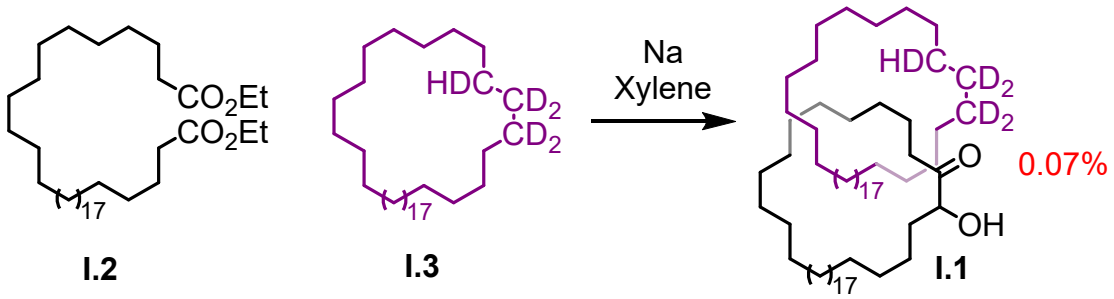

Figure I.1. First [*n*]catenane synthesis. Wasserman's statistical approach to [2]catenane **I.1** achieved via random threading events during the sodium-mediated acyloin condensation of diester **I.2** in the presence of hydrocarbon macrocycle **I.3**.

Of course, with no thermodynamic (or otherwise significant) driving force for the catenation event, the likelihood of forming **I.1** via shear happenstance is vanishingly small. Indeed,

even when conducting this experiment where **I.3** is used as the reaction solvent, the yield of catenane **I.1** is astonishingly low. In fact, no yield was offered in the original report. Wasserman's 1960 synthesis of **I.1** was met with reasonable scrutiny, and many questioned the validity of their claims owing to the distinct lack of experimental detail and only indirect evidence supporting the formation of the proposed structure (**I.1**). Only 63 years later did researchers take it upon themselves to repeat Wasserman's experiments and unequivocally prove that **I.1** is in fact generated under these conditions in 0.07% yield.[20] Whilst Wasserman's claims from 1960 were eventually validated, this statistical approach to mechanically interlocked molecules is highly contrived and remarkably inefficient. Unsurprisingly this synthetic methodology gained very little traction apart from a publication seven years later from Harrison and Harrison in which a similar method was used for the synthesis of the first rotaxane molecule.[21] Still, this initial synthesis sparked a great deal of interest amongst the controversy and encouraged researchers to search for alternative methods that would allow interlocking structures to be prepared in a more efficient manner.

Four years later, Schill and Luttringhaus improved upon Wasserman's statistical approach by using a cleavable covalent template to encourage catenane formation (Figure I.2).[22] This was accomplished by synthesizing key intermediate **I.4**. Nucleophilic displacement reactions of the alkyl halides by the phenylamine gives the tertiary amine **II.5** which is linked intra-annularly with the N-alkyl chains are situated on opposite sides of the benzene ring. It was noted that the chain lengths of the alkyl halides of **I.4** were precisely chosen to inhibit the extra-annular cyclization reaction which would result in an isomer of **I.5** having the N-alkyl chains situated on the same side of the benzene ring. Cleavage of the ketal and subsequent oxidation and acid catalyzed hydrolysis of the aryl-N bond liberates the covalent attachment between the two macrocycles resulting in

[2]catenane **I.7**. While this represents an impressive show of synthetic *tour de force,* and the first rational synthesis of a MIM, the synthetic procedure reported was long and arduous. Furthermore, the key intermediate **I.4** needed to be carefully designed to arrive at the desired structure making this methodology challenging to extend to the general synthesis of MIMs of varying structure and composition.

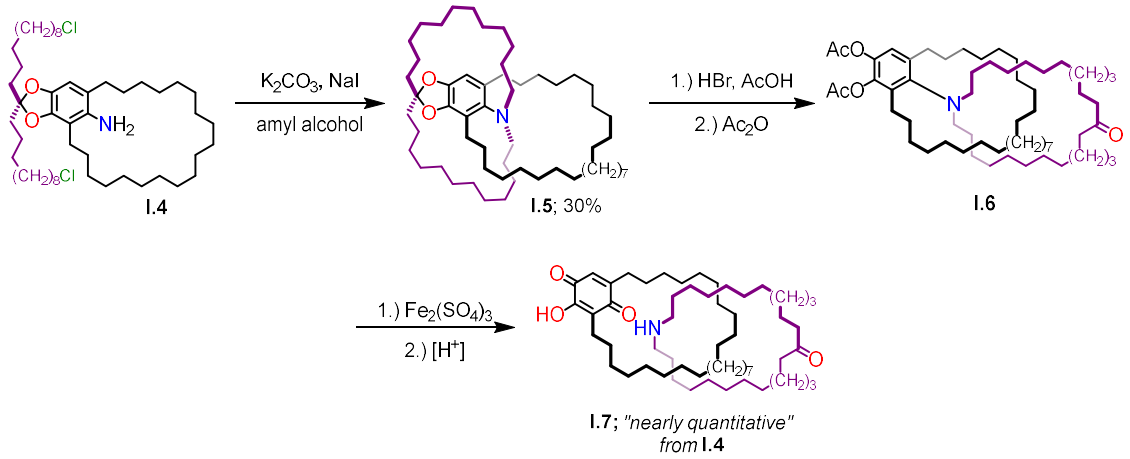

Figure I.2. Covalent template approach to [2]catenane **I.7** reported by Schill and Luttringhaus in which cleavable covalent tethers are used to aid in the formation of intra-annularly linked macrocycles.

I.3 Metal-ion templates in MIMs syntheses.

The renaissance of MIMs began in 1983 when J. P. Sauvage and co-workers demonstrated, for the first time, a method in which MIMs could be synthesized in high yield from simple starting materials by using passive metal-ion templates.[23] This was accomplished by leveraging metal-ligand interactions to pre-organize molecular substrates in such a way that subsequent bond-forming reactions could be performed to leave two mechanically bound macrocycles (i.e., a

[2]catenane) (Figure I.3). Specifically, phenanthroline containing macrocycle **I.9** was treated with Cu(I) and, subsequently, **I.10**, to give the heteroleptic Cu(I) complex **I.11**. The tetrahedral coordination geometry of Cu(I) orients the two ligands in such a way that the Williamson ether macrocyclization of the diol-containing unit occurs exclusively in an intra-annular fashion to provide [2]catenane **I.12** in an impressive 42% overall yield. This report demonstrated the power of reversible, non-covalent interactions in the construction of mechanically interlocked structures and an explosion of research began to surface in the field following its publication.[24]

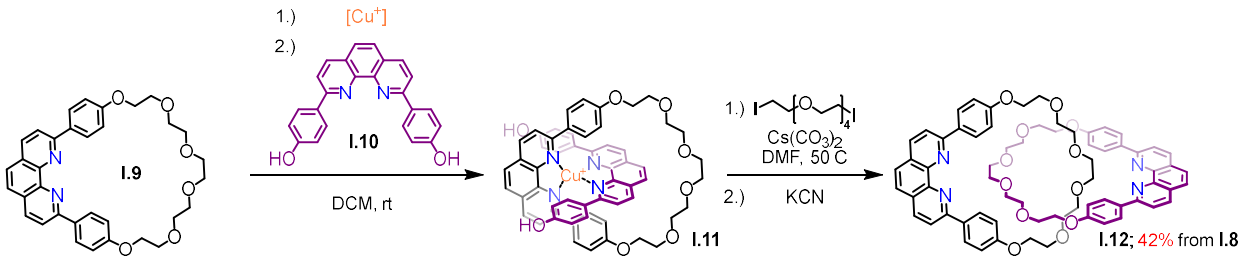

Figure I.3. Sauvage's passive template synthesis of [2]catenane **I.12**, using a Cu(I) to form a preorganized complex which is then covalently captured via Williamson ether synthesis.

In 2006, Leigh and co-workers reported an alternative strategy using a transition metal ion template, termed the "active template" (AT) approach.[25] In contrast to the passive metal template (PT) approach developed by Sauvage, the templating moiety in this case is *actively* involved in the formation of the mechanical bond. Specifically, the AT approach relies on a macrocycle to coordinate a catalytic metal ion endotopically (i.e., at the interior of its cavity). Bond forming reactions then are facilitated by this metal resulting in a product molecule that is threaded through the center of the macrocycle. Provided the threaded species is appropriately functionalized with large 'stopper' groups at either end, the 'thread' unit becomes mechanically entrapped and unable

to diffuse away from the macrocycle. This was first accomplished by conducting the copper-catalyzed azide-alkyne cycloaddition (CuAAC) reaction of **I.13** and **I.14** in the presence of the macrocyclic ligand **I.15** (Figure I.4). After optimization of the reaction conditions, [2]rotaxane **I.16** could be isolated in 94% yield, provided 5 equivalents **I.13** and **I.14** were used. AT offers certain advantages over PT in that the breadth of structures that may be formed are not dictated by the inherent molecular recognition between interlocking components, but by the catalytic character of the templating metal-ion. Indeed, since the initial report by Leigh, Goldup and others have shown the remarkable structural diversity and range of applications enabled by this strategy.[26]

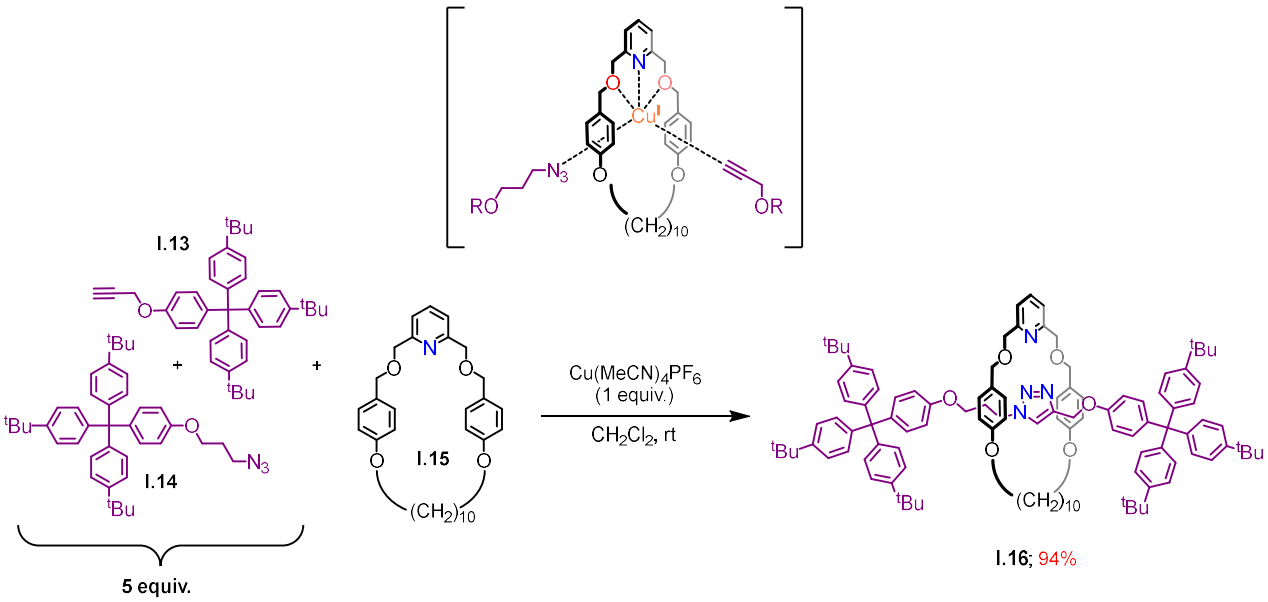

Figure I.4. Leigh and coworkers' active template synthesis of [2]rotaxane **I.16.**

Following Sauvage's demonstration of using passive metal-ion templates, researchers began to explore alternative supramolecular interactions for the synthesis of MIMs.[27] A particularly important example came in 1987 when Stoddart and colleagues reported that crown ether macrocycle **I.17** forms a 1:1 inclusion complex with the paraquat dictation by virtue of the

strong intermolecular π-π interaction between the electron deficient viologen and the electron rich arenes of **1.18** (Figure I.5a).[28] Two years later the same group aimed to take advantage of this supramolecular association to template the formation of a [2]catenane.[29] This was accomplished by the reaction of bis(pyridinium) salt **I.19** with *p*-xylene dibromide in the presence of the host macrocycle **I.17**. After the initial substitution reaction between **I.19** and *p*-xylene dibromide, the viologen unit becomes encapsulated within the cavity of **I.17** (**I.20**) such that the second intramolecular substitution reaction occurs to generate [2]catenane **I.21** which precipitates cleanly from the reaction mixture (70% yield).

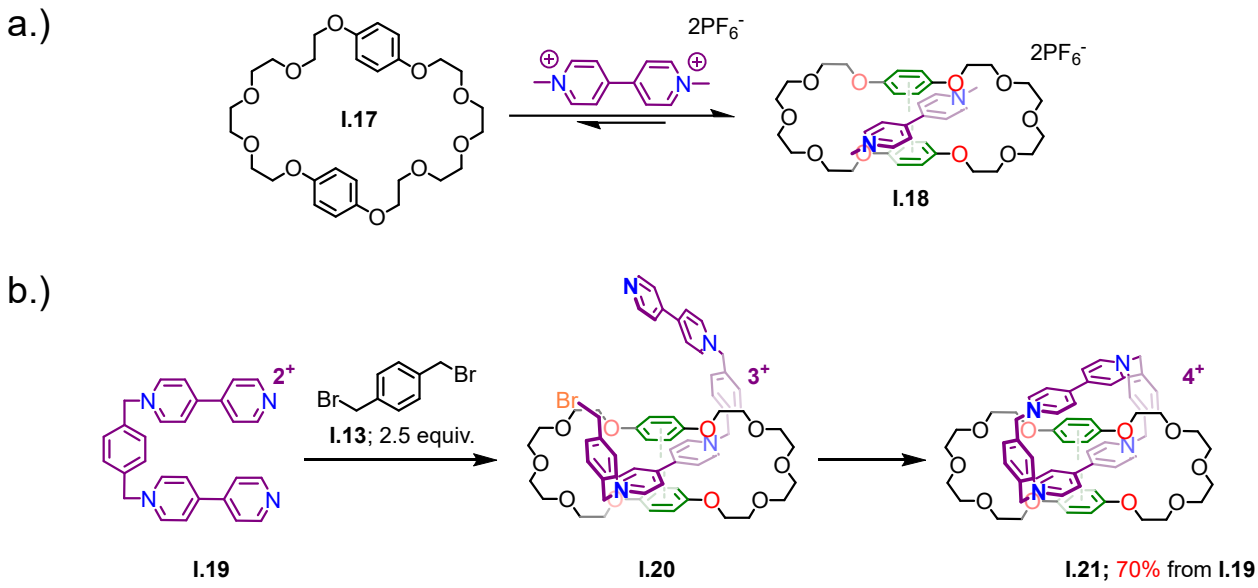

Figure I.5. Stoddart's donor-acceptor template approach to synthesize [2]catenane **I.21.**

1.4 Synthesis and properties of [n]cycloparaphenylenes.

[*n*]Cycloparaphenylenes ([*n*]CPPs), as the name implies, are a family of macrocyclic compounds composed entirely of *n*, *para*-linked, phenylene units. The act of bending *para*-

phenylene into a circular shape imparts a large amount of strain into these otherwise flat molecules and despite significant effort, the successful synthesis of [*n*]CPP eluded chemists for many years.[30] Indeed, the first efforts to synthesize [*n*]CPP can be traced back to 1934 when Parekh and Guha attempted to generate [2]CPP via the pyrolysis of the [2_2]paracyclophane, *p*,*p*′-diphenylenedisulfide though, unsurprisingly, these efforts were not successful. In the years following Vogtle and coworkers employed a variety of strategies to synthesize [*n*]CPPs from various macrocyclic precursors (**I.23**-**I.27**); however, they were ultimately unsuccessful in the final transformations.[31]

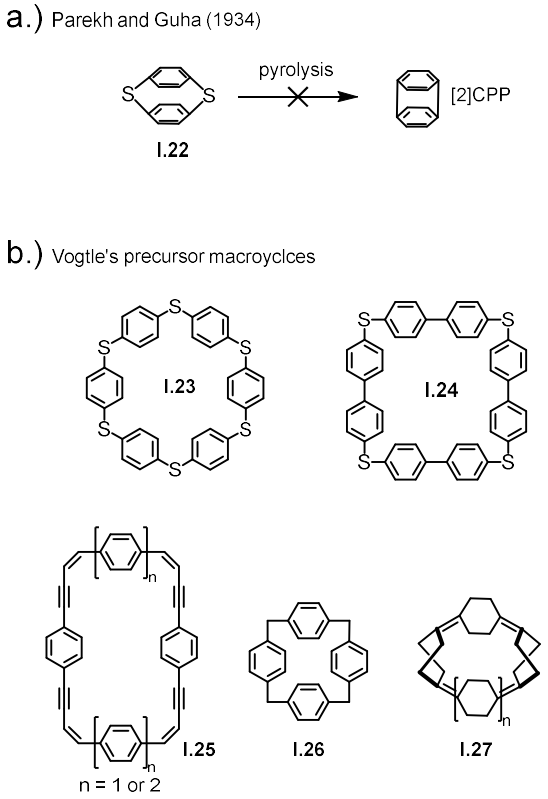

Figure I.6. (a) early attempt to synthesize [2]CPP by Parekh and Guha. (b) Examples of macrocyclic compounds synthesized by Vogtle in their attempts to synthesize [*n*]CPP.

Finally in 2008, the first [*n*]CPPs were synthesized by Jasti and Bertozzi.[32] This was accomplished by designing cis-dialkoxy cyclohexadiene motifs, **I.28** and **I.29**, as the key intermediates. The cyclohexadiene moieties impart the necessary curvature to these building blocks such that macrocycles of minimal strain could be produced. Indeed, under dilute conditions, the Suzuki-Miyaura macrocyclization reaction between **I.28** and **I.29** gave a statistical mixture of 9, 12, and 18-ring macrocycles (**I.30-32**). By treating **I.30-32** with sodium napthalenide, the cyclohexadiene corner units are converted to phenylene rings to give [9], [12], and [18]CPP (Figure I.7a). In this method, the gain in aromaticity compensates for the large increase in strain caused by bending the aromatic subunits. This strategy was later expanded upon the Jasti group to accomplish the selective syntheses of [5]-[12]CPP.[33–36]

After this seminal report, alternative methods were developed to synthesize [*n*]CPPs. In 2009, Itami and colleagues reported that cyclohexane moieties could be used in place of Jasti's cyclohexadiene motifs (**I.33**, **I.34**) in the construction of a low-strain macrocycle (**I.35**).[37] Then, through reaction with a strong oxidizing acid (p-TsOH) at elevated temperature, the cyclohexane motifs are aromatized to give [12]CPP. The following year Yamago and colleagues reported a highly streamlined approach based on the formation of tetraplatinum metallocycle via transmetalation of bis(stannane) **I.36** with $Pt(cod)Cl_2$.[38] After a ligand exchange reaction, and oxidation of the Pt nodes, four-fold reductive elimination ensues—presumably via a Pt(IV) intermediate—to furnish [8]CPP in an impressive 25% overall yield. While Yamago's method is elegant and attractive in terms of the high yield and the simplicity of the starting materials, the requirement of excess Pt in the synthesis of the metallocycle intermediates diminishes the economic viability of this approach at larger scales. More recently Tsuchido and Osakada reported

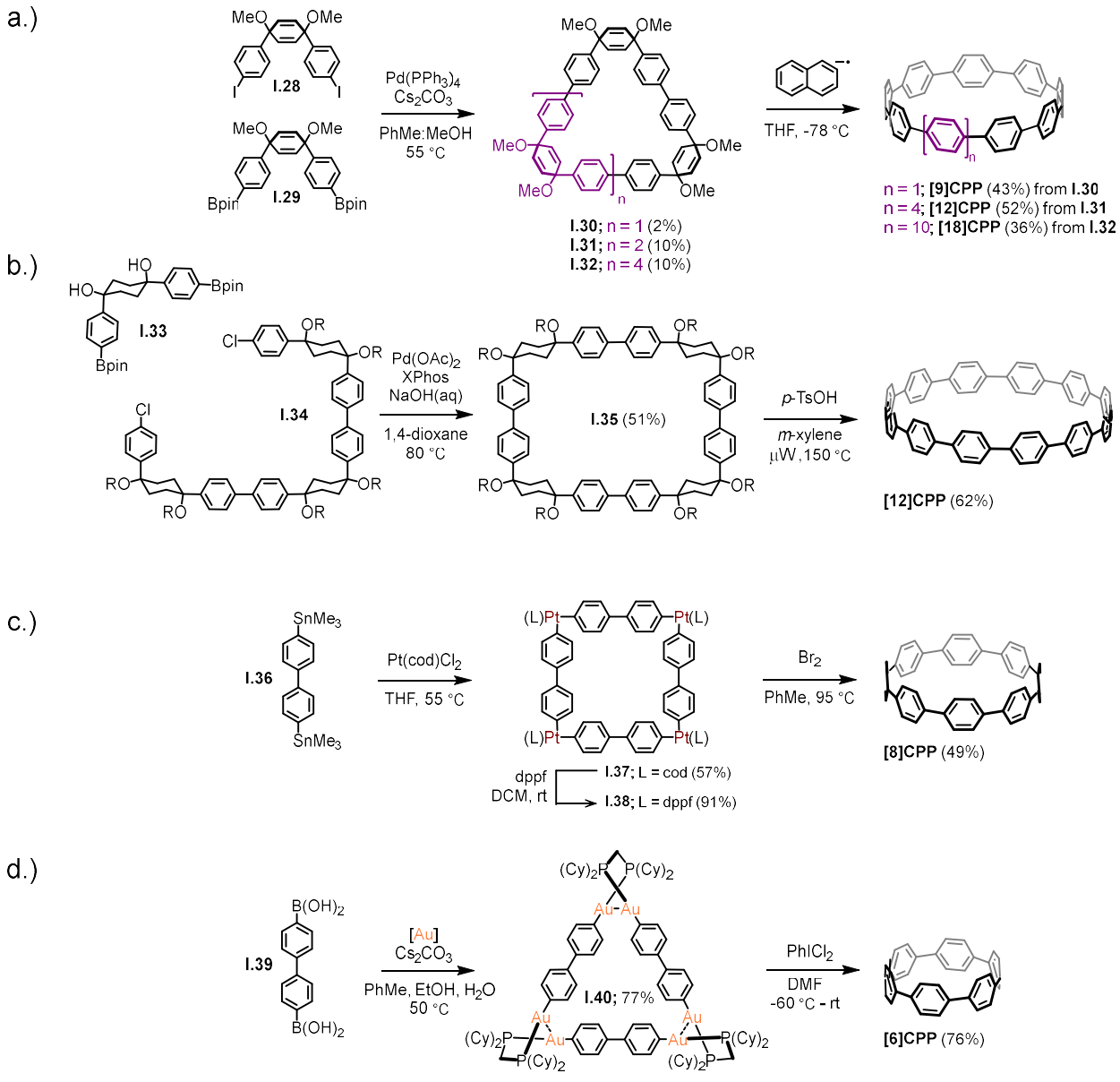

Figure 1.7. (a) Jasti and Bertozzi's seminal synthesis of [9], [12], and [18]CPP based on the reductive aromatization of cyclohexadiene containing macrocycles **I.30-32**. (b) Itami's synthesis of [12]CPP based on the oxidative aromatization of cyclohexane containing macrocycle **I.35**. (c) Yamago's Pt templated synthesis of [8]CPP. (b) Tsuchido and Osakada's Au templated synthesis of [6]CPP.

an alternative approach to Yamago's Pt-templated route in which twisted Au_2(diphosphine) corner units were used to construct metallocycle (**I.40**).[39] Similar to the previous example, treating **I.40** with an oxidant results in reductive elimination reactions to form the aryl-aryl bonds and gives the highly strained [6]CPP in 56% overall yield. In contrast to Yamago's approach, however, following the reductive elimination step, the Au complex can be recovered via column chromatography and reused in subsequent syntheses, justifying the use of super-stoichiometric amounts of the Au template in the construction of the metallocycle precursors.

One of the more striking features of the [*n*]CPP family are their size-dependent optoelectronic characteristics.[40] In contrast to their linear oligo-paraphenylene counterparts, the HOMO-LUMO energy gap of [*n*]CPPs decreases with the number of phenylene units in the CPP backbone. This is reflected in the fluorescence profiles of these compounds wherein decreasing the size of the [*n*]CPP results in a red shifting emission (Figure I.8)..

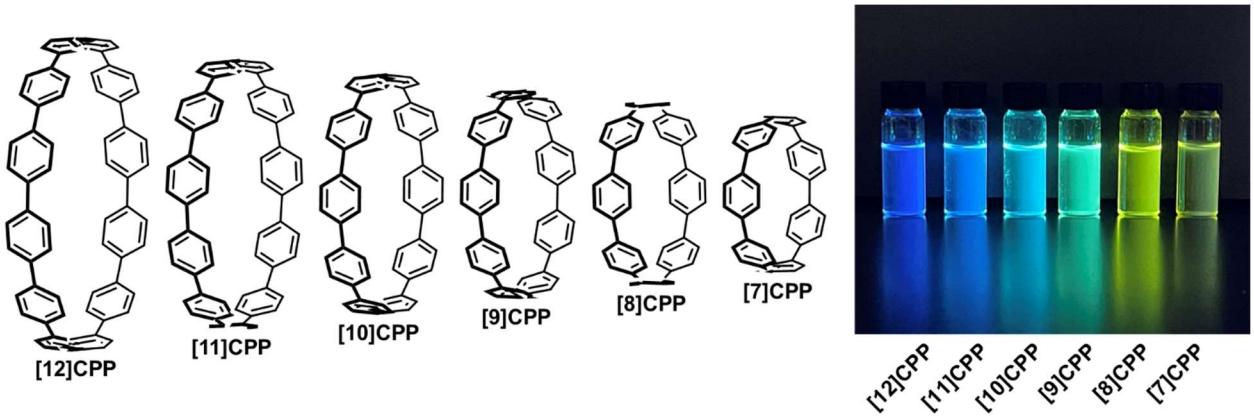

Figure I.8. Size dependent luminescent properties of [7]-[12]CPPs.

The origin of this counterintuitive phenomenon was described first by Wong et al. in 2009 in terms of their excited-state exciton binding energies.[41] In this study, it was concluded that the photogenerated electron-hole pair in [*n*]CPPs exhibit a larger columbic attraction energy than their

linear analogs which decreases more rapidly than the quasiparticle band gap as the ring size increases. The net effect is that the optical absorption energies of the cyclic compounds increase with larger ring sizes. Perhaps a more intuitive explanation could be gleaned by considering the effect of strain on the local aromaticity on the phenylene units and the dihedral angles between them: For [*n*]CPPs, as *n* becomes smaller, the phenylene units of the macrocycle become increasingly distorted from planarity resulting in a decrease in local aromaticity and an increase in quinoidal character. Additionally, the dihedral angles between adjacent phenylenes also decrease with decreasing ring size. As such, while the number of conjugated units decreases with *n*, the conjugation between the phenylene moieties is effectively enhanced.

In addition to their attractive photophysical characteristics, the radial π-system of [*n*]CPPs impart unexpected stability to their singly and doubly oxidized forms.[42] [*n*]CPPs (*n* = 5-13) each exhibit reversible one-electron oxidation and/or reduction events,[40] an important characteristic in organic electronic materials. Indeed, in a computational study based on the solid-state crystal packing of [*n*]CPPs, it was predicted that [*n*]CPPs should exhibit high hole-mobilities, substantially greater than that of the linear systems.[43] This was demonstrated experimentally in 2017 when Yamago *et al.* were able to show that a tetraalkoxy derivative of [10]CPP exhibit moderate conductivities in thin-film measurements.[44] Work from Bao et al. demonstrated that [*n*]CPPs may also be used as additives in conductive polymers to improve stretchability without adversely affecting charge mobility, further bolstering the potential of [*n*]CPPs in electronics applications. [45]

1.5. Integrating [*n*]CPPs into mechanically interlocked architectures.

The unique optical and electronic characteristics of [*n*]CPPs make them intriguing building blocks for the construction of interlocked molecules. Furthermore, the radially oriented π-system

of [*n*]CPPs renders them geometrically predisposed to electronic communication with guest molecules, offering the potential for the synthesis of interlocking systems with emergent properties. These features, coupled with strong structure-function relationships observed in carbon nanomaterials, make mechanically interlocked structures a new and exciting frontier in the search for nanocarbons with new topologies and properties. While this dissertation is geared specifically toward the development of novel carbon nanomaterial topologies, the knowledge gained through this pursuit will set the stage for the development of MIMs in any context.

A key feature of macrocyclic structures is their ability to accommodate guest molecules within their central cavities. Structural ridged macrocycles, such as [*n*]CPPs, tend to be much more selective in guest binding than more flexible hosts owing to the inability of their molecular structures to contort in accommodation of guest molecules of different shapes and sizes. As such, ridged macrocycles tend to selectively bind guest molecules that exhibit suitable shape and size complementarity with their shape persistent cavities. The smooth, circular π-surface formed by the radially situated phenylenes in [*n*]CPPs, for example, make these molecules perfect hosts for fullerenes. This was first demonstrated by Yamago *et al.,* who showed that [10]CPP forms a strong and highly selective complex with C_{60} (Figure I.9).[46] In this report, the authors showed that adding C_{60} to a mixture of [8]-[12]CPP results only in the shifting of the proton NMR signals of [10]CPP, evidencing the selectivity of C_{60} for [10]CPP over the larger or smaller macrocycles. The following year (2012), Jasti et al. published the crystal structure of the [10]CPP@C_{60} complex, proving that C_{60} does indeed form the predicted 1:1 endohedral complex with [10]CPP.[47]

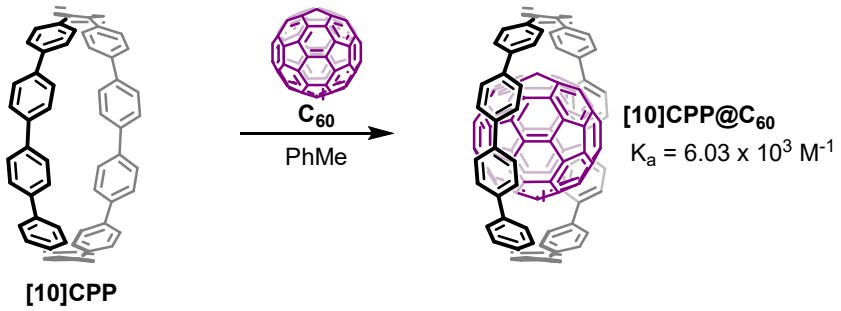

Figure 1.9. Encapsulation of C_{60} by [10]CPP and its binding strength in toluene (PhMe) as measured by Yamago *et al*.

Drawing inspiration from Stoddart's use of intermolecular π-π interactions to template the formation of MIMs, von Delius *et al.* demonstrated that C_{60} could effectively serve as a concave/convex π-π template to construct mechanically interlocked [2]rotaxanes with [10]CPP. This was accomplished via the route shown in Fig. I.10a. First, pseudo[2]rotaxane **I.41** was formed by virtue of the strong binding of C_{60} with [10]CPP. By subsequent functionalization of the incapsulated fullerene under Bingle reaction conditions with bromomalonic ester **I.42**, several different isomers (distinguished by the regiochemistry of the fullerene functionalization) of the [10]CPP [2]rotaxane **I.43** were identified. Importantly, it was found that the [10]CPP serves as a steric protecting group in the Bingle reaction, suppressing the formation of many regioisomers that are produced in the absence of this supramolecular interaction. This suggested that host-guest chemistry may be an effective tool for controlling the regiochemistry of fullerene functionalization. Indeed, this method was improved by the same group to achieve perfectly regioselective bis-functionalization of fullerene, eventually allowing for the synthesis of [10]CPP [2]catenane **I.44**. While reports of other guests such as pyridiniums, [*n*]CPPs themselves, corannulene, and cations are beginning to emerge, association constants are typically weak. The

[10]CPP@C_{60} complex is by far in a way the strongest host-guest system known for [*n*]CPPs and may be the only species known with sufficient affinity to be used as a supramolecular template in the synthesis of interlocked CPPs. As such, this π-π templated approach is difficult to generalize to the synthesis of mechanically interlocked [*n*]CPPs of diverse structure.

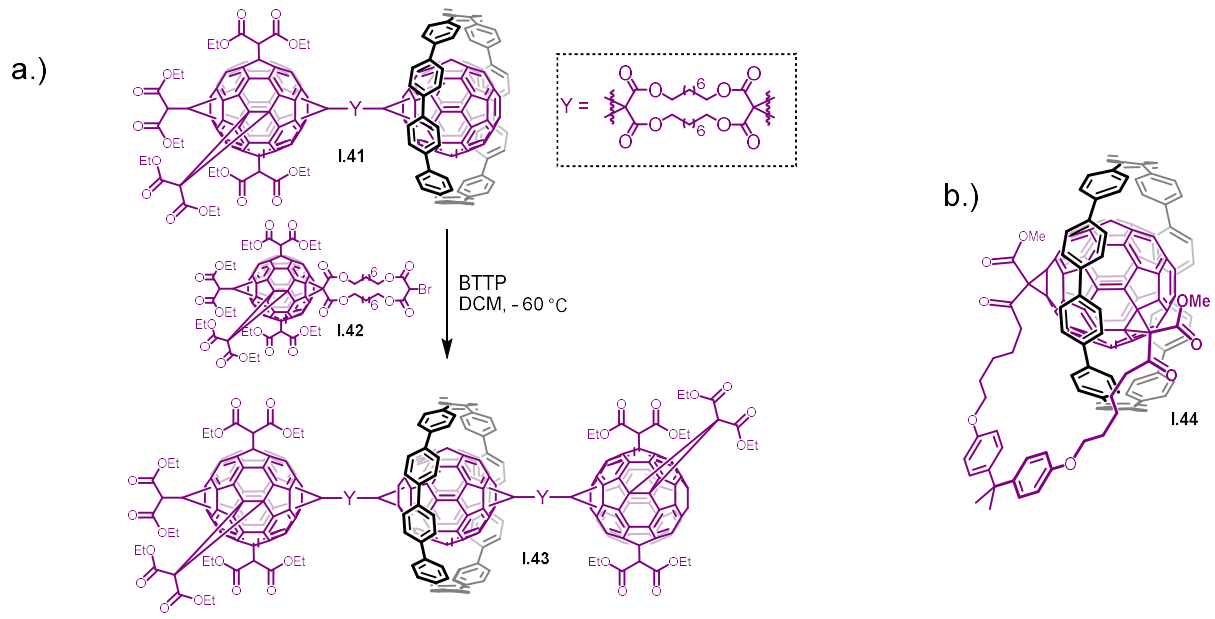

Figure 1.10. (a) von Delius' π-π template approach to [10]CPP [2]catenane **I.43**. (b) [10]CPP [2]catenane later synthesized by von Delius using similar methodology.

Owing to their limited host-guest chemistry and lack of inwardly directed functional groups, MIMs constructed from [*n*]CPP macrocycles pose a significant synthetic challenge. Work by Cong and Jasti independently showed that nanohoop macrocycles could be made amenable to metal ion templated MIM syntheses by making symmetry breaking modifications to the [*n*]CPP backbone so to arrive at ligand geometries suitable for endotopic metal coordination (Fig. 1.11).[8,9]

Cong's approach (Fig. 1.11a) relied on installing two of Jasti's bent cyclohexadiene containing motifs at the 2 and 9 positions of 1,10-phenathroline to arrive at bis(boronate) **I.45**. In accordance with Sauvage's passive template synthesis, coordination with Cu(I) results in homoleptic complex **I.46**, in which the two cleft shaped ligands are appropriately preorganized in a fashion conducive for catenane formation. Oxidative homocoupling of the aryl boronic esters followed by reductive aromatization of the cyclohexadiene moieties then results in the fully conjugated [2]catenane **I.47** made up of two interlocked 'kinked' cycloparaphenylene analogues. Interestingly, **I.47** was found to have Mobius topology in the solid state. This work highlights that nanohoop macrocycles, not only serve as building blocks for MIMs, but also represent a new class of compounds with Möbius topology.

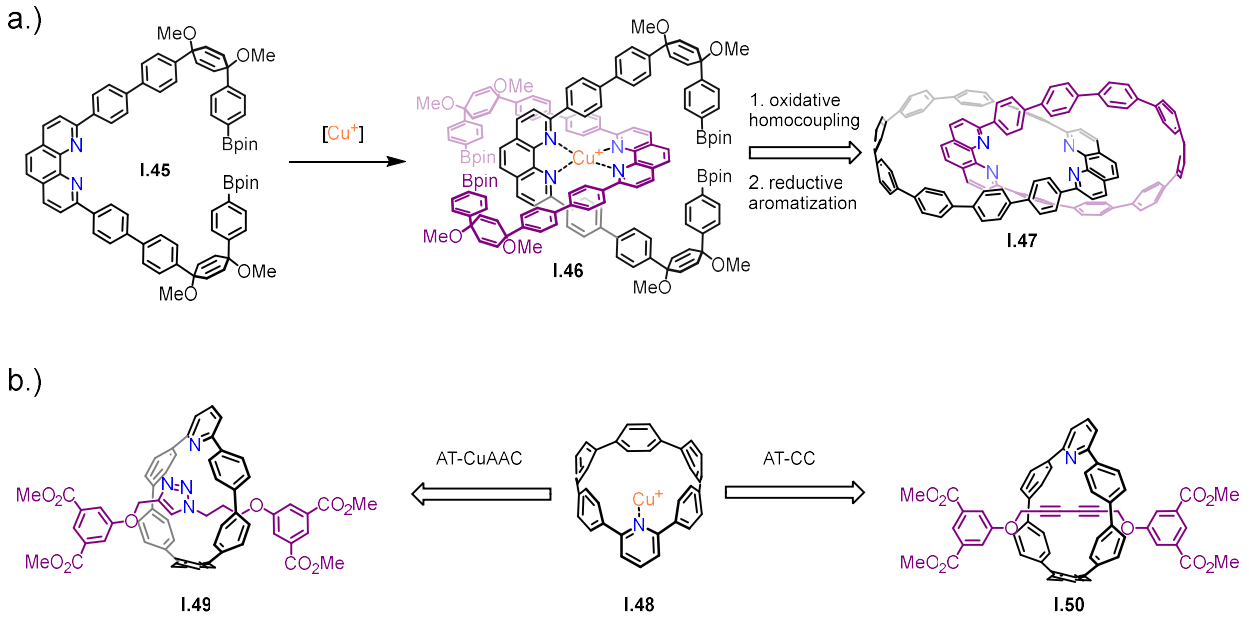

Figure 1.11. Symmetry broken nanohoops used in metal-ion templated MIM synthesis. (a) Cong's passive metal template synthesis of möbius [2]catenane **I.47**. (b) Jasti's active metal template synthesis of [2]rotaxanes **I.49** and **I.50**.

Jasti's approach, on the other hand (Figure 1.11b), was inspired by Leigh's active template method. By replacing a 1,4-phenylene unit of an [*n*]CPP with a 2,6-pyridyl moiety, it was found that macrocycle **I.48** could serve as an effective ligand for the synthesis of [2]rotaxanes via the active template azide-alkyne cycloaddition (AT-CuAAC) and active template Cadiot-Chodkiewicz (AT-CC) reactions (representative products for the AT-CuAAC and AT-CC reaction are given by **I.49** and **I.50**, respectively). While both approaches are more general—in terms of the breadth of structures that are potentially accessible—than the fullerene templated method used by von Delius, the symmetry breaking modifications required to facilitate the endotopic coordination of metal-ions comes at the expense of the radial π-conjugation of the nanohoop.

In 2019, Itami and Segawa reported a traceless covalent tethering approach to synthesize catenanes (**I.54**, **I.55**) and a trefoil knot (**I.56**) composed entirely of *para*-linked benzene rings (Figure I.12).[11] This was accomplished by using spirobis(dibenzosilole) moieties to covalently tether two [*n*]CPP building blocks (**I.51-I.53**) in such a way that Yamamoto coupling conditions could be applied to give statistical mixtures of intra-annularly and extra-annularly linked macrocycles. Treatment of the mixture with fluoride (removing the silicon template) followed by the reductive aromatization of the cyclohexadiene motifs then gives a mixture of interlocked and non-interlocked [*n*]CPPs, which were separable via gel permeation chromatography. While this is certainly an extraordinary feat of synthetic design, there are several drawbacks to this method. Namely, there is no means of controlling the Yamamoto macrocyclization reaction such that the intra-annular pathway is favored over the extra-annular pathway. As such, a significant quantity of the undesired non-interlocked side-products are always produced in the macrocyclization step. This is especially noticeable for the hetero[2]catenane, in which the non-interlocked [*n*]CPPs ([9] and [12]) are produced in a combined 20-fold excess over the desired [2]catenane.

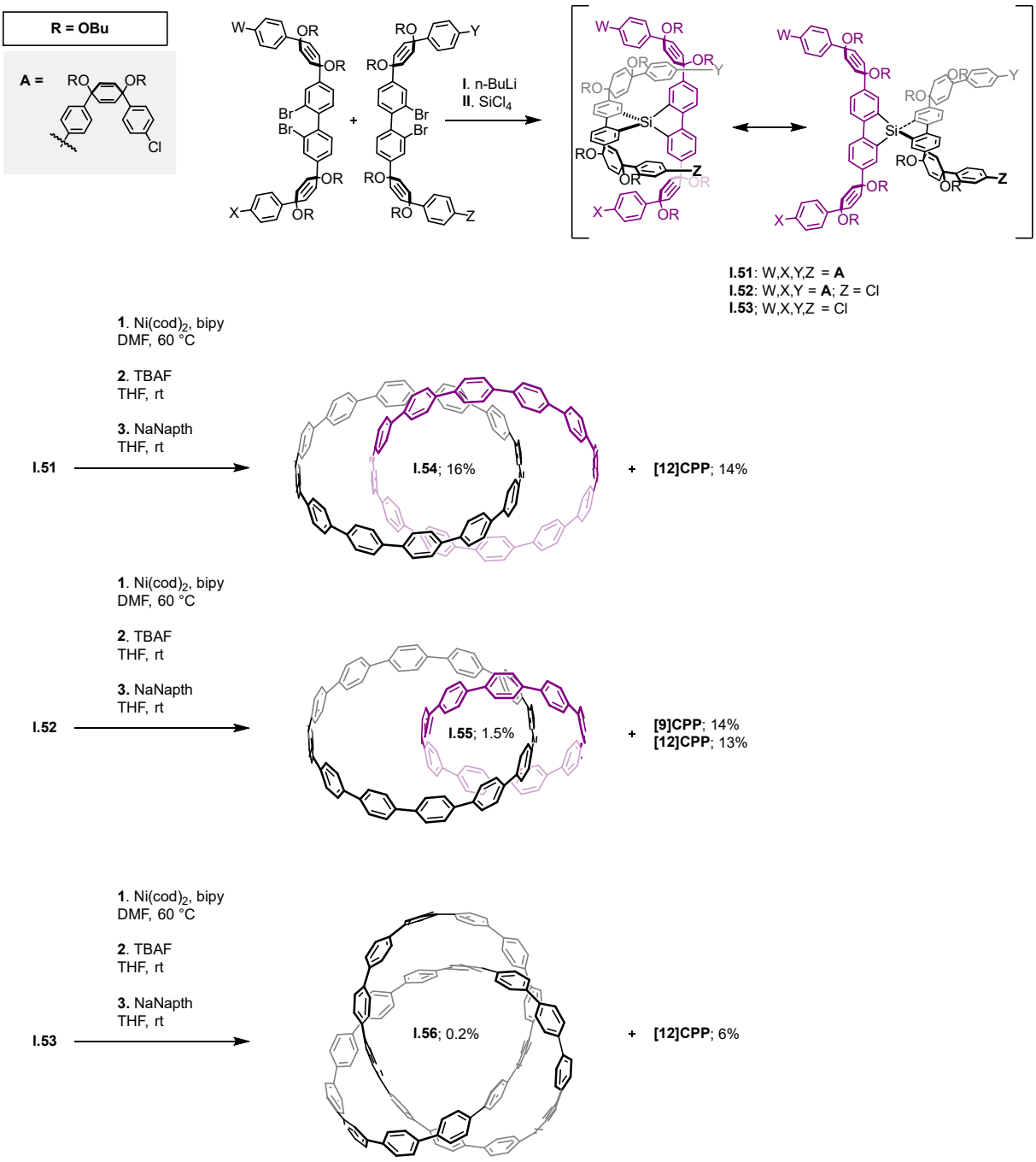

Figure I.12. Itami's traceless covalent template approach to synthesis all-benzene catenanes **I.54** and **I.55** and trefoil knot **I.56**.

1.6 Conclusion.

As our abilities to weave molecular components into complex interlocked architectures improve, new applications for mechanically interlocked molecules and materials continue to emerge. In merging the fields of carbon nanoscience with that of MIMs, we seek to take advantage of the strong structure function relationships observed in graphitic materials to uncover new properties hidden within nanocarbons with unrealized topologies. While significant strides have been made in incorporating [n]cycloparaphenylene and related nanohoop macrocycles into mechanically interlocked structures, the available methods are limited. Furthermore, general methods which would allow for the synthesis of a wide variety of structures are yet to be fully realized. This dissertation will focus on my efforts to address the drawbacks of the methods discussed above (in Chapter **1.5**) and develop new synthetic methods to efficiently incorporate [n]CPP macrocycles into a variety of interlocked architectures.

1.7 Bridge to Chapter II.

This chapter highlights the development of synthetic methods for the synthesis of mechanically interlocked molecules leading into the use of these methods for incorporating [*n*]CPPs and related macrocycles into such structures. In the following chapter, I will present an alternative approach in which active template chemistry is used to produce a variety of interlocking [*n*]CPP structures having the topologies of catenanes and rotaxanes.

CHAPTER II

ACTIVE METAL TEMPLATE SYTHESIS OF MECHANICALLY ITERLOCKED CYCLOPARAPHENYLENES VIA COPPER CATALYSED SP3-SP3 CROSS COUPLING REACTIONS

From May, J. H.; Van Raden, J. M.; Maust R. M.; Zakharov, L. N.; Jasti, R. *Nat. Chem*. **2023**, *15*, 170-176. Further permissions related to the use of the material excerpted in this chapter should be directed to Springer Nature Publishing. This manuscript was written by me with editorial assistance from Professor Ramesh Jasti. Experimental work in this chapter was performed by me.

Mechanically interlocked carbon nanostructures represent a relatively unexplored frontier in carbon nanoscience due to the difficulty in preparing these unusual topological materials. The development of synthetic methods to access such structures will help elucidate the implications of mechanical bonding for this emerging class of nanomaterials and allow structure-property relationships to be established. Here we illustrate an active template method in which [*n*]cycloparaphenylene([*n*]CPP)-precursor macrocycles, embedded with two convergent pyridine donors, enable cross-coupling reactions to be catalyzed within the central cavity of the macrocycle. The resultant interlocked products can then be converted into fully π-conjugated structures in subsequent synthetic steps. Specifically, we report the synthesis of a family of [*n*]catenanes (*n* = 2, 3) comprising two or three mutually interpenetrating [*n*]CPP-derived macrocycles. Additionally, a fully conjugated [3]rotaxane was synthesized by the same method, highlighting the versatility of this active template approach in preparing mechanically interlocked carbon nanostructures of varying topology.

2.1 Introduction.

The optical and electronic properties of carbon nanostructures are linked to their precise 3D arrangement of carbon atoms. Graphene, fullerene, and carbon nanotubes, while sharing very similar local bonding environments (i.e. exclusively sp^2-hybridized bonded carbon), display vastly different physical properties due to the differing topologies of the overall structure [5]. In recent years, using bottom-up organic synthesis strategies, carbon nanostructures can be prepared that were inaccessible by more traditional thermodynamically driven methods. For example, substructures of CNTs, often referred to as carbon nanohoops [6] and carbon nanobelts [48–50], can now be prepared in which the size [35], connectivity [51], and even heteroatom doping [52] can be controlled with atomic precision. These molecular nanocarbons are gaining traction for a wide array of possible applications in organic electronics, biology and polymer science [53–57]. A particularly exciting avenue is to use organic synthetic methods to prepare topologically unique carbon nanomaterials – in particular, mechanically interlocked structures. In 2019, Itami et al. reported the syntheses of catenanes and a trefoil knot composed entirely of *para*-linked phenylene units using a traceless silyl tethering strategy (Fig. II.1a) [11]. The catenated and knotted molecules are structurally related to the [*n*]cycloparaphenylenes ([*n*]CPPs), but the unique topologies of these structures give rise to dynamic motion and optical characteristics that differ from the parent [*n*]CPPs. General synthetic methods to access a wide array of interlocked carbon nanostructures where the structures can be altered via connectivity, size, and heteroatom doing would bring about a class of dynamic nanomaterials with engineerable optical and electronic properties. Herein, we disclose a versatile active template methodology that can deliver an array of mechanically interlocked nanocarbons of the catenane and rotaxane type, composed entirely of π-conjugated units (Fig. II.1b).

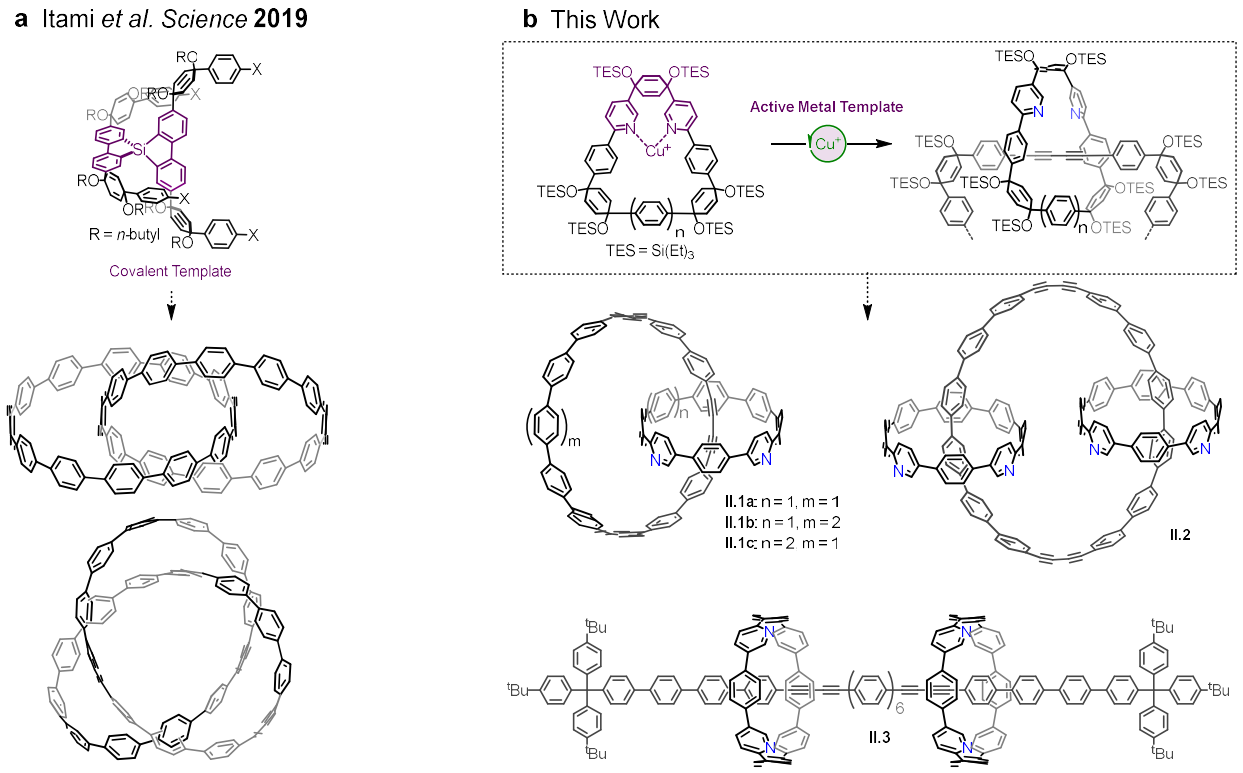

Figure II.1. (a) Itami and co-workers' covalent silicon tethering approach to all benzene catenanes and trefoil knot. **(b)** AT strategy for the synthesis of π-conjugated [*n*]catenanes **II.1a**–**II.1c**, **II.2** (*n* = 2 or 3) and π-conjugated [3]rotaxane **II.3**.

2.2 Results and Discussion

2.2.1 Method Design.

In 2006, Leigh and co-workers introduced the active template (AT) approach to mechanically interlocked molecules (MIMs) [58]. In contrast to more common passive-template (PT) approaches [23,59], the templating moiety in this case is actively involved in the formation of the mechanical bond. Specifically, the AT approach relies on a macrocycle to coordinate a catalytic metal ion endotopically (i.e. at the interior of its cavity). Bond forming reactions then are facilitated

by this metal resulting in a product molecule that is threaded through the center of the macrocycle. Provided the threaded species is appropriately functionalized with large 'stopper' groups at either end, the 'thread' unit becomes mechanically entrapped and unable to diffuse away from the macrocycle. AT offers certain advantages over PT in that the breadth of structures that may be formed are not dictated by the inherent molecular recognition between interlocking components, but by the catalytic character of the templating metal-ion. Indeed, since the initial report by Leigh, Goldup and others have shown the remarkable structural diversity and range of applications enabled by this strategy [26]. Macrocycles with radial π-systems, such as [*n*]CPPs, however, are challenging motifs to use in AT approaches due to their lack of inwardly directed functional groups that might facilitate the required endotopic metal coordination [8,9,60,61]. We envisioned an approach in which macrocyclic [*n*]CPP precursors, rather than the final aromatized structures, are used for the AT reaction. The methods developed in our lab for synthesizing [*n*]CPPs center on the use of cyclohexadiene motifs as bent units that allow for the construction of low-strain macrocyclic precursors, which are ultimately converted to π-conjugated molecules via reductive aromatization [6]. Advantageously, these precursors have been prepared with wide ranging structural diversity, incorporating non-benzenoid aromatics, heterocycles, and even antiaromatic molecules [52]. We envisioned that these same cyclohexadiene systems might also provide the basis of a ligand motif that could enable CPP precursors to endotopically coordinate metal-ions. We hypothesized that macrocyclic structures that contain a cyclohexadiene motif with two flanking pyridine rings would provide a general active templating system to prepare a wide array of π-conjugated, interlocked structures.

To assess the viability of this approach, pyridine containing macrocycles **II.4a** and **II.4b** (Fig. II.2) were prepared in high yields and on the gram and half-gram scale respectively. Half-

axle thread components were designed to be analogous to commonly used synthons in CPP syntheses but carrying a terminal alkyne (**II.5a**) or alkyne bromide (**II.5b**) functional group handle for the AT reation. The Cu^{I} catalyzed AT Cadiot-Chodkiewicz (AT-CC) reaction was chosen for this study as it is well established in MIM syntheses and allows for the creation of fully π-conjugated thread molecules [62,63]. Moreover, if so desired, the resultant diyne is easily converted to other π-conjugated units. We anticipated that the triethylsilyl (TES) ether substituents of **II.5a** and **II.5b** would provide sufficient steric bulk to serve as stopper units to prevent dethreading of the internally cross-coupled species. Accordingly, we envisioned accessing [2]rotaxane molecules that may serve as precursors to catenated structures consisting of a diaza[*n*]CPP and an [*n*+2]CPP, where the +2 of the latter denotes the sp-carbon atoms of the 1,4-butadyine moiety embedded in the CPP backbone.

2.2.2 Synthesis of π-conjugated [*n*]catenanes.

Gratifyingly, both macrocycles **II.4a** and **II.4b** efficiently template the AT-CC reaction to afford [2]rotaxanes **II.6a** and **II.6b** in 65% and 53% yield respectively, provided excess (2.5 eq) of the coupling partners (**II.5a**, **II.5b**) are used (Fig. II.2). [2]Rotaxanes **II.6a** and **II.6b** are subsequently transformed to the corresponding bis-boronates, **II.6c** and **II.6d**, via a Miyaura borylation reaction. Under dilute Suzuki-Miyaura cross coupling conditions **II.6c** and **II.6d** react with **II.S5**, affording [2]catenanes **II.7a** and **II.7b** in 74% and 50% yield respectively. Subjecting **II.6c** to similar macrocyclization reaction conditions using alternative coupling partner **II.S6** afforded [2]catenane **II.7c** in 58% yield. This demonstrates the modularity of these methods whereby [2]catenanes may be accessed in which the size of both the templating macrocycle and

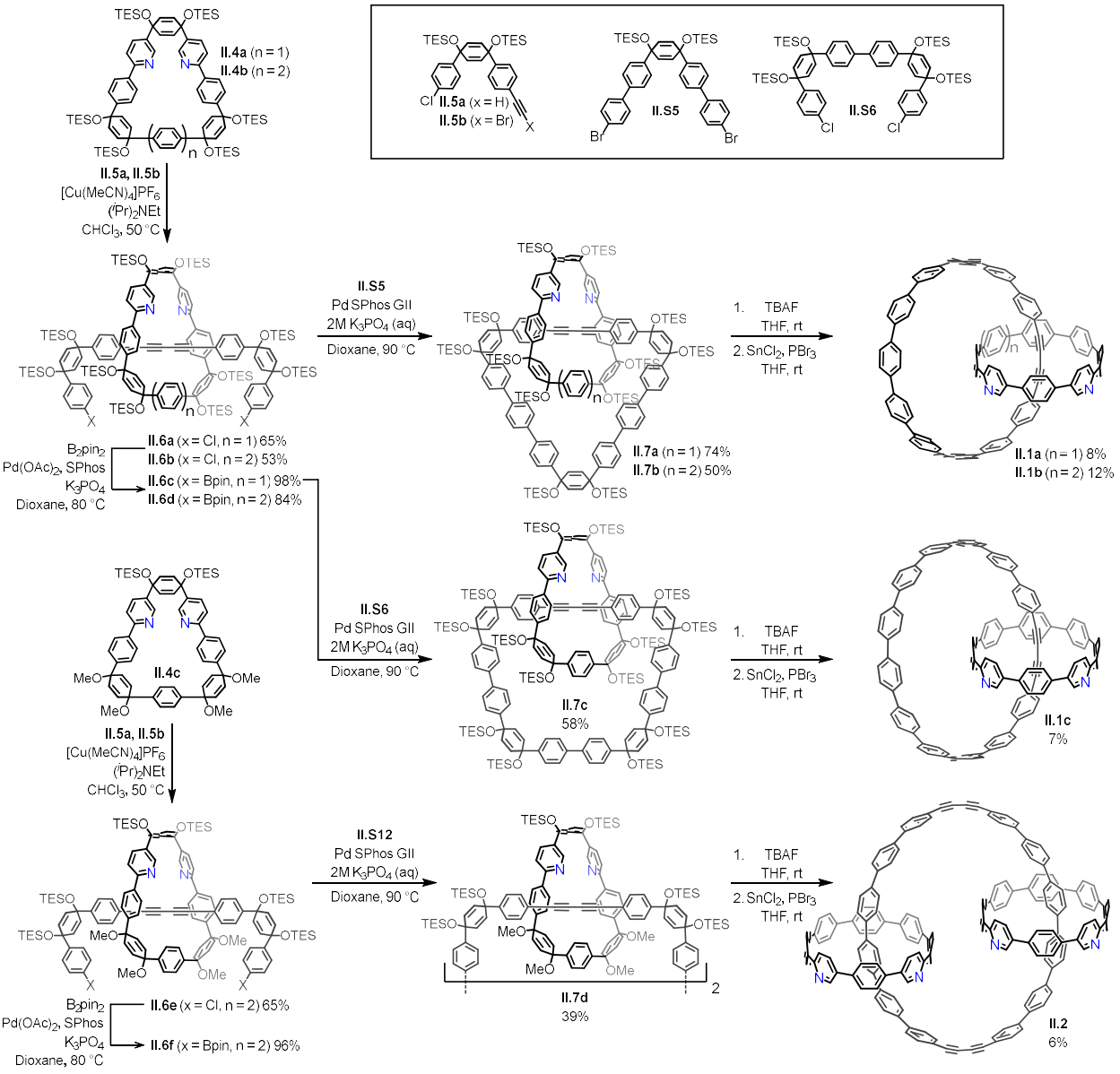

Figure II.2. Synthesis of π-conjugated catenanes. Synthetic routes to compounds **II.1a**–**c** and **II.2**. The general synthetic path to the final π-conjugated catenanes is as follows: AT-CC threading of macrocyclic ligands **II.4a**–**4c** to give [2]rotaxane intermediates **II.6a**, **II.6b** and **II.6e**; Miyuara borylation reactions to give [2]rotaxanes **II.6c**, **II.6d** and **II.6f** with pinacol boronic ester (Bpin)-terminated thread components; Suzuki–Miyuara cross coupling macrocyclization of [2]rotaxanes to give [2]catenanes **II.7a**–**c** or [3]catenane **II.7d**; reductive aromatization of the cyclohexadiene moieties in **II.7a**–**d** to furnish fully π-conjugated [2]catenanes **II.1a**–**c** and [3]catenane **II.2**. the

B_2pin_2, bis(pinacolato)diboron; $(^iPr)_2NEt$, *N*,*N*-diisopropylethylamine; Pd SPhos GII, chloro(2-dicyclohexylphosphino-2′,6′-dimethoxy-1,1′-biphenyl)[2-(2′-amino-1,1′-biphenyl)]palladium(II); r.t., room temperature; SPhos, dicyclohexylphosphino-2′,6′-dimethoxybiphenyl; TBAF, tetra-*n*-butylammonium fluoride.

---

secondary macrocycle formed in the last step may be varied. Aromatization reactions were performed via conditions adapted from those developed by Yamago et al. [64] to provide **II.1a**, **II.1b**, and **II.1c** in 7%, 11%, and 6% yield. While the yields for these final transformations are low, weighable quantities of the final compounds, sufficient for their characterization, could be obtained. In an attempt to access higher order interlocked molecules, **II.6a** and **II.6c** were subjected to dilute Suzuki-Miyaura cross-coupling to target a [3]catenane. This reaction, however, resulted only in a complex mixture of oligomeric products. Analysis of a space filling representation of the target molecule reveals a large degree of steric congestion created by clashing TES groups of the two pre-existing macrocycles, likely precluding macrocyclization and favoring oligomer formation. To circumvent these issues, analogous [2]rotaxane synthons, **II.6e** and **II.6f**, were prepared using the templating macrocycle **II.4c** in which the TES substituents on the lower half (as drawn) of the macrocycle are replaced with smaller methyl ether groups. Satisfyingly, subjecting **II.6e** and **II.6f** to macrocyclization reaction conditions afforded [3]catenane, **II.7d**, in modest yield (39%). Conversion to the aromatized structure was accomplished via conditions analogous to those used for **II.1a-c**, affording **2** in 6% yield. The resulting structure consists of a [12+4]CPP ('+4' now that there are two butadiyne moieties present) threading two diaza[8]CPPs and, to our knowledge, represents the first [3]catenane to be made up of entirely π-conjugated components.

2.2.3 X-ray crystallographic analysis.

Single crystals suitable for X-ray analysis were grown for **II.1a** (Fig. II.3a), **II.1b** (Fig. II.3b), and **II.2** (Fig. II.3c), unambiguously confirming their catenated structures. In the solid-state, **II.1a** exists as a dimer in which the diaza[8]CPP of one catenane occupies the void space of the **[11+2]CPP** from its dimeric partner. Increasing the size of the diaza[*n*]CPP by one phenylene unit prevents this dimer formation as evidenced by the solid-state structure of **II.1b** which displays a much more open packing motif. In contrast to the structures of **II.1a** and **II.1b**, the **diaza[8]CPP** components of **II.2** reside over the two opposing butadiyne moieties of the mutually encapsulated **[12+4]CPP**. This shift in preference is likely do to the sterically congested nature of the structure in which the most efficient separation of mass is achieved with the two **diaza[8]CPP** molecules existing along the major axis of the **[12+4]CPP**'s elliptical structure. Indeed, the structure of the diyne containing ring contorts significantly in accommodation of the two interlocking rings, displaying impressively acute -(C-C≡C)- angles as low as 163.8 ° (164.8 ° and 164.1 ° for **II.1a** and **II.1b** respectively). The solid-state packing of organic molecules is directly correlated to useful materials properties such as charge-transport characteristics [65], as well as their utility as porous molecular materials [66]. The introduction of mechanical linkages represents a unique approach to influence the crystal packing of CPPs beyond merely adjusting the diameter or atomic composition. Interestingly, many close contacts (≤ 3.5 Å) were observed in the crystal structures of **II.1a-c** and **II.2** when compared to the crystal structures of **diaza[8]CPP** and **diaza[9]CPP**. Not only do the catenated structures show a greater number of these contacts, but the mean distance between contacting atoms is markedly lower. This is most dramatic in the case of **II.1a** (Fig II.3d, left) in which 14 distinct intermolecular short contacts (≤ 3.5 Å) are observed between non-bonded

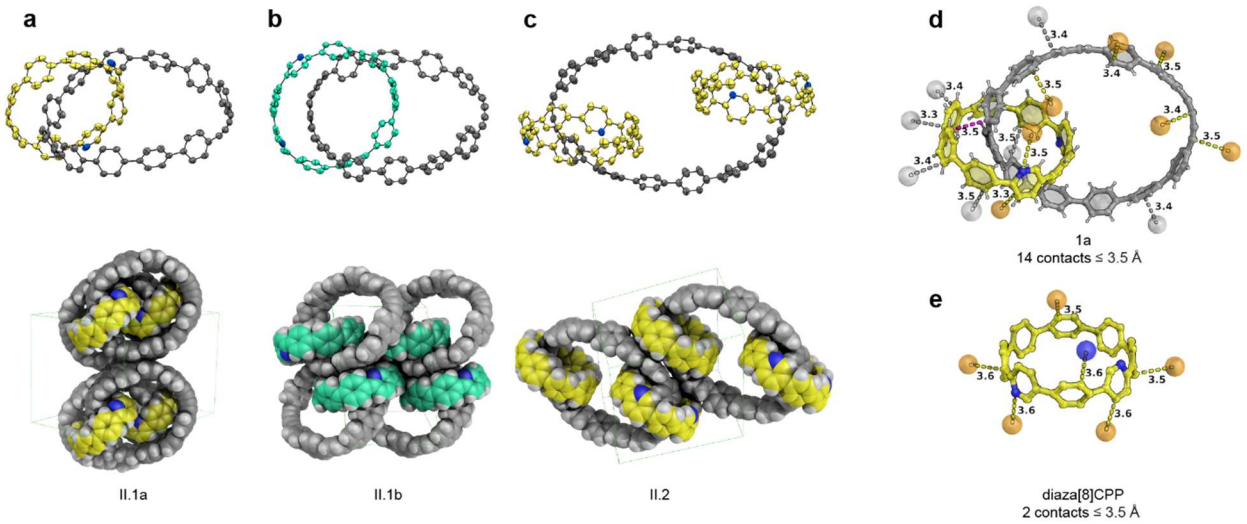

Figure II.3. X-ray structures of II.1a-b and II.2. (a–c) Structures of **II.1a** (a), **II.1b** (b) and **II.2** (c). Top: ORTEP (Oakridge thermal ellipsoid) drawings with thermal ellipsoids set to a 50% probability with the hydrogen atoms and solvent molecules omitted for clarity. Bottom: packing of the structures. Carbon, grey, yellow or green to distinguish different macrocycles; nitrogen, blue; hydrogen, white; solvent molecules omitted for clarity. (d, e) Short contacts (Å) observed in the X-ray structures of **II.1a** (d) and **diaza[8]CPP** (e) demonstrating the relatively large number of close contacts (distance ≤3.5 Å) in the catenated versus non-catenated structures. Contacted atoms are shown as semitransparent spheres and are coloured to distinguish between those that belong to neighbouring diaza[8]CPPs (orange) and neighbouring [11 + 2]CPPs (grey). The contact drawn in magenta (e) shows the closest contact existing between carbon atoms of the two catenated rings. Spheres coloured blue (e) denote closely contacted nitrogen atoms of an adjacent diaza[8]CPP.

carbon (or nitrogen) atoms of a catenane and its neighbors. This is in stark contrast to the structure of **diaza[8]CPP** in which only two contacts exist that are ≤ 3.5 Å (Fig II.3d, right), illustrating the large influence that catenation may have on the materials properties of molecular nanocarbons.

2.2.4 Synthesis of a π-conjugated [3]rotaxane.

Encouraged by our success in synthesizing catenated molecules, we envisioned that [2]rotaxane precursors similar to **II.6a-f** might also be used as intermediates in the synthesis of higher order [*n*]rotaxanes (*n* > 2) featuring fully conjugated threads. To investigate, [2]rotaxanes, **II.6g** and **II.6h**, were prepared (Fig. II.4) in which ^{t}Bu-substitued trityl groups are installed on one end of the thread. This bulky substituent serves as a permanent stopper that remains at the thread termini following the removal of silyl groups. [3]rotaxane **II.8** is readily prepared by the Suzuki cross-coupling of **II.6g** and **II.6h** in 92% yield which upon reductive aromatization provides [3]rotaxane **II.3** in 5% yield. Remarkably, despite the 14 unsubstituted phenyl rings and two interspacing butadiene moieties that make up the thread, **II.3** was completely soluble in common organic solvents and could be characterized by ^{1}H and ^{13}C NMR. Given the high solubility of **II.3**, one might imagine that [2]rotaxanes analogous to **II.6a** and **II.6g** could serve as monomer and end-capping units, respectively, in the formation of insulated π-conjugated wires, offering a new route to this class of electronic material. As it stands, the yields for the final reductive aromatization reaction are prohibitively low for such a pursuit, however, future work will seek alternative reaction conditions that provide more efficient conversion to the aromatized structures.

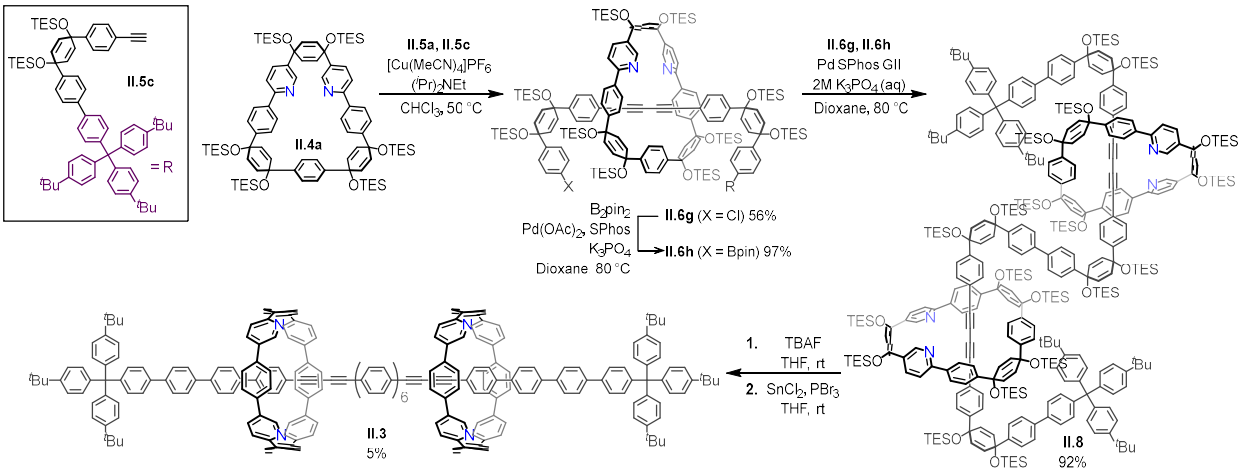

Figure II.4. Synthesis of [3]rotaxane II.3. AT-CC threading of macrocyclic ligand **II.4a** to give asymmetrical [2]rotaxane intermediate **II.6g**; Miyuara borylation reaction to give [2]rotaxane **II.6h** with Bpin-terminated thread components; Suzuki–Miyuara cross-coupling reaction of [2]rotaxanes **II.6g** and **II.6h** to give [3]rotaxane **II.8** or [3]catenane **II.7d**; reductive aromatization of the cyclohexadiene moieties in **II.8** to furnish fully π-conjugated [3]rotaxane **II.3**.

2.2.5 Photophysical analysis of the interlocked structures.

To examine the impact of the mechanical bond on the photophysical properties of these molecules, we independently synthesized and characterized control molecules **diaza[8]CPP**, **diaza[9]CPP** along with **[11+2]CPP** and **[12+2]CPP**. As shown in II.Fig. 5, the photophysical properties of these molecules are consistent with parent CPPs, where the UV-Vis max absorption is independent of size (λ_{max} ~ 345 nm), but the emission maximum redshifts with decreasing size (e.g. **diaza[8]CPP** is redshifted in comparison to **diaza[9]CPP**) [40]. The photophysical characteristics of **II.1a-c**, **II.2**, and **II.3** were also assessed via UV-Vis and fluorescence spectroscopy (Fig. II.5).

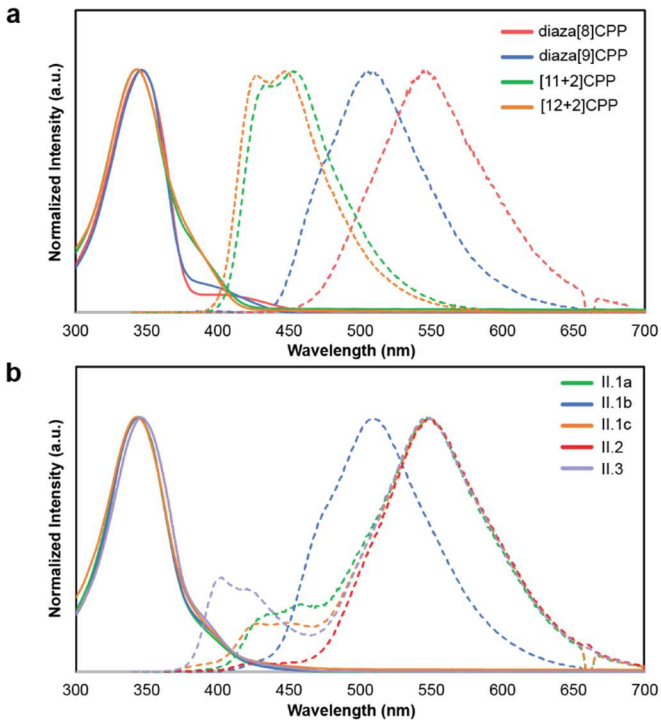

Figure II.5. Photophysical characteristics of compounds. (a) UV–vis absorbance (solid lines) and fluorescence (dashed lines) spectra of diaza[*n*]CPPs (*n* = 8 and 9) and [*n* + 2]CPPs (*n* = 11 and 12) free of mechanical linkage. (**b)** UV–vis absorbance (solid lines) and fluorescence (dashed lines) spectra of interlocked structures **II.1a—c**, **II.2** and **II.3** demonstrating the dominant emission of the diaza[*n*]CPP component(s) over the diyne-containing components. a.u., arbitrary units.

The UV-Vis absorbance profiles of all the interlocked structures are nearly identical to the control molecules, each having a λ_{max} ~ 345 nm. In contrast, the emission profiles of the interlocked structures vary depending on the exact composition. In each case, the dominant emission is that of the smaller diaza[*n*]CPP, with **1c** having an emission maximum centered around 509 nm and **II.1a-b**, **II.2**, and **II.3** having an emission maximum centered around 550 nm. In addition to the emission

from the diaza[*n*]CPP, the fluorescence profiles of each interlocked structure also display a weak blue shoulder stemming from the emission of the diyne containing CPPs (or linear thread component in the case of **II.3**). As the brightness of CPP emission is known to increase with increasing ring size [40], the rather modest contribution of the diyne containing CPP to the catenanes' overall fluorescence profile is consistent with energy transfer from the larger hoop to the smaller hoop [11]. Further study of the photophysics of these dynamic catenane and rotaxane systems is an exciting prospect for the future.

2.2.6 Effect of N-atom placement on ligand behavior.

Very few types of macrocycles have been used in AT chemistry [26], typically being flexible ethereal macrocycles with embedded phenanthrene or bipyridine motifs. Owing to the unusual nature of macrocyclic ligands **II.4a** and **II.4b**, we sought to gain a better understanding of the interaction of these molecules with the Cu catalyst. Specifically, we were curious to whether both pyridine rings are required to direct reactivity toward the interior of the macrocycle as we had originally designed both pyridine rings are required to direct reactivity toward the interior of the macrocycle as we had originally designed. To test this, macrocycle **II.S15** was synthesized, which is identical to **II.4a** but features only a single pyridine ring. However, no interlocked products were observed for AT-CC reactions with **II.S15**, which is consistent with both pyridines acting cooperatively in the endotopic binding of the Cu ion (Fig. II.6). We were also interested whether alternative ligand geometries could be amenable to AT chemistry. To probe this, macrocycle **II.4d** was synthesized which, like **II.4a**, carries two nitrogen atoms but placed at different positions along the macrocycle. Surprisingly, despite a wider bite angle and an increased distance between the two N-atom donors **II.4d** outperforms **II.4a** in the AT-CC reaction, providing [2]rotaxane **II.6i**

in 82% yield (Fig II.6). While it seems that both pyridine rings are essential in sequestering the Cu ion within the interior cavity of the macrocycle, the success of the AT-CC reaction using **II.4d** suggests that a bidentate binding model is likely an oversimplification of a more complex/dynamic interaction(s). This is significant as it demonstrates that macrocycles with atypical ligand motifs may be effectively employed in AT chemistry. As such, we anticipate that a wider array of macrocyclic motifs might be made suitable for AT chemistry than were previously appreciated. Further mechanistic investigations are warranted to fully understand the nature of these unusual ligands.

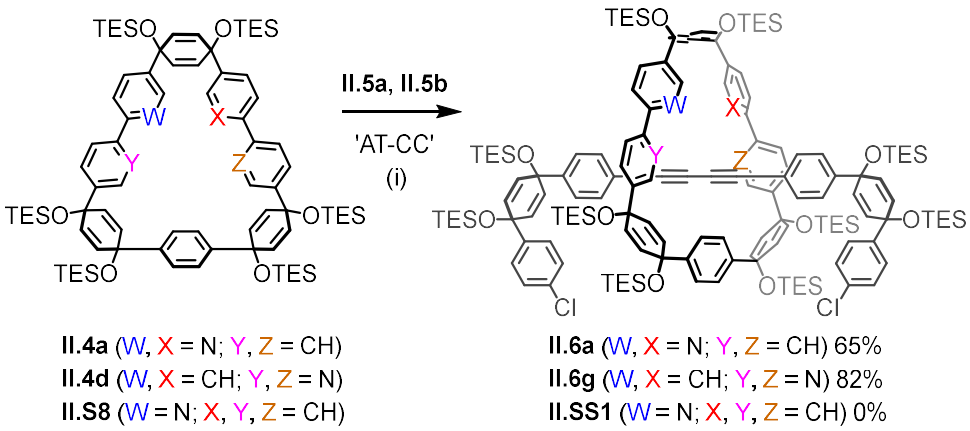

Figure II.4. Effect of N-atom positioning on the AT reaction. [2]rotaxane yields from AT-CC reactions run using macrocyclic ligands in which the number and positioning of the N atoms were varied, highlighting the necessity for more than one N donor atom but a tolerance for their relative positions.

2.2.7 Concerning the reductive aromatization of the interlocked compounds.

Despite the efficiency with which the interlocked precursors (**II.7a-c**, **II.8**) to the title compounds (**II.1a-c**, **II.2**, **II.3**) may be prepared, the synthesis of the fully aromatized structures

is plagued by a low yielding reduction in the final step. The low yield of the reductive aromatization reactions may be attributed to the incompatibility of the reaction conditions required to produce diaza[*n*]CPP and those that will be tolerated in the formation of the aromatized butadiyne containing structures. For the synthesis of **[11+2]CPP** and **[12+2]CPP**, independent of mechanical bonds, it was found that both compounds could be prepared in moderate to good yield via reduction of their macrocyclic precursors by H_2SnCl_4 (Supplementary Fig. II.7a). These mild reducing conditions, however, proved insufficient for the conversion of **II.4a** to **diaza[8]CPP**, instead providing the partially reduced compound **II.SS3** in which the cyclohexadiene unit central to the two pyridine rings is retained (Fig. II.7b). Complete reduction of **II.4a** required more forcing conditions, being accomplished either by reaction with PBr_3 and anhydrous $SnCl_2$ ($PBr_3/SnCl_2$) or by reaction with NaNaph as reported previously*(31)*. Interestingly, subjecting **II.SS3** to $PBr_3/SnCl_2$ resulted only the recovery of **II.SS3** with no evidence for further reduction of the compound. This suggests that **II.SS3** must not be an important intermediate to **diaza[8]CPP** when **II.4a** is directly subjected to these conditions. Attempts to synthesize the [n+2]CPP via reduction with $PBr_3/SnCl_2$ were largely unsuccessful, producing large amounts of insoluble biproducts. However, small amounts of the desired [n+2]CPPs were observed to form under these conditions. In attempts to synthesize [n+2]CPPs via reduction by NaNaph, none of the desired products were observed. Presumably this is due to deleterious reduction of the alkynes to alkenes/alkanes. Given these results, the $PBr_3/SnCl_2$ reduction offered the only conditions found in which full reduction to the diaza[*n*]CPP could be achieved whilst not resulting in the complete degradation of the diyne containing component. We believe that the efficiency of these transformation would be dramatically improved by eliminating the unstable diyne moiety from the system, either by conversion of this unit to a more stable species (thiophene for example) prior to the reductive

aromatization, or by pursuing an alternative active-template reaction, such as the Cu-catalyzed azide alkyne cycloaddition (AT-CuAAC).

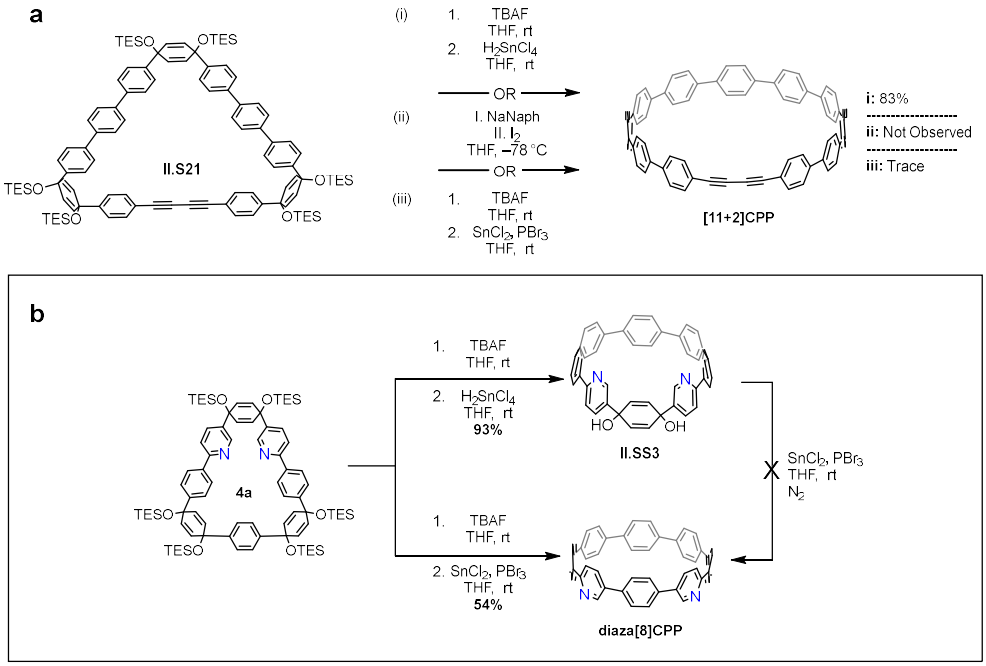

Figure II.7. Results from the reductive aromatization of **II.S21** and **II.4a** by various conditions.

2.3 Conclusion

In summary, we report a new active template synthesis by which mechanically interlocked CPPs of varying substructure and topology may be prepared. The methods disclosed in this report dramatically increase the structural space that may be explored in the context of topological nanocarbon species and lay the synthetic groundwork for the preparation of structures of even greater complexity than those presented here. Importantly, the synthetic method leverages the well-established building block approach to nanohoop architectures, which is already being

employed by numerous research groups. While we have confirmed the validity of this approach for the precursors of diaza[8]CPP and diaza[9]CPP, we anticipate that both smaller and larger macrocycles bearing these ligand motifs would be capable of participating in the AT-CC reaction, allowing for a detailed analysis of the influence of relative ring size on the properties of nanohoop catenanes. Further, owing to the simplicity of the mechanical bond forming reaction, we envision that this AT methodology may be adapted to produce a wide array of interlocked structures including those decorated with functional groups or even extended polymeric materials. We anticipate that the generality of this approach will provide access to topological carbon nanostructures with emergent optical and electronic characteristics that were previously inaccessible.

2.4 Methods and Materials

2.4.1 General Experimental Details.

Commercially available materials were used without purification. **II.S1** [51], **II.S4** [51], **II.S5** [51], **II.S6** [51], **II.S7** [51], **II.S14** [51], **II.S10**, **II.S11**, **II.S12** [61], and **II.S17** [67] were prepared according to modified protocols from the literature. Moisture and oxygen sensitive reactions were carried out in flame-dried glassware and under an inert atmosphere of purified nitrogen using syringe/septa technique. Tetrahydrofuran (THF), and 1,4-dioxane were dried by filtration through alumina according to the methods described by Grubbs. Column chromatography was conducted with Zeochem Zeoprep n60 Eco 40-63 μm silica gel. Alumina column chromatography was conducted with Sorbtech Alumina, basic (pH 10), Act. II-III, 50-200 μm. 1H and 13C NMR spectra were recorded on either a Bruker Avance III HD 500 (1H: 500 MHz, 13C: 126 MHz) or Bruker Avance III HD 600 MHz (1H: 600 MHz, 13C: 151 MHz) NMR spectrometer equipped with a Prodigy

multinuclear cryoprobe, respectively. All samples were measured at 25 °C. ^{1}H and ^{13}C NMR spectra were taken in either $CDCl_3$ (referenced to TMS, δ = 0.00 ppm) or CD_2Cl_2 (referenced to dichloromethane δ(1H) = 5.32 ppm, δ(13C) = 54.00 ppm). Coupling constants (J) are given in Hz and the apparent resonance multiplicity is reported as s (singlet), d (doublet), t (triplet), q (quartet), quint (quintet) or m (multiplet). Absorbance and fluorescence spectra were obtained in a 1 cm Quartz cuvette with dichloromethane using an Agilent Cary 100 UV-Vis spectrometer and a Horiba Jobin Yvon Fluoromax-4 Fluorimeter respectively. Solutions of PBr_3 and $SnCl_2$ used for the reductive aromatization of the interlocked species, **II.1a**, **II.1b**, **II.1c**, **II.2**, and **II.3**, were prepared immediately prior to use. Anhydrous $SnCl_2$ is used for reactions involving PBr_3. Unless stated otherwise, H_2SnCl_4 was prepared in the following manner: To a solution of $SnCl_2 \cdot 2H_2O$ (465.0 mg, 2.06 mmol) in 5 mL THF was added conc. HCl (0.33 mL, 4.00 mmol). The resulting solution was then stirred for 15 minutes and used as needed.

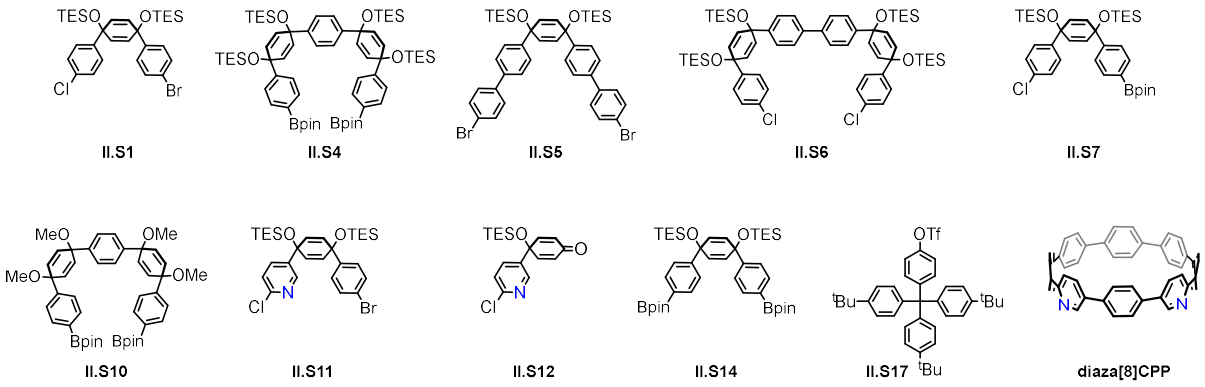

Figure II.8. Previously reported compounds pertinent to the syntheses recorded in chapter **II**.

2.4.2 Synthetic Procedures.

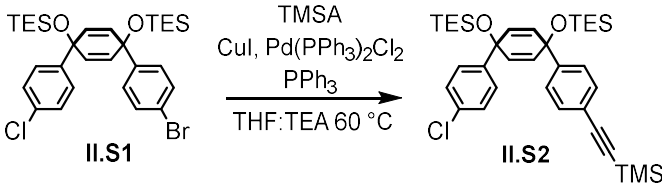

Synthesis of II.S2. To a 100 mL round bottom flask was added **II.S1** (6.00 g, 9.90 mmol), $Pd(PPh_3)_2Cl_2$ (0.174 g, 0.25 mmol), CuI (0.024 g, 0.12 mmol), and triphenylphosphine (PPh_3, 0.260 g, 0.990 mmol). The flask was evacuated and backfilled with N_2 gas five times before adding THF (10 mL), triethylamine (TEA, 10 mL) and trimethylsilyl acetylene (TMSA, 5.64 mL, 39.6 mmol). The mixture stirred at 60 °C for 48 h after which the reaction was removed from heat and the solvent was evaporated under reduced pressure. The crude material was run though a short silica plug using hexanes as eluent, providing **II.S2** as a viscous, pale-yellow oil. (6.15 g, 99%). ^{1}H NMR (500 MHz, Chloroform-*d*) δ 7.37 (d, *J* = 8.1 Hz, 2H), 7.24 (d, *J* = 8.0 Hz, 2H), 7.21 (s, 4H), 5.98 (d, *J* = 10.1 Hz, 2H), 5.93 (d, *J* = 10.1 Hz, 2H), 0.92 (dt, *J* = 12.0, 7.9 Hz, 18H), 0.59 (dq, *J* = 21.3, 7.9 Hz, 12H), 0.24 (s, 9H). ^{13}C NMR (126 MHz, Chloroform-*d*) δ 146.25, 144.45, 133.05, 131.91, 131.50, 131.36, 128.27, 127.25, 125.76, 122.12, 104.99, 93.34, 71.28, 71.17, 7.05, 7.03, 6.46, 6.44, 0.00. HRMS (ASAP) (m/z): [M]+ calculated for $C_{35}H_{51}ClO_2Si_3$, 622.2885; found, 622.2775.

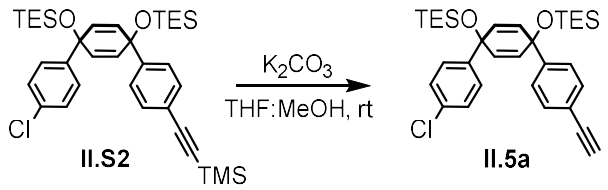

Synthesis of 5a. To a 50 mL round bottom flask were added **II.S2** (3.00 g, 4.81 mmol), THF (10 mL) and MeOH (10 mL). Potassium carbonate (K_2CO_3, 3.00 g, 21.7 mmol) was added, and the slurry was stirred for 30 min at room temperature. The solvent was removed under reduced pressure and the crude material was run through a short silica plug using hexanes as eluent, providing **II.5a** as a pale-yellow oil (2.6 g, 98%). ^{1}H NMR (500 MHz, Chloroform-*d*) δ 7.40 (d, *J* = 8.5 Hz, 2H), 7.26 (d, *J* = 8.4 Hz, 2H), 7.22 (s, 4H), 5.99 – 5.93 (m, 4H), 3.06 (s, 1H), 0.94 – 0.91 (m, 18H), 0.62 – 0.56 (m, 12H). ^{13}C NMR (126 MHz, Chloroform-*d*) δ 146.60, 144.44, 133.07, 132.03, 131.51, 131.35, 128.28, 127.26, 125.82, 121.02, 83.52, 71.28, 71.09, 7.01, 6.42. HRMS (ASAP) (m/z): [M]+ calculated for $C_{32}H_{43}ClO_2Si_2$, 550.2490; found, 550.2395.

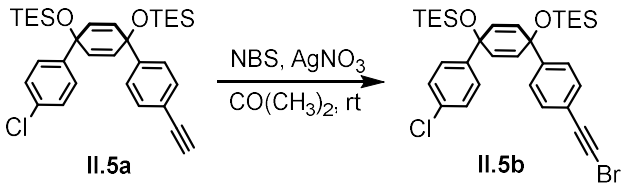

Synthesis of II.5b. To a 50 mL round bottom flask were added **5a** (1.22 g, 2.21 mmol), *N*-bromosuccinimide (NBS, 0.512 g, 2.88 mmol) and silver nitrate ($AgNO_3$, 0.038 g, 0.221 mmol). Acetone (25 mL) was added, and the solution was stirred for 1 h at room temperature. The solvent was removed under reduced pressure and the crude material was run through a short alumina plug using hexanes as eluent, providing **5b** as a pale-yellow oil. (1.05 g, 75%). ^{1}H NMR (500 MHz, Chloroform-*d*) δ 7.35 (d, *J* = 8.4 Hz, 2H), 7.25 (d, *J* = 8.5 Hz, 2H), 7.22 (s, 4H), 5.96 – 5.95 (m,

4H), 0.94 – 0.90 (m, 18H), 0.62 – 0.56 (m, 12H). ^{13}C NMR (126 MHz, Chloroform-*d*) δ 146.47, 144.42, 133.09, 131.90, 131.53, 131.32, 128.28, 127.26, 125.85, 121.63, 79.92, 71.28, 71.10, 49.83, 7.02, 6.43. HRMS (ASAP) (m/z): [M]+ calculated for $C_{32}H_{42}BrClO_2Si_2$, 628.1595; found, 628.1551.

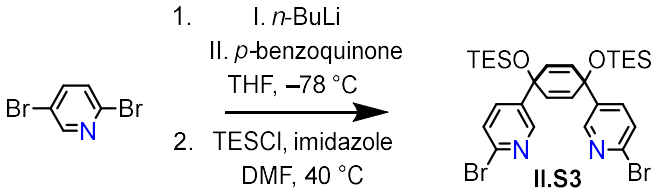

Synthesis of II.S3. Three flasks (**A-C**) were prepared as follows: **Flask A**: To a flame dried 250 mL round bottom flask was added 2,5-dibromopyridine (10 g, 42.2 mmol). The flask was evacuated and backfilled with N_2 gas three times before introducing THF (40 mL). The resulting solution was used at room temperature. **Flask B:** A flame dried 250 mL round bottom flask was evacuated and backfilled with N_2 gas three times. THF (60 mL) and *n*-butyllithium (*n*-BuLi, 16.0 mL, 40.0 mmol, 2.5 M in hexanes) were then added and the solution was cooled to –78 °C. **Flask C:** To a flame dried 500 mL round bottom flask containing stir bar were added *p*-benzoquinone (1.52 g, 14.1 mmol). The flask was evacuated and backfilled with N_2 gas three times before introducing THF (90 mL) and cooling to –78 °C. The contents of **Flask A** were added to **Flask B** via dropwise canula transfer over a period of 20 minutes. The resulting solution was allowed to stir at temperature for 30 minutes before radialy canulating the lithiate into **Flask C**. The resulting blue/green suspension was allowed to stir at –78 °C for 2 hrs. H_2O (100 mL) was added, and the reaction mixture was allowed to warm to room temperature. THF was removed under reduced pressure and the resulting aqueous suspension was extracted with EtOAc (4 x 50 mL). The organic

layers were combined and washed with H_2O (50 mL) and brine (50 mL) before drying over sodium sulfate (Na_2SO_4). The solvent was removed under reduced pressure to give a redish-brown oil. The crude oil was transferred into a flame-dried 250 mL round bottom flask. Imidazole (3.9 g, 57 mmol) was added, and the flask was evacuated and backfilled with N_2 gas three times before introducing DMF (60 mL). The solution was heated to 40 °C with stirring and chlorotriethylsilane (TESCl, 7.1 mL 42 mmol) was added. The reaction was allowed to stir for 4 h before quenching with a saturated aqueous solution of sodium bicarbonate (sat'd $NaHCO_3$). The resulting suspension was removed from heat and stirred until gasses ceased to evolve. The reaction mixture transferred into a separatory funnel and extracted with Et_2O (4 x 40 mL). The organic layers were combined and washed with H_2O (50 mL) and brine (50 mL) before drying over Na_2SO_4. The product was purified by column chromatography (SiO_2, 0-5% EtOAc in Hexanes) to give **II.S3** as a clear oil that solidifies upon standing (6.01 g, 66%). mp: 107 – 108 °C; ^{1}H NMR (500 MHz, Chloroform-*d*) δ 8.32 (s, 2H), 7.38 (s, 4H), 6.02 (s, 4H), 0.93 (t, *J* = 7.9 Hz, 18H), 0.60 (q, *J* = 7.9 Hz, 12H). ^{13}C NMR (126 MHz, Chloroform-*d*) δ 148.15, 141.23, 140.45, 135.88, 131.36, 127.65, 69.76, 6.94, 6.39. HRMS (ASAP) (m/z): [M]+ calculated for $C_{28}H_{40}Br_2N_2O_2Si_2$, 650.0995; found, 650.0933.

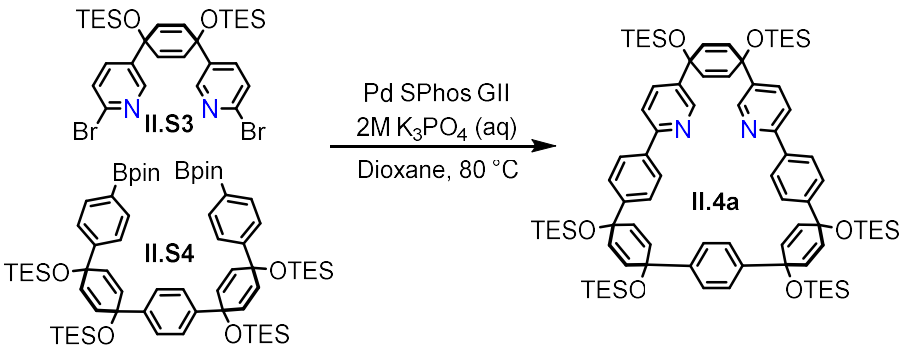

Synthesis of II.4a. To a 500 mL round bottom flask were added **II.S3** (0.562 g, 0.86 mmol), **II.S4** (1.10 g, 0.95 mmol) and Pd SPhos GII (0.031 g, 0.04 mmol). The flask was evacuated and backfilled with N_2 gas five times before introducing 1,4-dioxane (250 mL). The resulting mixture was heated to 80 °C with stirring at which point an aqueous solution of K_3PO_4 (2M, 10 mL) was added. After 1.5 h a small aliquot (0.2 mL) was removed from the reaction mixture, concentrated, and analyzed via ^{1}H NMR which showed total consumption of starting materials. The reaction was removed from heat and the solvent was removed under reduced pressure. The crude residue was transferred into a separatory funnel with the aid of 50 mL H_2O and 20 mL DCM. The organic layer was collected, and the aqueous layer was extracted with an additional 10 mL fresh DCM. The organic layers were combined and dried over Na_2SO_4 before running the solution through a short silica plug using DCM as eluent. The eluate was evaporated under reduced pressure and the resulting oily solid was triturated with acetone (5 mL) to produce a filterable solid precipitate. After chilling in an ice bath for 30 min, the precipitate was collected by vacuum filtration and washed with cold acetone (3 mL) and methanol (10 mL) to give **II.4a** as a white powder (1.10 g, 91%). mp: (decomp. 249 °C); ^{1}H NMR (500 MHz, Chloroform-*d*) δ 8.39 (d, *J* = 2.4 Hz, 2H), 7.86 (d, *J* = 8.4 Hz, 4H), 7.46 – 7.42 (m, 10H), 7.26 (dd, *J* = 8.3, 2.3 Hz, 1H), 6.14 (s, 4H), 6.03 (d, *J* = 10.1 Hz, 4H), 5.93 (d, *J* = 10.1 Hz, 4H), 1.00 – 0.92 (m, 54H), 0.70 – 0.66 (m, *J* = 7.9 Hz, 24H), 0.56 (q, *J* = 7.9 Hz, 12H). ^{13}C NMR (126 MHz, Chloroform-*d*) δ 156.09, 147.88,

147.18, 145.80, 137.78, 137.51, 134.36, 132.00, 131.67, 131.19, 126.70, 125.99, 125.82, 119.42, 71.28, 71.25, 70.76, 7.12, 7.01, 6.51, 6.46, 6.43. HRMS (ASAP) (m/z): [M]+ calculated for $C_{82}H_{120}N_2O_6Si_6$, 1396.7762; found, 1396.7507.

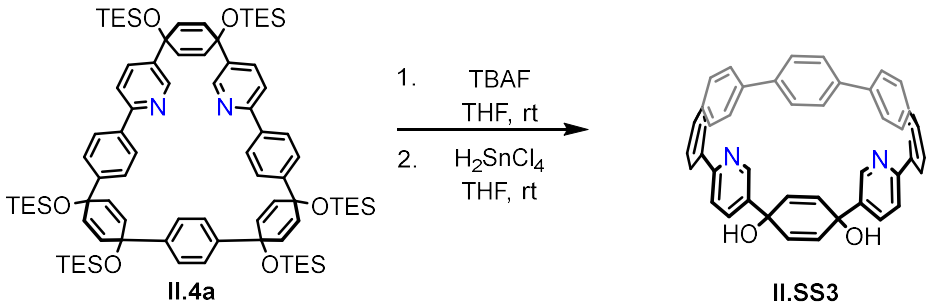

II.4a II.SS3

Synthesis of II.SS3. To a flame-dried 100 mL round bottom flask was added **II.S21** (0.166 g, 0.12 mmol). The flask was evacuated and backfilled with N_2 gas three times before dissolving in THF (30 mL). TBAF (0.95 mL, 0.95 mmol, 1M in THF) was added. was added and the reaction was stirred for 1 h at room temperature. The solvent was removed under reduced pressure and the resulting yellow-brown oil was triturated with 5 mL H_2O until a filterable solid had formed. The precipitate was collected by vacuum filtration and washed with H_2O (10 mL) and DCM (10 mL) which after drying under vacuum affords the intermediate product as a white solid. The desilylated material was then transferred into a separate 100 mL round bottom flask. The flask was evacuated and backfilled with N_2 gas three times before introducing THF (25 mL). H_2SnCl_4 (2.6 mL, 0.52 mmol, 0.20 M in THF) was added and the resulting solution was stirred in the exclusion of light for 3 h before quenching the reaction with sat'd $NaHCO_3$ (25 mL). The reaction mixture was then transferred into a separatory funnel with the aid of EtOAc (20 mL) and H_2O (20 mL). The organic layer was collected and the aqueous layer was extracted twice more with EtOAc (2 x 10 mL). The organic layers were combined and dried over Na_2SO_4 before removing the solvent under reduced

pressure. The crude material was then suspended in EtOAc and rinsed through a short silica plug using EtOAc (50 mL) to elute impurities followed by MeOH to elute the partially aromatized product. The MeOH was removed under reduced pressure and the resulting residue was triturated with 15 mL DCM until a freely flowing precipitate was obtained. The solids were collected by vacuum filtration, washing with DCM (5 mL) followed by pentane (5 mL) to afford **II.SS3** as a light-yellow solid. (0.071 g, 93%). mp: (decomp. 121 °C); 1H NMR (500 MHz, DMSO-d6) δ 8.39 (d, J = 2.3 Hz, 1H), 7.88 (dd, J = 8.4, 2.4 Hz, 1H), 7.76 (d, J = 8.5 Hz, 2H), 7.73 (d, J = 8.3 Hz, 1H), 7.69 (s, 2H), 7.65 (d, J = 8.9 Hz, 2H), 7.58 (d, J = 8.7 Hz, 2H), 7.54 (d, J = 8.6 Hz, 2H), 6.08 (s, 2H), 6.03 (s, 1H). 13C NMR (126 MHz, DMSO-d6) δ 155.14, 146.18, 139.50, 139.11, 137.72, 136.69, 136.34, 136.02, 134.59, 131.13, 127.71, 127.63, 127.46, 127.37, 127.00, 119.88, 66.58. HRMS (ASAP) (m/z): [M]+ calculated for $C_{46}H_{32}N_2O_2$, 644.2464; found, 644.2350.

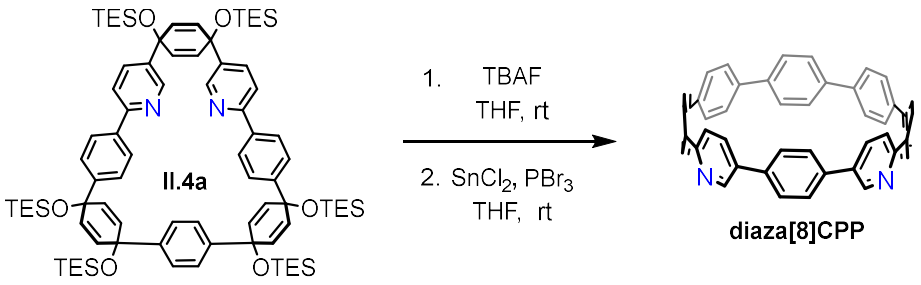

Synthesis of diaza[8]CPP. To a flame died 100 mL round bottom flask was added **II.4a** (0.041 g, 0.029 mmol). The flask was evacuated and backfilled with N_2 gas three times before dissolving in THF (10 mL). TBAF (0.29 mL, 0.29 mmol, 1M in THF) was added. was added and the reaction was stirred for 1 h at room temperature. The solvent was removed under reduced pressure and the resulting yellow-brown oil was triturated with 5 mL H_2O until a filterable solid had formed. The precipitate was collected by vacuum filtration and washed with H_2O (10 mL) and

DCM (10 mL). The desilylated material was rigorously dried under vacuum before transferring into a separate flame-dried 250 mL round bottom flask. The flask was evacuated and backfilled with N_2 gas three times before adding THF (15 mL). $SnCl_2$ (0.47 mL, 0.23 mmol, 0.5 M in THF) was added and the mixture was stirred until the starting material had dissolved. PBr_3 (0.47 mL, 0.23 mmol, 0.5 M in THF) was then introduced via slow, dropwise addition and the resulting solution was stirred in the exclusion of light for 30 minutes before quenching the with sat'd $NaHCO_3$ (20 mL). THF was removed under reduced pressure and the remaining aqueous suspension was extracted with DCM (3 x 15 mL). The organic layers were combined and dried over Na_2SO_4 before passing the solution through a short alumina plug using DCM as eluent. The eluate was evaporated under reduced pressure. The resulting material was then suspended in MeOH (10 mL) with sonication and collected by vacuum filtration, washing with MeOH (10 mL) and pentane (10 mL) to give **diaza[8]CPP** as a bright yellow solid (9.7 mg, 54%). Spectroscopic data of the product agrees with that found in the literature *(31)*.

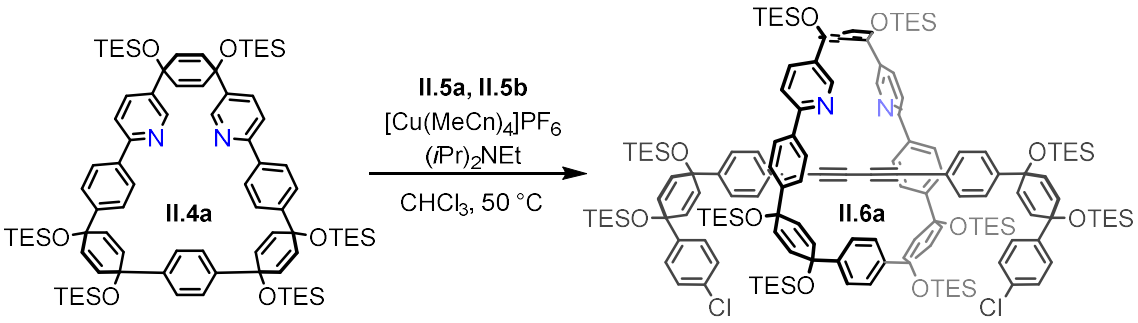

Synthesis of II.6a. To a flame-dried 100 mL round bottom flask were added, **II.4a** (0.635 g, 0.45 mmol), **II.5a** (0.626 g, 1.13 mmol), **II.5b**, (0.715 g, 1.13 mmol), and $[Cu(MeCN)_4]PF_6$ (0.161 g, 0.43 mmol). The flask was evacuated and backfilled with N_2 gas five times before adding $CHCl_3$ (30 mL). The mixture was sonicated while sparging with N_2 gas until $[Cu(MeCN)_4]PF_6$ had

completely dissolved (typically 5-10 minutes). The resulting solution was heated to 50 °C and *N,N*-diisoproylethylamine (DIPEA, 0.24 mL, 0.32 mmol) was added. The reaction was then stirred at 50 °C for 3 h at which point the reaction mixture was transferred into a separatory funnel along with an aqueous solution of ammonia (18 w/w%) containing ethylenediaminetetraacetic acid disodium salt (NH_3-EDTA, 20 mL). The mixture was emulsified and allowed to separate twice before collecting the organic layer. The aqueous layer was extracted with an additional 10 mL fresh DCM and the organic layers were combined and dried over Na_2SO_4. The reaction products were separated via column chromatography (SiO_2, 0-40% DCM in hexanes) to afford **II.6a** as an off-white solid (0.742 g, 65% yield). A secondary gradient (SiO_2, 0-5% EtOAc in hexanes) was used to elute unthreaded **II.4a** from the column (0.213 g, 33%). ^{1}H NMR (500 MHz, Chloroform-*d*) δ 8.87 (d, *J* = 2.4 Hz, 2H), 7.84 (d, *J* = 8.1 Hz, 4H), 7.43 – 7.33 (m, 10H), 7.28 – 7.23 (m, 8H), 7.08 (d, *J* = 8.0 Hz, 4H), 6.90 (dd, *J* = 8.4, 2.5 Hz, 2H), 6.70 (d, *J* = 8.1 Hz, 4H), 6.20 (s, 4H), 5.95 (q, *J* = 10.1 Hz, 8H), 5.87 (d, *J* = 9.8 Hz, 4H), 5.71 (d, *J* = 9.8 Hz, 4H), 1.00 – 0.91 (m, 72H), 0.83 (t, *J* = 7.9 Hz, 18H), 0.71 – 0.58 (m, 48H), 0.46 (q, *J* = 7.9 Hz, 12H). ^{13}C NMR (126 MHz, Chloroform-*d*) δ 156.01, 148.60, 147.06, 146.59, 145.01, 144.45, 137.73, 137.31, 133.80, 133.26, 132.22, 132.09, 131.73, 131.49, 131.30, 131.00, 128.38, 127.31, 127.25, 125.97, 125.63, 125.32, 120.61, 119.73, 81.55, 71.31, 71.20, 71.02, 70.96, 70.51, 7.14, 7.08, 7.04, 7.02, 6.50, 6.48, 6.44, 6.34. MS (MALDI–TOF) [M]+ calculated for $C_{146}H_{204}Cl_2N_2O_{10}Si_{10}$, 2495.2586; found, 2495.3.

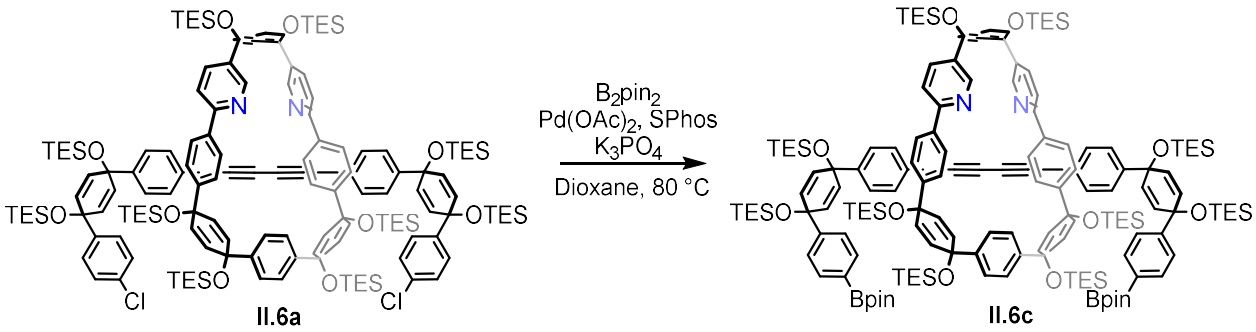

Synthesis of II.6c. To a flame dried 25 mL round bottom flask were added **II.6a** (0.670 g, 0.27 mmol)**,** B_2pin_2 (0.340 g, 1.34 mmol), $Pd(OAc)_2$ (0.012 g, 0.05 mmol), SPhos (0.044 g, 0.11 mmol), and tribasic potassium phosphate (K_3PO_4, 0.455 g, 2.14 mmol). The flask was evacuated and backfilled with N_2 gas five times before introducing 1,4-dioxane (5 mL). The mixture was stirred at 80 °C for 1 h. The solvent was then removed under reduced pressure and the crude material was run through a short silica plug using DCM as eluent. The eluate was concentrated under reduced pressure and the resulting residue was sonicated with MeOH (10 mL) until a flocculent precipitate had formed. The precipitate was collected by vacuum filtration and washed with MeOH (20 mL) to give **II.6c** as a tan colored solid (706 mg, 98%). ^{1}H NMR (500 MHz, Chloroform-*d*) δ 8.84 (d, *J* = 2.3 Hz, 2H), 7.87 (d, *J* = 8.4 Hz, 4H), 7.77 (d, *J* = 8.0 Hz, 4H), 7.41 – 7.33 (m, 14H), 7.09 (d, *J* = 8.4 Hz, 4H), 6.89 (dd, *J* = 8.4, 2.4 Hz, 2H), 6.64 (d, *J* = 8.4 Hz, 4H), 6.17 (s, 4H), 6.01 (d, *J* = 10.2 Hz, 4H), 5.87 (dd, *J* = 18.0, 10.1 Hz, 8H), 5.71 (d, *J* = 10.1 Hz, 4H), 1.33 (s, 24H), 1.01 – 0.94 (m, 54H), 0.91 (t, *J* = 7.9 Hz, 18H), 0.83 (t, *J* = 7.9 Hz, 18H), 0.69 – 0.63 (m, 36H), 0.55 (q, *J* = 7.9 Hz, 12H), 0.47 (q, *J* = 7.9 Hz, 12H). ^{13}C NMR (126 MHz, Chloroform-*d*) δ 156.09, 149.02, 148.39, 146.99, 146.99, 146.77, 144.94, 137.58, 137.33, 134.84, 133.89, 132.19, 132.02, 131.66, 131.61, 131.10, 131.00, 127.36, 126.02, 125.63, 125.27, 125.13, 120.48, 119.83, 119.83, 83.77, 71.26, 71.18, 70.95, 70.57, 24.87, 7.13, 7.11, 7.04, 7.03, 7.01, 6.48,

6.46, 6.45, 6.34. MS (MALDI–TOF) [M]+ calculated for $C_{158}H_{228}B_2N_2O_{14}Si_{10}$, 2679.5069; found, 2679.6.

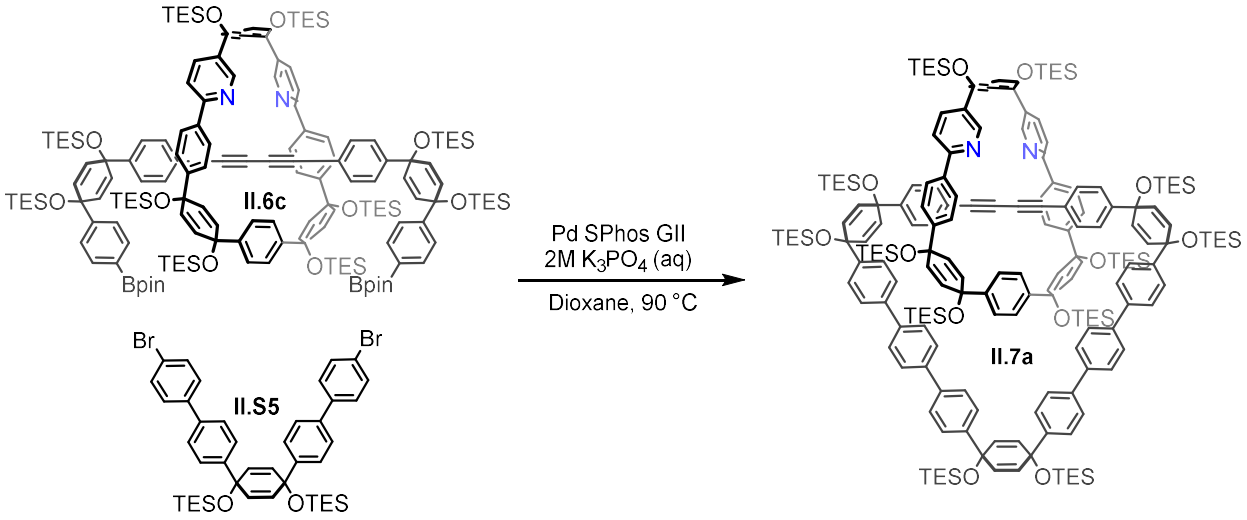

Synthesis of II.7a. To a 250 mL round bottom flask were added **II.6c** (0.250 g, 0.09 mmol), **II.S5** (0.075 g, 0.09 mmol) and Pd SPhos GII (0.013 g, 0.002 mmol). The flask was evacuated and backfilled with N_2 gas five times before introducing 1,4-dioxane (150 mL). The resulting mixture was heated to 90 °C with stirring at which point an aqueous solution of K_3PO_4 (2M, 3 mL) was added. After 1.5 h a small aliquot (0.2 mL) was removed from the reaction mixture, concentrated, and analyzed via ^{1}H NMR which showed total consumption of starting materials. The solvent was removed under reduced pressure and the crude residue was transferred into a separatory funnel with the aid of H_2O (50 mL) and DCM (20 mL). The organic layer was collected, and the aqueous layer was extracted with again with DCM (10 mL). The organic layers were combined and dried over Na_2SO_4. The product was purified via column chromatography (SiO_2, 0-40% DCM in hexanes), providing **II.7a** as an off-white solid (0.213 g, 74%).

*Product isolated from the column is sufficiently pure to be used in subsequent steps. Purity is marginally improved by washing with acetone at the cost of significant loss of product to the filtrate. This step was only performed on small scale in order to acquire an analytically pure sample for characterization.

^{1}H NMR (500 MHz, Chloroform-*d*) δ 8.83 (d, *J* = 2.3 Hz, 2H), 7.88 (d, *J* = 8.0 Hz, 4H), 7.74 – 7.67 (m, 8H), 7.63 (d, *J* = 8.2 Hz, 4H), 7.59 (d, *J* = 8.1 Hz, 4H), 7.48 – 7.44 (m, 8H), 7.41 (d, *J* = 8.1 Hz, 4H), 7.38 – 7.35 (m, 6H), 7.17 (d, *J* = 8.0 Hz, 4H), 6.88 (dd, *J* = 8.4, 2.3 Hz, 2H), 6.73 (d, *J* = 8.0 Hz, 4H), 6.13 (s, 4H), 6.08 – 6.04 (m, 8H), 5.94 (d, *J* = 9.8 Hz, 4H), 5.87 (d, *J* = 9.8 Hz, 4H), 5.71 (d, *J* = 9.8 Hz, 4H), 0.99 – 0.87 (m, 93H), 0.79 (t, *J* = 7.9 Hz, 18H), 0.67 – 0.57 (m, 64H), 0.43 (q, *J* = 8.0 Hz, 12H). ^{13}C NMR (126 MHz, Chloroform-*d*) δ 156.03, 148.55, 147.03, 146.94, 145.30, 145.06, 145.00, 139.83, 139.62, 139.47, 139.41, 137.69, 137.41, 133.86, 132.24, 132.02, 131.78, 131.71, 131.48, 131.05, 131.02, 127.39, 126.87, 126.71, 126.27, 126.00, 125.66, 125.35, 120.50, 119.69, 81.57, 75.32, 71.45, 71.42, 71.29, 71.15, 70.93, 70.54, 7.11, 7.09, 7.07, 7.03, 6.94, 6.52, 6.51, 6.48, 6.43, 6.32. MS (MALDI–TOF) [M]+ calculated for $C_{188}H_{254}N_2O_{12}Si_{12}$, 3067.6558; found, 3067.6.

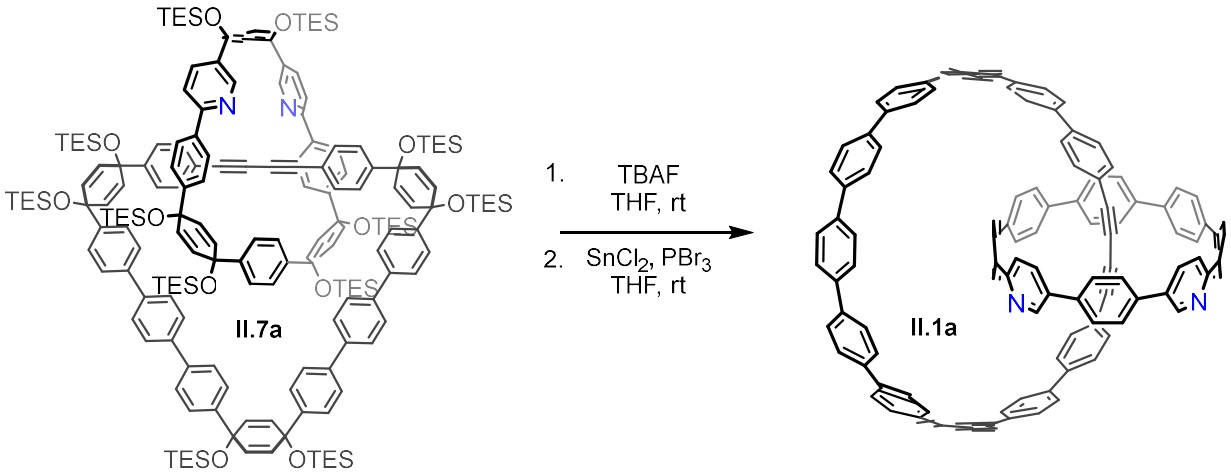

Synthesis of II.1a. To a flame died 100 mL round bottom flask was added **II.7a** (0.100 g, 0.032 mmol). The flask was evacuated and backfilled with N_2 gas three times before dissolving in THF (50 mL). tetra *n*-butylammonium fluoride (TBAF, 0.65 mL, 0.65 mmol, 1M in THF) was added and the reaction was stirred for 1 h at room temperature. The solvent was removed under reduced pressure and the resulting yellow-brown oil was triturated with H_2O (10 mL) until a filterable solid had formed. The precipitate was collected by vacuum filtration and washed with H_2O (10 mL) and DCM (10 mL). The desilylated material was rigorously dried under vacuum before transferring into a separate flame-dried 250 mL round bottom flask. The flask was evacuated and backfilled with N_2 gas three times before adding THF (100 mL). Stannous chloride ($SnCl_2$, 2.17 mL, 0.39 mmol, 0.18 M in THF) was added and the mixture was stirred until the starting material had dissolved. Phosphorous tribromide (PBr_3, 0.55 mL, 0.39 mmol, 0.18 M in THF) was then introduced via slow, dropwise addition and the resulting solution was stirred in the exclusion of light for 30 minutes before quenching the with sat'd $NaHCO_3$ (20 mL). THF was removed under reduced pressure and the remaining aqueous suspension was extracted with DCM (3 x 15 mL). The organic layers were combined and dried over Na_2SO_4. The product was purified via preparatory TLC (alumina, 60% DCM in hexanes) to furnish **II.1a** as a yellow solid (0.004 g,

8%). ^{1}H NMR (500 MHz, Chloroform-*d*) δ 8.56 (d, *J* = 2.4 Hz, 2H), 7.76 (s, 4H), 7.62 – 7.53 (m, 4H), 7.52 – 7.06 (m, 64H). ^{13}C NMR (126 MHz, Chloroform-*d*) δ 154.61, 147.12, 141.22, 139.56, 139.28, 139.07, 138.92, 138.78, 138.74, 138.72, 138.70, 138.37, 138.16, 137.94, 137.35, 137.33, 135.34, 133.03, 132.52, 130.37, 128.63, 127.86, 127.74, 127.70, 127.66, 127.63, 127.14, 121.41, 119.50, 91.19, 79.49. HRMS (ESI–TOF) [M+1]+ calculated for $C_{116}H_{75}N_2$, 1495.5930; found, 1495.5948.

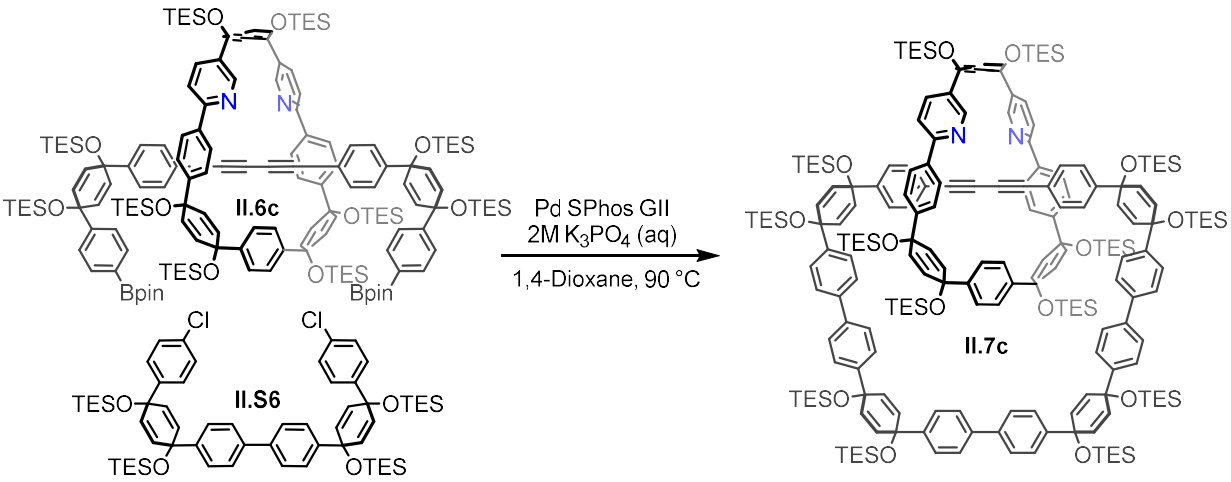

Synthesis of II.7c. To a 250 mL round bottom flask were added **II.6c** (0.250 g, 0.09 mmol), **II.S6** (0.098 g, 0.09 mmol) and Pd SPhos GII (0.013 g, 0.002 mmol). The flask was evacuated and backfilled with N_2 gas five times before introducing 1,4-dioxane (150 mL). The resulting mixture was heated to 90 °C with stirring at which point an aqueous solution of K_3PO_4 (2M, 3 mL) was added. After 1.5 h a small aliquot (0.2 mL) was removed from the reaction mixture, concentrated, and analyzed via ^{1}H NMR which showed total consumption of starting materials. The solvent was removed under reduced pressure and the crude residue was transferred into a separatory funnel with the aid of H_2O (50 mL) and DCM (20 mL). The organic layer was collected, and the aqueous layer was extracted with an additional 10 mL fresh DCM. The organic layers were combined and

dried over Na_2SO_4. The product was purified via column chromatography (SiO_2, 0-40% DCM in hexanes) providing **II.7c** as an off-white solid (0.184 g, 58%).

*Product isolated from the column is sufficiently pure to be used in subsequent steps. Purity is marginally improved by wash with acetone at the cost of significant loss of product to the filtrate. This step was only performed on small scale in order to acquire an analytically pure sample for characterization.

^{1}H NMR (500 MHz, Chloroform-*d*) δ 8.60 (d, *J* = 2.4 Hz, 2H), 7.75 (d, *J* = 8.1 Hz, 4H), 7.47 – 7.39 (m, 20H), 7.35 – 7.29 (m, 12H), 7.19 (d, *J* = 8.3 Hz, 2H), 7.01 (d, *J* = 8.1 Hz, 4H), 6.96 (dd, *J* = 8.3, 2.4 Hz, 2H), 6.56 (d, *J* = 8.1 Hz, 4H), 6.05 – 5.99 (m, 16H), 5.90 (d, *J* = 9.9 Hz, 4H), 5.75 (d, *J* = 10.0 Hz, 4H), 5.70 (d, *J* = 9.9 Hz, 4H), 1.01 (t, *J* = 7.9 Hz, 18H), 0.96 – 0.91 (m, 73H), 0.86 (t, *J* = 7.9 Hz, 18H), 0.81 (t, *J* = 7.9 Hz, 18H), 0.71 – 0.54 (m, 72H), 0.46 (q, *J* = 7.9 Hz, 12H). ^{13}C NMR (126 MHz, Chloroform-*d*) δ 155.97, 147.85, 146.76, 146.32, 145.27, 145.16, 145.10, 144.58, 139.79, 139.61, 139.42, 137.65, 137.23, 133.76, 132.24, 131.80, 131.69, 131.46, 131.40, 131.21, 131.15, 127.20, 126.85, 126.83, 126.81, 126.23, 126.14, 125.95, 125.82, 125.15, 120.53, 119.70, 81.78, 75.60, 71.58, 71.22, 71.20, 71.02, 70.93, 70.75, 70.61, 7.11, 7.07, 7.05, 7.03, 7.01, 6.50, 6.48, 6.46, 6.44, 6.38. MS (MALDI–TOF) [M]+ calculated for $C_{206}H_{288}N_2O_{14}Si_{14}$, 3405.8655; found, 3406.9.

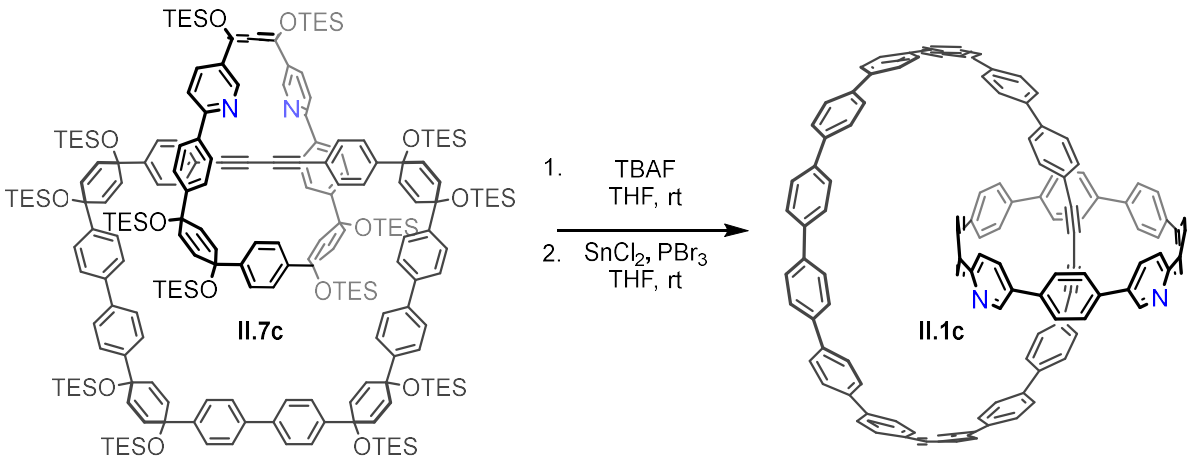

Synthesis of II.1c. To a flame died 100 mL round bottom flask was added **II.7c** (0.105 g, 0.031 mmol) The flask was evacuated and backfilled with N_2 gas three times before dissolving in THF (50 mL). TBAF (0.62 mL, 0.62 mmol, 1M in THF) was added and the reaction was stirred for 1 h at room temperature. The solvent was removed under reduced pressure and the resulting yellow-brown oil was triturated with 5 mL H_2O until a filterable solid had formed. The precipitate was collected by vacuum filtration and washed with H_2O (10 mL) and DCM (10 mL). The desilylated material was rigorously dried under vacuum before transferring into a separate flame-dried 250 mL round bottom flask. The flask was evacuated and backfilled with N_2 gas three times before adding THF (100 mL). $SnCl_2$ (2.33 mL, 0.43 mmol, 0.18M in THF) was added and the mixture was stirred until the starting material had dissolved. PBr_3 (0.68 mL, 0.43 mmol, 0.63 M in THF) was then introduced via slow, dropwise addition and the resulting solution was stirred in the exclusion of light for 30 minutes before quenching the with sat'd $NaHCO_3$ (20 mL). THF was removed under reduced pressure and the remaining aqueous suspension was extracted with DCM (3 x 15 mL). The organic layers were combined and dried over Na_2SO_4. The product was purified via preparatory TLC (alumina, 60% DCM in hexanes) to furnish **II.1c** as a yellow solid (0.003 g, 7%). ^{1}H NMR (600 MHz, Methylene Chloride-d_2) δ 8.62 (d, J = 2.3 Hz, 2H), 7.80 (s, 4H), 7.65

(dd, J = 8.6, 2.3 Hz, 2H), 7.55 – 7.46 (m, 34H), 7.45 (d, J = 8.6 Hz, 4H), 7.41 (d, J = 9.1 Hz, 4H), 7.38 – 7.25 (m, 28H). ^{13}C NMR (126 MHz, Methylene Chloride-d_2) δ 154.05, 146.54, 140.68, 139.05, 138.72, 138.61, 138.48, 138.36, 138.30, 138.28, 138.27, 137.90, 137.60, 137.38, 136.79, 136.75, 134.80, 132.47, 132.06, 129.80, 128.05, 127.29, 127.16, 127.12, 127.09, 127.08, 127.06, 126.57, 120.78, 118.91, 89.58, 78.37. HRMS (ESI–TOF) [M+1]+ calculated for $C_{122}H_{79}N_2$, 1571.6243; found, 1571.6272.

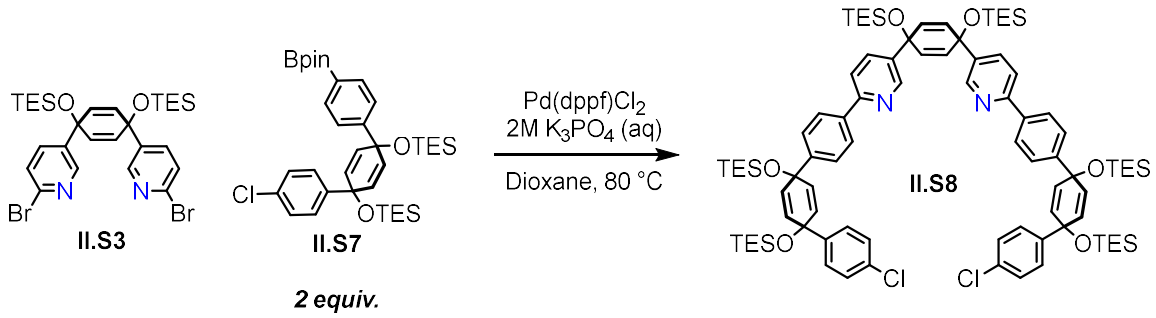

Synthesis of II.S8. To a 50 mL round bottom flask were added **II.S3** (0.390 g, 0.60 mmol), **II.S7** (0.780 g, 1.20 mmol) and Pd(dppf)Cl_2·DCM (0.024 g, 0.03 mmol). The flask was evacuated and backfilled with N_2 gas five times before introducing 1,4-dioxane (15 mL) and an aqueous solution of K_3PO_4 (2M, 3 mL). The mixture was stirred at 80 °C for 3 h after which the solvent was removed under reduced pressure. The crude residue was then transferred into a separatory funnel with the aid of H_2O (20 mL) and DCM (10 mL). The organic layer was collected, and the aqueous layer was extracted with an additional 10 mL fresh DCM. The organic layers were combined and dried over Na_2SO_4 before running the solution through a short silica plug using DCM as eluent. The eluate was evaporated under reduced pressure and the resulting oily solid was triturated with 20 mL EtOH to produce a filterable solid precipitate. After chilling in an ice bath for 30 min, the precipitate was collected by vacuum filtration and washed with cold EtOH (15 mL)

to provide **II.S8** as a white powder (0.892 g, 96%). mp: 168-169 °C; ^{1}H NMR (500 MHz, Chloroform-*d*) δ 8.73 (d, *J* = 2.1 Hz, 2H), 7.90 (d, *J* = 8.1 Hz, 4H), 7.66 – 7.57 (m, 4H), 7.41 (d, *J* = 8.2 Hz, 4H), 7.26 (d, *J* = 8.0 Hz, 4H), 7.21 (d, *J* = 8.4 Hz, 4H), 6.10 (s, 4H), 6.04 (d, *J* = 9.9 Hz, 4H), 5.95 (d, *J* = 10.0 Hz, 4H), 0.97-0.91 (m, 54H), 0.66-0.57 (m, 36H). ^{13}C NMR (126 MHz, Chloroform-*d*) δ 155.98, 147.69, 146.70, 144.60, 139.55, 137.99, 134.08, 132.96, 131.61, 131.43, 131.31, 128.26, 127.28, 126.75, 126.28, 119.85, 71.29, 71.17, 70.12, 7.05, 7.02, 6.48, 6.46, 6.42. HRMS (ASAP) (m/z): [M]+ calculated for $C_{88}H_{124}Cl_2N_2O_6Si_6$, 1542.7452; found, 1542.7400.

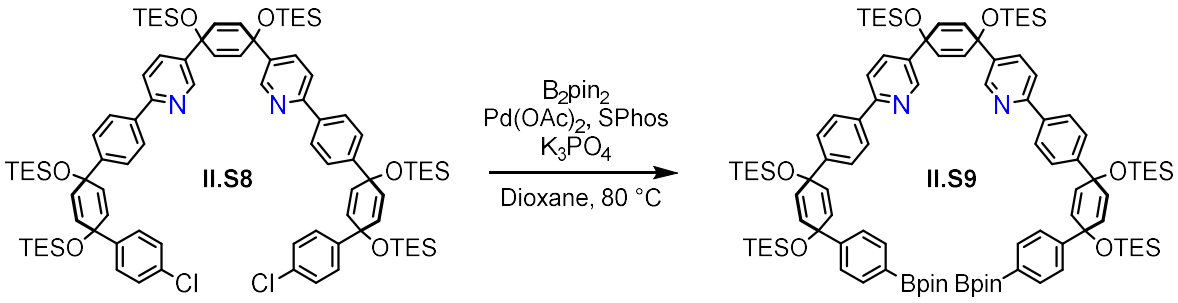

Synthesis of II.S9. To a flame dried 25 mL round bottom flask were added **II.S8** (0.892 g, 0.58 mmol)**,** B_2pin_2 (0.585 g, 2.31 mmol), $Pd(OAc)_2$ (0.006 g, 0.03 mmol), SPhos (0.024 g, 0.06 mmol), and K_3PO_4 (0.980 g, 4.62 mmol). The flask was evacuated and backfilled with N_2 gas five times before introducing 1,4-dioxane (10 mL). The mixture was stirred at 80 °C for 1 h. The solvent was then removed under reduced pressure and the crude material run through a short silica plug using DCM as eluent. The eluate was concentrated under reduced pressure and the resulting residue was sonicated with MeOH (10 mL) until a flocculent precipitate had formed. The precipitate was collected by vacuum filtration and washed with MeOH (20 mL) to give **II.S9** as a tan colored solid (0.852 g, 85%). mp: 136-138 °C; ^{1}H NMR (500 MHz, Chloroform-*d*) δ 8.77 (d, *J* = 2.3 Hz, 2H), 7.89 (d, *J* = 8.1 Hz, 4H), 7.71 (d, *J* = 7.8 Hz, 4H), 7.63 (d, *J* = 8.3 Hz, 2H), 7.58

(dd, J = 8.3, 2.4 Hz, 2H), 7.42 (d, J = 8.1 Hz, 4H), 7.36 (d, J = 7.9 Hz, 4H), 6.11 (s, 4H), 6.06 – 5.93 (m, 8H), 1.31 (s, 24H), 1.07 – 0.81 (m, 54H), 0.71 – 0.49 (m, 36H). ^{13}C NMR (126 MHz, Chloroform-*d*) δ 156.06, 149.09, 147.71, 146.87, 139.46, 137.83, 134.73, 134.00, 131.48, 131.42, 126.71, 126.28, 125.18, 119.85, 83.71, 71.57, 71.39, 70.13, 24.86, 7.07, 7.05, 7.03, 6.47. HRMS (ASAP) (m/z): [M]+ calculated for $C_{100}H_{148}B_2N_2O_{10}Si_6$, 1726.9936; found, 1726.9763.

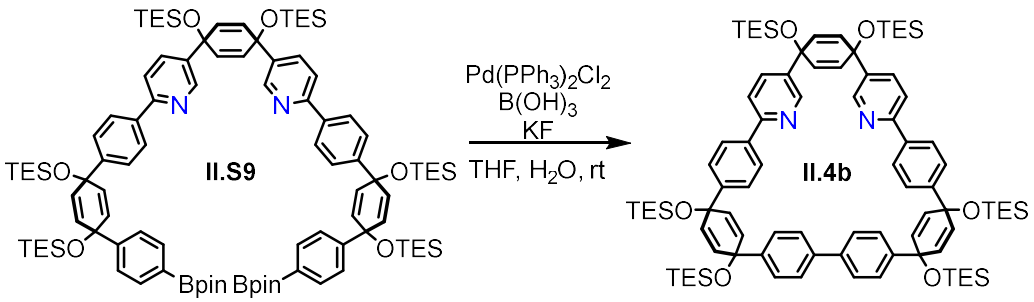

Synthesis of II.4b. To a 500 mL round bottom flask was added **II.S9** (0.850 g, 0.49 mmol), $Pd(PPh_3)_2Cl_2$ (0.069 g, 0.10 mmol), $B(OH)_3$ (4.92 mmol), and KF (0.286 g, 4.92 mmol). THF (250 mL) and H_2O (10 mL) were added, and the solution was stirred for 16 h at room temperature, open to air. The THF was removed under reduced pressure and the resulting aqueous suspension was extracted with DCM (3 x 10 mL). The organic layers were combined and dried over Na_2SO_4 before running through a short silica plug using DCM as eluent. The eluate was evaporated under reduced pressure and the resulting residue was triturated with 5 mL acetone to produce a filterable solid precipitate. After chilling in an ice bath for 30 min, the precipitate was collected by vacuum filtration and washed with ice-cold hexanes (3 mL) and methanol (3 mL) to give **II.4b** as an off-white powder. (0.531 g, 73%). mp: (decomp. 281 °C); ^{1}H NMR (500 MHz, Chloroform-*d*) δ 8.68 (d, J = 2.2 Hz, 2H), 7.97 (d, J = 8.5 Hz, 4H), 7.70 (d, J = 8.3 Hz, 2H), 7.66 (dd, J = 8.3, 2.3 Hz, 2H), 7.54 (d, J = 8.4 Hz, 4H), 7.49 (d, J = 8.5 Hz, 4H), 7.39 (d, J = 8.4 Hz, 4H), 6.08 (s, 4H), 6.03

(d, J = 10.2 Hz, 4H), 6.00 (d, J = 10.4 Hz, 4H), 0.98 – 0.94 (m, 54H), 0.66 – 0.62 (m, 36H). ^{13}C NMR (126 MHz, Chloroform-*d*) δ 155.81, 147.61, 147.12, 145.02, 139.62, 139.29,137.63, 134.05, 131.69, 131.35, 131.17, 126.63, 126.59, 126.38, 126.20, 119.78, 71.59, 71.51, 70.20, 7.09, 7.08, 7.03, 6.51, 6.49, 6.47. HRMS (ASAP) (m/z): [M]+ calculated for $C_{88}H_{124}N_2O_6Si_6$, 1472.8075; found, 1472.7859.

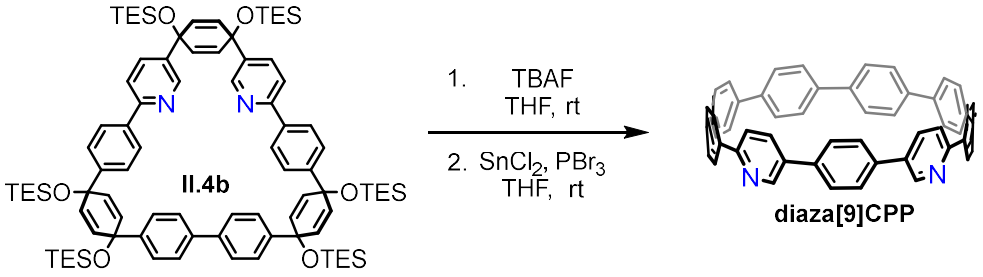

Synthesis of diaza[9]CPP. To a flame died 50 mL round bottom flask was added **II.4b** (0.034 g, 0.02 mmol). The flask was evacuated and backfilled with N_2 gas three times before dissolving in THF (10 mL). TBAF (0.46 mL, 0.46 mmol, 1M in THF) was added and the reaction was stirred at room temperature for 1 h. The solvent was removed under reduced pressure and the resulting yellow oil was triturated with 5 mL H_2O until a filterable solid had formed. The precipitate was collected by vacuum filtration and washed with H_2O (10 mL) and DCM (10 mL) which, after drying under vacuum, affords the product as a white solid. The desilylated material was then transferred into a separate flame-dried 50 mL round bottom flask. The flask was evacuated and backfilled with N_2 gas three times before adding THF (15 mL). The suspension was stirred and $SnCl_2$ (0.37 mL, 0.18 mmol, 0.5 M in THF) was added followed by the dropwise addition of PBr_3 (0.37 mL, 0.18 mmol, 0.5 M in THF). The resulting solution was allowed to stir in the exclusion of light for 30 minutes before quenching the reaction with sat'd $NaHCO_3$ (5 mL).

THF was removed under reduced pressure and the remaining aqueous suspension was extracted with DCM (3 x 10 mL). The organic layers were combined and dried over Na_2SO_4 before running through an alumina plug using DCM as eluent. The eluate was evaporated under reduced pressure and the resulting residue was suspended with sonication in 10 mL MeOH. Solids were collected by vacuum filtration to give **diaza[9]CPP** as a yellow-green solid (9.7 mg, 69%). mp: (decomp. 187 °C); ^{1}H NMR (500 MHz, Chloroform-*d*) δ 8.77 (d, *J* = 2.3 Hz, 2H), 7.91 (d, *J* = 8.4 Hz, 4H), 7.83 (dd, *J* = 8.6, 2.3 Hz, 2H), 7.65 (d, *J* = 8.5 Hz, 2H), 7.59 – 7.49 (m, 24H). ^{13}C NMR (126 MHz, Chloroform-*d*) δ 154.69, 147.13, 139.54, 138.36, 138.00, 137.90, 137.63, 137.01, 135.68, 133.18, 130.91, 128.05, 127.67, 127.50, 127.37, 127.23, 119.29. HRMS (ESI–TOF) [M+H]+ calculated for $C_{52}H_{35}N_2$, 687.2795; found, 697.2783.

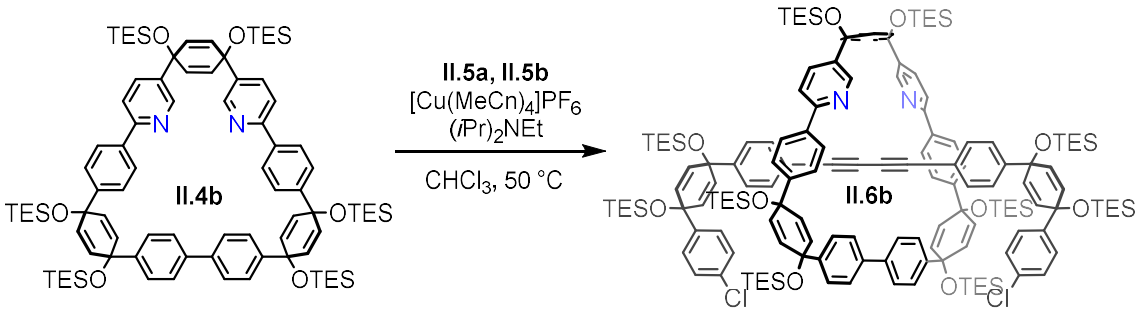

Synthesis of II.6b. To a flame-dried 100 mL round bottom flask were added, **II.4b** (0.237 g, 0.16 mmol), **II.5a** (0.177 g, 0.32 mmol), **II.5b**, (0.203 g, 0.32 mmol), and $[Cu(MeCN)_4]PF_6$ (0.057 g, 0.15 mmol). The flask was evacuated and backfilled with N_2 gas five times before adding $CHCl_3$ (30 mL). The mixture was sonicated while sparging with N_2 until $[Cu(MeCN)_4]PF_6$ had completely dissolved (typically 5-10 minutes). The resulting solution was heated to 50 °C and DIPEA (0.24 mL, 0.32 mmol) was added. The reaction was then stirred at 50 °C for 3 h at which point the reaction mixture was transferred into a separatory funnel along with an aqueous NH_3-

EDTA solution (20 mL). The mixture was emulsified and allowed to separate twice before collecting the organic layer. The aqueous layer was extracted with an additional 10 mL fresh DCM after which and the organic layers were combined and dried over Na_2SO_4. The reaction products were separated via column chromatography (SiO_2, 0-40% DCM in hexanes) to afford **II.6b** as an off-white solid (0.219 g, 53 % yield). A secondary gradient (SiO_2, 0-5% EtOAc in hexanes) was used to elute unthreaded **II.4b** from the column (0.086 g, 36%). ^{1}H NMR (500 MHz, Chloroform-*d*) δ 8.94 (d, *J* = 2.4 Hz, 2H), 8.04 (d, *J* = 8.2 Hz, 4H), 7.76 (d, *J* = 8.4 Hz, 2H), 7.60 (d, *J* = 8.2 Hz, 4H), 7.44 (d, *J* = 8.2 Hz, 4H), 7.34 (d, *J* = 8.2 Hz, 4H), 7.26 (dd, *J* = 8.4, 2.4 Hz, 2H), 7.21 (s, 8H), 6.93 (d, *J* = 8.1 Hz, 4H), 6.62 (d, *J* = 8.2 Hz, 4H), 6.01 (s, 4H), 5.99 – 5.93 (m, 8H), 5.91 (d, *J* = 10.1 Hz, 4H), 5.84 (d, *J* = 10.1 Hz, 4H), 1.02 – 0.88 (m, 90H), 0.69 – 0.54 (m, 60H). ^{13}C NMR (126 MHz, Chloroform-*d*) δ 155.57, 147.77, 146.92, 146.69, 144.89, 144.42, 139.26, 139.24, 137.54, 133.62, 133.26, 132.25, 131.69, 131.45, 131.39, 131.28, 131.15, 128.42, 127.24, 126.77, 126.16, 126.07, 125.38, 119.97, 119.59, 82.28, 74.50, 71.65, 71.52, 71.26, 70.94, 70.62, 7.11, 7.09, 7.06, 7.01, 6.55, 6.51, 6.50, 6.45. MS (MALDI–TOF) [M]+ calculated for $C_{152}H_{208}Cl_2N_2O_{10}Si_{10}$, 2571.2899; found, 2571.4.

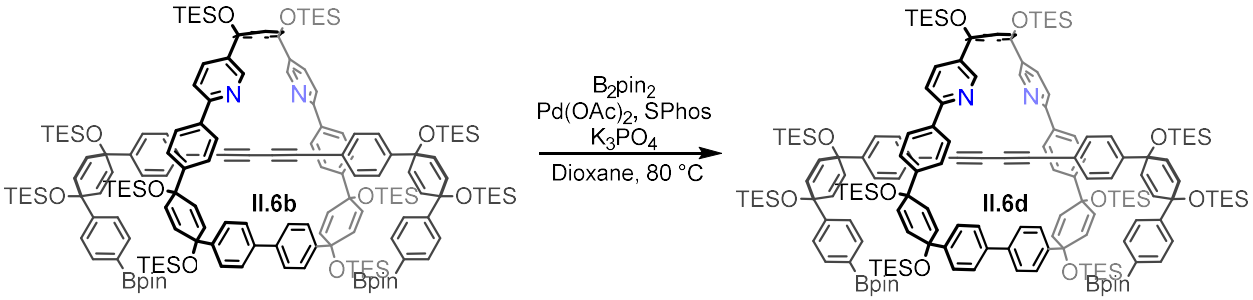

Synthesis of II.6d. To a flame dried 25 mL round bottom flask were added **II.6b** (0.200 g, 0.08 mmol)**,** B_2pin_2 (0.197 g, 0.78 mmol), $Pd(OAc)_2$ (0.004 g, 0.02 mmol), SPhos (0.016 g, 0.04

mmol), and K_3PO_4 (0.132 g, 0.62 mmol). The flask was evacuated and backfilled with N_2 gas five times before introducing 1,4-dioxane (5 mL). The mixture was stirred at 80 °C for 1 h. The solvent was then removed under reduced pressure and the crude material was run through a short silica plug using DCM as eluent. The eluate was concentrated under reduced pressure and the resulting residue was sonicated with MeOH (10 mL) until a flocculent precipitate had formed. The precipitate was collected by vacuum filtration and washed with MeOH (20 mL) to provide **II.6d** as a tan colored solid (0.119 g, 84%). 1H NMR (500 MHz, Chloroform-*d*) δ 8.91 (d, *J* = 2.4 Hz, 2H), 8.06 (d, *J* = 8.2 Hz, 4H), 7.77 – 7.69 (m, 6H), 7.63 (d, *J* = 8.2 Hz, 4H), 7.43 (d, *J* = 8.1 Hz, 4H), 7.34 – 7.29 (m, 8H), 7.22 (dd, *J* = 8.3, 2.5 Hz, 2H), 6.94 (d, *J* = 8.2 Hz, 4H), 6.57 (d, *J* = 8.1 Hz, 4H), 6.01 – 5.94 (m, 12H), 5.90 (d, *J* = 10.0 Hz, 4H), 5.79 (d, *J* = 9.8 Hz, 4H), 1.33 (s, 24H), 0.97 – 0.88 (m, 90H), 0.67 – 0.58 (m, 48H), 0.53 (q, *J* = 7.9 Hz, 12H). ^{13}C NMR (126 MHz, Chloroform-*d*) δ 155.69, 148.90, 147.57, 146.85, 146.82, 144.75, 139.18, 139.11, 137.60, 134.88, 133.75, 132.21, 131.62, 131.52, 131.41, 131.15, 131.09, 126.87, 126.79, 126.15, 126.04, 125.35, 125.13, 119.86, 119.71, 83.76, 82.28, 74.44, 71.64, 71.57, 71.32, 71.28, 24.90, 7.11, 7.09, 7.05, 7.02, 6.54, 6.50, 6.45, 6.44. MS (MALDI–TOF) [M]+ calculated for $C_{164}H_{232}B_2N_2O_{14}Si_{10}$, 2755.5382; found, 2755.6.

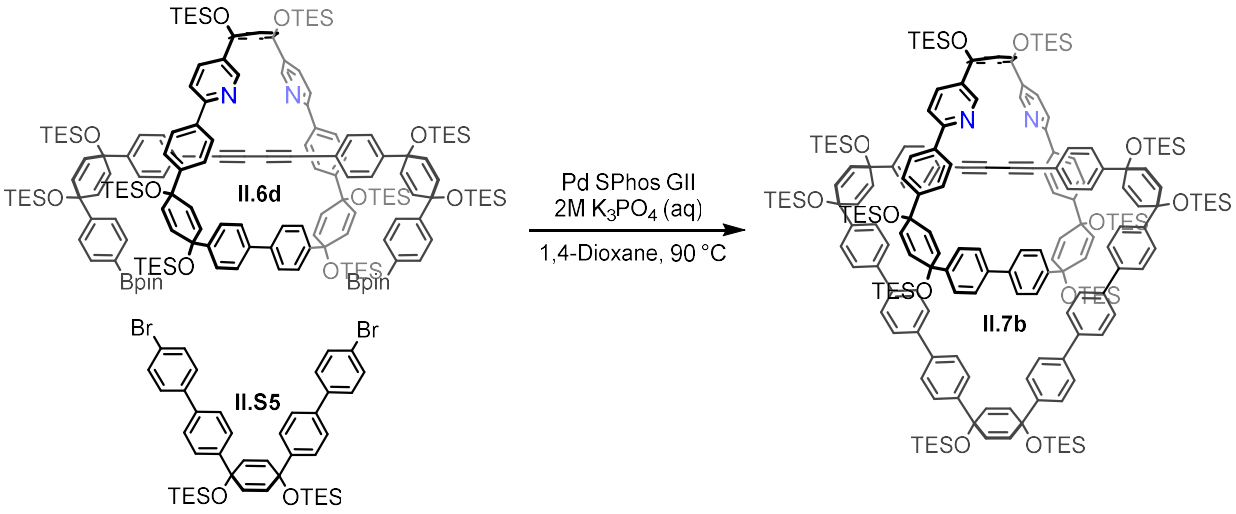

Synthesis of II.7b. To a 100 mL round bottom flask were added **II.6d** (0.094 g, 0.03 mmol), **II.S5** (0.027 g, 0.03 mmol) and Pd SPhos GII (0.006 g, 0.009 mmol). The flask was evacuated and backfilled with N_2 gas five times before introducing 1,4-dioxane (60 mL). The resulting mixture was heated to 90 °C with stirring at which point an aqueous solution of K_3PO_4 (2M, 2 mL) was added. After 1.5 h a small aliquot (0.2 mL) was removed from the reaction mixture, concentrated, and analyzed via ^{1}H NMR which showed total consumption of starting materials. The solvent was removed under reduced pressure and the crude residue was transferred into a separatory funnel with the aid of H_2O (50 mL) and DCM (20 mL). The organic layer was collected, and the aqueous layer was extracted with an additional 10 mL fresh DCM. The organic layers were combined and dried over Na_2SO_4. The product was purified via column chromatography (SiO_2, 0-40 % DCM in hexanes) providing **II.7b** as an off-white solid (0.054 g, 50%).

*Product isolated from the column is sufficiently pure to be used in subsequent steps. Purity is marginally improved by washing with acetone at the cost of significant loss of product to the

filtrate. This step was only performed on small scale in order to acquire an analytically pure sample for characterization.

^{1}H NMR (500 MHz, Chloroform-*d*) δ 8.89 (d, *J* = 2.4 Hz, 2H), 8.05 (d, *J* = 8.2 Hz, 4H), 7.74 (d, *J* = 8.3 Hz, 2H), 7.69 – 7.64 (m, 8H), 7.61 – 7.55 (m, 12H), 7.48 (d, *J* = 8.1 Hz, 4H), 7.43 – 7.37 (m, 8H), 7.33 (d, *J* = 8.1 Hz, 4H), 7.24 – 7.21 (m, 2H), 7.02 (d, *J* = 8.1 Hz, 4H), 6.63 (d, *J* = 8.1 Hz, 4H), 6.08 – 6.03 (m, 8H), 5.96 (s, 4H), 5.93 (d, *J* = 10.0 Hz, 4H), 5.90 – 5.85 (m, 8H), 0.98 – 0.87 (m, 108H), 0.67 – 0.54 (m, 72H). ^{13}C NMR (126 MHz, Chloroform-*d*) δ 155.57, 147.71, 146.98, 146.88, 145.31, 144.93, 144.89, 139.62, 139.45, 139.35, 139.19, 137.56, 133.61, 132.23, 131.75, 131.59, 131.49, 131.40, 131.17, 130.97, 127.36, 127.34, 126.79, 126.76, 126.73, 126.29, 126.25, 126.12, 126.07, 125.42, 119.86, 119.57, 82.31, 74.46, 71.60, 71.52, 71.46, 71.43, 71.26, 70.59, 7.11, 7.07, 7.05, 6.98, 6.69, 6.52, 6.50, 6.49, 6.46, 6.44, 6.22. MS (MALDI–TOF) [M]+ calculated for $C_{194}H_{258}N_2O_{12}Si_{12}$, 3143.6871; found, 3143.9.

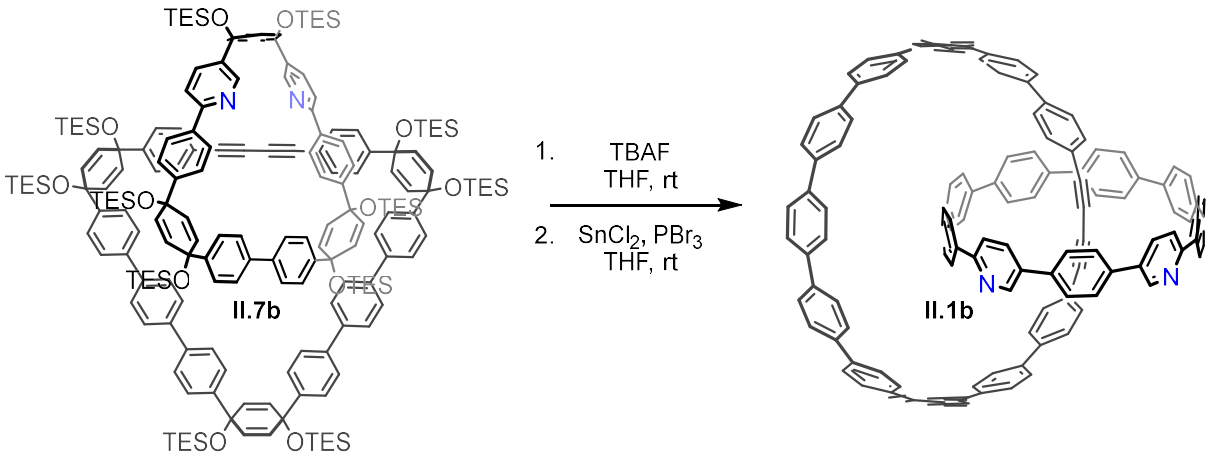

Synthesis of II.1b. To a flame died 100 mL round bottom flask was added **II.7b** (0.178 g, 0.06 mmol). The flask was evacuated and backfilled with N_2 gas three times before dissolving in THF (50 mL). TBAF (1.13 mL, 1.13 mmol, 1M in THF) was added and the reaction was stirred

for 1 h at room temperature. The solvent was removed under reduced pressure and the resulting yellow-brown oil was triturated with 5 mL H_2O until a filterable solid had formed. The precipitate was collected by vacuum filtration and washed with H_2O (10 mL) and DCM (10 mL). The desilylated material was rigorously dried under vacuum before transferring into a separate flame-dried 100 mL round bottom flask. The flask was evacuated and backfilled with N_2 gas three times before adding THF (50 mL). $SnCl_2$ (3.68 mL, 0.68 mmol, 0.18M in THF) was added and the mixture was stirred until the starting material had dissolved. PBr_3 (1.07 mL, 0.68 mmol, 0.18M in THF) was then introduced via slow, dropwise addition and the resulting solution was stirred in the exclusion of light for 30 minutes before quenching the with sat'd $NaHCO_3$ (20 mL). THF was removed under reduced pressure and the remaining aqueous suspension was extracted with DCM (3 x 10 mL). The organic layers were combined and dried over Na_2SO_4. The product was purified via preparatory TLC (alumina, 60% DCM in hexanes) to furnish **II.1b** as a yellow solid (0.011 g, 12%). ^{1}H NMR (600 MHz, Methylene Chloride-d_2) δ 8.54 (d, J = 2.4 Hz, 2H), 7.78 (d, J = 8.3 Hz, 4H), 7.59 (dd, J = 8.6, 2.4 Hz, 2H), 7.45 – 7.40 (m, 32H), 7.38 – 7.36 (m, 6H), 7.35 – 7.32 (m, 8H), 7.29 (s, 8H), 7.27 – 7.25 (m, 8H), 7.21 (d, J = 8.4 Hz, 4H), 7.17 (d, J = 8.3 Hz, 4H). ^{13}C NMR (151 MHz, Methylene Chloride-d_2 δ 154.71, 147.35, 141.16, 139.73, 139.52, 139.07, 138.90, 138.79, 138.75, 138.73, 138.70, 138.31, 138.24, 138.17, 137.93, 137.40, 135.85, 133.31, 132.50, 131.12, 128.35, 127.84, 127.78, 127.76, 127.67, 127.64, 127.63, 127.41, 127.08, 121.30, 119.58, 91.06, 79.40. HRMS (ESI–TOF) [M+1]+ calculated for $C_{122}H_{79}N_2$, 1571.6243; found, 1571.6240.

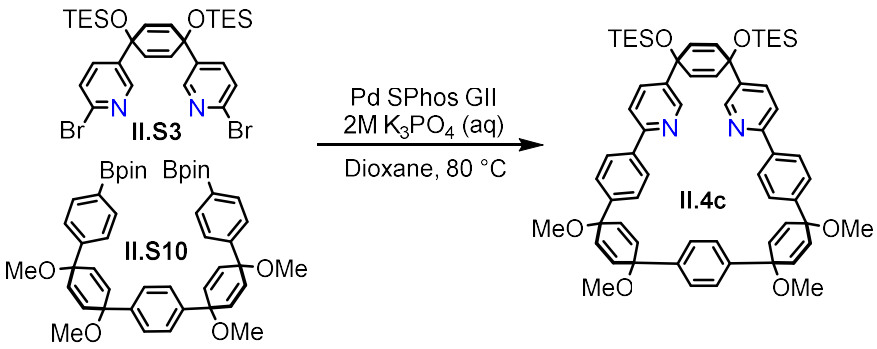

Synthesis of II.4c. To a 500 mL round bottom flask were added **II.S3** (0.562 g, 0.86 mmol), **II.S10** (0.785 g, 1.03 mmol) and Pd SPhos GII (0.031 g, 0.04 mmol). The flask was evacuated and backfilled with N_2 gas five times before introducing 1,4-dioxane (250 mL). The resulting mixture was heated to 80 °C with stirring at which point an aqueous solution of K_3PO_4 (2M, 10 mL) was added. After 1.5 h a small aliquot (0.2 mL) was removed from the reaction mixture, concentrated, and analyzed via ^{1}H NMR which showed total consumption of starting materials. The reaction was removed from heat and the solvent was removed under reduced pressure. The crude residue was transferred into a separatory funnel with the aid of H_2O (50 mL) and DCM (20 mL). The organic layer was collected, and the aqueous layer was extracted with an additional 10 mL fresh DCM. The organic layers were combined and dried over Na_2SO_4. The product was purified via column chromatography (SiO_2, 0-60% DCM in hexanes to elute impurities, followed by a secondary gradient of 0-10% EtOAc in hexanes to elute the product) giving **II.4c** as a white solid. (0.549 g, 63%). mp: (decomp. 261 °C); ^{1}H NMR (500 MHz, Chloroform-*d*) δ 8.37 (d, *J* = 2.4 Hz, 2H), 7.92 (d, *J* = 8.4 Hz, 4H), 7.53 – 7.46 (m, 10H), 7.34 – 7.32 (m, 2H), 6.15 – 6.11 (m, 8H), 6.05 (d, *J* = 10.2 Hz, 4H), 3.48 (s, 6H), 3.41 (s, 6H), 0.98 (t, *J* = 7.9 Hz, 18H), 0.67 (q, *J* = 8.0 Hz, 12H).^{13}C NMR (126 MHz, $CDCl_3$) δ 155.89, 147.81, 144.47, 143.30, 138.09, 137.73, 134.39, 133.38, 132.89, 131.99, 126.84, 126.24, 126.20, 119.46, 74.68,

74.11, 71.21, 52.11, 51.85, 7.01, 6.45. HRMS (ASAP) (m/z): [M]+ calculated for $C_{62}H_{72}N_2O_6Si_2$, 996.4929; found, 996.4715.

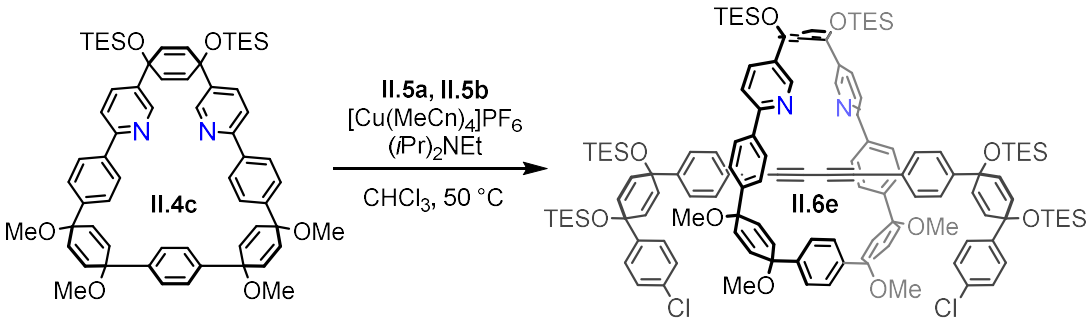

Synthesis of II.6e. To a flame-dried 100 mL round bottom flask were added, **II.4c** (0.455 g, 0.46 mmol), **II.5a** (0.629 g, 1.14 mmol), **II.5b**, (0.719 g, 1.14 mmol), and $[Cu(MeCN)_4]PF_6$ (161 mg, 0.43 mmol). The flask was evacuated and backfilled with N_2 gas five times before adding $CHCl_3$ (40 mL). The mixture was sonicated while sparging with N_2 until $[Cu(MeCN)_4]PF_6$ had completely dissolved (typically 5-10 minutes). The resulting solution was heated to 50 °C and DIPEA (0.24 mL, 0.32 mmol) was added. The reaction was then stirred at 50 °C for 3 h at which point the reaction mixture was transferred into a separatory funnel along with an aqueous NH_3-EDTA solution (20 mL). The mixture was emulsified and allowed to separate twice before collecting the organic layer. The aqueous layer was extracted with an additional 10 mL fresh DCM and the organic layers were combined and dried over Na_2SO_4. The product was purified via column chromatography (SiO_2, 0-100% DCM in hexanes) to afford **II.6e** as an off-white solid (0.618 g, 65% yield). ^{1}H NMR (500 MHz, Chloroform-*d*) δ 8.79 (d, *J* = 2.4 Hz, 2H), 7.90 (d, *J* = 8.1 Hz, 4H), 7.45 (s, 4H), 7.44 – 7.38 (m, 6H), 7.30 (d, *J* = 8.6 Hz, 4H), 7.25 (d, *J* = 8.6 Hz, 4H), 7.05 (d, *J* = 8.0 Hz, 4H), 7.02 (dd, *J* = 8.4, 2.4 Hz, 2H), 6.66 (d, *J* = 8.0 Hz, 4H), 6.17 (s, 4H), 6.01 – 5.95 (m, 8H), 5.92 (d, *J* = 9.9 Hz, 4H), 5.84 (d, *J* = 10.0 Hz, 4H), 3.38 (d, 12H), 1.01 – 0.89 (m, 54H),

0.70 – 0.56 (m, 36H). ^{13}C NMR (126 MHz, Chloroform-*d*) δ 155.77, 148.27, 146.58, 144.49, 144.04, 142.83, 137.90, 137.48, 133.84, 133.26, 133.02, 132.72, 132.19, 132.00, 131.49, 131.28, 128.40, 127.47, 127.26, 126.20, 126.14, 125.27, 120.57, 119.59, 81.75, 75.48, 74.17, 74.14, 71.26, 71.08, 70.97, 52.00, 51.72, 7.08, 7.02, 6.47, 6.46, 6.43. MS (MALDI–TOF) [M]+ calculated for $C_{126}H_{156}Cl_2N_2O_{10}Si_6$, 2094.9753; found, 2094.4.

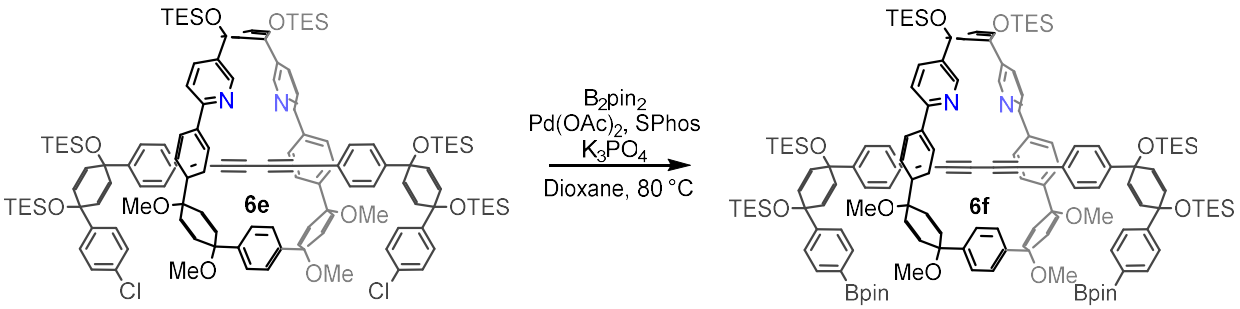

Synthesis of II.6f. To a flame dried 25 mL round bottom flask were added **II.6e** (0.350 g, 0.167 mmol)**,** B_2pin_2 (0.254 g, 1.00 mmol), $Pd(OAc)_2$ (0.009 g, 0.04 mmol), SPhos (0.034 g, 0.08 mmol), and K_3PO_4 (0.283 g, 1.33 mmol). The flask was evacuated and backfilled with N_2 gas five times before introducing 1,4-dioxane (5 mL). The mixture was stirred at 80 °C for 1 h. The solvent was then removed under reduced pressure and the crude material was run through a short silica plug using DCM as eluent. The eluate was concentrated under reduced pressure and the resulting residue was sonicated with MeOH (10 mL) until a flocculent precipitate had formed. The precipitate was collected by vacuum filtration and washed with MeOH (20 mL) to give **II.6f** as a tan colored solid (0.364 g, 96%). ^{1}H NMR (600 MHz, Chloroform-*d*) δ 8.81 (d, *J* = 2.4 Hz, 2H), 7.95 (d, *J* = 8.4 Hz, 4H), 7.82 (d, *J* = 8.0 Hz, 4H), 7.48 – 7.44 (m, 10H), 7.39 (d, *J* = 8.1 Hz, 4H), 7.09 (d, *J* = 8.3 Hz, 4H), 7.04 (dd, *J* = 8.4, 2.4 Hz, 2H), 6.62 (d, *J* = 8.4 Hz, 4H), 6.19 (s, 4H), 6.05 (d, *J* = 10.1 Hz, 4H), 6.00 (d, *J* = 10.3 Hz, 4H), 5.91 (d, *J* = 10.1 Hz, 4H), 5.87 (d, *J* = 10.2 Hz,

4H), 3.39 (d, J = 5.8 Hz, 12H), 1.37 (s, 24H), 1.02 – 0.98 (m, 36H), 0.94 (t, J = 7.9 Hz, 18H), 0.68 – 0.62 (m, 26H), 0.61 – 0.57 (m, 12H). ^{13}C NMR (126 MHz, Chloroform-*d*) δ 155.85, 148.99, 148.11, 146.72, 144.02, 142.75, 137.78, 137.47, 134.84, 133.92, 132.95, 132.72, 132.13, 131.95, 131.61, 131.07, 127.46, 126.25, 126.20, 125.23, 125.13, 120.42, 119.69, 83.80, 83.51, 81.78, 75.40, 74.18, 74.12, 71.28, 71.06, 51.99, 51.69, 25.03, 24.90, 24.60, 7.11, 7.04, 7.01, 6.46, 6.44. MS (MALDI–TOF) [M]+ calculated for $C_{138}H_{180}B_2N_2O_{14}Si_6$, 2279.2236; found, 2279.6.

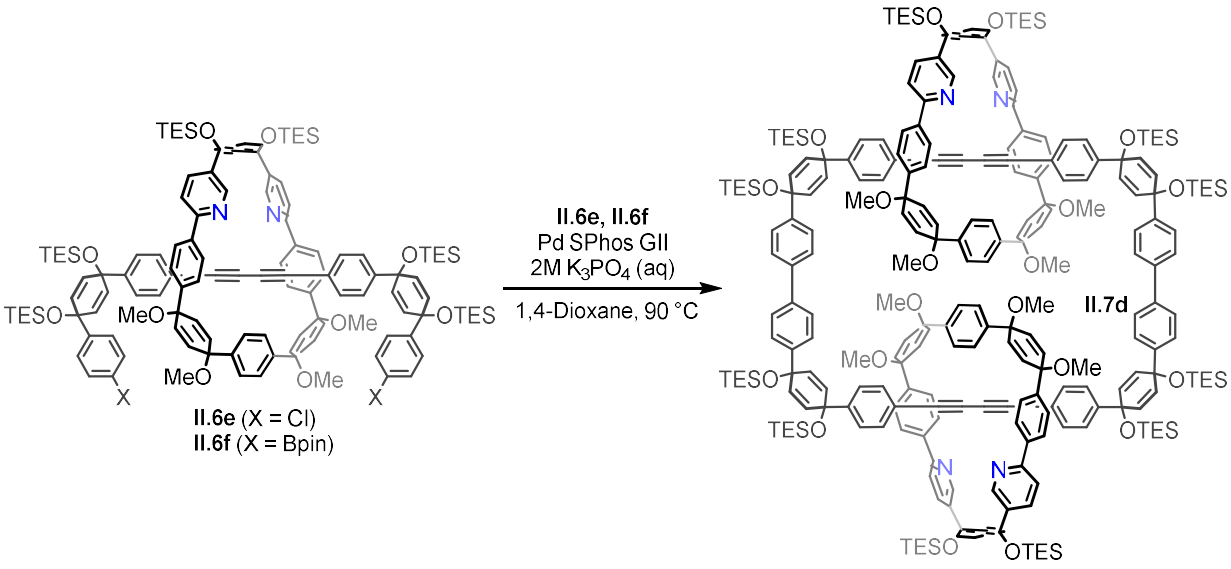

Synthesis of II.7d. To a 250 mL round bottom flask were added **II.6e** (0.275 g, 0.13 mmol), **II.6f** (0.300 g, 0.13 mmol) and Pd SPhos GII (0.009 g, 0.013mmol). The flask was evacuated and backfilled with N_2 gas five times before introducing 1,4-dioxane (150 mL). The resulting mixture was heated to 90 °C with stirring at which point an aqueous solution of K_3PO_4 (2M, 3 mL) was added. After 2 h a small aliquot (0.2 mL) was removed from the reaction mixture, concentrated, and analyzed via ^{1}H NMR which showed total consumption of starting materials. The solvent was removed under reduced pressure and the crude residue was transferred into a

separatory funnel with the aid of 50 mL H_2O and 20 mL DCM. The organic layer was collected, and the aqueous layer was extracted with an additional 10 mL fresh DCM. The organic layers were combined and dried over Na_2SO_4. The product was purified via column chromatography (SiO_2, 0-100% DCM in hexanes) providing **II.7d** as a tan colored solid (0.209 g, 39%). ^{1}H NMR (500 MHz, Chloroform-*d*) δ 8.74 (d, *J* = 2.4 Hz, 4H), 7.86 (d, *J* = 8.1 Hz, 8H), 7.53 (d, *J* = 8.1 Hz, 8H), 7.39 (d, *J* = 8.2 Hz, 12H), 7.34 – 7.30 (m, 16H), 7.08 (d, *J* = 8.0 Hz, 8H), 7.01 (dd, *J* = 8.2, 2.4 Hz, 4H), 6.56 (d, *J* = 8.0 Hz, 8H), 6.12 (s, 8H), 6.05 (d, *J* = 9.8 Hz, 8H), 5.90 (d, *J* = 9.9 Hz, 8H), 5.81 (d, *J* = 10.0 Hz, 8H), 3.21 (s, 12H), 3.16 (s, 12H), 1.01 – 0.91 (m, 108H), 0.68 – 0.58 (m, 72H). ^{13}C NMR (126 MHz, Chloroform-*d*) δ 155.74, 148.14, 146.80, 145.07, 144.00, 142.78, 139.46, 137.87, 137.44, 133.75, 132.76, 132.59, 132.24, 131.91, 131.66, 131.02, 127.41, 126.75, 126.22, 126.16, 125.16, 120.37, 119.63, 81.72, 75.34, 74.07, 74.05, 71.34, 71.04, 71.01, 51.83, 51.50, 7.14, 7.04, 6.99, 6.49, 6.45. MS (MALDI–TOF) [M]+ calculated for $C_{252}H_{312}N_4O_{20}Si_{12}$, 4050.0751; found, 4049.7.

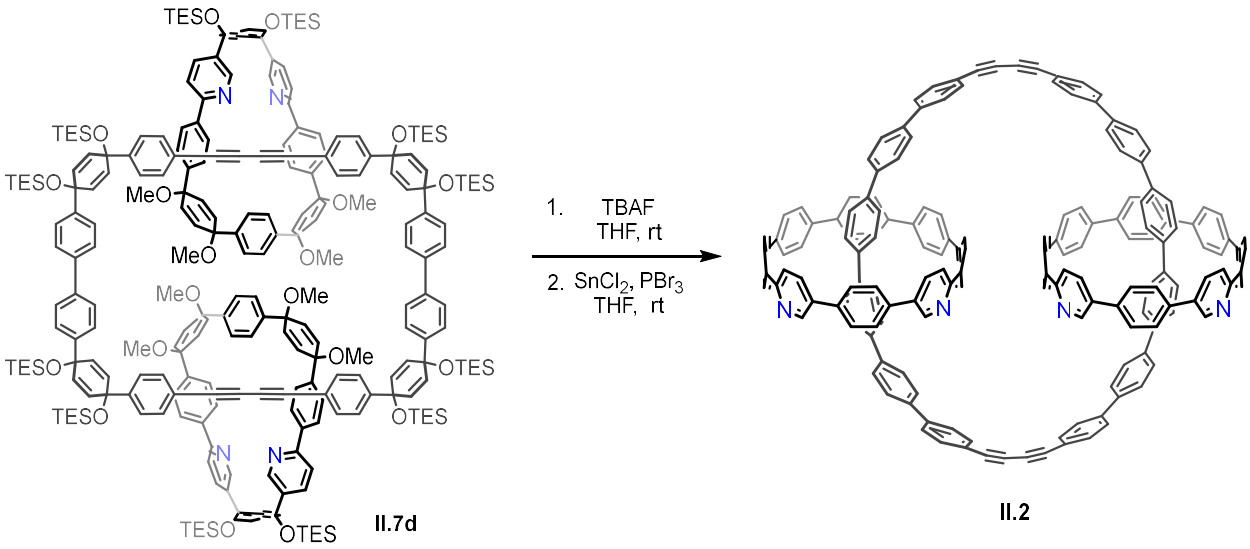

Synthesis of II.2. To a flame died 100 mL round bottom flask was added **II.7d** (0.209 g, 0.05 mmol). The flask was evacuated and backfilled with N_2 gas three times before dissolving in THF (50 mL). TBAF (0.72 mL, 0.72 mmol, 1M in THF) was added and the reaction was stirred for 1 h at room temperature. The solvent was removed under reduced pressure and the resulting yellow oil was triturated with 5 mL H_2O until a filterable solid had formed. The precipitate was collected by vacuum filtration and washed with H_2O (10 mL) and DCM (10 mL) to provide a tan colored solid. The desilylated material was rigorously dried under vacuum before transferring into a separate flame-dried 250 mL round bottom flask. The flask was evacuated and backfilled with N_2 gas three times before adding THF (100 mL). $SnCl_2$ (4.60 mL, 0.82 mmol, 0.18M in THF was added and the mixture was stirred until the starting material had dissolved. PBr_3 (1.15 mL, 0.82 mmol, 0.72 M in THF) was then introduced via slow, dropwise addition and the resulting solution was stirred in the exclusion of light for 30 minutes before quenching the with saturated sodium bicarbonate (20 mL). THF was removed under reduced pressure and the remaining aqueous suspension was extracted with DCM (3 x 15 mL). The organic layers were combined and dried over Na_2SO_4. The product was purified via preparatory TLC (alumina, 60% DCM in hexanes) to

furnish **II.2** as a yellow solid (7 mg, 6%). ^{1}H NMR (600 MHz, Methylene Chloride-d_2) δ 8.65 – 8.61 (m, 4H), 7.82 (s, 8H), 7.66 (dd, 4H), 7.48 (d, J = 8.7 Hz, 4H), 7.42 (d, J = 8.6 Hz, 8H), 7.38 – 7.30 (m, 48H), 7.24 (d, J = 7.9 Hz, 8H), 7.09 – 6.97 (m, 24H). ^{13}C NMR (151 MHz, CD_2Cl_2) δ 154.62, 147.20, 141.05, 139.42, 139.30, 139.05, 138.89, 138.37, 138.16, 137.94, 137.38, 137.32, 135.40, 133.07, 132.46, 130.39, 128.67, 127.90, 127.77, 127.52, 127.46, 127.44, 126.97, 121.20, 119.52, 90.40, 79.02. MS (MALDI–TOF) [M]+ calculated for $C_{172}H_{108}N_4$, 2228.9; found, 2229.1.

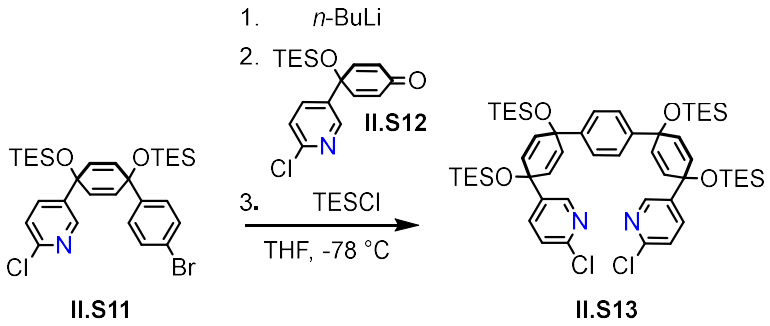

Synthesis of II.S13. To a flame-dried 100 mL round bottom flask was added **II.S11** (4.32 g, 7.11 mmol). The flask was evacuated and backfilled with N_2 gas three times before introducing THF (30 mL). To a separate flame-dried 50 mL round bottom flask was added **II.S12** (2.39 g, 7.11 mmol). Likewise, this flask was evacuated and backfilled with N_2 gas three times before introducing THF (10 mL). Both solutions were cooled to –78 °C and *n*-BuLi (2.85 mL, 7.11 mmol, 2.5 M in hexanes) was added via slow dropwise addition to the flask containing **II.S11**. The mixture was stirred for 20 minutes before canulating the solution of **II.S12** into the lithiate. The reaction was stirred at –78 °C for 1 h after which TESCl (1.43 mL, 8.54 mmol) was added. The reaction was then allowed to warm to room temperature over the course of 1.5 h. The reaction mixture was transferred into a separatory funnel along with EtOAc (10 mL) and washed with sat'd $NaHCO_3$ (50 mL), H_2O (20 mL) and brine (20 mL). The organic layer was collected and dried

over Na_2SO_4 before concentrating under reduced pressure. The resulting crude oil was triturated with 50 mL EtOH to produce light-colored precipitate. The precipitate was collected via vacuum filtration and washed with EtOH (20 mL) to provide **II.S13** as a white solid (5.21 g, 75%). mp: 97 - 98 °C; ^{1}H NMR (500 MHz, Chloroform-*d*) δ 8.34 (d, *J* = 2.5 Hz, 2H), 7.47 (dd, *J* = 8.3, 2.5 Hz, 2H), 7.28 (s, 4H), 7.23 (d, *J* = 8.4 Hz, 2H), 6.10 (d, *J* = 10.1 Hz, 4H), 5.89 (d, *J* = 10.1 Hz, 4H), 0.96 (t, *J* = 8.0 Hz, 18H), 0.90 (t, *J* = 7.9 Hz, 20H), 0.66 (q, *J* = 7.9 Hz, 12H), 0.54 (q, *J* = 7.9 Hz, 12H). ^{13}C NMR (126 MHz, Chloroform-*d*) δ 150.20, 147.80, 144.97, 140.56, 136.41, 132.34, 130.47, 125.84, 123.56, 70.85, 70.12, 7.01, 7.00, 6.45, 6.35. HRMS (ASAP) (m/z): [M]+ calculated for $C_{52}H_{78}N_2O_4Si_4$, 976.4416; found, 976.4077.

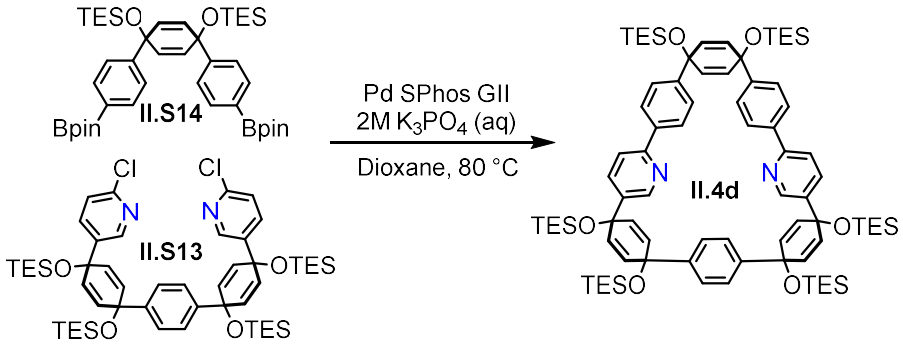

Synthesis of II.4d. To a 500 mL round bottom flask were added **II.S14** (0.562 g, 0.75 mmol), **II.S13** (0.738 g, 0.75 mmol) and Pd SPhos GII (0.054 g, 0.075 mmol). The flask was evacuated and backfilled with N_2 gas five times before introducing 1,4-dioxane (200 mL). The resulting mixture was heated to 80 °C with stirring at which point an aqueous solution of K_3PO_4 (2M, 10 mL) was added. After 1.5 h a small aliquot (0.2 mL) was removed from the reaction mixture, concentrated, and analyzed via ^{1}H NMR which showed total consumption of starting materials. The reaction was removed from heat and the solvent was removed under reduced

pressure. The crude residue was transferred into a separatory funnel with the aid of H_2O (50 mL) and DCM (20 mL). The organic layer was collected, and the aqueous layer was extracted with an additional 10 mL fresh DCM. The organic layers were combined and dried over Na_2SO_4 before evaporating the DCM under reduced pressure. The crude material was then chromatographed (SiO_2, 0-80% DCM in hexanes). The product containing fractions were combined and evaporated under reduced pressure. The resulting residue was triturated with 5 mL acetone to produce a solid precipitate. The precipitate was collected via vacuum filtration to provide **II.4d** as a white solid (0.316 g, 30%). mp: (decomp. 279 °C); ^{1}H NMR (500 MHz, Chloroform-*d*) δ 8.73 (d, *J* = 2.2 Hz, 1H), 7.72 (d, *J* = 8.0 Hz, 2H), 7.60 (dd, *J* = 8.4, 2.1 Hz, 1H), 7.54 (d, *J* = 8.3 Hz, 1H), 7.47 (s, 2H), 7.11 (d, *J* = 8.1 Hz, 2H), 6.14 – 6.05 (m, 4H), 5.92 (d, *J* = 9.7 Hz, 2H), 1.02 – 0.90 (m, 27H), 0.70 (q, *J* = 7.9 Hz, 6H), 0.64 (q, *J* = 7.9 Hz, 6H), 0.54 (q, *J* = 8.0 Hz, 6H). ^{13}C NMR (126 MHz, $CDCl_3$) δ 155.85, 147.45, 145.76, 144.78, 139.86, 138.02, 134.22, 132.04, 131.67, 131.20, 126.85, 126.34, 125.94, 119.76, 72.49, 70.54, 70.22, 7.10, 7.05, 6.52, 6.50, 6.37. HRMS (ASAP) (m/z): [M]+ calculated for $C_{82}H_{120}N_2O_6Si_6$, 1396.7762; found, 1396.7250.

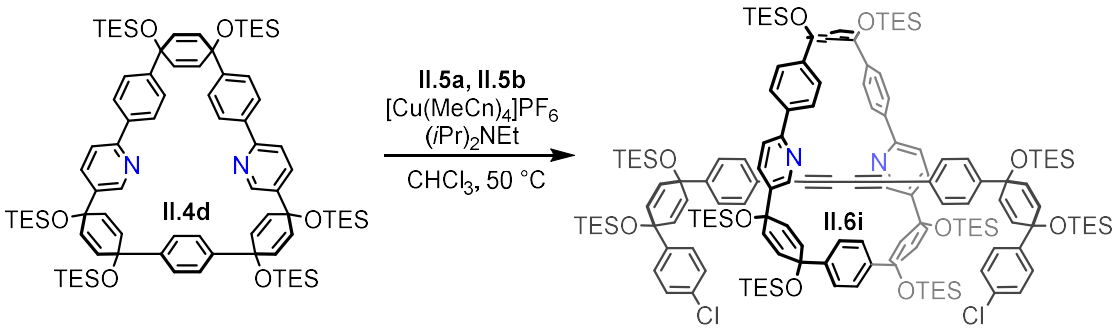

Synthesis of II.6i. To a flame-dried 100 mL round bottom flask were added, **II.4d** (0.150 g, 0.11 mmol), **II. 5a** (0.149 g, 0.27 mmol), **II.5b**, (0.169 g, 0.27 mmol), and $[Cu(MeCN)_4]PF_6$ (0.038 g, 0.04 mmol). The flask was evacuated and backfilled with N_2 gas five times before adding

$CHCl_3$ (15 mL). The mixture was sonicated while sparging with N_2 until $[Cu(MeCN)_4]PF_6$ had completely dissolved (typically 5-10 minutes). The resulting solution was heated to 50 °C and DIPEA (0.24 mL, 0.32 mmol) was added. The reaction was then stirred at 50 °C for 3 h at which point the reaction mixture was transferred into a separatory funnel along with NH_3-EDTA (20 mL). The mixture was emulsified and allowed to separate twice before collecting the organic layer. The aqueous layer was extracted with an additional 10 mL fresh DCM and the organic layers were combined and dried over Na_2SO_4. The was purified via column chromatography (SiO_2, 0-40% DCM in hexanes) to afford **II.6i** as an off-white solid (0.221 g, 82% yield). ^{1}H NMR (500 MHz, Chloroform-*d*) δ 8.72 (d, *J* = 1.8 Hz, 2H), 7.83 (d, *J* = 8.0 Hz, 4H), 7.48 (s, 4H), 7.35 (s, 4H), 7.29 – 7.23 (m, 8H), 7.19 (d, *J* = 8.1 Hz, 4H), 7.08 (d, *J* = 8.4 Hz, 4H), 6.68 (d, *J* = 7.9 Hz, 4H), 6.12 (s, 4H), 5.97 (d, *J* = 10.5 Hz, 4H), 5.92 (d, *J* = 10.5 Hz, 4H), 5.84 (d, *J* = 10.4 Hz, 4H), 5.77 (d, *J* = 9.8 Hz, 4H), 1.06 – 0.88 (m, 72H), 0.85 (t, *J* = 7.9 Hz, 18H), 0.71 – 0.54 (m, 48H), 0.50 (q, *J* = 7.9 Hz, 12H). ^{13}C NMR (126 MHz, $CDCl_3$) δ 155.68, 147.84, 146.57, 144.96, 144.93, 144.44, 139.77, 138.36, 133.28, 133.24, 132.25, 131.98, 131.47, 131.32, 130.27, 128.40, 127.27, 126.75, 126.55, 125.71, 125.38, 120.47, 120.44, 81.56, 75.13, 72.25, 71.32, 71.03, 70.76, 69.54, 7.11, 7.08, 7.06, 7.02, 6.99, 6.53, 6.50, 6.47, 6.44, 6.38. HRMS (ESI–TOF) [M+1]+ calculated for $C_{146}H_{205}Cl_2N_2O_{10}Si_{10}$, 2496.2664; found, 2495.2742.

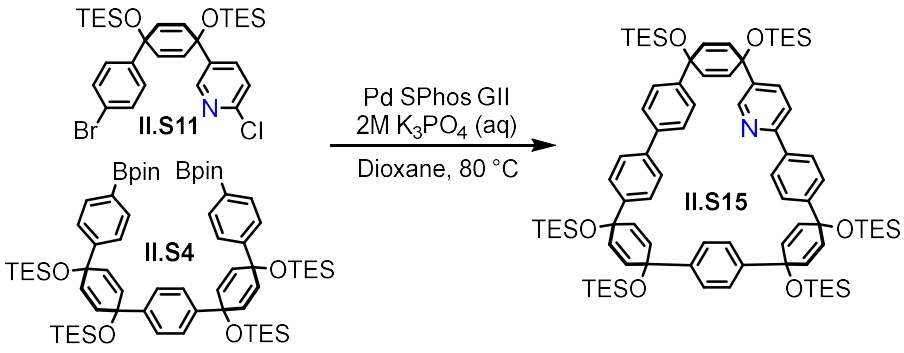

Synthesis of II.S15. To a 500 mL round bottom flask were added **II.S11** (0.530 g, 0.86 mmol), **II.S4** (1.00 g, 0.87 mmol) and Pd SPhos GII (0.031 g, 0.04 mmol). The flask was evacuated and backfilled with N_2 gas five times before introducing 1,4-dioxane (250 mL). The resulting mixture was heated to 80 °C with stirring at which point an aqueous solution of K_3PO_4 (2M, 10 mL) was added. After 1.5 h a small aliquot (0.2 mL) was removed from the reaction mixture, concentrated, and analyzed via ^{1}H NMR which showed total consumption of starting materials. The reaction was removed from heat and the solvent was removed under reduced pressure. The crude residue was transferred into a separatory funnel with the aid of H_2O (50 mL) and DCM. The organic layer was collected, and the aqueous layer was extracted with an additional 10 mL fresh DCM (20 mL). The organic layers were combined and dried over Na_2SO_4 before running through a short silica plug using DCM as eluent. The eluate was evaporated under reduced pressure and the resulting oily solid was triturated with 10 mL 1:1 acetone:MeOH to produce a filterable solid precipitate. After chilling in an ice bath for 30 min, the precipitate was collected by vacuum filtration and washed with cold acetone (3 mL) and methanol (10 mL) to give **II.S15** as a white powder (1.02 g, 84%). mp: (decomp. 279 °C); ^{1}H NMR (500 MHz, Chloroform-*d*) δ 8.38 (d, *J* = 2.4 Hz, 1H), 7.87 (d, *J* = 8.4 Hz, 2H), 7.48 – 7.45 (m, 8H), 7.43 – 7.39 (m, 3H), 7.35 (d, *J* = 8.3 Hz, 2H), 7.24 (dd, J =8.3, 2.3 Hz, 1H), 7.08 (d, *J* = 8.3 Hz, 2H), 6.16 (d, *J* = 9.9 Hz, 2H), 6.09 – 6.02 (m, 6H), 5.92 (d, *J* = 10.1 Hz, 4H), 1.01 – 0.91 (m, 54H), 0.73 – 0.63 (m, 24H), 0.55 (q, *J* = 7.9 Hz, 12H). ^{13}C NMR (126 MHz, Chloroform-*d*) δ 155.71, 148.18, 147.11, 145.90, 145.39, 142.71, 139.88, 139.32, 137.91, 134.65, 132.86, 131.87, 131.76, 131.26, 131.15, 131.03, 126.73, 126.60, 126.58, 126.01, 125.98, 125.88, 119.16, 72.33, 71.45, 71.27, 71.24, 70.77, 70.71, 7.12, 7.04, 6.53, 6.48, 6.43, 6.41. HRMS (ASAP) (m/z): [M]+ calculated for $C_{83}H_{121}N_1O_6Si_6$, 1395.7809; found, 1395.8252.

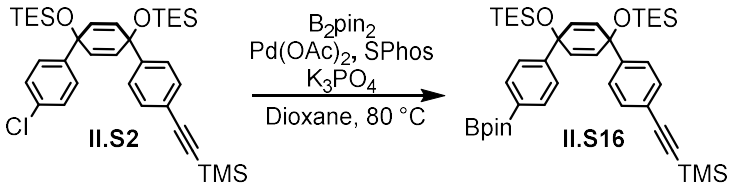

Synthesis of II.S16. To a flame-dried 25 mL round bottom flask were added **II.S2** (3.60 g, 5.77 mmol)**,** B_2pin_2 (2.93 g, 11.55 mmol), $Pd(OAc)_2$ (0.065 g, 0.29 mmol), SPhos (0.237 g, 0.58 mmol), and K_3PO_4 (6.12 g, 28.87 mmol). The flask was evacuated and backfilled with N_2 gas five times before introducing 1,4-dioxane (10 mL). The mixture was stirred at 80 °C for 1 h. The solvent was then removed under reduced pressure and the crude material was run through a short silica plug using DCM as eluent. The eluate was concentrated under reduced pressure and the resulting residue was sonicated with MeOH (30 mL) until a flocculent precipitate had formed. The precipitate was collected by vacuum filtration and washed with MeOH (20 mL) to give **II.S16** as a tan colored solid (3.92 g, 91%). mp: (decomp. 131 °C); ^{1}H NMR (500 MHz, Chloroform-*d*) δ 7.70 (d, *J* = 8.3 Hz, 2H), 7.35 (d, *J* = 8.6 Hz, 2H), 7.30 (d, *J* = 8.4 Hz, 2H), 7.25 (d, *J* = 8.5 Hz, 2H), 5.97 (d, *J* = 9.9 Hz, 2H), 5.94 (d, *J* = 10.2 Hz, 2H), 1.34 (s, 12H), 0.92 (t, *J* = 7.9 Hz, 18H), 0.59 (q, *J* = 7.9 Hz, 12H), 0.25 (s, 9H). ^{13}C NMR (126 MHz, Chloroform-*d*) δ 148.93, 146.41, 134.71, 131.82, 131.64, 131.14, 125.76, 125.14, 121.89, 105.13, 94.11, 83.75, 71.55, 71.37, 24.88, 7.03, 6.45, 6.43, 0.00. HRMS (ASAP) (m/z): [M]+ calculated for $C_{41}H_{63}BO_4Si_3$, 714.4127; found, 714.4250.

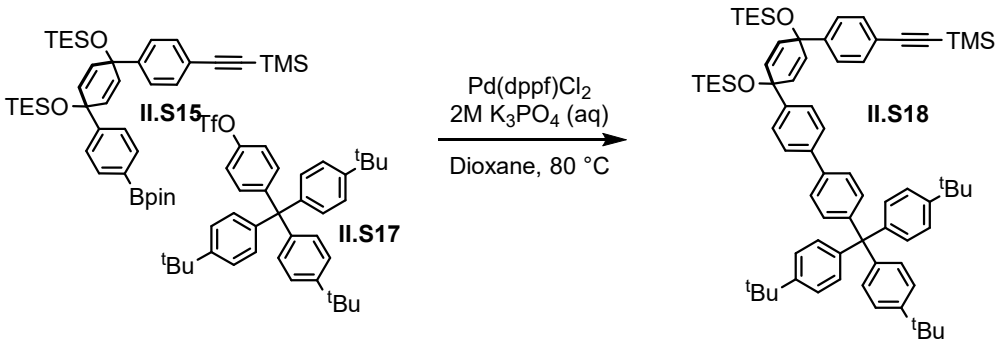

Synthesis of II.S18. To a 50 mL round bottom flask were added **II.S16** (0.800 g, 1.12 mmol), **II.S17** (0.713 g, 1.12 mmol) and Pd(dppf)Cl_2·DCM (0.040 gg, 0.06 mmol). The flask was evacuated and backfilled with N_2 gas five times before introducing 1,4-dioxane (10 mL) and an aqueous solution of K_3PO_4 (2M, 2 mL). The mixture was stirred at 80 °C for 16 h after which the solvent was removed under reduced pressure. The crude residue was then transferred into a separatory funnel with the aid of H_2O (20 mL) and DCM (10 mL). The organic layer was collected, and the aqueous layer was extracted with an additional 10 mL DCM. The organic layers were combined and dried over Na_2SO_4. Product was purified by column chromatography (SiO_2, 0-20% DCM in Hexanes) to provide **II.S18** as a white solid (1.10 g, 91%). mp: (decomp. 153 °C); ^{1}H NMR (500 MHz, Chloroform-*d*) δ 7.50 (d, *J* = 8.1 Hz, 2H), 7.46 (d, *J* = 8.3 Hz, 2H), 7.37 – 7.32 (m, 4H), 7.28 (d, *J* = 8.1 Hz, 2H), 7.25 – 7.24 (m, 8H), 7.13 (d, *J* = 8.4 Hz, 6H), 6.03 (d, *J* = 9.7 Hz, 2H), 5.96 (d, *J* = 10.0 Hz, 2H), 1.30 (s, 27H), 0.96 – 0.91 (m, 18H), 0.66 – 0.56 (m, 12H), 0.23 (s, 9H). ^{13}C NMR (126 MHz, $CDCl_3$) δ 148.41, 146.55, 146.47, 144.63, 143.88, 139.64, 137.72, 131.81, 131.64, 131.06, 130.82, 126.62, 126.20, 125.80, 125.66, 124.13, 121.91, 105.10, 94.08, 71.43, 71.34, 63.55, 34.31, 31.40, 7.07, 7.05, 6.47, 6.45, 0.00. HRMS (ASAP) (m/z): [M]+ calculated for $C_{72}H_{94}O_2Si_3$, 1074.6562; found, 1074.6365.

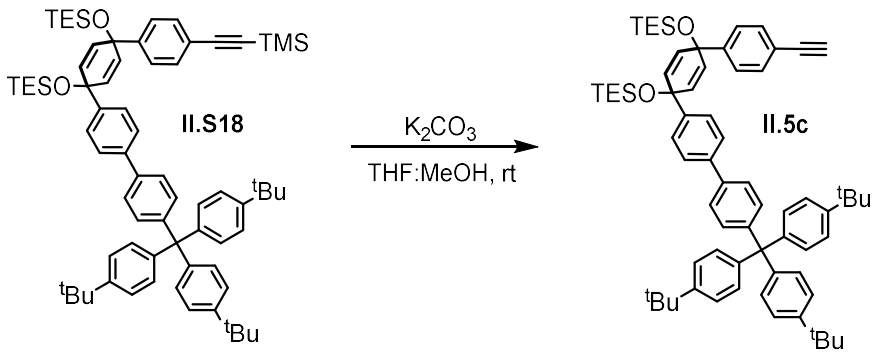

Synthesis of II.5c. To a 50 mL round bottom flask was added **II.S18** (1.10 g, 1.02 mmol. 10 mL THF was added, and the resulting solution was made to stir open to air. MeOH was then added, followed by K_2CO_3 (0.500 g, 3.62 mmol). The slurry was allowed to stir for 30 min, monitoring reaction progress by TLC. The solvent was removed under reduced pressure and the crude material was passed through a short silica plug using DCM as eluent. The eluate was evaporated under reduced pressure and the resulting residue was triturated with MeOH (20 mL) to produce a filterable precipitate. The precipitate was collected by vacuum filtration, washing with 10 mL MeOH, to provide the **II.5c** as a white solid (0.972 g, 95%). mp: 144 - 148 °C; ^{1}H NMR (500 MHz, Chloroform-*d*) δ 7.50 (d, *J* = 8.1 Hz, 2H), 7.44 (d, *J* = 8.2 Hz, 2H), 7.37 (d, *J* = 7.8 Hz, 4H), 7.30 (d, *J* = 8.1 Hz, 2H), 7.23 (d, *J* = 8.7 Hz, 8H), 7.13 (d, *J* = 8.3 Hz, 6H), 6.06 (d, *J* = 9.9 Hz, 2H), 5.96 (d, *J* = 9.8 Hz, 2H), 2.96 (s, 1H), 1.30 (s, 27H), 0.96 – 0.92 (m, *J* = 8.0, 5.1 Hz, 18H), 0.66 – 0.58 (m, 12H). ^{13}C NMR (126 MHz, Chloroform-*d*) δ 148.35, 146.74, 146.57, 144.56, 143.86, 139.67, 137.62, 131.93, 131.82, 131.64, 131.06, 131.00, 130.80, 126.60, 126.22, 125.84, 125.63, 124.10, 120.88, 83.56, 77.13, 71.43, 71.27, 63.53, 34.26, 31.38, 7.04, 6.47, 6.43. HRMS (ASAP) (m/z): [M]+ calculated for $C_{69}H_{86}O_2Si_2$, 1002.6166; found, 1002.6036.

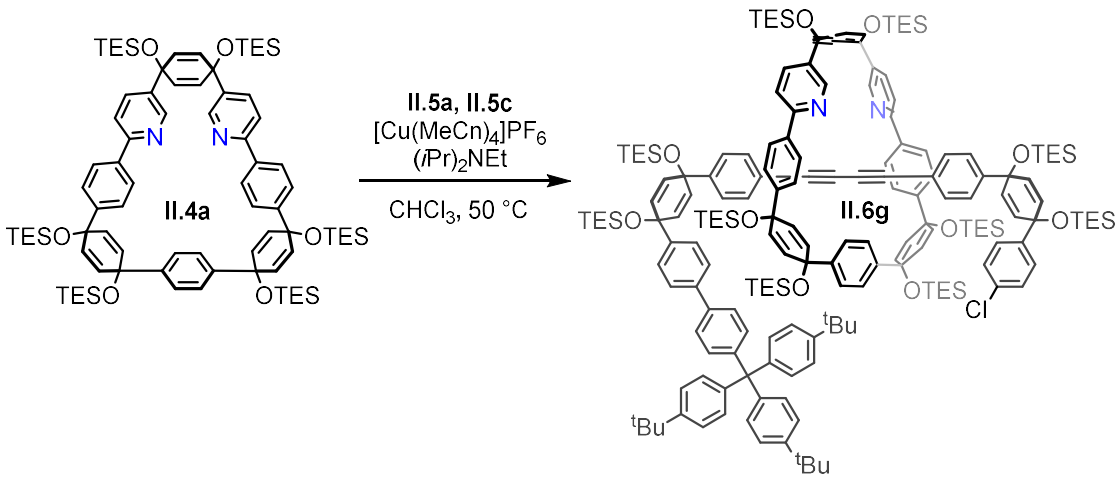

Synthesis of II.6g. To a flame-dried 100 mL round bottom flask were added, **II.4a** (0.600 g, 0.43 mmol), **II.5a** (1.100 g, 1.08 mmol), **II.5c**, (0.676 g, 1.08 mmol), and $[Cu(MeCN)_4]PF_6$ (0.152 g, 0.41 mmol). The flask was evacuated and backfilled with N_2 gas five times before adding $CHCl_3$ (40 mL). The mixture was sonicated while sparging with N_2 until $[Cu(MeCN)_4]PF_6$ had completely dissolved (typically 5-10 minutes). The resulting solution was heated to 50 °C and DIPEA (0.19 mL, 1.07 mmol) was added. The reaction was then stirred at 50 °C for 3 h at which point the reaction mixture was transferred into a separatory funnel along with an NH_3-EDTA solution (20 mL). The mixture was emulsified and allowed to separate twice before collecting the organic layer. The aqueous layer was extracted with an additional 10 mL fresh DCM and the organic layers were combined and dried over Na_2SO_4. The reaction products were separated via column chromatography (SiO_2, 0-40% DCM in hexanes) to afford **II.6g** as an off-white solid (0.712 g, 56% yield). ^{1}H NMR (500 MHz, Methylene Chloride-d_2) δ 8.67 (d, J = 2.4 Hz, 2H), 7.88 (d, J = 8.2 Hz, 4H), 7.59 (d, J = 8.1 Hz, 2H), 7.51 (d, J = 8.3 Hz, 2H), 7.46 – 7.40 (m, 8H), 7.39 – 7.34 (m, 6H), 7.31 – 7.26 (m, 10H), 7.23 (d, J = 8.3 Hz, 6H), 7.20 (d, J = 8.1 Hz, 2H), 7.16 (dd, J = 8.4, 2.4 Hz, 2H), 7.07 (d, J = 8.1 Hz, 2H), 6.77 (d, J = 8.2 Hz, 2H), 6.65 (d, J = 8.1 Hz, 2H), 6.24 – 6.19 (m, 4H), 6.09 (d, J = 10.0 Hz, 2H), 6.03 – 5.96 (m, 8H), 5.92 (dd, J = 10.2, 2.6 Hz,

2H), 5.80 (dd, J = 10.0, 2.6 Hz, 2H), 5.76 (dd, J = 10.1, 2.3 Hz, 2H), 1.31 (s, 27H), 1.03 – 0.94 (m, 72H), 0.86 (t, J = 8.0 Hz, 18H), 0.71 – 0.62 (m, 48H), 0.52 (q, J = 7.8 Hz, 12H). ^{13}C NMR (126 MHz, Methylene Chloride-d_2) δ 156.31, 149.06, 148.58, 147.57, 147.45, 147.06, 145.76, 145.69, 145.26, 144.83, 140.20, 138.53, 138.28, 137.93, 134.41, 133.65, 132.82, 132.79, 132.59, 132.40, 132.27, 132.12, 132.05, 131.98, 131.90, 131.68, 131.62, 131.04, 128.88, 127.96, 127.77, 127.31, 126.84, 126.57, 126.49, 126.33, 126.31, 125.94, 125.82, 124.97, 121.26, 121.18, 120.00, 82.24, 76.14, 75.92, 71.90, 71.82, 71.67, 71.64, 71.61, 71.45, 71.17, 64.22, 34.79, 31.68, 7.52, 7.50, 7.46, 7.43, 7.39, 7.03, 7.02, 7.00, 6.97, 6.94. MS (MALDI–TOF) [M]+ calculated for $C_{183}H_{247}ClN_2O_{10}Si_{10}$, 2947.6262; found, 2947.6.

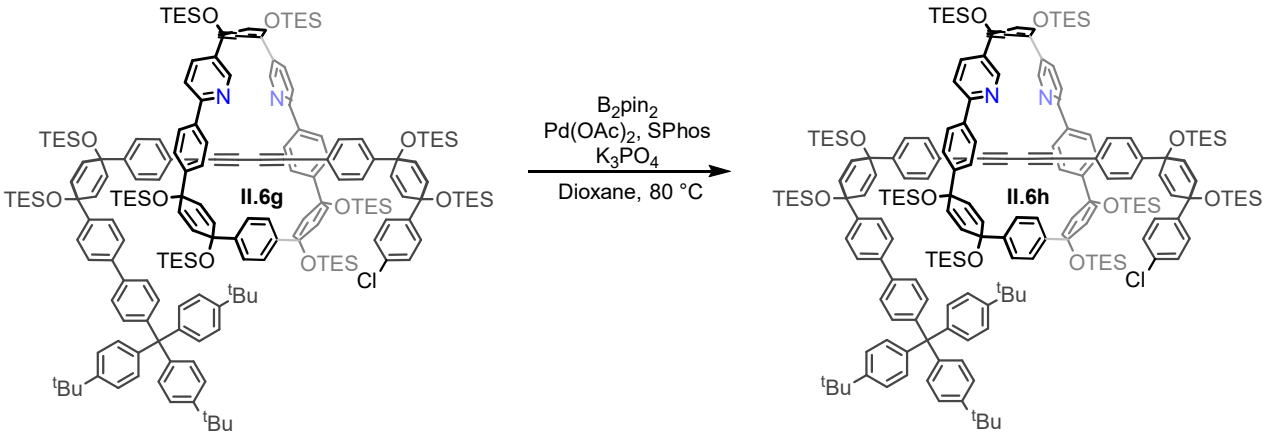

Synthesis of II.6h. To a flame dried 15 mL round bottom were added **II.6h** (0.210 g, 0.71 mmol)**,** B_2pin_2 (0.090 g, 0.35 mmol), $Pd(OAc)_2$ (0.008 g, 0.04 mmol), SPhos (0.030 g, 0.07 mmol), and K_3PO_4 (0.121 g, 0.57 mmol). The flask was evacuated and backfilled with N_2 gas five times before introducing 1,4-dioxane (5 mL). The mixture was stirred at 80 °C for 1 h. The solvent was then removed under reduced pressure and the crude material was run through a short silica plug using DCM as eluent. The eluate was concentrated under reduced pressure and the resulting

residue was sonicated with MeOH (10 mL) until a flocculent precipitate had formed. The precipitate was collected by vacuum filtration and washed with MeOH (20 mL) to give **II.6h** as a tan colored solid (0.209 g, 97%). ^{1}H NMR (500 MHz, Methylene Chloride-d_2) δ 8.65 (d, J = 2.3 Hz, 2H), 7.88 (d, J = 8.1 Hz, 4H), 7.74 (d, J = 7.8 Hz, 2H), 7.58 (d, J = 8.1 Hz, 2H), 7.50 (d, J = 8.2 Hz, 2H), 7.47 – 7.40 (m, 8H), 7.42 – 7.31 (m, 8H), 7.27 (d, J = 8.3 Hz, 6H), 7.21 (d, J = 8.3 Hz, 6H), 7.18 – 7.12 (m, 4H), 7.09 (d, J = 8.1 Hz, 2H), 6.70 – 6.61 (m, 4H), 6.21 – 6.14 (m, 4H), 6.10 – 6.02 (m, 4H), 5.99 – 5.88 (m, 8H), 5.77 (d, J = 10.1 Hz, 4H), 1.33 (s, 12H), 1.30 (s, 27H), 1.03 – 0.89 (m, 72H), 0.85 (t, J = 8.0 Hz, 18H), 0.71 – 0.54 (m, 48H), 0.51 (q, J = 8.0 Hz, 12H). ^{13}C NMR (126 MHz, Methylene Chloride-d_2) δ 156.31, 149.57, 149.03, 148.46, 147.42, 147.40, 147.33, 145.73, 145.69, 144.82, 140.17, 138.47, 138.27, 137.91, 135.29, 134.42, 132.79, 132.72, 132.54, 132.34, 132.20, 132.08, 131.87, 131.84, 131.77, 131.73, 131.61, 131.01, 127.76, 127.29, 126.81, 126.57, 126.48, 126.32, 125.86, 125.82, 125.75, 124.95, 121.14, 120.01, 84.36, 83.81, 82.24, 82.18, 76.07, 75.93, 71.91, 71.77, 71.64, 71.58, 71.43, 71.17, 64.20, 34.77, 31.66, 25.44, 25.27, 7.49, 7.47, 7.41, 7.37, 7.00, 6.97, 6.92. MS (MALDI–TOF) [M]+ calculated for $C_{189}H_{259}BN_2O_{12}Si_{10}$, 3039.7504; found, 3039.8.

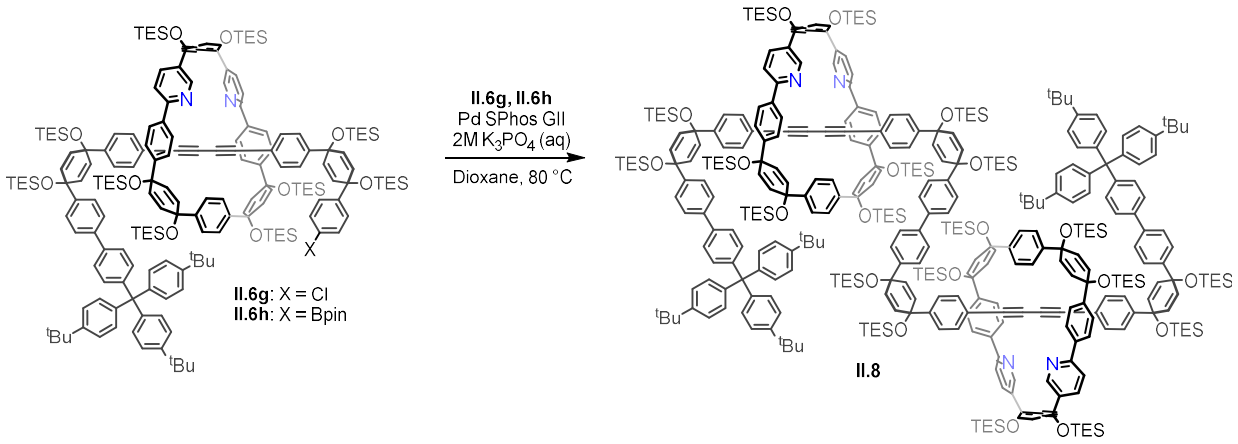

Synthesis of II.8: To a 50 mL round bottom flask were added **II.6g** (0.193 g, 0.07 mmol), **II.6h** (0.200 g, 0.07 mmol) and Pd SPhos GII (0.012 mg, 0.017 mmol). The flask was evacuated and backfilled with N_2 gas five times before introducing 1,4-dioxane (15 mL) and an aqueous solution of K_3PO_4 (2M, 2 mL). The mixture was stirred at 80 °C for 16 h after which the solvent was removed under reduced pressure. The crude residue was then transferred into a separatory funnel with the aid of H_2O (20 mL) and DCM (10 mL). The organic layer was collected, and the aqueous layer was extracted with an additional 10 mL DCM. The organic layers were combined and dried over Na_2SO_4. Product was purified by column chromatography (SiO_2, 0-40% DCM in Hexanes) to give **II.8** as an off-white solid (0.315 g, 92%). ^{1}H NMR (500 MHz, Methylene Chloride-d_2) δ 8.62 (d, J = 2.4 Hz, 4H), 7.85 (d, J = 8.1 Hz, 8H), 7.59 – 7.53 (m, 8H), 7.50 (d, J = 8.6 Hz, 4H), 7.44 – 7.37 (m, 20H), 7.37 – 7.32 (m, 12H), 7.27 (d, J = 8.7 Hz, 12H), 7.21 (d, J = 8.6 Hz, 12H), 7.19 – 7.14 (m, 8H), 7.12 (d, J = 8.2 Hz, 4H), 6.74 (d, J = 8.1 Hz, 4H), 6.64 (d, J = 8.2 Hz, 4H), 6.20 – 6.14 (m, 8H), 6.08 – 6.02 (m, 8H), 5.98 – 5.89 (m, 16H), 5.79 – 5.73 (m, 8H), 1.29 (s, 54H), 1.02 – 0.88 (m, 142H), 0.83 (t, J = 7.9 Hz, 36H), 0.71 – 0.56 (m, 96H), 0.48 (q, J = 7.9 Hz, 24H). ^{13}C NMR (126 MHz, Methylene Chloride-d_2) δ 156.28, 149.03, 148.44, 147.51, 147.41, 147.40, 145.74, 145.69, 144.81, 140.17, 140.11, 138.50, 138.50, 138.26, 137.90, 134.38, 132.79, 132.53, 132.44, 132.31, 132.19, 132.09, 131.87, 131.76, 131.61, 131.50, 131.01, 127.72,

127.34, 127.28, 126.81, 126.78, 126.55, 126.47, 126.33, 125.92, 125.77, 124.94, 121.24, 121.09, 119.96, 82.37, 82.10, 78.16, 77.90, 77.65, 76.09, 75.94, 71.77, 71.75, 71.67, 71.62, 71.54, 71.40, 71.14, 64.19, 34.76, 31.65, 30.27, 7.49, 7.47, 7.41, 7.39, 7.35, 7.01, 6.98, 6.96, 6.91. MS (MALDI–TOF) [M]+ calculated for $C_{366}H_{494}N_4O_{20}Si_{20}$, 5825.3; found, 5825.9.

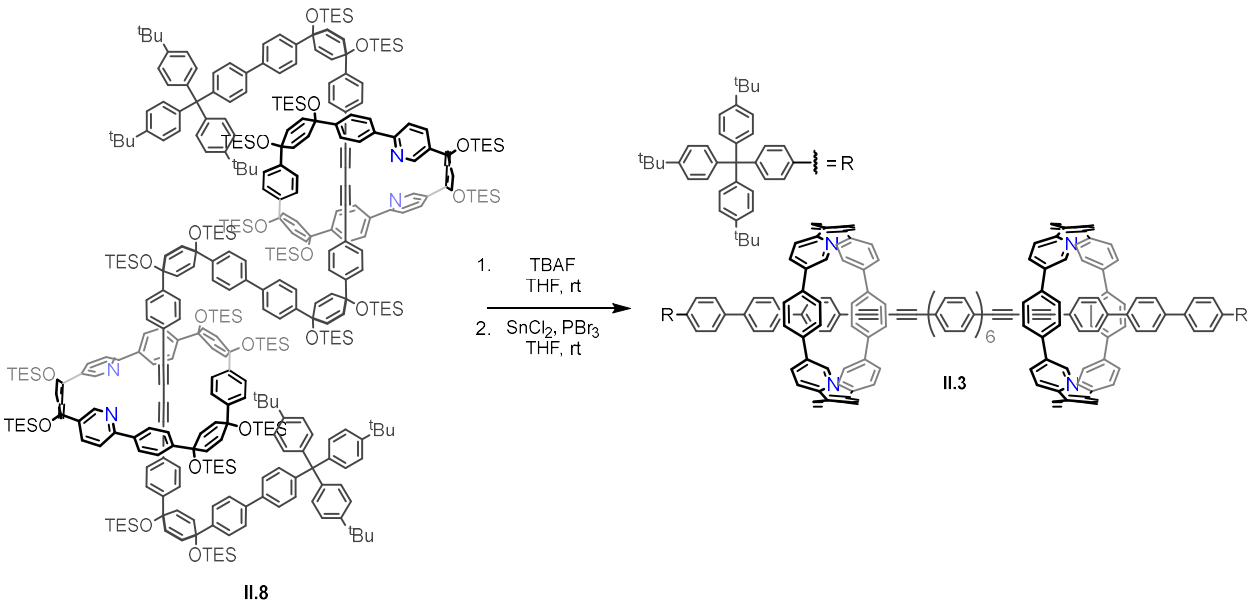

Synthesis of II.3. To a flame died 100 mL round bottom flask was added **II.8** (0.200 g, 0.034 mmol). The flask was evacuated and backfilled with N_2 gas three times before dissolving in THF (50 mL). TBAF (0.86 mL, 0.86 mmol, 1M in THF) was added. was added and the reaction was stirred for 1 h at room temperature. The solvent was removed under reduced pressure and the resulting yellow-brown oil was triturated with 5 mL H_2O until a filterable solid had formed. The precipitate was collected by vacuum filtration and washed with H_2O (10 mL) and DCM (10 mL). The desilylated material was rigorously dried under vacuum before transferring into a separate flame-dried 250 mL round bottom flask. The flask was evacuated and backfilled with N_2 gas three times before adding THF (100 mL). $SnCl_2$ (3.06 mL, 0.55 mmol, 0.18M in THF) was added and

the mixture was stirred until the starting material had dissolved. PBr_3 (0.72 mL, 0.55 mmol, 0.72 M in THF) was then introduced via slow, dropwise addition and the resulting solution was stirred in the exclusion of light for 30 minutes before quenching the with sat'd $NaHCO_3$ (20 mL). THF was removed under reduced pressure and the remaining aqueous suspension was extracted with DCM (3 x 15 mL). The organic layers were combined and dried over Na_2SO_4. The product was purified via preparatory TLC (alumina, 60% DCM in hexanes) to furnish **II.3** as a yellow solid (6 mg, 5.5%). ^{1}H NMR (500 MHz, Methylene Chloride-d_2) δ 8.78 (d, J = 2.3 Hz, 4H), 8.08 – 7.68 (m, 12H), 7.57 (d, J = 8.6 Hz, 4H), 7.52 – 7.44 (m, 46H), 7.41 – 7.27 (m, 46H), 7.26 – 7.18 (m, 16H), 7.16 – 7.10 (m, 8H), 7.04 (d, J = 7.7 Hz, 4H), 1.35 (s, 54H). ^{13}C NMR (126 MHz, CD_2Cl_2) δ 154.78, 149.21, 147.43, 147.32, 144.89, 141.69, 140.26, 140.20, 139.89, 139.76, 139.64, 139.41, 139.06, 138.85, 138.27, 138.07, 137.98, 137.53, 137.43, 135.59, 133.34, 133.32, 133.23, 131.76, 131.06, 130.53, 128.79, 128.08, 128.04, 127.89, 127.70, 127.68, 127.64, 127.59, 127.52, 127.33, 127.24, 127.21, 126.37, 125.07, 119.71, 82.50, 75.12, 64.28, 34.85, 31.70. MS (MALDI–TOF) [M]+ calculated for $C_{246}H_{194}N_4$, 3203.5; found, 3203.4.

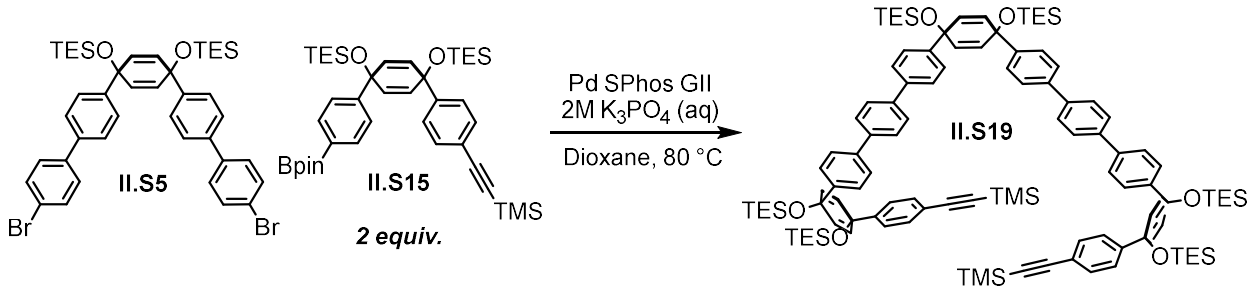

Synthesis of II.S19. To a 50 mL round bottom flask were added **II.S16** (0.305 g, 0.38 mmol), **II.S5** (0.543 g, 0.76 mmol) and Pd SPhos GII (0.014 g, 0.02 mmol). The flask was evacuated and backfilled with N_2 gas five times before introducing 1,4-dioxane (10 mL) and an

aqueous solution of K_3PO_4 (2M, 2 mL). The mixture was stirred at 80 °C for 1 h after which the solvent was removed under reduced pressure. The crude residue was then transferred into a separatory funnel with the aid of H_2O (20 mL) and DCM (10 mL). The organic layer was collected, and the aqueous layer was extracted with an additional 10 mL DCM. The organic layers were combined and dried over Na_2SO_4 before running the solution through a short silica plug using DCM as eluent. The eluate was evaporated under reduced pressure and the resulting brownish residue was triturated in 50 mL EtOH until a filterable solid had formed. Solids were collected by vacuum filtration, washing with an additional 20 mL EtOH to give **II.S19** as a tan colored solid. (0.682 g, 99 %). ^{1}H NMR (500 MHz, Chloroform-*d*) δ 7.69 – 7.60 (m, 8H), 7.57 (d, *J* = 8.1 Hz, 4H), 7.53 (d, *J* = 8.3 Hz, 4H), 7.46 (d, *J* = 8.2 Hz, 4H), 7.40 – 7.33 (m, 8H), 7.30 (d, *J* = 8.1 Hz, 4H), 6.06 (s, 4H), 6.02 (d, *J* = 10.5 Hz, 4H), 5.98 (d, *J* = 10.4 Hz, 4H), 0.99 – 0.90 (m, 54H), 0.67 – 0.56 (m, 36H), 0.23 (s, 18H). ^{13}C NMR (126 MHz, Chloroform-*d*) δ 146.51, 145.25, 144.99, 139.66, 139.64, 139.51, 131.86, 131.56, 131.09, 127.38, 126.75, 126.73, 126.41, 126.28, 125.86, 121.96, 71.42, 71.40, 71.37, 7.10, 7.08, 7.05, 6.51, 6.48, 0.00. HRMS (ESI–TOF) [M]+ calculated for $C_{112}H_{152}O_6Si_8$, 1816.9743; found, 1816.9660.

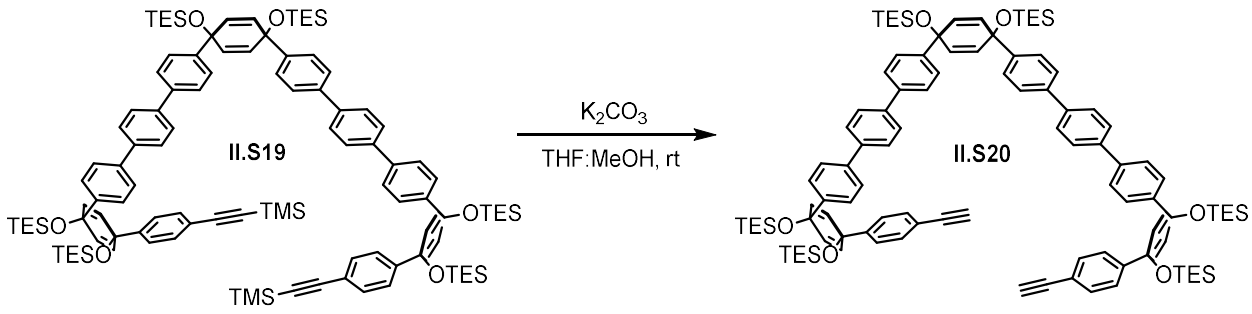

Synthesis of II.S20. To a 50 mL round bottom was added **II.S19** (0.630 g, 0.35 mmol), THF (10 mL) and MeOH (10 mL). K_2CO_3 (0.382 g, 2.77 mmol) was added was stirred for 30 min

at room temperature. The solvent was removed under reduced pressure and the crude material was run through a short silica plug using DCM as eluent. The eluate was evaporated under reduced pressure and the resulting residue was triturated with 10 mL EtOH to produce a solid precipitate. The precipitate was collected by vacuum filtration, washing with 10 mL EtOH, to provide the **II.S20** as a brown solid (0.437 g, 75%). ^{1}H NMR (600 MHz, Chloroform-*d*) δ 7.68 – 7.63 (m, 8H), 7.57 (d, *J* = 8.4 Hz, 4H), 7.54 (d, *J* = 8.4 Hz, 4H), 7.46 (d, *J* = 8.4 Hz, 4H), 7.42 – 7.36 (m, 8H), 7.32 (d, *J* = 8.4 Hz, 4H), 6.07 – 6.03 (m, 8H), 5.98 (d, *J* = 10.1 Hz, 4H), 3.04 (s, 2H), 0.98 – 0.92 (m, 48H), 0.68 – 0.59 (m, 36H). ^{13}C NMR (151 MHz, Chloroform-*d*) δ 146.84, 145.22, 144.95, 139.66, 139.56, 139.54, 139.46, 131.99, 131.86, 131.54, 131.08, 127.37, 127.36, 127.33, 126.73, 126.39, 126.30, 125.92, 120.87, 83.61, 71.39, 71.37, 71.33, 53.43, 7.09, 7.06, 7.04, 6.48, 6.45, 6.43. HRMS (ESI–TOF) [M]+ calculated for $C_{105}H_{136}O_6Si_6$, 1672.8953; found, 1672.903.

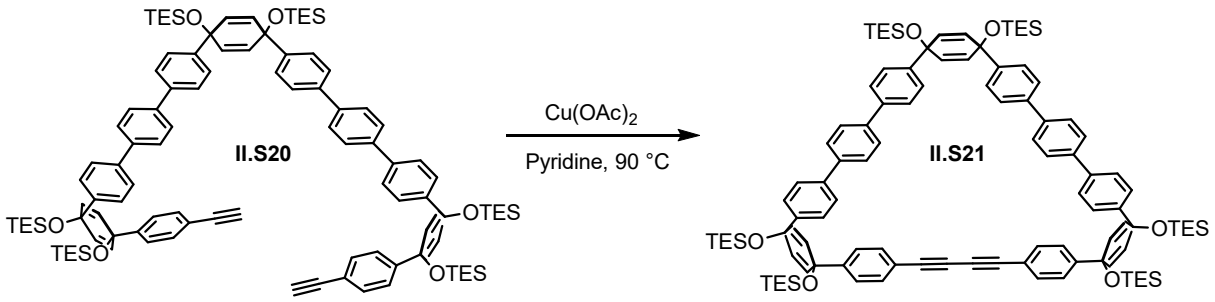

Synthesis of II.21. To a 250 mL three neck flask fitted with a water-cooled condenser, were added copper(II)acetate monohydrate ($Cu_2(OAc)_4(H_2O)_2$, 0.104 g, 0.52 mmol) and pyridine (60 mL). The resulting blue solution was heated to 90 °C, stirring open to air, at which point **II.S20** (40 mL, 0.26 mmol, 6.5 mM in pyridine) was added dropwise over 20 minutes. The reaction was allowed to stir for 1 h following complete addition of starting material. The solvent was removed under reduced pressure and the crude material was run through a short silica plug using 30% DCM

in hexanes as eluent. The eluate was evaporated under reduced pressure and the resulting residue was triturated with 10 mL hexanes. The precipitate was collected by vacuum filtration and washed with 10 mL EtOH to provide **II.S21** as an off-white solid. (0.107 g, 20%). ^{1}H NMR (500 MHz, Chloroform-*d*) δ 7.72 – 7.62 (m, 8H), 7.60 (d, *J* = 8.2 Hz, 4H), 7.57 (d, *J* = 8.3 Hz, 4H), 7.49 (d, *J* = 8.4 Hz, 4H), 7.44 (d, *J* = 8.4 Hz, 4H), 7.40 (d, *J* = 8.4 Hz, 4H), 7.34 (d, *J* = 8.3 Hz, 4H), 6.04 (d, *J* = 7.2 Hz, 8H), 5.96 (d, *J* = 10.0 Hz, 4H), 1.02 – 0.84 (m, 54H), 0.69 – 0.55 (m, 36H). ^{13}C NMR (126 MHz, Chloroform-*d*) δ 147.34, 145.41, 144.98, 139.51, 139.50, 139.36, 132.39, 131.88, 131.47, 130.98, 127.36, 127.33, 126.74, 126.71, 126.34, 126.32, 126.02, 120.56, 81.46, 74.01, 71.53, 71.41, 7.09, 7.06, 7.04, 6.51, 6.49, 6.45. HRMS (ESI–TOF) [M]+ calculated for $C_{105}H_{134}O_6Si_6$, 1670.8796; found, 1670.8714.

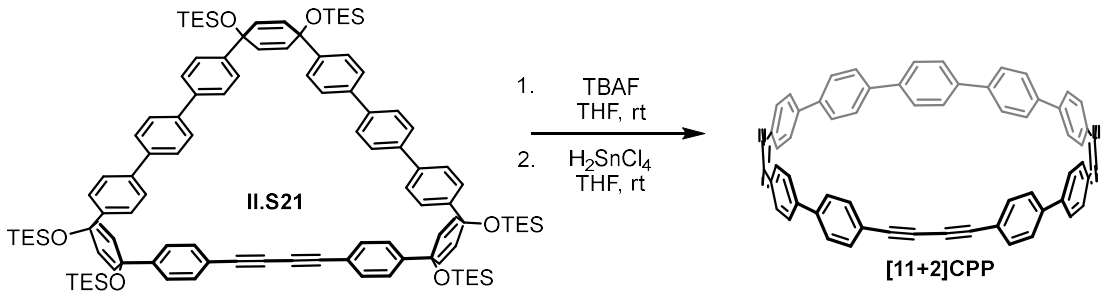

Synthesis of [11+2]CPP. To a flame-dried 100 mL round bottom flask was added **II.S21** (0.025 g, 0.015 mmol). The flask was evacuated and backfilled with N_2 gas three times before dissolving in THF (15 mL). TBAF (0.18 mL, 0.18 mmol, 1M in THF) was added. was added and the reaction was stirred for 1 h at room temperature. The solvent was removed under reduced pressure and the resulting yellow-brown oil was triturated with 5 mL H_2O until a filterable solid had formed. The precipitate was collected by vacuum filtration and washed with H_2O (10 mL) and DCM (10 mL) which after drying under vacuum affords the intermediate product as a white solid.

The desilylated material was then transferred into a separate 100 mL round bottom flask. The flask was evacuated and backfilled with N_2 gas three times before introducing THF (25 mL). H_2SnCl_4 (0.16 mL, 0.07 mmol, 0.41 M in THF) was added and the resulting solution was stirred in the exclusion of light for 1 h before quenching the reaction with sat'd $NaHCO_3$ (10 mL). THF was removed under reduced pressure and the remaining aqueous suspension was extracted with DCM (3 x 15 mL). The organic layers were combined and dried over Na_2SO_4. The product was purified via column chromatography (alumina, 0-50% DCM in hexanes) to furnish **[11+2]CPP** as an off-white solid (11 mg, 83%). ^{1}H NMR (500 MHz, Chloroform-*d*) δ 7.65 – 7.59 (m, 32H), 7.58 (d, *J* = 8.3 Hz, 4H), 7.54 (d, *J* = 8.3 Hz, 4H), 7.45 (d, *J* = 8.3 Hz, 4H). ^{13}C NMR (126 MHz, Chloroform-*d*) δ 140.95, 139.39, 138.88, 138.67, 138.56, 138.49, 138.25, 132.24, 127.43, 127.39, 127.37, 127.35, 126.84, 121.27, 90.71, 79.33. HRMS (ESI–TOF) [M]+ calculated for $C_{70}H_{44}$, 884.3443; found, 884.3417.

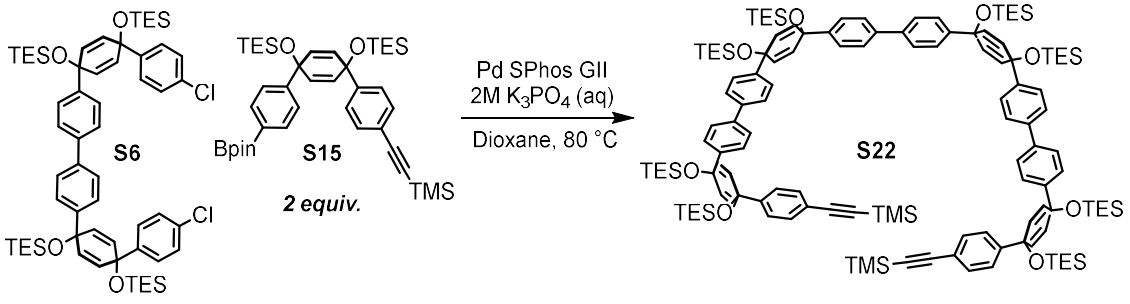

Synthesis of II.S22. To a 50 mL round bottom flask were added **II.S6** (0.400 g, 0.38 mmol), **II.S16** (0.543 g, 76 mmol) and Pd SPhos GII (0.014 g, 0.02 mmol). The flask was evacuated and backfilled with N_2 gas five times before introducing 1,4-dioxane (10 mL) and an aqueous solution of K_3PO_4 (2M, 2 mL). The mixture was stirred at 80 °C under N_2 for 1 h. The solvent was removed under reduced pressure and the crude residue was transferred into a separatory funnel with the aid

of H_2O (20 mL) and DCM (10 mL). The organic layer was collected, and the aqueous layer was extracted with an additional 10 mL DCM. The organic layers were combined and dried over Na_2SO_4 before running the solution through a short silica plug using DCM as eluent. The eluate was evaporated under reduced pressure and the resulting brownish residue was triturated in 50 mL EtOH. The resulting precipitate was collected by vacuum filtration, washing with an additional 20 mL EtOH to give **II.S22** as a tan colored solid. (0.756 g, 92 %). ^{1}H NMR (500 MHz, Chloroform-*d*) δ 7.52 – 7.44 (m, 12H), 7.41 (d, *J* = 8.0 Hz, 8H), 7.36 (d, *J* = 8.0 Hz, 4H), 7.33 (d, *J* = 8.1 Hz, 4H), 7.28 (d, *J* = 8.2 Hz, 4H), 6.04 – 5.94 (m, 16H), 0.99 – 0.88 (m, 72H), 0.66 – 0.55 (m, 48H), 0.22 (s, 18H). ^{13}C NMR (126 MHz, Chloroform-*d*) δ 146.51, 145.16, 145.13, 144.87, 139.65, 139.62, 138.58, 131.85, 131.54, 131.52, 131.07, 126.78, 126.31, 126.21, 125.84, 121.94, 105.10, 94.16, 71.39, 71.37, 7.10, 7.08, 7.05, 6.51, 6.47, 0.00. HRMS (ESI–TOF) [M]+ calculated for $C_{130}H_{186}O_8Si_{10}$, 2155.1840; found, 2155.1761.

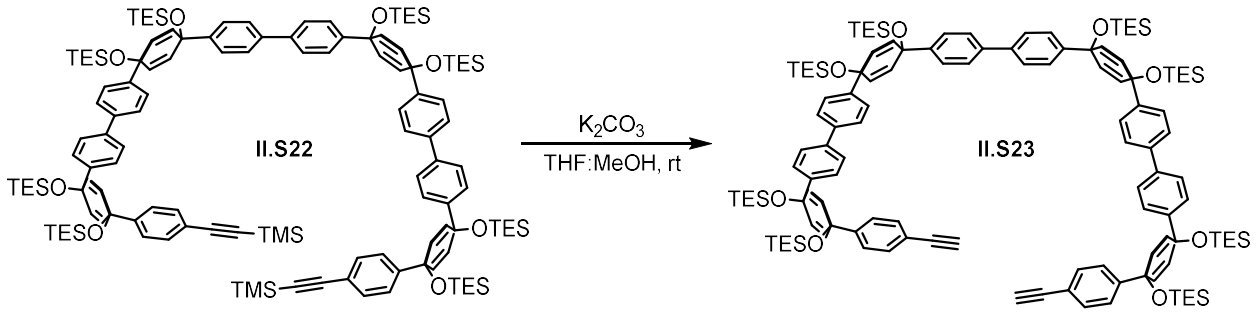

Synthesis of II.S23. To a 50 mL round bottom flask were added **II.S22** (0.720 g, 0.33 mmol), THF (10 mL) and MeOH (10 mL). K_2CO_3 (0.369 g, 2.67 mmol) was added, and the slurry was stirred at room temperature for 30 min. The solvent was removed under reduced pressure and the crude material was run through a short silica plug using DCM as eluent. The eluate was evaporated under reduced pressure and the resulting residue was triturated with EtOH (10 mL).

The resulting precipitate was collected by vacuum filtration, washing with 10 mL EtOH, to provide **II.S23** as a brown solid (0.597 g, 89%). ^{1}H NMR (500 MHz, Chloroform-*d*) δ 7.53 – 7.46 (m, 12H), 7.43 – 7.34 (m, 16H), 7.30 (d, *J* = 8.1 Hz, 4H), 6.05 – 6.00 (m, 12H), 5.96 (d, *J* = 10.1 Hz, 4H), 2.99 (s, 2H), 0.97 – 0.91 (m, 72H), 0.66 – 0.58 (m, 48H). ^{13}C NMR (126 MHz, Chloroform-*d*) δ 146.84, 145.17, 145.12, 144.82, 139.67, 139.61, 139.51, 131.98, 131.87, 131.52, 131.07, 126.77, 126.75, 126.31, 126.23, 125.90, 120.88, 83.59, 77.13, 71.38, 71.37, 71.34, 71.31, 7.08, 7.05, 7.03, 6.48, 6.46, 6.43. HRMS (ESI–TOF) [M]+ calculated for $C_{124}H_{170}O_8Si_8$, 2011.1050; found, 2011.0969.

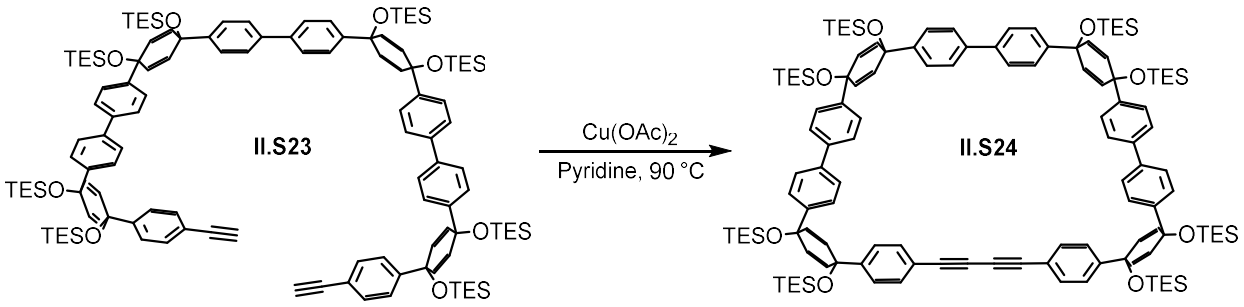

Synthesis of II.S24. To a 250 mL three neck flask fitted with a water-cooled condenser were added $Cu_2(OAc)_4(H_2O)_2$ (0.118 g, 0.59 mmol) and pyridine (60 mL). The resulting blue solution was heated to 90 °C, stirring open to air. **II.S23** (40 mL, 0.30 mmol, 7.4 mM in pyridine) was added dropwise over 20 minutes after which the reaction was stirred for 1 h. The solvent was removed under reduced pressure and the product was purified via column chromatography (SiO_2, 0-30 % DCM in hexanes) to provide **II.S24** as a yellow solid. (0.197 g, 33%). ^{1}H NMR (500 MHz, Chloroform-*d*) δ 7.50 – 7.40 (m, 20H), 7.34 – 7.28 (m, 8H), 7.21 (d, *J* = 8.4 Hz, 4H), 6.07 (d, *J* = 10.0 Hz, 4H), 6.03 (s, 8H), 5.95 (d, *J* = 10.1 Hz, 4H), 0.97 – 0.91 (m, 72H), 0.65 – 0.57 (m, 48H). ^{13}C NMR (126 MHz, Chloroform-*d*) δ 146.85, 145.18, 145.13, 144.37, 139.94, 139.71, 139.59,

132.24, 131.95, 131.17, 126.85, 126.81, 126.35, 126.28, 126.24, 126.05, 120.51, 81.42, 73.92, 71.77, 71.44, 71.32, 71.18, 7.08, 7.06, 7.03, 6.47, 6.46, 6.44. HRMS (ESI–TOF) [M]+ calculated for $C_{124}H_{168}O_8Si_8$, 2009.0893; found, 2009.0845.

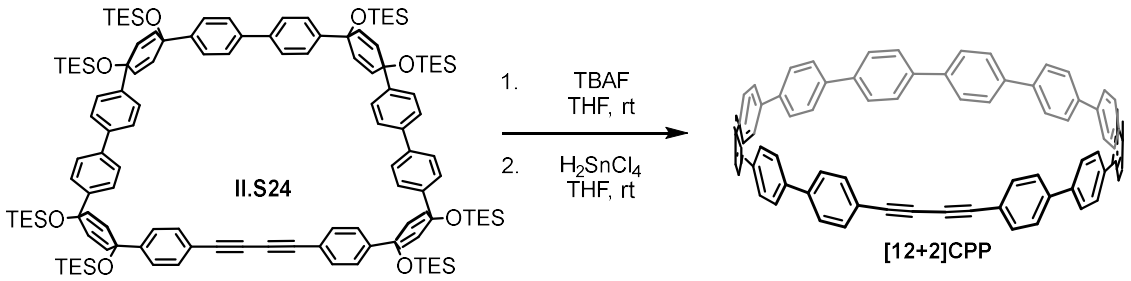

Synthesis of [12+2]CPP. To a flame-dried 100 mL round bottom flask was added **II.S24** (0.035 g, 0.017 mmol). The flask was evacuated and backfilled with N_2 gas three times before introducing THF (15 mL). TBAF (0.21 mL, 0.21 mmol, 1M in THF) was added and the reaction was stirred for 1 h at room temperature. The solvent was removed under reduced pressure and the resulting yellowish oil was triturated with 5 mL H_2O until a filterable solid had formed. The precipitate was collected by vacuum filtration, washing with H_2O (10 mL) and DCM (10 mL) which, after drying under vacuum, affords the intermediate product as a white solid. The desilylated material was then transferred into a separate 100 mL round bottom flask. The flask was evacuated and backfilled with N_2 gas three times before introducing THF (25 mL). H_2SnCl_4 (0.19 mL, 0.09 mmol, 0.41 M in THF) was added and the resulting solution was stirred in the exclusion of light for 1 h before quenching the reaction with sat'd $NaHCO_3$ (10 mL). THF was removed under reduced pressure and the remaining aqueous suspension was extracted with DCM (3 x 15 mL). The organic layers were combined and dried over Na_2SO_4. The product was purified via column chromatography (alumina, 0- 50% DCM in hexanes) to furnish **[12+2]CPP** as an off-white

solid (8 mg, 52%). ^{1}H NMR (500 MHz, Chloroform-*d*) δ 7.68 – 7.62 (m, 36H), 7.60 (d, *J* = 8.6 Hz, 4H), 7.55 (d, *J* = 8.5 Hz, 4H), 7.47 (d, *J* = 8.5 Hz, 4H). ^{13}C NMR (126 MHz, Chloroform-*d*) δ 140.94, 139.44, 138.96, 138.80, 138.69, 138.65, 138.63, 138.61, 138.58, 138.36, 132.35, 127.44, 127.40, 127.37, 126.85, 121.21, 89.51, 78.70. HRMS (ESI–TOF) [M]+ calculated for $C_{76}H_{48}$, 960.3756; found, 960.3781.

2.4.3 X-Ray Crystallographic Details.

Single crystals of **II.1a**, **II.1b** and **II.1c** were grown by slow vapor diffusion of pentane into solutions of the compounds in 1,4-dioxane (**II.1a**, **II.2**), THF (**diaza[8]CPP**), $CHCl_3$ (**diaza[9]CPP**), or a mixture of THF and 1,4-dioxane (**II.1b**) at room temperature.

Diffraction intensities for **II.1a**, **II.1b**, **II.1c**, **diaza[8]CPP** and **diaza[9]CPP** were collected at 173 K on a Bruker Apex2 CCD DUO diffractometer using MoKα (**diaza[9]CPP**) and CuKα radiation, 0.71073 Å and 1.54178 Å, respectively. Space groups were determined based on systematic absences. Absorption corrections were applied by SADABS *(32).* Structures were solved by direct methods and Fourier techniques and refined on F^2 using full matrix least-squares procedures. All non-H atoms were refined with anisotropic thermal parameters. H atoms in **diaza[9]CPP** and **diaza[8]CPP** were found on the residual density maps and refined with isotropic thermal parameters except those in solvent molecules $CHCl_3$ in **diaza[9]CPP**. The H atoms in these solvent molecules were treated in calculated positions in a rigid group model. All H atoms in **II.1a**, **II.1b** and **II.2** were refined in calculated positions in a rigid group model. In the crystal structures of **1a**, **II.1b** and **II.2** there are a lot of $C_4H_8O_2$ solvent molecules filling empty spaces in the packing: five in **II.1a**, three in **II.1b** and two in **II.2**. These solvent molecules were found

from the diffraction data and refined. Some additional solvent molecules in **II.1b**, **diaza[8]CPP** and **II.2** are highly disordered. It was not possible to resolve these disordered molecules (which could be $C_4H_8O_2$, pentane and tetrahydrofuran molecules as well or a mix of them) and they were treated by SQUEEZE *(33)*. Two solvent molecules $CHCl_3$ in **diaza[9]CPP** are disordered over two positions and were refined with restrictions on its geometry; the standard C-Cl distances were used as the target for corresponding bond lengths. The structure of **diaza[8]CPP** seems to have higher pseudo symmetry, but it was determined in space group with low symmetry to avoid possible disorder of the N atoms in the structure. The main molecules in both **diaza[9]CPP** and **diaza[8]CPP** structures are not disordered and that allowed finding positions of the N atoms. Crystals of **II.1a** and **II.2** are very thin plates. X-ray diffraction from these crystals at high angles was very weak due to its small scattering volume and the disorder inside them. Even by using a strong *Incoatec* Cu *I*μ*S* source it was possible to collected diffraction data only up to $2\theta_{max} = 99.81°$ (**II.1a**) and 88.93° (**II.2**). The collected data provide an appropriate number of measured reflections per refined parameters; 10454 per 1352 in **II.1a** and 7332 reflections per 874 in **II.2**. RIGU command in SHELX was used for refinement of **II.2**. The structure of **II.2** is clear but not very precisely determined. All calculations were performed by the Bruker SHELXL-2014/7 package *(34)*.

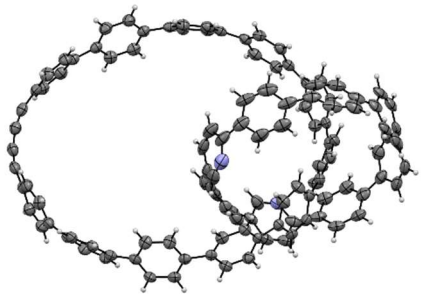

II.1a

Crystallographic Data for ***II.1a*** (CCDC 2159304): $C_{136}H_{114}N_2O_{10}$, M = 1936.29, 0.16 x 0.08 x 0.03 mm, T = 173(2) K, Monolinic, space group $P2_1/n$, a = 19.850(5) Å, b = 19.447(5) Å, c = 26.797(8) Å, β = 97.516(5)°, V = 10256(5) Å^3, Z = 4, Dc = 1.254 Mg/m^3, μ(Cu) = 0.612 mm^{-1}, F(000) = 4096, $2\theta_{max}$ = 99.81°, 41249 reflections, 10451 independent reflections [R_{int} = 0.0688], R1 = 0.0616, wR2 = 0.1621 and GOF = 1.035 for 10451 reflections (1352 parameters) with I>2σ(I), R1 = 0.0955, wR2 = 0.1873 and GOF = 1.035 for all reflections, max/min residual electron density +0.0828/-0.317 eÅ^{-3}.

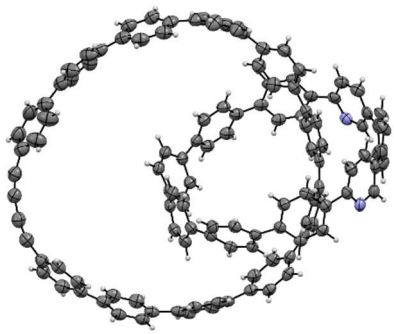

II.1b

Crystallographic Data for ***1b*** (CCDC 2159303): $C_{139}H_{114}N_2O_5$, M = 1892.32, 0.16 x 0.09 x 0.04 mm, T = 173(2) K, Triclinic, space group P-1, a = 15.3267(6) Å, b = 15.5999(5) Å, c = 22.6516(10) Å, α = 99.295(3)°, β = 97.318(3)°, γ = 93.967(3)°, V = 5278.9(4) Å3, Z = 2, D_c =

1.190 Mg/m^3, μ(Cu) = 0.547 mm^{-1}, F(000) = 2004, $2\theta_{max}$ = 134.69°, 57932 reflections, 18664 independent reflections [R_{int} = 0.0765], R1 = 0.0826, wR2 = 0.2275 and GOF = 1.040 for 18664 reflections (1225 parameters) with I>2σ(I), R1 = 0.1231, wR2 = 0.2550 and GOF = 1.042 for all reflections, max/min residual electron density +0.337/-0.481 eÅ^{-3}.

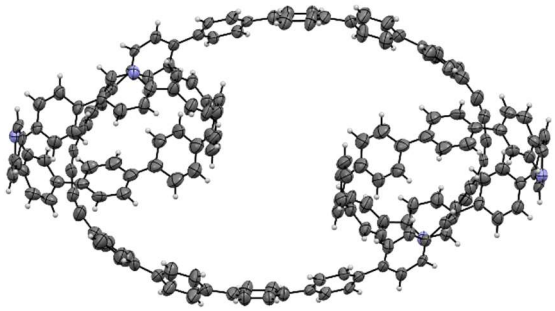

II.2

*Crystallographic Data for **2*** (CCDC 2159302): $C_{224}H_{212}N_4O_{26}$, M = 3375.96, 0.21 x 0.09 x 0.03 mm, T = 173(2) K, Triclinic, space group *P*-1, a = 13.797(3) Å, b = 18.823(4) Å, c = 20.955(4) Å, α = 107.275(7)°, β = 102.060(7)°, γ = 106.952(7)°, V = 4703.4(17) Å^3, Z = 1, D_c = 1.192 Mg/m^3, μ(Cu) = 0.614 mm^{-1}, F(000) = 1792, $2\theta_{max}$ = 88.93°, 26498 reflections, 7332 independent reflections [R_{int} = 0.1103], R1 = 0.0894, wR2 = 0.2498 and GOF = 1.023 for 7332 reflections (874 parameters) with I>2σ(I), R1 = 0.1503, wR2 = 0.2742 and GOF = 1.068 for all reflections, max/min residual electron density +0.257/-0.182 eÅ^{-3}.

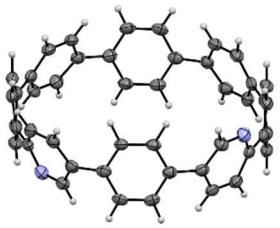

diaza[8]CPP

Crystallographic Data for ***diaza[8]CPP*** (CCDC 2159305): $C_{50}H_{38}N_2O$, M = 682.82, 0.15 x 0.11 x 0.07 mm, T = 173(2) K, Monolinic, space group $P2_1/c$, a = 26.954(6) Å, b = 8.3874(18) Å, c = 17.525(5) Å, β = 107.284(17)°, V = 3783.1(16) Å^3, Z = 4, Dc = 1.199 Mg/m^3, μ(Cu) = 0.547 mm^{-1}, F(000) = 1440, $2\theta_{max}$ = 133.63°, 18967 reflections, 6517 independent reflections [R_{int} = 0.0783], R1 = 0.0829, wR2 = 0.2181 and GOF = 1.063 for 6517 reflections (553 parameters) with I>2σ(I), R1 = 0.1055, wR2 = 0.2357 and GOF = 1.063 for all reflections, max/min residual electron density +0.350/-0.284 eÅ^{-3}.

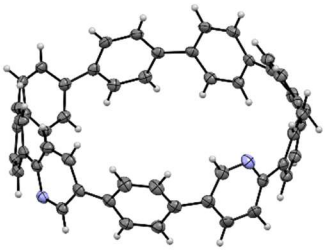

diaza[9]CPP

Crystallographic Data for ***diaza[9]CPP*** (CCDC 2159306): $C_{54}H_{36}N_2Cl_6$, M = 925.55, 0.19 x 0.18 x 0.08 mm, T = 173(2) K, Monolinic, space group $P2_1/c$, a = 15.3818(19) Å, b = 16.5721(19) Å, c = 18.914(2) Å, β = 111.379(2)°, V = 4489.6(9) Å^3, Z = 4, Dc = 1.369 Mg/m^3, μ(Mo) = 0.423 mm^{-1}, F(000) = 1904, $2\theta_{max}$ = 56.72°, 50923 reflections, 11157 independent reflections [R_{int} = 0.0778], R1 = 0.0692, wR2 = 0.1776 and GOF = 1.043 for 11157 reflections

(760 parameters) with I>2σ(I), R1 = 0.1089, wR2 = 0.2039 and GOF = 1.063 for all reflections, max/min residual electron density +0.666/-0.776 $eÅ^{-3}$.

2.5 Bridge to Chapter III

In Chapter **II** we discussed an active template strategy to synthesize mechanically interlocked [*n*]cycloparaphenylenes in which bis(pyridyl) macrocycles are used as ligands for the active-template Cadiot-Chodkiewicz reaction. While this work provided solid proof of concept for using AT chemistry in the synthesis of these topologically complex nanocarbons, the synthesis proved very challenging owing to the instability of the 1,4-butadiyne moiety under final reductive aromatization reaction conditions. Consequently, only small quantities of the target molecules could be prepared, precluding detailed analysis of their physical properties. Following the completion of this work, we sought an alternative approach that would allow these types of interlocked structures to be prepared more efficiently. In Chapter III we will discuss a 2,2'-bipyridine embedded macrocycle (a precursor to bipy[9]CPP) which effectively templates the active template copper catalyzed azide-alkyne cycloaddition reaction (AT-CuAAC) to give mechanically interlocked [2]rotaxane molecules. Not only do we find that replacing the butadiyne (AT-CC) with a triazole (AT-CuAAC) dramatically increases the yield of the reductive aromatization reaction, we also see that the AT reaction can be optimized to give quantitative yields of the [2]rotaxane intermediates. The work described in Chapter III provides a highly efficient method to incorporate [*n*]CPPs into mechanically interlocked architectures.

CHAPTER III

A QUANTITATIVE ACTIVE TEMPLATE 'CLICK' REACTION (AT-CUAAC) FOR THE SYNTHESIS OF MECHANICALLY INTERLOCKED NANOHOOPS

This chapter outlines a manuscript in preparation at the time of writing this thesis: May, J. H.; Fehr, J. M.; Lorenz, J.; Zakharov, L. N.; Jasti, R. *in preparation*. This manuscript was written by me with editorial assistance from Professor Ramesh Jasti. The synthetic work was performed by me. The photophysical analysis was performed by me and Julia Fehr. Single crystals were grown by me, and the data collection and analysis were performed by Dr. Lev N. Zakharov.

Mechanically interlocked molecules (MIMs) represent an exciting yet underexplored area of research in the context of carbon nanoscience. Recently, work from our group and others have shown that small carbon nanotube fragments—[*n*]cycloparaphenylenes ([*n*]CPPs) and related *nanohoop* macrocycles—may be integrated into mechanically interlocked architectures by leveraging supramolecular interactions, covalent tethers, or metal-ion templates. Still, available synthetic methods are typically difficult and low yielding and general methods that allow for the creation of a wide variety of these structures are limited. Here we report an efficient route to interlocked nanohoop structures via active template Cu-catalyzed azide-alkyne cycloaddition (AT-CuAAC) reaction. With the appropriate choice of substituents, a macrocyclic precursor to 2,2'-bipyridyl embedded [9]CPP (bipy[9]CPP) participates in the AT-CuAAC reaction to provide [2]rotaxanes in near-quantitative yield, which can then be converted to fully π-conjugated structures. Through this approach two nanohoop[2]catenanes are synthesized which consist of a bipy[9]CPP catenated with either Tz[10]CPP or Tz[12]CPP (where 'Tz' denotes a 1,2,3-triazole moiety replacing one phenylene ring in the [*n*]CPP backbone).

3.1 Introduction.

Graphitic carbon nanomaterials hold tremendous promise for applications across many fields of science and technology.[5] The broad scope of applications for these materials is largely correlated with their profound structure-function relationships, illustrated by the distinct sets of properties observed within, and between families of graphitic carbon allotropes (e.g., graphene, carbon nanotubes, fullerenes). While this strong structure-function dependency potentially provides a powerful platform wherein certain properties may be tailored via seemingly small structural perturbations, the precise synthesis of carbon nanomaterials of specific identity remains challenging. As such, significant interest has manifested for the synthesis of molecular analogues of these materials whose structure and composition may be meticulously controlled via bottom-up synthetic strategies. Notable among these so-called *molecular nanocarbons* are [*n*]cycloparaphenylenes ([*n*]CPPs) and related oligoparaphenylene-derived 'nanohoop' macrocycles, which represent molecular substructures of carbon nanotubes. Since the synthesis of the first [*n*]CPPs in 2008,[6] nanohoops have been the focus of many research efforts owing to their unique radial conjugation and accompanying size-dependent optoelectronic characteristics. More recently, researchers have begun to develop methods to integrate nanohoops into mechanically interlocked architectures (e.g., rotaxanes, catenanes, and knots), providing an opportunity to interrogate the effects of topological manipulation on the properties of these molecular nanocarbons.[7–18] While methods using passive templates,[8] supramolecular assemblies,[7,17,68] or covalent tethering groups[11–13] have proven successful, the active template (AT) strategy offers an attractive approach for the selective synthesis of asymmetrical structures via kinetically driven reactions. [9,10,14–16,69] Here, we show that a macrocyclic precursor to 2,2'-bipyridyl embedded [9]CPP (bipy[9]CPP) participates in the AT Cu-catalyzed azide-alkyne cycloaddition (AT-

CuAAC) reaction. Provided the appropriate design of the macrocyclic ligand, quantitative conversion to [2]rotaxanes could be achieved which then serve as intermediates to nanohoop[2]catenanes.

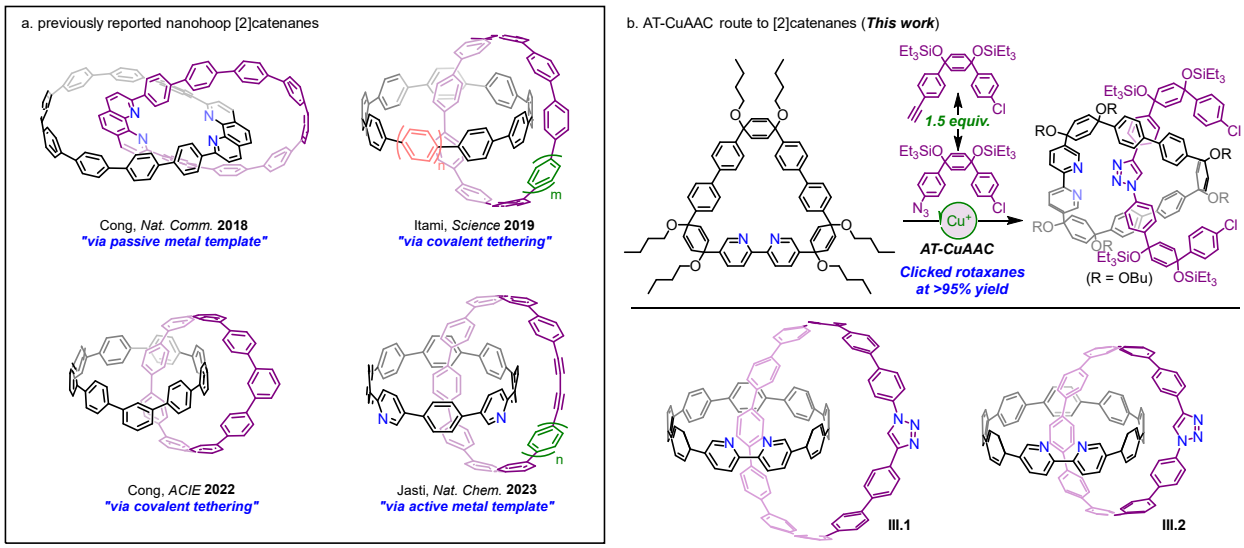

Figure III.1. (a) previously reported nanohoop [2]catenanes. (b) Active template Cu catalyzed azide-alkyne cycloaddition reaction (AT-CuAAC) reported herein for the synthesis of nanohoop [2]catenanes **III.1** and **III.2**.

3.2 Results and Discusion.

3.2.1 Method Design

Since the initial report by Leigh and coworkers in 2006,[25] the active template (AT) method has proven a powerful tool for generating mechanically interlocked molecules (MIMs) with complex structure and function.[26] This approach takes advantage of a macrocyclic ligand which sequesters a metal ion within the interior of its cavity. Chemical reactions that are facilitated by this metal ion result in a product molecule which threads through the center of the macrocycle.

Provided the reactants are functionalized with sufficiently bulky *stopper* groups that prevent the macrocycle from slipping over either end of the newly formed molecule, the two species are left mechanically bound, and unable to diffuse apart without the breaking of covalent bonds. We recently applied this AT approach to the synthesis of interlocked nanohoop structures wherein the Cadiot-Chodkiewicz C*sp*-C*sp* cross-coupling (AT-CC) was used as the mechanical bond forming reaction.[14] This synthesis suffered, however, due to the instability of the 1,3-diyne moiety under the conditions required to aromatize the penultimate intermediates to the fully conjugated nanohoop structures. If the 1,3-diyne could be eliminated in favor of a more robust functional group—that is, by using an alternative AT reaction—the target interlocked nanohoops might be prepared more efficiently. Unfortunately, other AT reactions such as the AT-CuAAC reaction, failed to provide interlocked products with our original ligand design(s). Though macrocycles with isolated pyridine donors have been shown to be effective ligands for the AT-CuAAC reaction, those featuring 2,2'-bipyridine ligands have been among the most powerful, occasionally providing near quantitative yields of the interlocked targets.[70–73] Previously our group reported 2,2'-bipyridyl embedded nanohoops (bipy[*n*]CPPs) which form well defined organometallic complexes by virtue of the bipyridine moiety.[74] While the bipy[*n*]CPPs do not exhibit coordination geometries conducive to the AT formation of mechanical bonds—binding metal ions above/below the rim of the nanohoop rather than at their interior—their macrocyclic precursors should possess the conformational flexibility to adopt the desired endotopic coordination geometry.

3.2.2 Synthesis of nanohoop [2]catenanes.

With this we turned our attention to a macrocyclic precursor to bipy[9]CPP, **III.3a**, which can be reliably prepared on multi-gram scale (Fig. III.2). Half-axel thread components, **III.4a** and **III.4b**, were designed to carry complementary reactive handles for the CuAAC reaction as well as

distal silyl-ether groups which serve as stoppers to prevent the dethreading of any encapsulated cycloaddition products. Initially attempts to produce [2]rotaxane, **III.5a**, via the AT-CuAAC reaction were performed by reacting the thread components **III.4a** and **III.4b** (5 equiv. each) in the presence of macrocyclic ligand **III.5a** and a Cu^{I} catalyst ($Cu(MeCN)_4PF_6$; 0.9 equiv.). These reactions, however, proceeded sluggishly, requiring more than 16 h for the starting materials (**III.4a**, **III.4b**) to be consumed, and gave no indication of the intended [2]rotaxane formation. The addition of base is known to increase the rate of CuAAC reactions,[75] and we hypothesized that enhancing the rate of the cycloaddition may favor the formation of the kinetic, interlocked products.

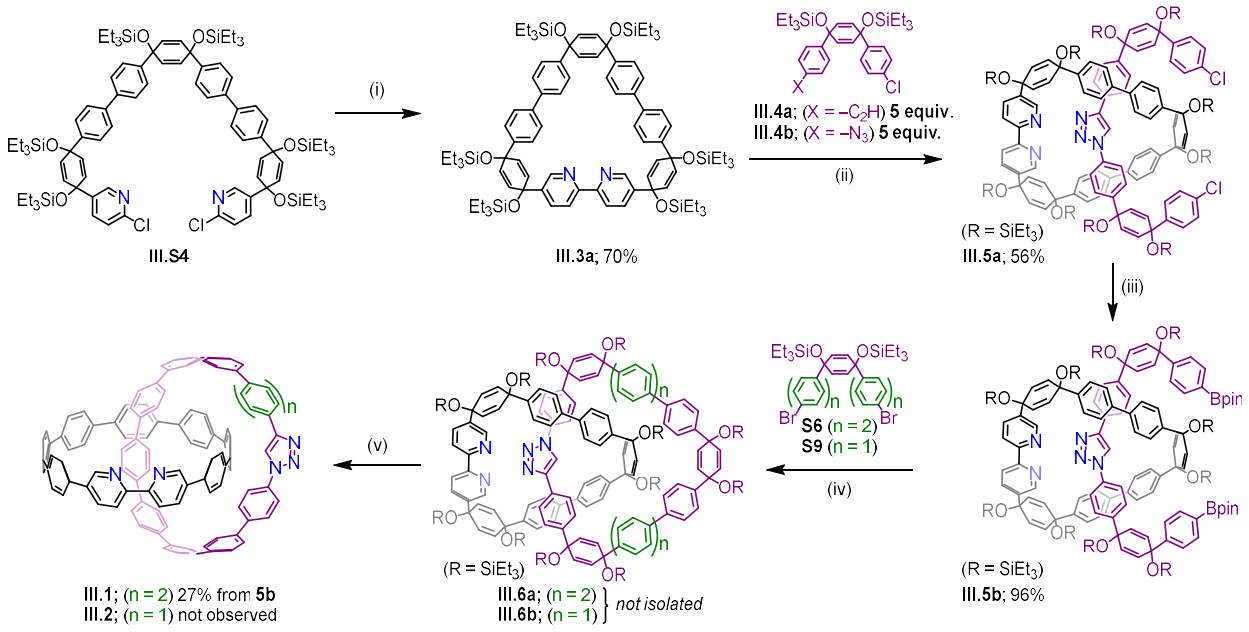

Figure III.2. Synthetic route to nanohoop [2]catenane **III.1** (a). Conditions: (i) $Ni(PPh_3)_2Br_2$, PPh_3, Mn, DMF, 60 ℃; (ii) $Cu(MeCN)_4PF_6$, $^{i}Pr_2NEt$, Toluene, 70 ℃; (iii) bis(pinacolato)diboron, $Pd(OAc)_2$, SPhos, K_3PO_4, dioxane, 80 ℃; (iv) SPhos Pd G3, 2M K_3PO_4 (aq) , dioxane, 80 ℃; Sodium naphthalenide, THF, -78 ℃.

Indeed, running the AT-CuAAC reaction under the same conditions, but with ^{i}PrNEt$_3$ as an additive, provided a dramatic rate increase (<10 min to reach completion) and, fortuitously, afforded [2]rotaxane **III.5a** in 56% isolated yield with respect to **III.3a**. **III.5a** could then be converted to bis(boronate) **III.5b** under standard Miyaura borylation conditions (96% yield), which further reacts with the V-shaped dihalide, **III.S6** via dilute Suzuki-Miyuara cross-coupling to give [2]catenane **III.6a** (not isolated). Finally, reduction of **III.6a** with sodium naphthalenide gives the fully π-conjugated [2]catenane **III.1** (101 mg, 27% two step yield), comprising a bipy[9]CPP catenated with a triazole embedded [12]CPP (Tz[12]CPP). This represents a substantial improvement in yield in comparison to our previous report in which the analogous 1,3-butadiyne containing structures gave yields ranging from 2-6% over the final two steps.

In an attempt to synthesize a more constricted [2]catenane, bis(boronate) **III.5b** was reacted with **III.S9** under the conditions used to access **III.6a**. However, this reaction gave only complex mixtures of oligomeric products and no clear evidence of the desired catenane formation. This is likely explained by a prohibitive degree of steric hindrance created by the large -SiEt$_3$ groups of **III.3a** that would have to be overcome to achieve the desired ring closure. To circumvent this issue, the -SiEt$_3$ substituents of **III.3a** were replaced with ^{n}Bu chains via desilylation and subsequent alkylation with n-bromobutane, providing macrocycle **III.3b** in 96% from **III.3a** (Fig. III.3a). ^{n}Bu groups were selected over shorter alkyl chains to maintain good solubility while still offering significant steric relief in comparison to the -SiEt$_3$ groups of **III.3a**. After performing the AT-CuAAC reaction with ligand **III.3b**, we were delighted to observe total conversion to the interlocked structure **III.5c** (95% isolated yield). Even after reducing the equivalents of the thread components **III.4a** and **III.4b** (1.5 equivalent each), complete conversion to **III.5c** (96% isolated

yield) was still observed (Fig. III.3b). These results demonstrate a profound substituent effect on the fidelity of macrocyclic ligand in the AT reaction that we had not previously anticipated. This seems especially interesting in that there is no clear explanation as to why the CuAAC reaction displays such a high degree of specificity towards the endotopic reaction pathway (i.e., forming interlocked products instead of externally catalyzing the cycloaddition reaction) considering the free rotation of the 2,2'-bipyridyl moiety in **III.3b**(**a**). Regardless, the efficiency of **III.3b** ranks among the most effective macrocyclic ligands known for the AT synthesis of MIMs.

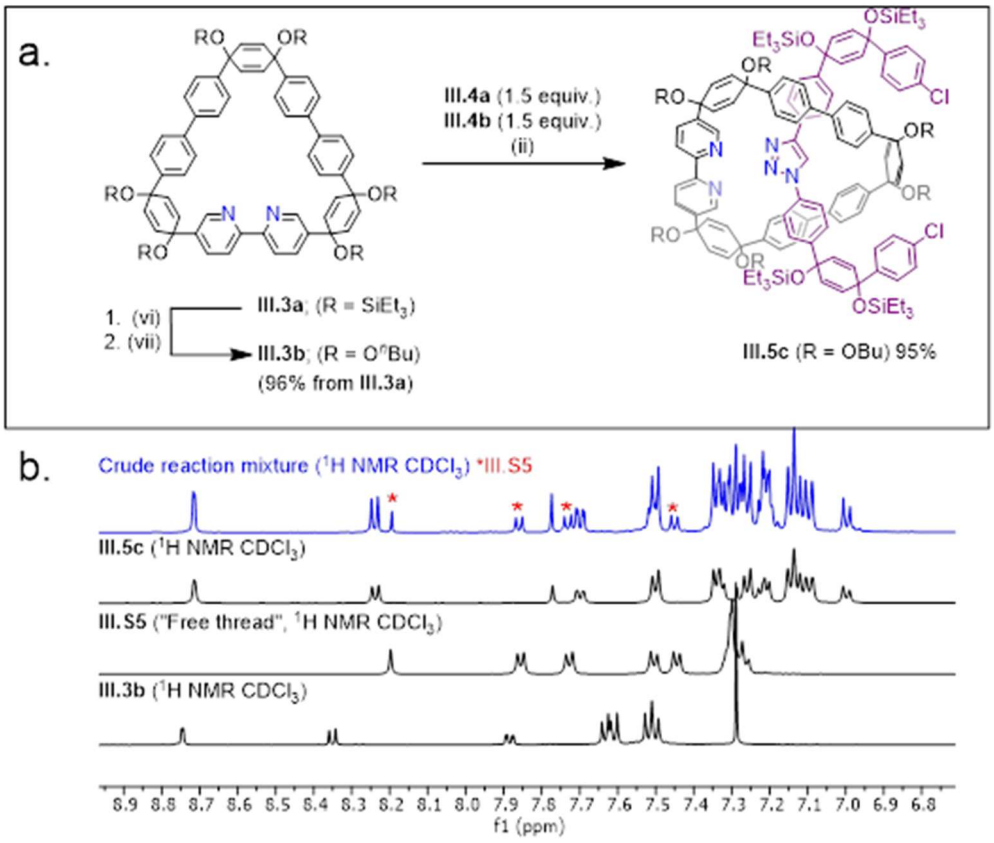

Figure III.3. (**a**) ^{1}H NMR spectrum of the crude reaction mixture for the AT-CuAAC reaction shown above, stacked against that of pure compounds **III.5c** (b), **III.S5** (c), and **III.3b** (d). Red asterisks in the upper (blue) spectrum mark peaks corresponding to the free thread, **III.S5.**

Conditions: (vi) TBAF, THF, rt; (vii) NaH, *n*-bromobutane, DMF, rt. (ii) $Cu(MeCN)_4PF_6$, $^iPr_2NEt$, Toluene, 70 ℃.

To test our ability to access the more tightly constricted [2]catenane now that the bipyridyl macrocycle had been decorated with less bulky *n*-butyl groups, **III.5c** was converted to bis(boronate) **III.5d**, and subsequently reacted **III.S9** under dilute Suzuki-Miyuara macrocyclization conditions. ^{1}H NMR spectra of the crude reaction mixture still indicated a complex mixture of products; however, distinct peaks in the spectrum were present that were consistent with the target molecule. While, in our hands, [2]catenane **III.6b** could not be isolated in high purity via traditional chromatographic methods, many of the impurities could be removed and, after subjecting the product-enriched mixture to reductive aromatization by sodium naphthalenide, **III.2**, was isolated in 8% yield from **III.5d** (Fig. III.4). Despite reducing the steric profile of the macrocyclic ligand, the formation of compact catenated structures via this Suzuki-Miyuara macrocyclization route remains challenging. However, the efficiency of the AT-CuAAC reaction renders this a highly efficient route for integrating nanohoops into interlocked architectures.

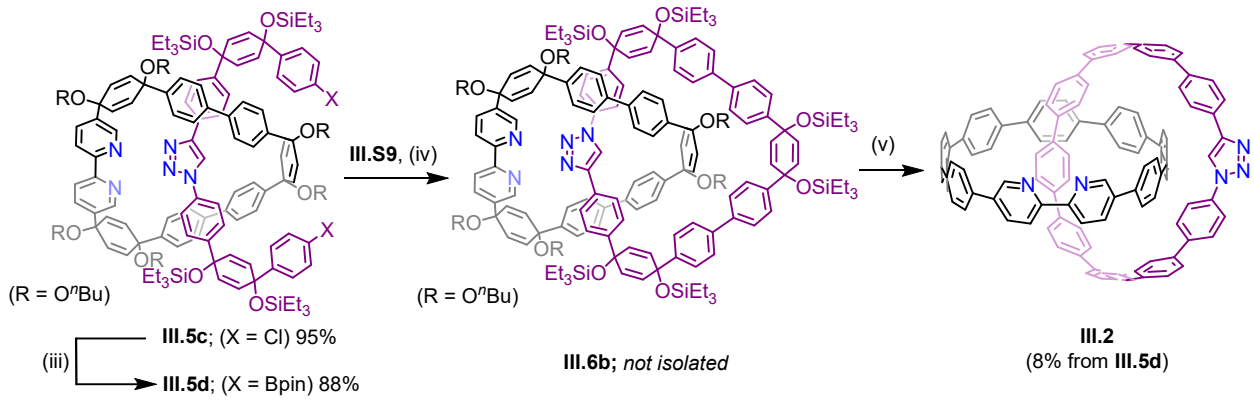

Figure III.4. Synthetic route to nanohoop[2]catenane **III.2**. Conditions: (iii) bis(pinacolato)diboron, $Pd(OAc)_2$, SPhos, K_3PO_4, dioxane, 80 ℃; (iv) SPhos Pd G3, 2M K_3PO_4 (aq) , dioxane, 80 ℃; Sodium naphthalenide, THF, -78 ℃.

3.2.3 X-ray crystallography and mass spectral analysis.

Single crystals of **III.1** suitable for x-ray diffraction were grown by vapor diffusion of hexanes into a solution of **III.1** in 1,4-dioxane unambiguously confirming its catenated structure (Fig. III.5a). The structure is highly solvated with many dioxane molecules being incorporated into the crystalline lattice (not shown). This largely precludes any significant intermolecular interactions between the π-surfaces of adjacent catenanes in the solid state. On the other hand, close contacts are observed between the interlocking bipy[9]CPP and Tz[12]CPP macrocycles, with the short contacts observed between non-bonded benzene rings being 3.41 Å. Despite our best efforts, we were unable to obtain suitable diffraction data from crystals of **III.2** to allow for the detailed analysis of the solid-state parameters. However, preliminary diffraction data from crystals grown via vapor diffusion of pentanes into a solution of **III.2** in $CHCl_3$ was sufficient to confirm the interlocked structure (Fig. III.5b). Additionally, isotopic distributions obtained via

HR-MS (ESI-TOF) are in excellent agreement with the calculated values further supporting our structural assignments (Fig. III.5c-d).

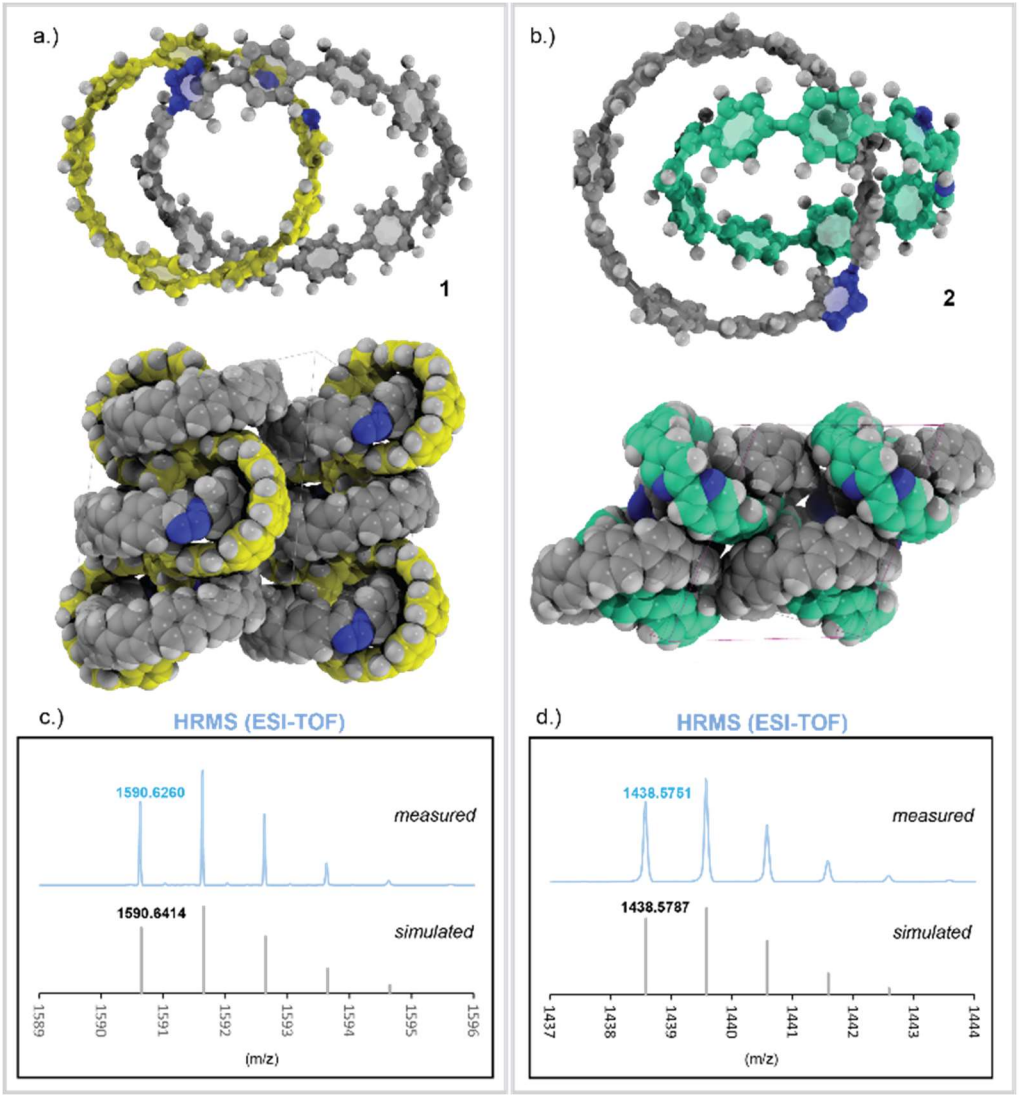

Figure III.5. (a-b) x-ray crystal structures of **III.1** (a) and **III.2** (b); showing the single-molecule (top) and their packing structures (bottom). Solvent molecules have been omitted for clarity. Carbon atoms are coloured yellow, green, or grey to distinguish between different macrocycles;

nitrogen atoms are coloured blue; hydrogen atoms are white. (c-d) Isotopic distributions for the molecular ions $[M+H]^+$ of catenanes **III.1** (c) and **III.2** (d) as measured by HRMS-ESI (blue trace) compared to their simulated distributions (grey trace).

3.2.4 Photophysical analysis.

The photophysical characteristics of **III.1** and **III.2** were probed via UV-Visible and fluorescence spectroscopy. The absorbance spectra of each catenane are consistent with the sum of the absorbance of the individual components suggesting that the nanohoop ground-state electronic properties are not significantly perturbed by the mechanical bond (Fig. III.6a-b). The emission profiles, however, are dominated by the **bipy[9]CPP** emission with no evidence of emission from the Tz[*n*]CPP component (Fig. III.6c). This phenomenon is now well established for nanohoop *hetero*[*n*]catenanes wherein energy transfer between the interlocked units results in emission being observed only from the smaller (furthest red emitting) nanohoop.[11,14] The effect of this process on the brightness of the emissive species, however, has not been directly studied. Specifically, we were curious if the **bipy[9]CPP** emission is sensitized by the Tz[*n*]CPP absorbance or if the quenching of the Tz[*n*]CPP emission occurs non-radiatively. In general, the fluorescent quantum yields of nanohoop catenanes **III.1** (Φ_F = 0.18) and **III.2** (Φ_F = 0.19) are similar to that of the free **bipy[9]CPP** (Φ_F = 0.22), while the molar extinction coefficients are significantly larger due to the presence of two absorbing species ($\varepsilon_{(\mathbf{III.1})}$ = 2.55 x 10^5 M^{-1}, $\varepsilon_{(\mathbf{III.2})}$ = 1.78 x 10^5 M^{-1}, $\varepsilon_{(\mathbf{bipy[9]CPP})}$= 1.09 x 10^5 M^{-1}). Taken together, **III.1** and **III.2** exhibit a 1.9 and 1.4 fold increase in apparent brightness, (brightness = ε x Φ_F) respectively, relative to *free* **bipy[9]CPP**. These results strongly suggest that the energy transfer in these systems is productive in terms of stimulating emission of the **bipy[9]CPP** component. This is further supported by

comparing the fluorescent excitation spectra of **III.1** and **III.2** at 510 nm which display profiles that are hypsochromically shifted relative to that of bipy[9]CPP, consistent with the contribution of Tz[*n*]CPP absorbance to **bipy[9]CPP** emission (Fig. III.6d). These results suggest that these types of systems, which exhibit high efficiency energy transfer between interlocking components, may be applicable in light harvesting systems.

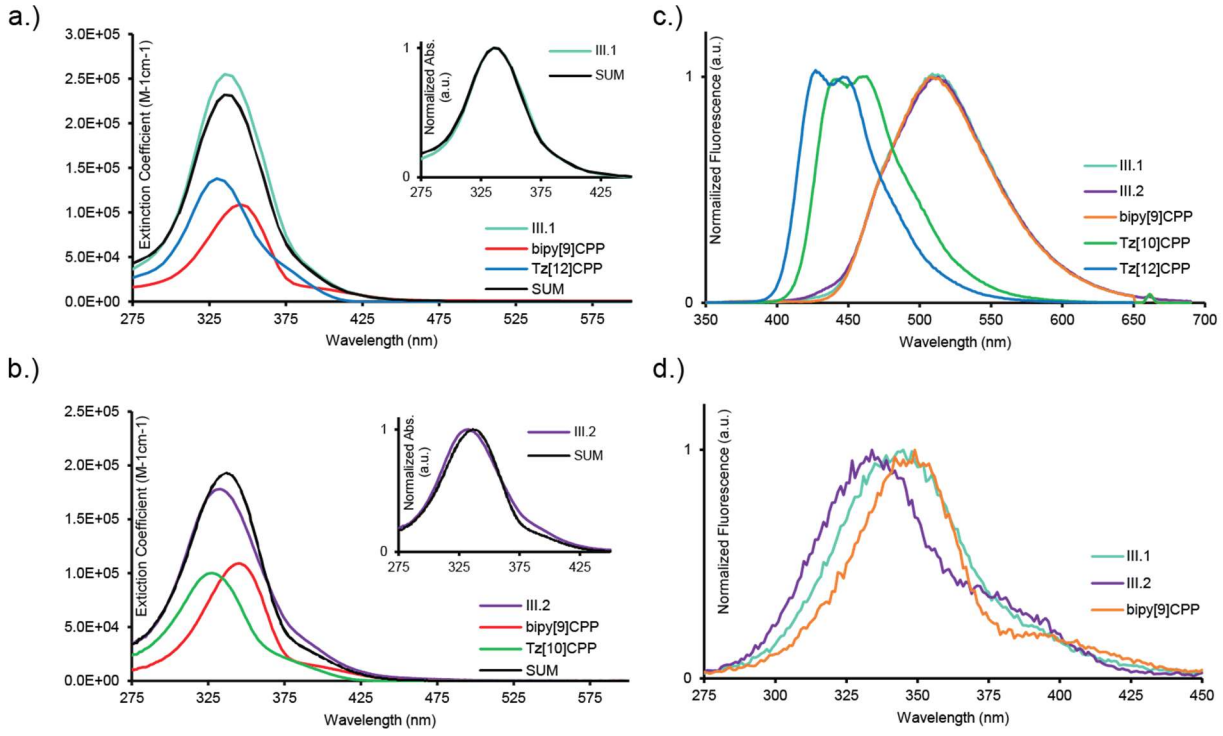

Figure III.6. (a-b) absorbance spectra of nanohoop[2]catenanes **III.1** (a) and **III.2** (b) plotted against their non-interlocked constituent macrocycles and normalized to their respective molar extinction coefficients. Traces labeled SUM (black traces) are given by the summation of the absorbance curves of bipy[9]CPP and Tz[12]CPP (a) or Tz[10]CPP (b). (c) normalized emission spectra of **III.1** and **III.2** plotted against that of their non-interlocked components. (d) normalized excitation spectra of **III.1** and **III.2** compared to that of bipy[9]CPP.

3.2.5 Complexation of III.1 with Pd(II)

Next, we were curious to investigate to the ability of the nanohoop catenanes to coordinate transition metals via the 2,2'-bipyridyl moiety of the **bipy[9]CPP** component. As a control, pristine **bipy[9]CPP** was treated with one equivalent of $Pd(MeCN)_2Cl_2$ in DCM which resulted in clean conversion to the metalated product and complete quenching of the **bipy[9]CPP** fluorescence (Fig. III.7a-b). Repeating this process with **III.1** also resulted in fluorescence quenching; however, ^1H NMR spectra of the crude product(s) indicates the formation of a mixture of metalated species (Fig. III.7c-d). Presumably this is due to the ability of both the 2,2'-bipyridine and triazole moiety to coordinate Pd(II), which could result in over-metalation of the catenane or, perhaps, the formation of oligomeric species with bridging metal centers. To investigate the evolution of these different complexes, a ^1H NMR titration experiment was conducted in which $Pd(MeCN)_2Cl_2$ was incrementally added to a solution of **III.1** in CD_2Cl_2 (Fig. III.7c-d). At lower sub-stochiometric equivalents of $Pd(MeCN)_2Cl_2$, only **III.1** and **Pd[III.1]diCl** are apparent in the NMR spectrum. However, upon subsequent additions of the Pd source, secondary species arise, even prior to the consumption of non-complexed **III.1**. Nevertheless, the monometallic **Pd[III.1]diCl** complex could be isolated from the filtrate of repeatedly washing the crude solids with hot acetone. Interestingly, the ^1H NMR spectrum of **Pd[III.1]diCl** shows a doubling of proton signals compared to that of **III.1**. This is especially pronounced in benzene-d_6 where there is greater degree of discrimination between aromatic proton signals (Fig. III.8) We hypothesize that this is due to the inability of the 2,2'-bipyridine unit to rotate on the NMR timescale when chelated to the metal ion, resulting in two discrete isomers differentiated by the orientation two possible orientations of the 1,2,3-triazole of the **Tz[12]CPP** relative to the 2-2'-bipyridine unit. The UV-Visible absorbance

of **Pd[III.1]diCl** is closely replicated by taking weighted sums of the absorbance spectra of **Pd[bipy[9]CPP]diCl** and **Tz[12]CPP** indicating that the optical properties of the metal complex are minimally influenced by the mechanical bond (Fig. III.9a).

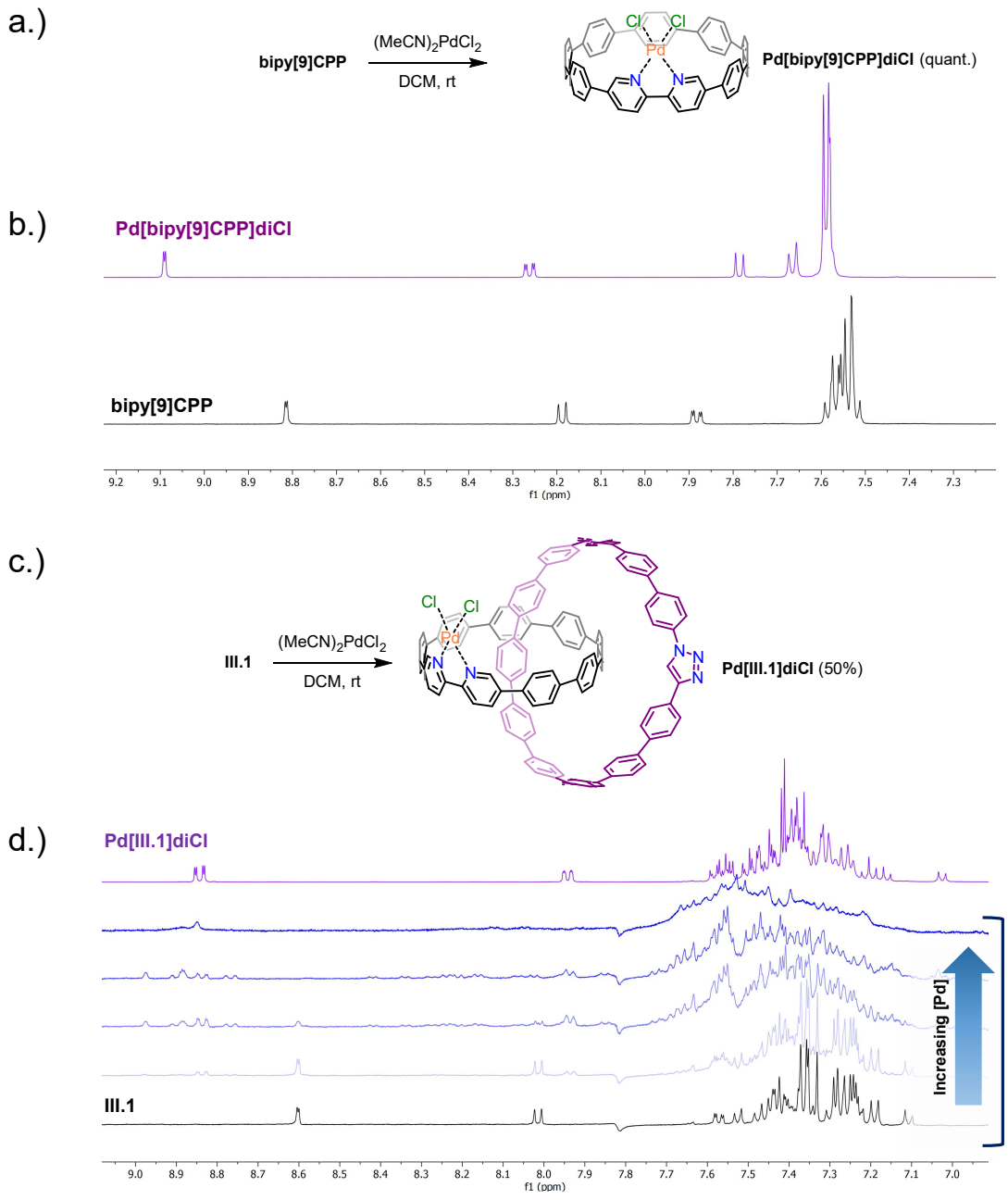

Figure III.7. Complexation of **bipy[9]CPP** and **III.1** with Pd[II]. (a) synthesis of

Pd[bipy[9]CPP]diCl. (b) 1H NMR (aromatic region) of **bipy[9]CPP** stacked with that of **Pd[bipy[9]CPP]diCl**. (c) synthesis of **Pd[III.1]diCl**. (d) 1H NMR titration of **III.1** with $Pd(MeCN)_2Cl_2$ (lower 5 traces) stacked below the purified **Pd[III.1]diCl** (top, purple trace).

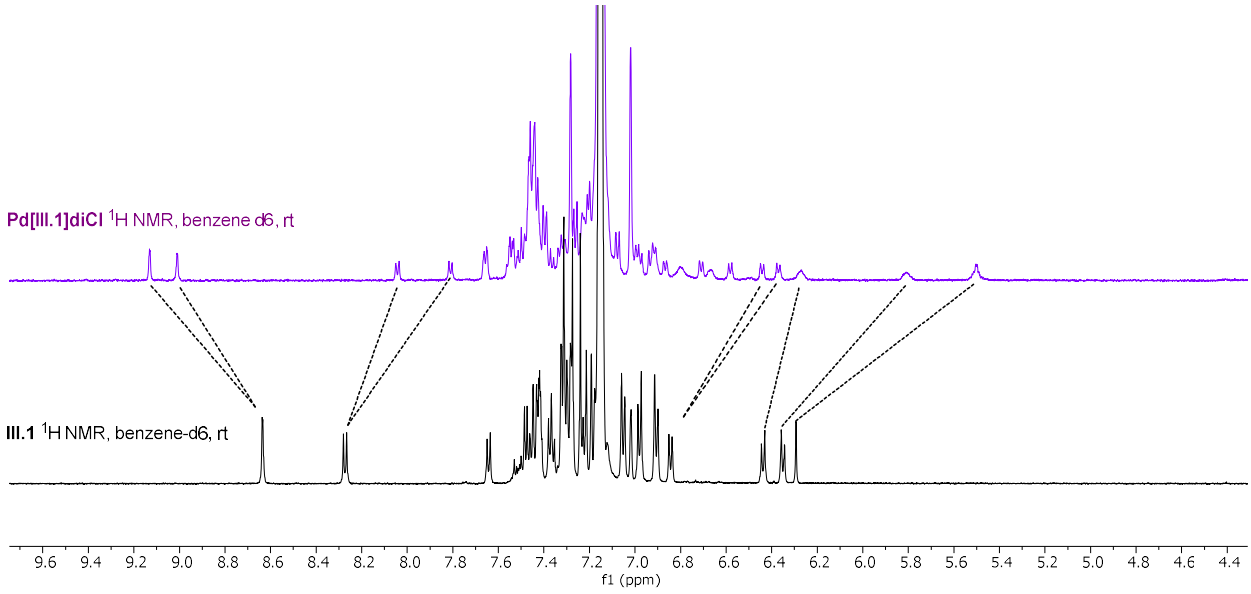

Figure III.8. ^{1}H NMR (600 MHz, benzene d6, rt) of **Pd[III.1]diCl** showing the doubling of proton signals compared to that of **III.1** demonstrating the broken symmetry of the complex.

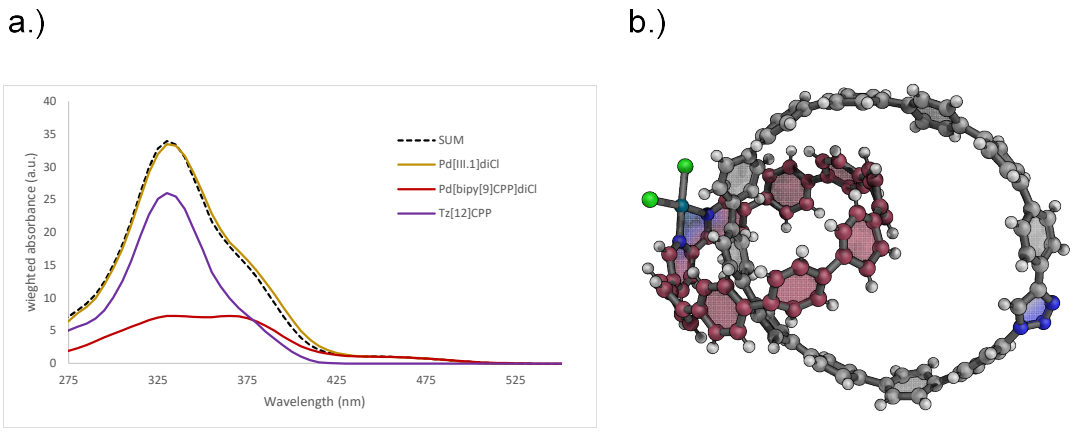

Figure III.9. (a) UV-Visible absorbance spectrum of **Pd[III.1]diCl** ploted against that of **Pd[bipy[9]CPP]diCl** and **Tz[12]CPP**. Weighted absorbance values are arbitrary and were chosen

such that $abs(\lambda)_{Pd[bipy[9]CPP]diCl} + abs(\lambda)_{Tz[12]CPP} \sim abs(\lambda)_{Pd[1.III]diCl}$. (b) X-ray crystal strucure of **Pd[III.1]diCl** unambigiously confirming its molecular structure.

3.2.6 Multicomponent AT-CuAAC reactions.

Owing to the effieicincy obvserved in the AT-CuAAC reaction under the conditions optimized for macrocycle **III.3b**, we were interested in the possibility of generating catenated structures directly from the mechanical bond forming step. To accomplish this we designed thread unit **III.4c** which containes both azide and alkyne functionalities. Indeed, by slowly adding solution of **III.4c** (6 equiv.) to a solution of **III.3b**, $Cu(MeCN)_4PF_6$, and $^{i}Pr_2NEt$ over the course of the 2 h, [2]catenane **III.6c** was obtained in 30% yield (Fig. III.10). Dispite the the three click reactions which occur to formation of the trimeric macrocycle, higher-order catenanes were not observed in the reaction mixture. This might be explained by steric inhibition of the intramolecular cyclization reaction resulting in the polymerization of higher any order [*n*]rotaxanes intermediates. Alternatively, it may be that the existence of a mechanical bond discorages AT reactions at the adjacent reaction cites, also due to steric constraints.

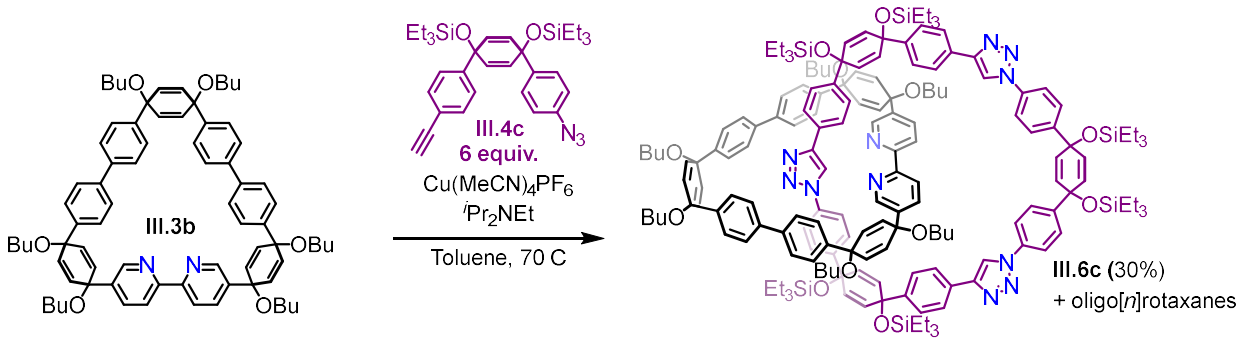

Figure III.10. Multicomponent AT-CuAAC synthesis of [2]catenane **III.6c.**

To test this, we conducted a multicomponet AT-CuAAC reaction between dialkyne **III.4d** (1 equiv.) and azide **III.4b** (2 equiv.) in the presence of ligand **III.3b** (1 equiv.) and the Cu^{I} catalyst (0.9 equiv.) (Fig. III.11a). Following the consumption of **III.4d** and **III.4b**, the reaction mixture was analyzed via ^{1}H NMR spectroscopy (Fig. III.11b). The crude mixture consists of one major descrete interlocked product in addition to unreacted **III.3b** in approximately an 1:1 ratio. While separation of the products proved difficult, after column chromatography a less complex ("Purified" mixture) mixture could be obtained which clearly indicates the presence of both [2]rotaxane **III.5e** and [3]rotaxane **III.5f**.

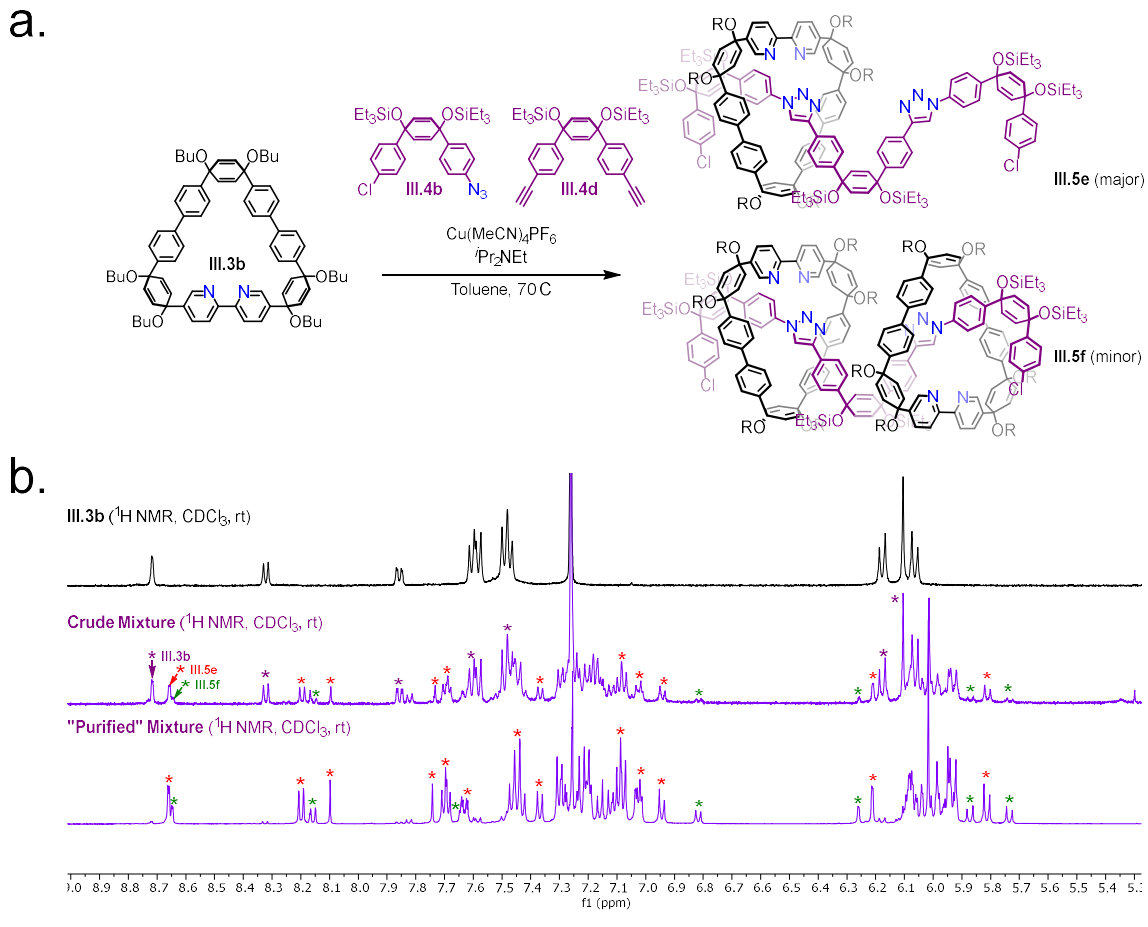

Fig III.11. (a) Multicompent AT-CuAAC reaction between **III.4b** and **III.4d** with ligand **III.3b**. (b) 1H NMR spectra ($CDCl_3$, rt) of the crude reaction mixture (middle purple trace) and the purified mixture (lower purple trace) stacked with that of **III.3b**. Colored asterisks are used to mark peaks assigned to **III.3b** (purple), **III.5e** (red) and **III.5f** (green).

The major interlocked product signals are easily assigned to [2]rotaxane **III.5e** owing to the two distinct triazole proton signals (d = 7.742 ppm, d = 8.098 ppm), which are indicative of the assmetrical [2]rotaxane. While the purified mixture is enriched in **III.5f**, the relative integrations of ^{1}H signals in the crude mixture shows that the [2]rotaxane (**III.5e**) is formed in a roughly ten-fold excess over **III.5f**, clearly demonstrating the inhibitory effect of the initial mechanical bond formation on adjacent AT reactions.

3.3 Conclusion.

In conclusion, we report a highly efficient active template route to nanohoop[2]catenanes via the azide-alkyne cycloaddition (AT-CuAAC) reaction. Specifically, we show that, with the correct choice of substituents, a macrocyclic precursor to bipy[9]CPP can participate in the AT-CuAAC to give quantitative conversion to [2]rotaxanes even at low loadings of the cycloaddition precursors. The efficiency observed for the AT reactions reported herein places **3b** among the most effective macrocyclic ligands reported and represents a powerful approach to integrate nanohoops into mechanically interlocked systems.

3.4 Methods and Materials

3.4.1. General Experimental Details

Commercially available materials were used without purification. Moisture and oxygen sensitive reactions were carried out in flame-dried glassware and under an inert atmosphere of purified nitrogen using syringe/septa technique. Tetrahydrofuran (THF), and 1,4-dioxane were dried by filtration through alumina according to the methods described by Grubbs. Column chromatography was conducted with Zeochem Zeoprep n60 Eco 40-63 μm silica gel. Alumina column chromatography was conducted with Sorbtech Alumina ,basic (pH 10), Act. II-III, 50-200 μm. 1H and 13C NMR spectra were recorded on either a Bruker Avance III HD 500 (1H: 500 MHz, 13C: 126 MHz) or Bruker Avance III HD 600 MHz (1H: 600 MHz, 13C: 151 MHz) NMR spectrometer equipped with a Prodigy multinuclear cryoprobe, respectively. All samples were measured at 25 °C. ^{1}H and ^{13}C NMR spectra were taken in either $CDCl_3$ (referenced to TMS, δ = 0.00 ppm) or CD_2Cl_2 (referenced to dichloromethane δ(1H) = 5.32 ppm, δ(13C) = 54.00 ppm). Coupling constants (J) are given in Hz and the apparent resonance multiplicity is reported as s (singlet), d (doublet), t (triplet), q (quartet), quint (quintet) or m (multiplet). Absorbance and fluorescence spectra were obtained in a 1 cm Quartz cuvette with dichloromethane using an Agilent Cary 100 UV-Vis spectrometer and a Horiba Jobin Yvon Fluoromax-4 Fluorimeter respectively. Compounds **III.S1**, **III.S2**, **III.S3**, **III.S6**, **III.4a**, **III.S7**, **III.S9**, and **bipy[9]CPP** were synthesized according to literature procedures.

3.4.2. Synthetic Procedures

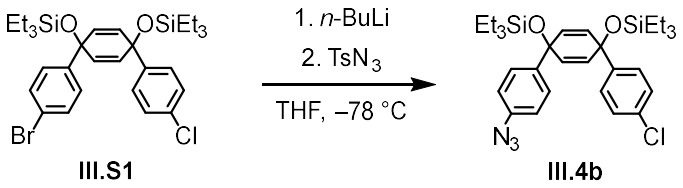

Synthesis of III.4b. To a flame dried 50 mL round bottom flask was added **III.S1** (5.00 g, 8.25 mmol). The flask was evacuated and backfilled with N_2 gas three times before introducing THF (40 mL). The flask was then submerged in a dry-ice acetone bath and the solution was stirred for 20 minutes before adding n-butyl lithium (*n*-BuLi; 3.30 mL, 8.25 mmol, 2.5 M solution in hexanes) dropwise. The mixture was stirred for 5 minutes after which tosyl azide (1.63 g, 8.25 mmol) was added, causing the reaction mixture to become a deep purple color. The reaction was stirred for an additional 20 minutes before quenching the reaction with H_2O (20 mL). The THF was removed under reduced pressure and the remaining aqueous mixture was extracted with hexanes (3 x 15 mL). The organic layers were combined and dried over Na_2SO_4 before passing the solution through a short silica plug, using hexanes as eluent. Removal of the solvent provides **III.4b** as a pale yellow-brown colored oil (4.43 g, 95%). ^{1}H NMR (500 MHz, Chloroform-*d*) δ 7.29 (d, *J* = 8.7 Hz, 2H), 7.23 (s, 4H), 6.93 (d, *J* = 8.6 Hz, 2H), 5.97 (d, *J* = 10.3 Hz, 3H), 5.94 (d, *J* = 10.3 Hz, 4H), 0.95 – 0.90 (m, 18H), 0.63 – 0.56 (m, 12H). ^{13}C NMR (126 MHz, Chloroform-*d*) δ 144.52, 142.74, 139.04, 133.07, 131.54, 131.33, 128.28, 127.32, 127.24, 118.79, 71.09, 71.05, 7.02, 6.44, 6.42. HRMS (ASAP) (m/z): [M]+ calculated for $C_{30}H_{42}N_3O_2Si_2$, 567.2504; found, 567.2476.

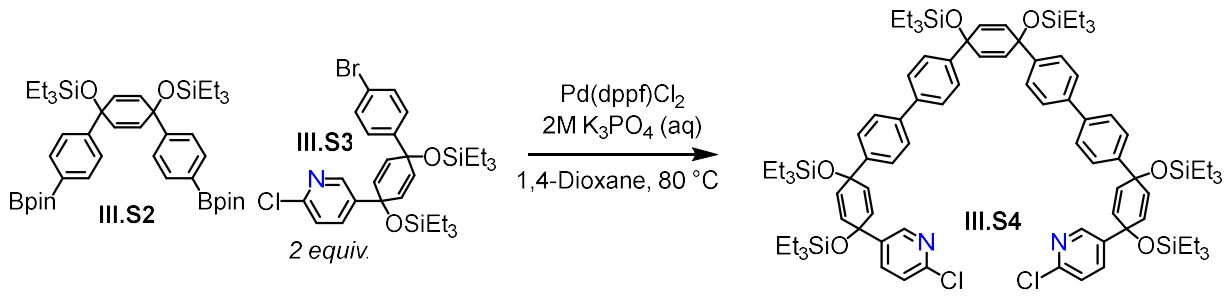

Synthesis of III.S4. To a 50 mL round bottom flask were added **III.S2** (3.10 g, 4.16 mmol), **III.S3** (5.05 g, 8.32 mmol) and **Pd(dppf)Cl$_2$-CH$_2$Cl$_2$** (0.340 g, 0.42 mmol) The flask was then evacuated and backfilled with N_2 gas three times before introducing 1,4-dioxane (50 mL). The resulting mixture was heated to 80 °C at which point K_3PO_4 (2 mL, 2M in H_2O) was introduced. The resulting red-black solution was stirred at 80 °C for 16 h. The reaction was removed from heat and allowed to cool to room temperature before transferring the reaction mixture into a separatory funnel with the aid of EtOAc (20 mL) and H_2O (20 mL). The organic layer was collected, and the aqueous layer was washed with two additional 10 mL portions of EtOAc. The organic layers were combined and washed with H_2O (20 mL) and brine (20 mL) before drying over sodium sulfate (Na_2SO_4). The solvent was evaporated under reduced pressure and the crude material was purified via column chromatography (SiO_2; 0-3% EtOAc in hexanes) to give **III.S4** as a white foam (5.25 g, 82%). ^{1}H NMR (500 MHz, Chloroform-*d*) δ 8.36 (d, *J* = 2.5 Hz, 2H), 7.56 – 7.49 (m, 10H), 7.43 (d, *J* = 8.4 Hz, 4H), 7.36 (d, *J* = 8.4 Hz, 4H), 7.17 (d, *J* = 8.4 Hz, 2H), 6.13 (d, *J* = 10.1 Hz, 4H), 6.04 (s, 4H), 5.92 (d, *J* = 10.1 Hz, 4H), 0.99 – 0.88 (m, 55H), 0.68 – 0.61 (m, 24H), 0.57 (q, *J* = 8.0 Hz, 12H). ^{13}C NMR (126 MHz, Chloroform-*d*) δ 150.13, 147.88, 145.29, 144.36, 140.66, 140.01, 139.33, 136.51, 132.55, 131.52, 130.36, 127.03, 126.77, 126.35, 126.10, 123.52, 71.38, 70.97, 70.14, 7.09, 7.01, 6.50, 6.47, 6.39. HRMS (ASAP) (m/z): [M]+ calculated for $C_{88}H_{124}Cl_2N_2O_6Si_6$, 1542.7452; found, 1542.7366.

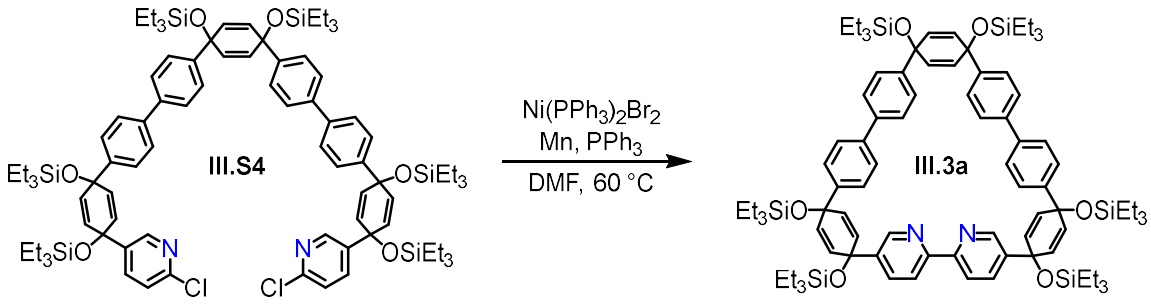

Synthesis of III.3a. To a flame dried 250 mL three-neck flask fitted with a 100 mL addition funnel were added $Ni(PPh_3)_2Br_2$ (2.16 g, 2.91 mmol, 1.5 equiv.), Mn (0.320 g, 5.82 mmol, 3 equiv.) and PPh_3 (1.56 g, 5.82 mmol, 3 equiv.). The apparatus was evacuated and backfilled with N_2 gas three times before introducing DMF (50 mL). The resulting mixture was sparged with sonication for 20 min causing the initially green mixture to become red-orange in color. The mixture was then made to stir in an oil bath set to 60 °C for 1 h. An N_2 sparged solution of **III.S4** (3.00 g, 1.94 mmol, 1 equiv.) was then transferred into the addition funnel and added to the catalyst mixture dropwise over the course of 2 h. Following complete addition of **III.S4**, the reaction was stirred at 60 °C for 1 h under an N2 atmosphere. The reaction mixture was then transferred into a separatory funnel along with an aqueous solution of ammonia (18 w/w%) containing ethylenediaminetetraacetic acid disodium salt (NH_3-EDTA, 200 mL) and extracted with Et_2O (4 x 60 mL). the organic layers were combined and washed with NH_3-EDTA (150 mL), H_2O (100 mL), and brine (100 mL) before drying over Na_2SO_4. The solvent was evaporated under reduced pressure and the crude material was purified via column chromatography (Al_2O_3; 0-30% DCM in hexanes) to provide **III.3a** as a white solid (1.96 g, 68%). ^{1}H NMR (500 MHz, Methylene Chloride-d_2) δ 8.63 (d, J = 2.3 Hz, 2H), 8.34 (d, J = 8.3 Hz, 2H), 7.77 (dd, J = 8.3, 2.3 Hz, 2H), 7.65 – 7.58 (m, 8H), 7.48 – 7.42 (m, 8H), 6.14 (d, J = 10.1 Hz, 4H), 6.06 (s, 4H), 6.03 (d, J = 10.1 Hz, 8H), 1.03 – 0.94 (m, 56H), 0.73 – 0.61 (m, 39H). ^{13}C NMR (126 MHz, Methylene Chloride-d_2) δ 154.71, 147.31, 145.40, 145.07, 141.78, 139.46, 139.10, 134.34, 132.22, 131.59, 130.80, 126.69, 126.57, 126.46, 126.33, 120.20,

71.65, 71.30, 70.66, 6.93, 6.90, 6.59, 6.53, 6.51. HRMS (ASAP) (m/z): [M]+ calculated for $C_{88}H_{124}N_2O_6Si_6$, 1472.8075; found, 1472.8063.

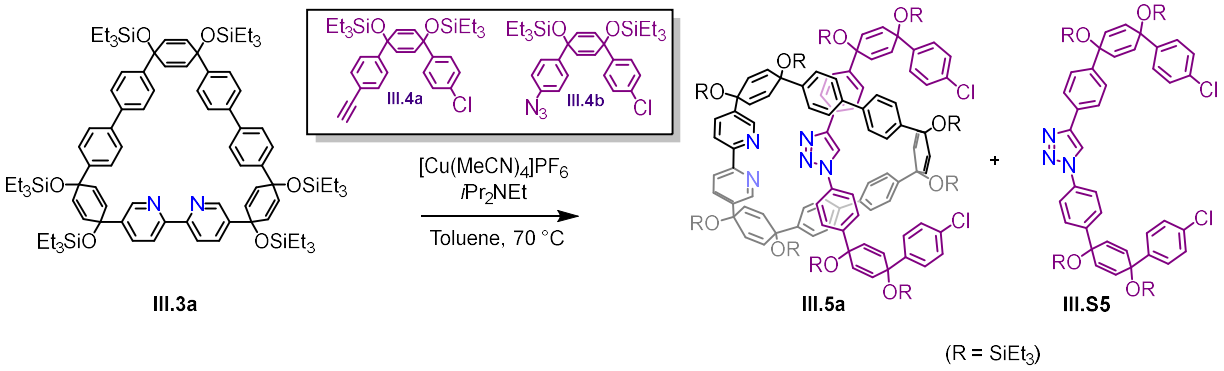

Synthesis of 5a. To a flame dried 100 mL round bottom flask was added **III.3a** (0.700 g, 0.47 mmol) and $[Cu(MeCN)_4]PF_6$ (0.159 g, 0.43 mmol). The flask was evacuated and backfilled with N_2 gas three times before introducing toluene (50 mL). The resulting mixture was sparged with N_2 while sonicating for 15 minutes before heating to 70 °C. The mixture was stirred at this temperature for an additional 15 minutes before adding N,N-diisoproylethylamine (iPr$_2$NEt, 0.41 mL, 2.37 mmol) and, subsequently, a solution containing **III.4a** (1.31 g, 2.37 mmol) and **III.4b** (1.35 g, 2.37 mmol) in toluene (30 mL). The reaction mixture was stirred at 70 °C under a N_2 atmosphere for 1.5 h at which point the reaction mixture was transferred into a separatory funnel along with an aqueous solution of ammonia (18 w/w%) containing ethylenediaminetetraacetic acid disodium salt (NH_3-EDTA (aq), 20 mL). The mixture was emulsified and allowed to separate before collecting the organic layer. The aqueous layer was then extracted with EtOAc (2 x 10 mL) before combining and drying organic layers over Na2SO4. The solvent was evaporated under reduced pressure and the crude residue was triturated with 10 mL acetone before cooling in a brine-ice bath for 30 minutes. The resulting precipitate was collected by vacuum filtration and washed

with cold acetone (5 mL) to recover unthreaded **III.3a** as a white crystalline solid (0.274 mg, 39%). The filtrate was consolidated, and the solvent was removed under reduced pressure. The resulting material was then purified via column chromatography (Al_2O_3; 0 - 3% EtOAc in hexanes) to give **III.5a** (first to elute) as a white foam (0.687 g, 56%) and the free cycloaddition product, **III.S5**, as a viscous yellow oil which crystallizes over several weeks (1.98 g, 75%). **III.5a**: ^{1}H NMR (500 MHz, Methylene Chloride-d_2) δ 8.65 (d, J = 2.4 Hz, 2H), 8.13 (d, J = 8.4 Hz, 2H), 7.60 (dd, J = 8.4, 2.3 Hz, 2H), 7.52 (s, 1H), 7.43 (d, J = 8.2 Hz, 4H), 7.35 – 7.30 (m, 6H), 7.27 – 7.19 (m, 8H), 7.19 – 7.13 (m, 6H), 7.13 – 7.08 (m, 4H), 7.06 (d, J = 8.5 Hz, 2H), 7.02 (d, J = 8.5 Hz, 2H), 6.19 (s, 2H), 6.11 – 6.06 (m, 6H), 6.02 – 5.90 (m, 12H), 1.01 – 0.91 (m, 90H), 0.71 – 0.57 (m, 60H). ^{13}C NMR (126 MHz Methylene Chloride-d_2) δ 155.00, 147.82, 147.49, 146.58, 146.10, 145.82, 145.32, 145.24, 145.21, 142.43, 139.93, 139.31, 136.29, 134.68, 133.63, 133.42, 133.04, 132.39, 132.19, 132.17, 132.01, 131.94, 131.76, 131.61, 130.85, 130.04, 128.89, 128.76, 127.85, 127.84, 127.48, 127.29, 127.05, 126.71, 126.46, 126.43, 120.90, 120.86, 119.34, 71.74, 71.70, 71.67, 71.60, 71.52, 71.44, 70.98, 7.46, 7.44, 7.42, 7.39, 7.38, 7.03, 7.01, 6.99, 6.95. MS (MALDI) (m/z): [M+H]+ calculated for $C_{150}H_{210}Cl_2N_5O_{10}Si_{10}$, 2591.3147; found, 2591.7; **III.S5**: ^{1}H NMR (500 MHz, Chloroform-*d*) δ 8.17 (s, 1H), 7.83 (d, J = 8.0 Hz, 2H), 7.70 (d, J = 8.2 Hz, 2H), 7.48 (d, J = 8.3 Hz, 2H), 7.42 (d, J = 8.2 Hz, 2H), 7.31 – 7.21 (m, 8H), 6.09 – 5.94 (m, 8H), 1.02 – 0.89 (m, 36H), 0.70 – 0.55 (m, 24H). ^{13}C NMR (126 MHz, Chloroform-*d*) δ 148.11, 146.73, 146.12, 144.56, 144.38, 136.03, 133.24, 133.00, 131.70, 131.60, 131.35, 131.30, 129.26, 128.40, 128.27, 127.29, 127.25, 127.23, 126.44, 125.71, 120.20, 117.50, 77.28, 77.03, 76.78, 71.30, 71.20, 71.16, 71.00, 7.05, 7.02, 6.46, 6.43, 6.42. HRMS (ASAP) (m/z): [M]+ calculated for $C_{62}H_{85}Cl_2N_3O_4Si_4$, 1117.4994; found, 1117.4994.

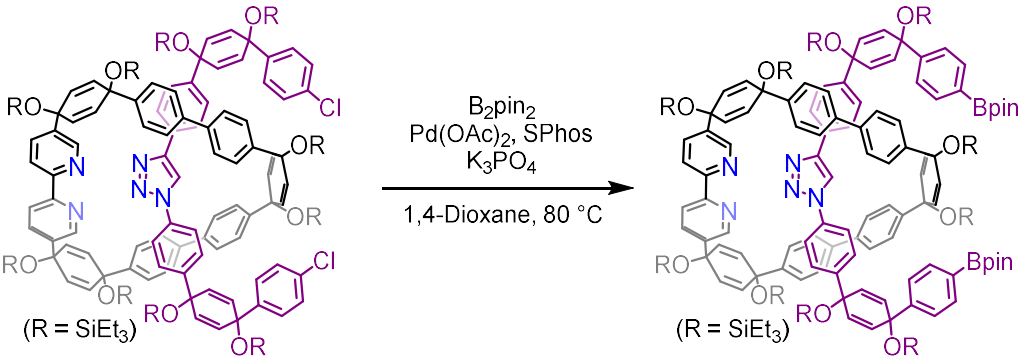

III.5a III.5b

Synthesis of 5b. To a flame dried 50 mL round bottom flask were added **III.5a** (0.687 g, 0.26 mmol)**,** bis(pinacolato)diboron (B_2pin_2, 0.336 g, 1.32 mmol), $Pd(OAc)_2$ (0.030 g, 0.13 mmol), SPhos (0.076 g, 0.19 mmol), and tribasic potassium phosphate (K_3PO_4, 0.450 g, 2.12 mmol). The flask was evacuated and backfilled with N_2 gas five times before introducing 1,4-dioxane (10 mL). The mixture was stirred at 80 °C for 5 h. The reaction was removed from heat and diluted with 30 mL hexanes. After cooling to room temperature, the reaction mixture was poured over a short silica plug topped with celite. The plug was washed with hexanes (50 mL) followed by DCM (150 mL). The eluate was concentrated under reduced pressure and the resulting residue was sonicated with MeOH (50 mL) until a flocculent precipitate had formed. The precipitate was collected by vacuum filtration and washed with MeOH (50 mL) to give **III.5b** as a tan colored solid (0.705 g, 96%). 1H NMR (500 MHz, Methylene Chloride-*d*2) δ 8.61 (d, *J* = 2.3 Hz, 2H), 8.16 (d, *J* = 8.3 Hz, 2H), 7.66 (d, *J* = 8.2 Hz, 2H), 7.61 (d, *J* = 8.0 Hz, 2H), 7.58 (dd, *J* = 8.4, 2.3 Hz, 2H), 7.53 (s, 1H), 7.37 (d, *J* = 8.4 Hz, 4H), 7.34 – 7.25 (m, 10H), 7.21 (d, *J* = 8.5 Hz, 4H), 7.18 (d, *J* = 8.5 Hz, 4H), 7.08 (d, *J* = 8.5 Hz, 2H), 7.02 (d, *J* = 8.6 Hz, 2H), 6.95 (d, *J* = 8.8 Hz, 2H), 6.16 (d, *J* = 2.1 Hz, 2H), 6.07 – 5.96 (m, 12H), 5.94 – 5.90 (m, 4H), 5.84 (d, *J* = 10.1 Hz, 2H), 1.34 (s, 12H), 1.32 (s, 12H), 0.98 – 0.88 (m, 90H), 0.68 – 0.54 (m, 60H). ^{13}C NMR (126 MHz, Methylene Chloride-*d*2) δ 155.00, 149.60, 149.49, 147.82, 147.42, 146.73, 146.24, 145.68, 145.14, 142.27, 139.80,

139.25, 136.19, 135.38, 135.26, 134.61, 133.01, 132.30, 132.13, 131.98, 131.87, 131.72, 131.61, 130.78, 129.93, 127.47, 127.28, 126.99, 126.63, 126.43, 126.38, 126.35, 125.62, 120.97, 120.88, 119.40, 84.35, 84.26, 72.01, 71.84, 71.76, 71.65, 71.58, 71.44, 70.99, 25.30, 25.27, 7.47, 7.46, 7.42, 7.41, 7.39, 7.37, 6.99, 6.98, 6.96, 6.93. MS (MALDI) (m/z): [M]+ calculated for $C_{162}H_{234}B_2N_5O_{14}Si_{10}$, 2775.5631; found, 2775.9.

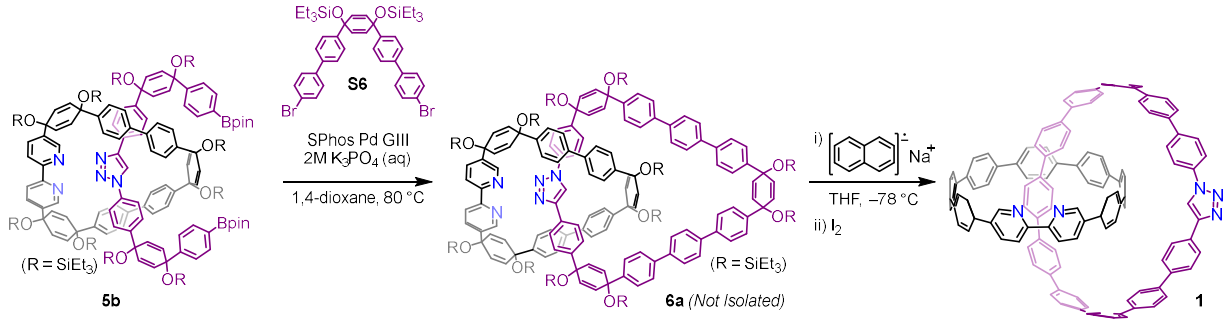

Synthesis of III.1. To a 500 mL round bottom flask were added **III.5b** (0.705 g, 0.25 mmol), **III.S6** (0.224 g, 0.28 mmol) and Pd SPhos GIII (0.100 g, 0.013 mmol). The flask was evacuated and backfilled with N_2 gas five times before introducing 1,4-dioxane (200 mL). The resulting mixture was heated to 80 °C. An aqueous solution of K_3PO_4 (2M, 5 mL) was then added and the reaction was stirred overnight. The following morning the reaction was removed from heat and allowed to cool to room temperature. NH_3-EDTA (aq) (50 mL) was added, and the mixture was stirred vigorously for 30 minutes. The solvent was removed under reduced pressure and the crude material was transferred into a separatory funnel with the aid of DCM (50 mL) and H_2O (100 mL). The organic layer was collected, and the aqueous layer was extracted twice more with DCM (2 x 25 mL). The organic layers were combined and dried over Na_2SO_4 before passing through a short silica plug, using DCM as eluent. The eluate was evaporated under reduced pressure and the crude material was transferred into a flame dried 100 mL round bottom flask. The

flask was evacuated and backfilled with N_2 gas three times before introducing THF (50 mL). The resulting solution was then cooled to -78 °C at which point sodium napthalenide (7.5 mL, 0.42 M in THF) was added, dropwise. The resulting dark purple solution was allowed to stir for 2 h at -78 °C after which point I_2 (0.4 M in THF) was added until the reaction mixture had turned orange. A saturated aqueous solution of $Na_2S_2O_3$ (25 mL) was then added quench any excess iodine. The THF was then removed under reduced pressure and the remaining aqueous suspension was extracted with DCM (5 x 20 mL). The organic layers were combined and dried over Na_2SO_4 before removing the solvent under reduced pressure. The product was purified via column chromatography (Al_2O_3: 60% DCM, 0-10% EtOAc in hexanes) to provide **III.1** as a bright yellow solid (0.101 g, 27% over two steps).

*Material of single crystalline purity may be achieved by diffusing hexanes into a concentrated solution of 1 in 1,4-dioxane.

^{1}H NMR (600 MHz, Methylene Chloride-d_2) δ 8.62 (d, J = 2.4 Hz, 2H), 8.03 (d, J = 8.5 Hz, 2H), 7.59 (dd, J = 8.5, 2.3 Hz, 2H), 7.54 (d, J = 8.6 Hz, 2H), 7.49 (d, J = 8.7 Hz, 4H), 7.48 – 7.33 (m, 41H), 7.34 – 7.22 (m, 27H), 7.20 (d, J = 8.8 Hz, 4H), 7.12 (d, J = 8.8 Hz, 2H). ^{13}C NMR (126 MHz, Methylene Chloride-d_2) δ 154.22, 148.36, 146.08, 140.16, 139.99, 139.03, 138.65, 138.56, 138.53, 138.43, 138.41, 138.22, 138.19, 138.18, 138.16, 138.12, 138.09, 137.91, 137.77, 137.55, 137.51, 137.16, 135.97, 134.57, 133.28, 132.15, 129.31, 127.61, 127.56, 127.38, 127.31, 127.27, 127.23, 127.19, 127.16, 127.14, 127.12, 127.08, 126.57, 125.54, 121.83, 120.9. MS (MALDI) (m/z): [M-N_2]+ calculated for $C_{120}H_{79}N_3$, 1561.6274; found, 1561.2.

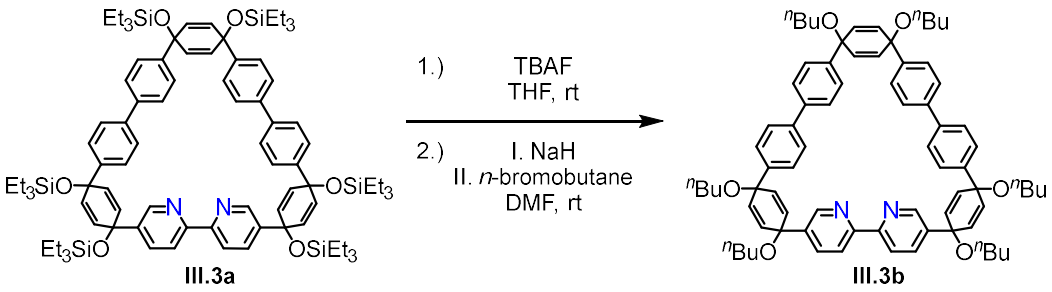

III.3a III.3b

Synthesis of III.3b. To a flame dried 100 mL round bottom flask was added **3a** (0.800 g, 0.54 mmol). The flask was evacuated and backfilled with N_2 gas three times before introducing THF (60 mL). tetra *n*-butylammonium fluoride (TBAF, 5.43 mL, 5.43 mmol, 1M in THF) was added and the reaction was stirred for 30 min. at room temperature. The solvent was removed under reduced pressure and the resulting yellow-brown oil was triturated with H_2O (25 mL) until a filterable solid had formed. The precipitate was collected by vacuum filtration and washed with H_2O (10 mL), acetone (10 mL), and DCM (10 mL). The desilylated material was allowed dried on the filter paper for 30 minutes before transferring the solid into a flame dried 100 mL round bottom flask. To a separate flame dried 100 mL round bottom flask was added sodium hydride (NaH, 0.269 g, 10.85 mmol). Both flasks were evacuated and backfilled with N_2 gas three times before introducing DMF (20 mL into each flask). The flask containing the NaH suspension was cooled to 0℃ with stirring after which the contents of the second flask were introduced via dropwise cannulation. The resulting suspension was stirred for 1 h, allowing the mixture to warm slowly to room temperature. *n*-bromobutane (1.17 mL, 10.85 mmol) was added and the reaction was stirred at room temperature for 24 hours. Excess NaH was quenched by adding MeOH in small portions until gasses ceased to evolve. The resulting mixture was then transferred into a separatory funnel with the aid of DCM (100 mL) and washed with NH_4Cl (aq) (sat'd, 100 mL), H_2O (100 mL) and brine (100 mL). The organic layer was collected and dried over Na_2SO_4 before passing through a short silica plug with DCM:EtOAc (9:1) as eluent. The filtrate was concentrated under reduced

pressure to give **3b** as an off white solid (0.589 g, 96%). ^{1}H NMR (500 MHz, Methylene Chloride-d_2) δ 8.67 (d, J = 2.2 Hz, 2H), 8.36 (d, J = 8.3 Hz, 2H), 7.84 (dd, J = 8.3, 2.3 Hz, 2H), 7.64 – 7.60 (m, 8H), 7.49 (d, J = 8.5 Hz, 8H), 6.17 (d, J = 10.2 Hz, 4H), 6.11 – 6.07 (m, 8H), 3.65 – 3.59 (m, 13H), 1.72 – 1.63 (m, 14H), 1.53 – 1.46 (m, 13H), 1.00 – 0.96 (m, 18H). ^{13}C NMR (126 MHz, Methylene Chloride-d_2) δ 148.06, 143.89, 143.61, 140.38, 140.17, 139.86, 135.08, 134.80, 134.05, 133.27, 127.32, 127.21, 127.19, 127.02, 120.82, 75.02, 74.72, 73.98, 64.45, 64.36, 33.13, 33.09, 33.01, 20.15, 20.13, 14.31, 14.30. HRMS (ASAP) (m/z): [M]+ calculated for $C_{76}H_{88}N_2O_6$, 1124.6642; found, 1124.6715.

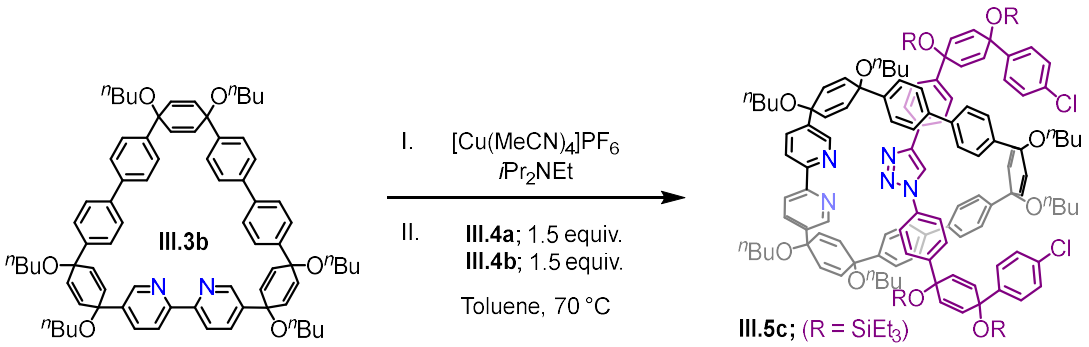

Synthesis of III.5c. To a flame dried 100 mL round bottom flask was added **III.3b** (0.210 g, 0.08 mmol) and $[Cu(MeCN)_4]PF_6$ (0.063 g, 0.06 mmol). The flask was evacuated and backfilled with N_2 gas three times before introducing toluene (10 mL). The resulting mixture sonicated for 5 minutes before heating to 70 °C. The mixture was stirred at this temperature for an additional 10 minutes before adding N,N-diisoproylethylamine (iPr$_2$NEt, 0.16 mL, 0.38 mmol). subsequently, a solution containing **III.4a** (1.31 g, 2.37 mmol) and **III.4b** (1.35 g, 2.37 mmol) in toluene (30 mL) was added dropwise via cannula. The reaction mixture was stirred at 70 °C under a N_2 atmosphere for 20 minutes at which point the reaction mixture was transferred into a separatory

funnel along with an aqueous solution of ammonia (18 w/w%) containing ethylenediaminetetraacetic acid disodium salt (NH_3-EDTA (aq), 20 mL). The mixture was emulsified and allowed to separate before collecting the organic layer. The aqueous layer was then extracted with EtOAc (2 x 10 mL) before combining and drying organic layers over Na2SO4. The solvent was evaporated under reduced pressure and the resulting material was purified via column chromatography (SiO_2; 0 – 10% EtOAc in hexanes) to give **III.5c** as a white foam (0.403 g, 96%). ^{1}H NMR (500 MHz, Chloroform-*d*) δ 8.67 (d, *J* = 2.2 Hz, 2H), 8.20 (d, *J* = 8.4 Hz, 2H), 7.73 (s, 1H), 7.66 (dd, *J* = 8.3, 2.3 Hz, 2H), 7.46 (d, *J* = 7.9 Hz, 4H), 7.32 – 7.27 (m, 6H), 7.22 (d, *J* = 8.0 Hz, 4H), 7.20 – 7.15 (m, 4H), 7.12 – 7.02 (m, 12H), 6.96 (d, *J* = 8.3 Hz, 2H), 6.23 (s, 2H), 6.13 – 6.05 (m, 6H), 6.01 – 5.89 (m, 10H), 5.82 (d, *J* = 9.9 Hz, 2H), 3.59 (q, *J* = 5.8 Hz, 8H), 3.53 (t, *J* = 6.5 Hz, 4H), 1.71 – 1.58 (m, 14H), 1.52 – 1.40 (m, 13H), 0.99 – 0.87 (m, 54H), 0.63 – 0.53 (m, 24H). ^{13}C NMR (126 MHz, $CDCl_3$) δ 154.59, 147.46, 147.21, 145.81, 145.38, 144.58, 144.49, 142.90, 142.25, 139.82, 139.78, 139.11, 135.66, 134.58, 134.43, 133.87, 133.45, 133.31, 133.19, 133.01, 132.79, 132.06, 131.54, 131.33, 131.27, 131.13, 129.32, 128.41, 128.28, 127.27, 127.17, 127.12, 126.96, 126.34, 126.31, 125.93, 125.87, 125.77, 120.56, 120.33, 118.71, 77.28, 77.03, 76.78, 74.14, 73.88, 73.29, 71.16, 71.06, 70.94, 70.82, 63.88, 63.80, 32.57, 32.46, 32.41, 19.57, 19.56, 19.53, 13.97, 13.94, 13.92, 7.08, 7.07, 7.03, 7.00, 6.47, 6.42. MS (MALDI) (m/z): [M+H]+ calculated for $C_{138}H_{174}Cl_2N_5O_{10}Si_4$, 2243.16; found, 2243.4.

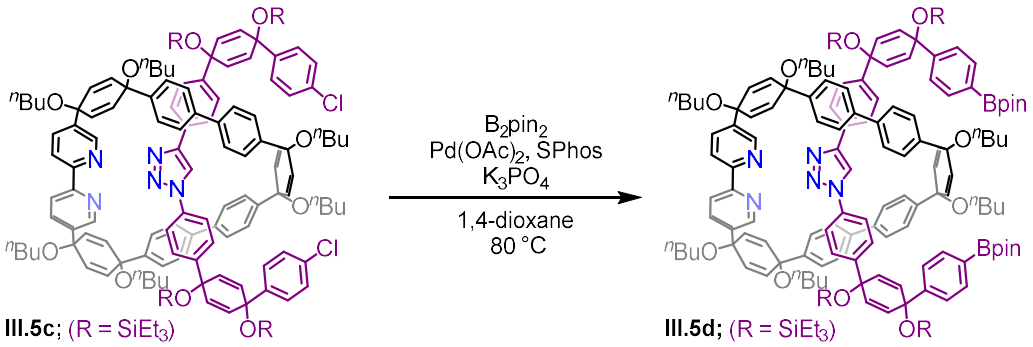

Synthesis of III.5d. To a flame dried 50 mL round bottom flask were added **III.5c** (0.345 g, 0.15 mmol)**,** bis(pinacolato)diboron (B_2pin_2, 0.195 g, 0.76 mmol), $Pd(OAc)_2$ (0.017 g, 0.08 mmol), SPhos (0.044 g, 0.04 mmol), and tribasic potassium phosphate (K_3PO_4, 0.261 g, 1.23 mmol). The flask was evacuated and backfilled with N_2 gas five times before introducing 1,4-dioxane (5 mL). The mixture was stirred at 80 °C for 5 h. The reaction was removed from heat and diluted with 30 mL hexanes. After cooling to room temperature, the reaction mixture was poured over a short silica plug topped with celite. The plug was washed with hexanes (50 mL) followed by DCM (150 mL). The eluate was concentrated under reduced pressure and the resulting residue was sonicated with MeOH (50 mL) until a flocculent precipitate had formed. The precipitate was collected by vacuum filtration and washed with MeOH (50 mL) to give **III.5b** as a tan colored solid (0.327 g, 88%). ^{1}H NMR (500 MHz, Chloroform-*d*) δ 8.66 (d, *J* = 2.3 Hz, 2H), 8.21 (d, *J* = 8.4 Hz, 2H), 7.75 (d, *J* = 8.0 Hz, 2H), 7.71 (d, *J* = 7.9 Hz, 2H), 7.64 (dd, *J* = 8.4, 2.3 Hz, 2H), 7.46 (s, 1H), 7.42 (d, *J* = 8.1 Hz, 4H), 7.33 (d, *J* = 7.8 Hz, 4H), 7.28 (d, *J* = 8.4 Hz, 6H), 7.22 (dd, *J* = 8.3, 3.6 Hz, 6H), 7.07 (dd, *J* = 8.4, 6.3 Hz, 7H), 6.96 (s, 4H), 6.24 (d, *J* = 2.1 Hz, 2H), 6.15 – 6.06 (m, 7H), 6.03 – 5.94 (m, 9H), 5.88 (d, *J* = 10.1 Hz, 2H), 5.77 (d, *J* = 10.1 Hz, 2H), 3.61 – 3.54 (m, 10H), 3.53 (t, *J* = 6.6 Hz, 4H), 1.70 – 1.58 (m, 19H), 1.52 – 1.39 (m, 16H), 1.33 (d, *J* = 10.2 Hz, 26H), 0.99 – 0.86 (m, 67H), 0.63 – 0.50 (m, 29H). ^{13}C NMR (126 MHz, Chloroform-*d*) δ 154.61, 149.04, 149.00, 147.44, 147.15, 145.98, 145.50, 142.75, 142.20, 139.71,

139.62, 139.14, 135.52, 135.00, 134.86, 134.45, 134.36, 133.81, 133.44, 133.31, 132.84, 132.22, 131.45, 131.42, 131.25, 131.19, 129.16, 127.30, 126.98, 126.26, 125.93, 125.79, 125.73, 125.11, 125.05, 120.60, 120.56, 118.66, 83.80, 83.71, 74.09, 73.86, 73.35, 71.42, 71.33, 71.16, 71.05, 63.87, 63.85, 63.77, 32.58, 32.47, 32.43, 25.03, 24.95, 24.91, 19.56, 19.53, 13.97, 13.95, 13.92, 7.13, 7.10, 7.05, 7.02, 6.48, 6.46, 6.44, 6.37. MS (MALDI) (m/z): [M+H]+ calculated for $C_{138}H_{174}Cl_2N_5O_{10}Si_4$, 2427.4193; found, 2427.6.

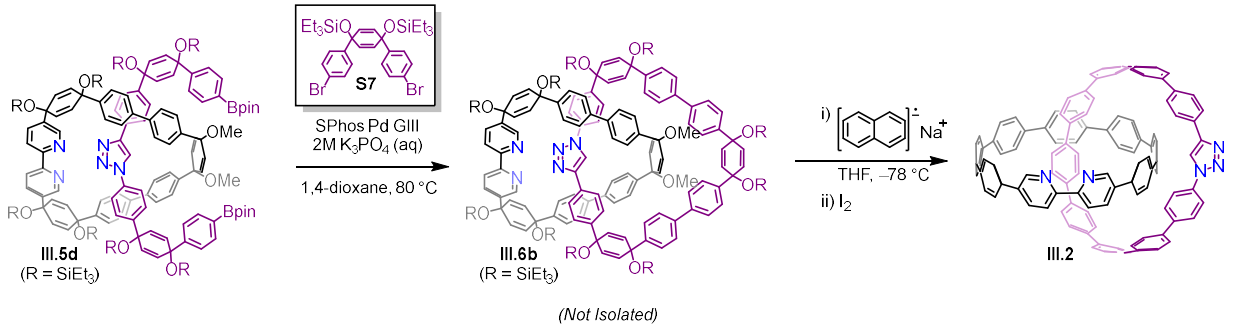

Synthesis of III.2. To a 250 mL round bottom flask were added **III.5d** (0.315 g, 0.12 mmol), **III.S7** (0.080 g, 0.12 mmol) and Pd SPhos GIII (0.019 g, 0.02 mmol). The flask was evacuated and backfilled with N_2 gas five times before introducing 1,4-dioxane (150 mL). The resulting mixture was heated to 80 °C. An aqueous solution of K_3PO_4 (2M, 5 mL) was then added and the reaction was stirred overnight. The following morning the reaction was removed from heat and allowed to cool to room temperature. NH_3-EDTA (aq) (50 mL) was added, and the mixture was stirred vigorously for 30 minutes. The solvent was removed under reduced pressure and the crude material was transferred into a separatory funnel with the aid of DCM (50 mL) and H_2O (100 mL). The organic layer was collected, and the aqueous layer was extracted twice more with DCM (2 x 25 mL). The organic layers were combined and dried over Na_2SO_4 before passing through a short silica plug, using DCM as eluent. The eluate was evaporated under reduced

pressure and the resulting material was transferred into a flame dried 100 mL round bottom flask. The flask was evacuated and backfilled with N_2 gas three times before introducing THF (25 mL). The resulting solution was then cooled to -78 °C at which point sodium napthalenide (4.18 mL, 0.47 M in THF) was added, dropwise. The resulting dark purple solution was allowed to stir for 2 h at -78 °C after which point I_2 (0.4 M in THF) was added until the reaction mixture had turned orange. A saturated aqueous solution of $Na_2S_2O_3$ (25 mL) was then added to quench any excess iodine. The THF was then removed under reduced pressure and the remaining aqueous suspension was extracted with DCM (5 x 15 mL). The organic layers were combined and dried over Na_2SO_4 before removing the solvent under reduced pressure. The product was purified via column chromatography (Al_2O_3: 60% DCM, 0-10% EtOAc in hexanes) to provide **III.2** as a bright yellow solid (0.014 g, 8% over two steps). ^{1}H NMR (500 MHz, Methylene Chloride-d_2) δ 8.50 (d, J = 2.3 Hz, 2H), 7.85 (d, J = 8.5 Hz, 2H), 7.46 (d, J = 8.6 Hz, 2H), 7.44 – 7.39 (m, 6H), 7.37 (d, J = 8.8 Hz, 4H), 7.35 – 7.31 (m, 4H), 7.29 – 7.16 (m, 30H), 7.14 – 7.08 (m, 16H), 7.05 (d, J = 8.6 Hz, 2H), 7.00 (s, 1H), 6.95 (d, J = 8.6 Hz, 2H). ^{13}C NMR (126 MHz, CD_2Cl_2) δ 154.63, 149.14, 146.54, 140.67, 140.41, 139.31, 139.01, 138.81, 138.66, 138.63, 138.56, 138.49, 138.47, 138.44, 138.40, 138.39, 138.32, 138.24, 138.20, 138.18, 137.93, 137.90, 137.03, 136.42, 134.90, 133.59, 132.58, 129.68, 128.18, 128.11, 127.98, 127.86, 127.84, 127.82, 127.79, 127.76, 127.72, 127.70, 127.65, 127.63, 127.60, 127.57, 127.51, 127.47, 127.29, 122.41, 121.34. MS (MALDI) (m/z): [M-N_2]+ calculated for $C_{108}H_{71}N_3$, 1409.5648; found, 1409.1.

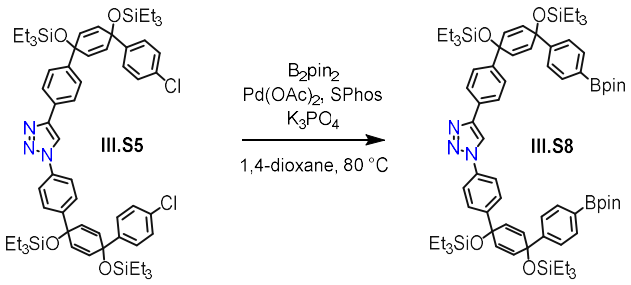

Synthesis of III.S8. To a flame dried 100 mL round bottom flask were added **III.S5** (6.00 g, 5.36 mmol), B_2pin_2 (5.44 g, 21.4 mmol), $Pd(OAc)_2$ (0.060 g, 0.27 mmol), SPhos (0.165 g, 0.40 mmol) and K_3PO_4 (5.69 g, 26.8 mmol). The flask was evacuated and backfilled with N_2 gas five times before introducing 1,4-dioxane (20 mL). The resulting suspension was heated to 80 °C and stirred overnight. The reaction was removed from heat and diluted with 60 mL hexanes. After cooling to room temperature, the reaction mixture was poured over a short silica plug topped with celite. The plug was washed with hexanes (50 mL) followed by DCM (200 mL). The eluate was concentrated under reduced pressure and the resulting residue was sonicated with MeOH (50 mL) until a flocculent precipitate had formed. The precipitate was collected by vacuum filtration and washed with MeOH (50 mL) to give **III.S8** as a brown colored solid (6.73 g, 96%). ^{1}H NMR (500 MHz, Chloroform-*d*) δ 8.17 (s, 1H), 7.82 (d, *J* = 8.5 Hz, 2H), 7.78 – 7.71 (m, 4H), 7.68 (d, *J* = 8.7 Hz, 2H), 7.49 (d, *J* = 8.7 Hz, 2H), 7.43 (d, *J* = 8.5 Hz, 2H), 7.38 (d, *J* = 8.2 Hz, 4H), 6.07 (d, *J* = 10.1 Hz, 2H), 6.01 (s, 4H), 5.98 (d, *J* = 10.1 Hz, 2H), 1.34 (d, *J* = 2.6 Hz, 24H), 0.99 – 0.91 (m, 36H), 0.69 – 0.56 (m, 24H). ^{13}C NMR (126 MHz, Chloroform-*d*) δ 149.07, 148.84, 148.14, 146.87, 146.27, 135.97, 134.82, 134.74, 131.88, 131.51, 131.42, 131.12, 129.17, 127.25, 126.44, 125.68, 125.19, 125.17, 120.18, 117.55, 83.80, 83.73, 71.58, 71.42, 71.32, 25.03, 24.89, 7.06, 7.05, 7.03, 6.70, 6.47, 6.44, 6.23. HRMS (ASAP) (m/z): [M]+ calculated for $C_{74}H_{109}B_2N_3O_8Si_4$, 1301.7478; found, 1301.7642.

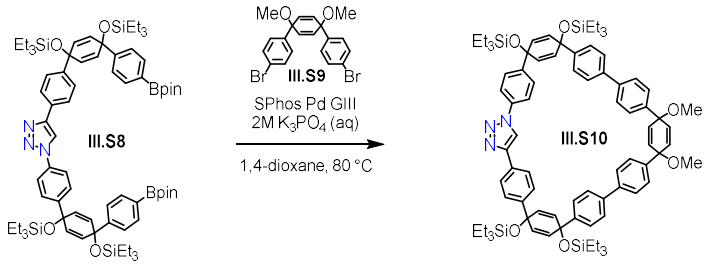

Synthesis of III.S10. To a 250 mL round bottom flask were added **III.S8** (0.500 g, 0.38 mmol), **III.S9** (0.173 g, 0.38 mmol) and Pd SPhos GIII (0.060 g, 0.06 mmol). The flask was evacuated and backfilled with N_2 gas five times before introducing 1,4-dioxane (125 mL). The resulting mixture was heated to 80 °C with stirring at which point an aqueous solution of K_3PO_4 (2M, 10 mL) was added. After 1.5 h a small aliquot (0.2 mL) was removed from the reaction mixture, concentrated, and analyzed via ^{1}H NMR which showed total consumption of starting materials. The reaction was removed from heat and the solvent was removed under reduced pressure. The crude residue was transferred into a separatory funnel with the aid of 50 mL H2O and 20 mL DCM. The organic layer was collected, and the aqueous layer was extracted with an additional 10 mL fresh DCM. The organic layers were combined and dried over Na_2SO_4 before running the solution through a short silica plug using DCM as eluent. The eluate was evaporated under reduced pressure and the resulting oily solid was triturated with acetone (5 mL) to produce a filterable solid precipitate. After chilling in an ice bath for 30 min, the precipitate was collected by vacuum filtration and washed with cold acetone (3 mL) and methanol (10 mL) to give **III.S10** as a white powder (0.472 g, 92%). ^{1}H NMR (500 MHz, Chloroform-*d*) δ 8.20 (s, 1H), 7.87 – 7.83 (m, 2H), 7.76 – 7.72 (m, 2H), 7.62 – 7.50 (m, 16H), 7.42 (d, *J* = 8.1 Hz, 4H), 6.15 (s, 4H), 6.08 – 5.99 (m, 8H), 3.47 (s, 6H), 1.00 – 0.93 (m, 36H), 0.69 – 0.60 (m, 24H). ^{13}C NMR (126 MHz, Chloroform-*d*) δ 148.22, 147.12, 146.55, 145.36, 145.11, 143.01, 142.86, 139.88, 139.73, 139.55, 139.34, 135.95, 133.30, 133.23, 131.95, 131.60, 131.30, 130.99, 129.20, 127.25, 127.06, 126.82,

126.72, 126.46, 126.36, 126.31, 126.21, 126.19, 125.79, 120.13, 117.57, 74.27, 71.39, 71.29, 71.25, 52.04, 7.09, 7.07, 6.70, 6.50, 6.47, 6.46, 6.23. HRMS (ASAP) (m/z): [M]+ calculated for $C_{82}H_{103}N_3O_6Si_4$, 1337.6924; found, 1337.6917.

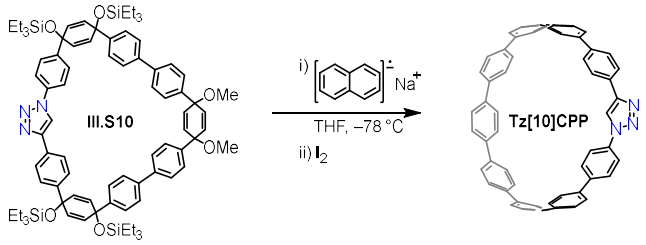

Synthesis of Tz[10]CPP. To a flame dried 100 mL round bottom flask was added **III.S10** (0.200 g, 0.15 mmol). The flask was evacuated and backfilled with N_2 gas three times before introducing THF (25 mL). The resulting solution was then cooled to -78 °C at which point sodium napthalenide (5.1 mL, 1.19 mmol, 0.23 M in THF) was added, dropwise. The resulting dark purple solution was allowed to stir for 2 h at -78 °C after which point I_2 (0.4 M in THF) was added until the reaction mixture had turned orange. A saturated aqueous solution of $Na_2S_2O_3$ (25 mL) was then added quench any excess iodine. The THF was then removed under reduced pressure and the remaining aqueous suspension was extracted with DCM (3 x 20 mL). The organic layers were combined and dried over Na_2SO_4 before passing through a short alumina plug using DCM as eluent. The eluate was evaporated under reduced pressure and the resulting material was suspended in hexanes (50 mL). The solids were collected via vacuum filtration and washed with hexanes (15 mL), Et_2O (15 mL), and MeOH (15 ml). The resulting material was dissolved in a minimal amount of chloroform and the product was crystallized via vapor diffusion with pentanes over three days. Provides **Tz[10]CPP** as pale-yellow plates (0.036 g, 32%). ^{1}H NMR (600 MHz, Methylene Chloride-d_2) δ 7.71 (d, J = 8.9 Hz, 2H), 7.62 – 7.56 (m, 32H), 7.53 (d, J = 8.9 Hz, 2H), 7.32 (s,

1H). ^{13}C NMR (126 MHz, Methylene Chloride-d_2) δ 149.20, 141.03, 140.53, 139.72, 139.01, 138.94, 138.92, 138.84, 138.81, 138.72, 138.68, 138.66, 138.63, 138.50, 137.61, 136.95, 129.95, 128.57, 128.24, 128.19, 128.06, 128.03, 127.96, 127.95, 127.92, 127.90, 127.87, 127.35, 122.77, 78.10. HRMS (ESI) (m/z): [M]+ calculated for $C_{56}H_{37}N_3$, 751.2987; not observed – [M-N_2]+ calculated for $C_{56}H_{37}N$, 723.2926; found, 723.2887.

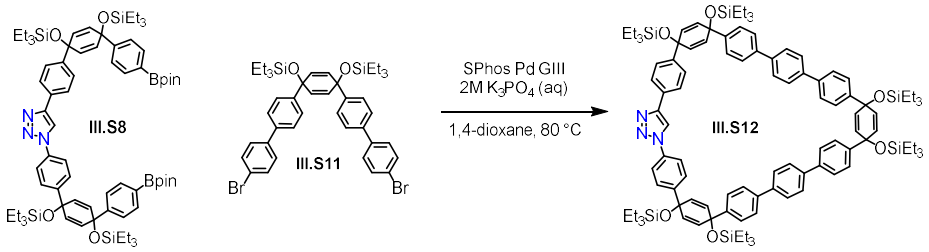

Synthesis of III.S12. To a 250 mL round bottom flask were added **III.S8** (0.500 g, 0.38 mmol), **III.S11** (0.308 g, 0.38 mmol) and Pd SPhos GIII (0.060 g, 0.06 mmol). The flask was evacuated and backfilled with N_2 gas five times before introducing 1,4-dioxane (125 mL). The resulting mixture was heated to 80 °C with stirring at which point an aqueous solution of K3PO4 (2M, 10 mL) was added. After 1.5 h a small aliquot (0.2 mL) was removed from the reaction mixture, concentrated, and analyzed via 1H NMR which showed total consumption of starting materials. The reaction was removed from heat and the solvent was removed under reduced pressure. The crude residue was transferred into a separatory funnel with the aid of 50 mL H2O and 20 mL DCM. The organic layer was collected, and the aqueous layer was extracted with an additional 10 mL fresh DCM. The organic layers were combined and dried over Na2SO4 before running the solution through a short silica plug using DCM as eluent. The eluate was evaporated under reduced pressure and the resulting oily solid was triturated with acetone (5 mL) to produce a filterable solid precipitate. After chilling in an ice bath for 30 min, the precipitate was collected

by vacuum filtration and washed with cold acetone (3 mL) and hexanes (3 mL) to give **III.S12** as a white powder (0.467 g, 72%). ^{1}H NMR (500 MHz, Chloroform-*d*) δ 8.23 (s, 1H), 7.93 (d, *J* = 8.0 Hz, 2H), 7.81 – 7.70 (m, 10H), 7.68 – 7.59 (m, 10H), 7.59 – 7.46 (m, 10H), 6.22 – 6.06 (m, 12H), 1.11 – 0.99 (m, 54H), 0.80 – 0.67 (m, 36H). ^{13}C NMR (126 MHz, $CDCl_3$) δ 148.13, 146.90, 146.32, 145.15, 145.07, 144.97, 144.75, 139.73, 139.68, 139.57, 139.52, 139.46, 139.41, 139.39, 136.09, 132.15, 131.87, 131.60, 131.52, 131.25, 131.03, 129.34, 127.38, 127.35, 127.28, 126.75, 126.66, 126.64, 126.61, 126.47, 126.44, 126.37, 126.34, 125.77, 120.21, 117.20, 71.69, 71.67, 71.63, 71.45. HRMS (ASAP) (m/z): [M]+ calculated for $C_{104}H_{135}N_3O_6Si_6$, 1689.8966; found, 1689.9110.

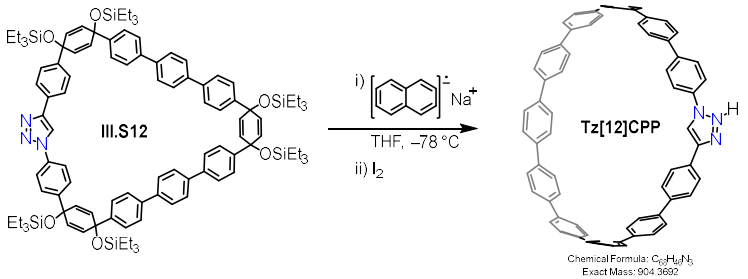

To a flame dried 100 mL round bottom flask was added **III.S12** (0.200 g, 0.12 mmol). The flask was evacuated and backfilled with N_2 gas three times before introducing THF (30 mL). The resulting solution was then cooled to -78 °C at which point sodium napthalenide (4.0 mL, 0.94 mmol, 0.23 M in THF) was added, dropwise. The resulting dark purple solution was allowed to stir for 2 h at -78 °C after which point I_2 (0.4 M in THF) was added until the reaction mixture had turned orange. A saturated aqueous solution of $Na_2S_2O_3$ (25 mL) was then added to quench any excess iodine. The THF was then removed under reduced pressure and the remaining aqueous suspension was extracted with DCM (3 x 20 mL). The organic layers were combined and dried

over Na_2SO_4 before passing through a short alumina plug using DCM as eluent. The eluate was evaporated under reduced pressure and the resulting material was suspended in hexanes (50 mL). The solids were collected via vacuum filtration and washed with hexanes (15 mL), Et_2O (15 mL), and MeOH (15 ml). The resulting material was dissolved in a minimal amount of chloroform and the product was crystallized via vapor diffusion with pentanes over three days giving **Tz[12]CPP** as thin white needles. The crystals were collected by vacuum filtration and washed with pentane to give an off-white powder (0.052 g, 49%). ^{1}H NMR (500 MHz, Methylene Chloride-d_2) δ 7.77 (d, J = 8.8 Hz, 2H), 7.71 (d, J = 8.6 Hz, 2H), 7.69 – 7.63 (m, 40H), 7.59 (s, 1H). ^{13}C NMR (126 MHz, $CDCl_3$) δ 149.11, 141.23, 140.72, 139.95, 139.35, 139.27, 139.20, 139.17, 139.08, 139.05, 139.03, 139.00, 138.97, 138.92, 138.08, 136.98, 130.02, 128.63, 128.11, 128.07, 127.99, 127.91, 127.89, 127.87, 127.84, 127.28, 126.06, 122.63, 54.43, 54.22, 54.00, 53.78, 53.57. HRMS (ESI) (m/z): [M+H]+ calculated for $C_{68}H_{46}N_3$, 904.3692; found, 904.3604.

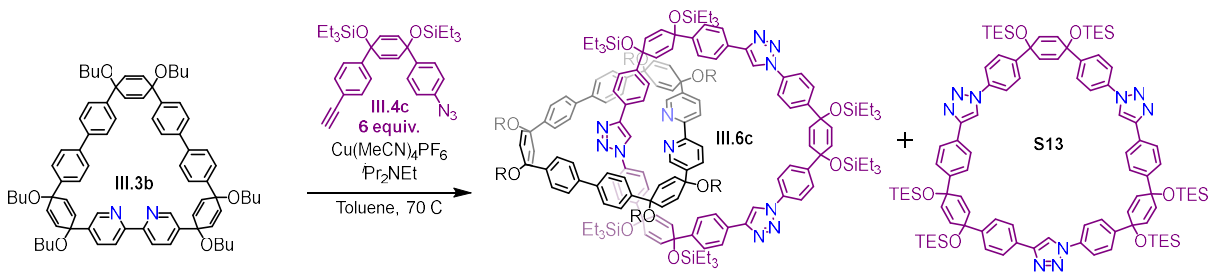

Synthesis of III.6c and S13. To a flame dried 100 mL round bottom flask was added **III.3b** (0.015 g, 0.013 mmol) and $[Cu(MeCN)_4]PF_6$ (0.004 g, 0.011 mmol). The flask was evacuated and backfilled with N_2 gas three times before introducing toluene (3 mL). The resulting mixture sonicated for 5 minutes before heating to 70 °C. The mixture was stirred at this temperature for an additional 10 minutes before adding N,N-diisoproylethylamine (iPr$_2$NEt, 0.02 mL, 0.13 mmol).

subsequently, a solution containing **III.4c** (0.045 g, 0.08 mmol) was added via syringe pump over 2 h. Following complete addition of III.4c the reaction mixture was stirred at 70 °C for an additional 10 minutes at which point the reaction mixture was transferred into a separatory funnel along with an aqueous solution of ammonia (18 w/w%) containing ethylenediaminetetraacetic acid disodium salt (NH_3-EDTA (aq), 20 mL). The mixture was emulsified and allowed to separate before collecting the organic layer. The aqueous layer was then extracted with EtOAc (2 x 10 mL) before combining and drying organic layers over Na2SO4. The solvent was evaporated under reduced pressure and the resulting material was purified via column chromatography (SiO_2; 0 – 10% EtOAc in hexanes) to give **III.6c** as a yellow foam (0.012 g, 32%) and **III.S13** as a white powder (0.014 mg, 31% from **III.4c**). **III.6c**; ^{1}H NMR (600 MHz, Methylene Chloride-d_2) δ 8.67 (d, J = 2.4 Hz, 2H), 8.23 (d, J = 8.4 Hz, 2H), 8.06 (s, 1H), 8.03 (s, 1H), 7.93 (d, J = 8.2 Hz, 2H), 7.79 (d, J = 8.2 Hz, 2H), 7.75 (d, J = 8.5 Hz, 3H), 7.67 (dd, J = 8.3, 2.4 Hz, 2H), 7.63 (d, J = 8.4 Hz, 2H), 7.61 – 7.56 (m, 4H), 7.48 (d, J = 8.1 Hz, 2H), 7.46 – 7.38 (m, 10H), 7.33 (d, J = 8.0 Hz, 4H), 7.21 (d, J = 8.2 Hz, 4H), 7.18 – 7.11 (m, 8H), 6.94 (d, J = 8.4 Hz, 2H), 6.27 – 6.23 (m, 2H), 6.19 – 6.10 (m, 10H), 6.06 – 5.98 (m, 12H), 5.97 – 5.94 (m, 2H), 3.57 (dt, J = 9.9, 6.5 Hz, 8H), 3.50 (t, J = 6.5 Hz, 4H), 1.66 – 1.54 (m, 19H), 1.50 – 1.36 (m, 14H), 1.06 – 0.90 (m, 86H), 0.76 – 0.62 (m, 38H). ^{13}C NMR (151 MHz, Methylene Chloride-d_2 δ 154.51, 147.51, 147.49, 147.14, 147.06, 146.92, 146.80, 146.08, 145.19, 143.09, 142.59, 139.91, 139.46, 139.05, 136.07, 135.94, 135.53, 134.39, 134.36, 133.99, 133.44, 133.29, 133.07, 132.60, 132.17, 132.09, 131.87, 131.77, 131.54, 131.39, 131.33, 131.09, 129.75, 129.69, 129.55, 128.05, 127.29, 127.17, 127.10, 127.05, 126.79, 126.51, 126.46, 126.44, 126.30, 125.94, 125.89, 125.74, 125.71, 125.64, 124.86, 120.46, 120.41, 120.25, 120.24, 120.15, 118.95, 117.84, 117.62, 74.05, 73.73, 73.11, 72.43, 71.25, 71.21, 71.14, 71.03, 70.80, 63.79, 63.76, 32.49, 32.39, 32.37, 19.51, 19.50, 19.47, 13.71, 13.70, 13.67,

6.93, 6.86, 6.83, 6.80, 6.41, 6.38, 6.36, 6.35. MS (MALDI) (m/z): [M+H]+ calculated for $C_{171}H_{218}N_{11}O_{12}Si_6$, 2797.5397; found, 2796.6. **III.S13**; ^{1}H NMR (600 MHz, Methylene Chloride-d_2) δ 7.92 (s, 3H), 7.53 (d, J = 8.0 Hz, 6H), 7.48 (d, J = 8.4 Hz, 6H), 7.20 (d, J = 8.6 Hz, 6H), 7.07 (d, J = 8.1 Hz, 6H), 6.23 (s, 12H), 0.99 (t, J = 7.9 Hz, 54H), 0.68 (q, J = 7.9 Hz, 36H). ^{13}C NMR (151 MHz, CD_2Cl_2) δ 148.68, 145.41, 144.70, 136.23, 133.62, 132.73, 129.61, 128.61, 127.62, 125.41, 119.46, 118.25, 72.98, 72.67, 54.36, 54.18, 54.00, 53.82, 53.64, 7.35, 7.33, 6.94, 6.92.

Photophysical Data.

Table III.1: Summery of optical properties

	λ_{max} (abs, nm)	ε ($M^{-1}cm^{-1}$)	λ_{max} (fluor, nm)	Φ_F	ε x Φ_F ($M^{-1}cm^{-1}$)
III.1	335	254500	515	0.181	46100
III.2	330	178007	515	0.193	34400
bipy[9]CPP	345	109308	515	0.223	24400
Tz[10]CPP	327	100312	461	0.704	70600
Tz[12]CPP	330	138388	446	0.690	95500

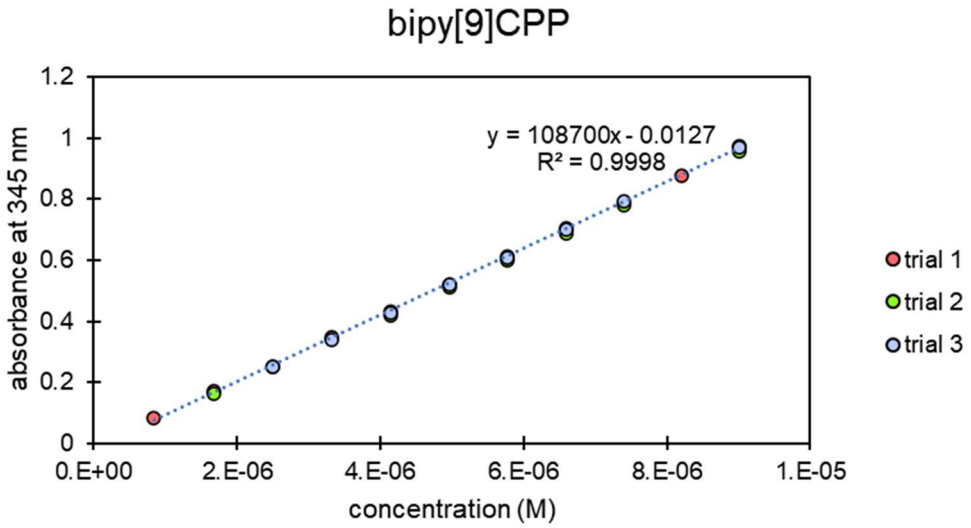

Figure III.12. Beer-Lambert plot for bipy[9]CPP in DCM.

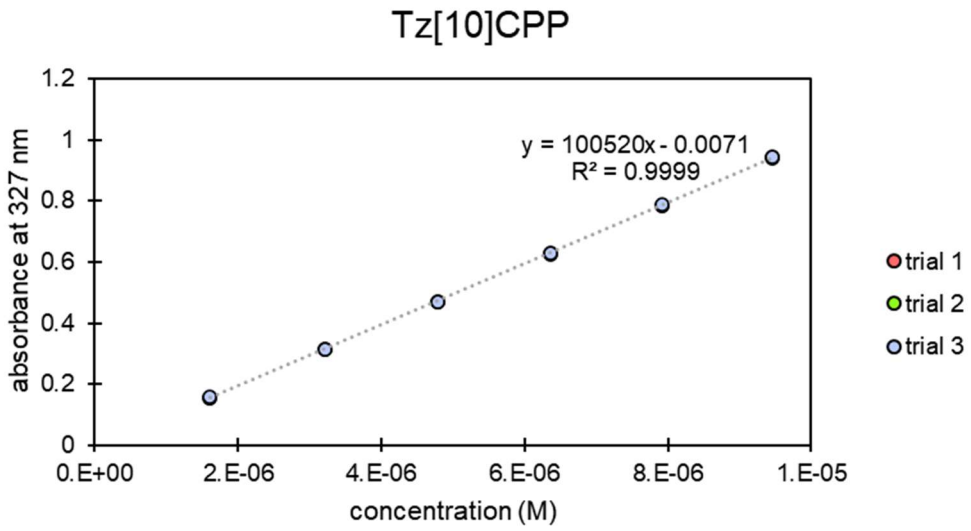

Figure III.13. Beer-Lambert plot for Tz[10]CPP in DCM.

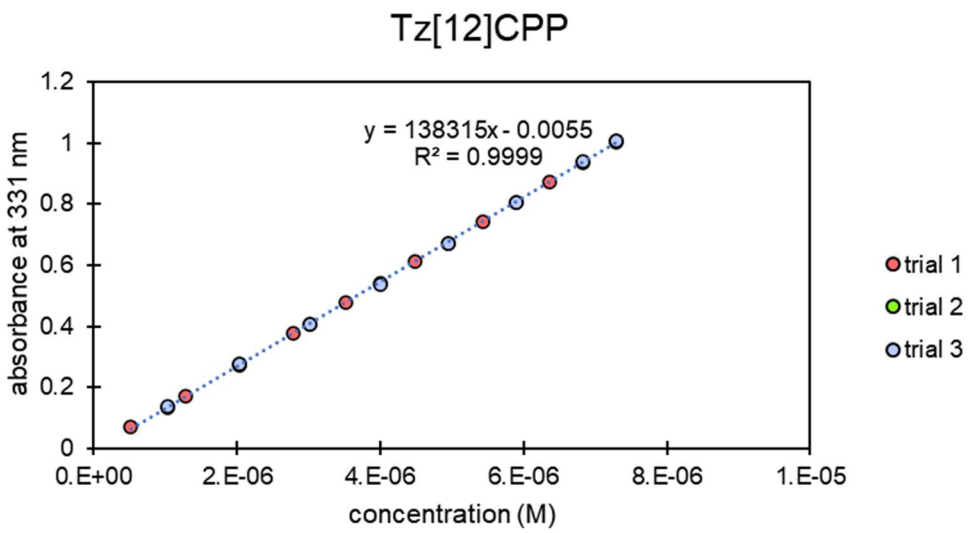

Figure III.14. Beer-Lambert plot for Tz[12]CPP in DCM.

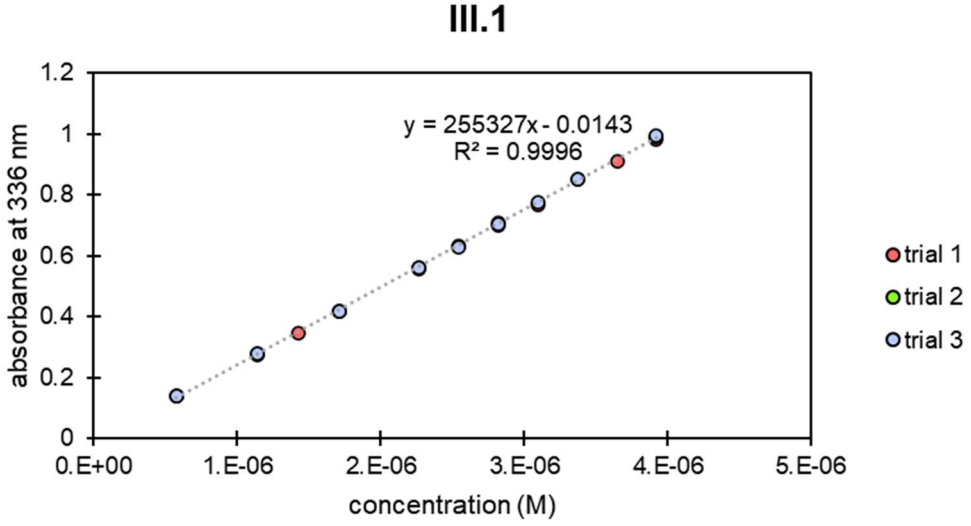

Figure III.15. Beer-Lambert plot for III.1 in DCM.

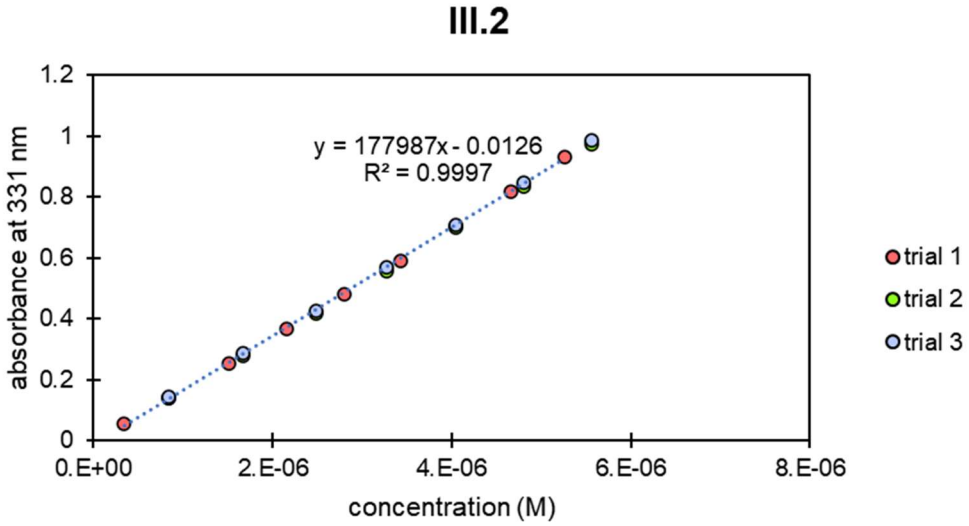

Figure III.16. Beer-Lambert plot for III.2 in DCM.

Quantum yields of **III.1**, **III.2**, **bipy[9]CPP**, **Tz[12]CPP** and **Tz[10]CPP** were measured according to the procedure reported by Jobin Yvon Horiba. Quinine and anthracene were used as standard reference compounds with known quantum yields. Absorbance values were measured at 330 nm. Emission spectra were acquired with the excitation monochromator set to 330 nm with the excitation and emission slit widths set to 1 nm and 2 nm respectively. The fluorescence spectra of **III.1**, **III.2** and **bipy[9]CPP** were integrated from 400-650 nm, **Tz[10]CPP** and **Tz[12]CPP** were integrated from 400-600 nm, anthracene was integrated from 360-480 nm and quinine sulfate was integrated from 400-600 nm.

Quantum yields were calculated using the following equation:

$$\phi_{unk} = \phi_{std}\left(\frac{\eta_{unk}^2}{\eta_{std}^2}\right)\left(\frac{Grad_{unk}^2}{Grad_{std}^2}\right)$$

$$\phi_{unk} = quantum\ yield\ of\ the\ unknown$$

$$\phi_{std} = quantum\ yield\ of\ the\ standard$$

$$\eta_{unk} = refractive\ index\ of\ the\ unknown\ soution$$

$$\eta_{std} = refractive\ index\ of\ the\ standard\ soution$$

$$Grad_{unk} = slope\ of\ the\ curve\ for\ unknown$$

$$Grad_{std} = slope\ of\ the\ curve\ for\ standard$$

The equation above was first used to cross-calibrate the standards and validate the method.

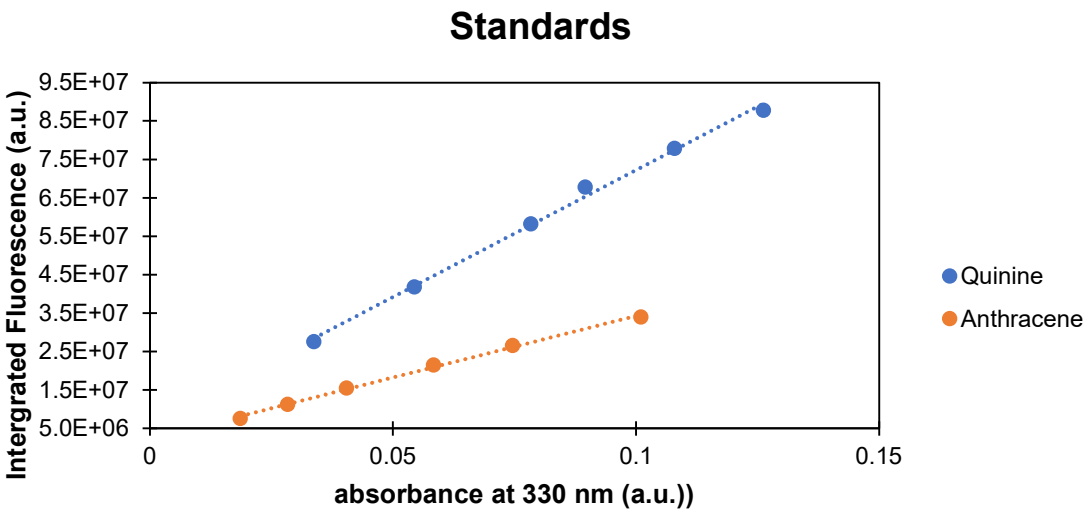

Figure III.17. Calibration curves (integrated fluorescence vs absorbance) for anthracene and quinine are used for the indirect determination of fluorescence quantum yields.

Table III.2: Cross calibration of standards

Standard	**Solvent**	**Refractive Index**	**Slope**	**$\Phi_{Lit.}$**	**$\Phi_{measured}$**	**error (%)**
Quinine	0.1M H_2SO_4(aq)	1.3333	660992984	0.54	0.533	1.21
Anthracene	EtOH	1.3614	320735920	0.27	0.273	1.22

`The above cross-calibration of quinine and anthracene produces good agreement between the measured quantum yields and their literature values. Furthermore, the errors of the two standard measurements are symmetric about 0 – as such the quantum yields of the analytes with be reported as the average of the result when calculated with respect to anthracene and when calculated with respect to quinine.

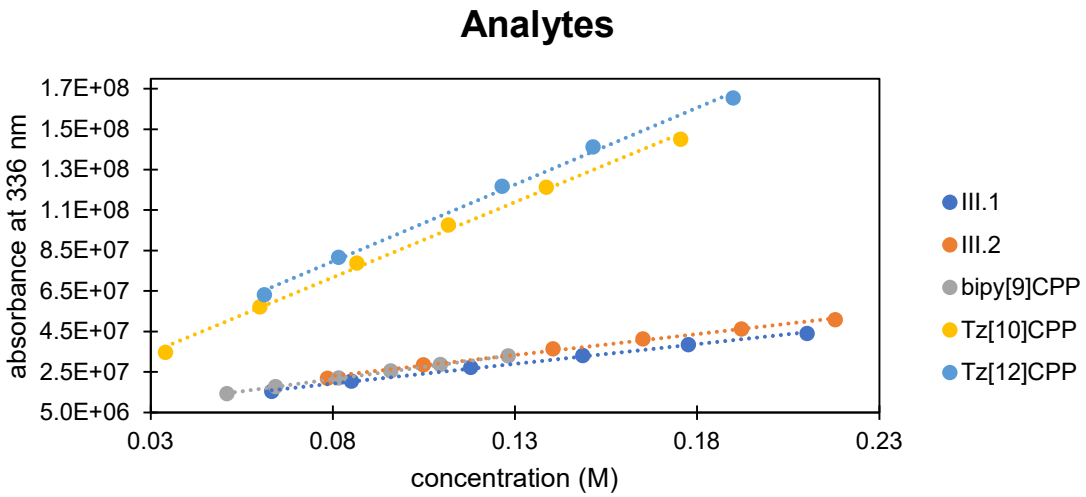

Figure III.18. Integrated fluorescence vs absorbance curves for **III.1**, **III.2 bipy[9]CPP**, **Tz[10]CPP** and **Tz[12]CPP.**

Table III.3: Pertinent data for determination of quantum yields						
Analyte	**Solvent**	**η**	**Slope**	**Φ** w.r.t anthracene	**Φ** w.r.t quinine	**Φ_{avg}**
III.1	DCM	1.4200	195,342,204.43	0.182	0.180	0.181
III.2	*	*	206,881,303.15	0.193	0.191	0.193
bipy[9]CPP	*	*	240291274.5	0.224	0.221	0.223
Tz[10]CPP	*	*	744011322.3	0.708	0.700	0.704
Tz[12]CPP	*	*	759631548.7	0.694	0.685	0.690

CHAPTER IV

CONCLUDING REMARKS

The discovery of new carbon nanomaterials has historically led to impactful and often unexpected developments in materials science and technology. In this dissertation, I outline my efforts to develop new synthetic methods to produce molecular nanocarbon structures bearing non-trivial topologies—particularly those featuring mechanical linkages. Specifically, I outline the methods I have developed that allow us to integrate [*n*]cycloparaphenylene macrocycles into interlocking architectures via active template (AT) chemistry. Though this work we have informed design principles for ligand motifs that may be incorporated into [*n*]CPP precursors to make them amenable for AT chemistry, ultimately expanding our ability to engender these interesting molecular nanocarbons with unique topologies. While our initial efforts based on the Cadiot-Chodkiewicz (AT-CC) reaction were hampered by a low yielding final transformation, this provided an important proof-of-principle for the utility of the AT approach in this context. By adapting the macrocyclic ligand to be suitable for the AT-CuAAC reaction, we were able to discover a highly efficient route to create mechanical bonds with [*n*]CPP precursors. While in this dissertation we focused specifically on the synthesis of catenated cycloparaphenylenes, the efficiency of this method is such that it may be adapted for the synthesis of a tremendous breadth of structures and will perhaps allow for the creation of new types of molecular machines in the future.

CITED REFERENCES

(1) Langton, M. J.; Beer, P. D. Rotaxane and Catenane Host Structures for Sensing Charged Guest Species. *Acc. Chem. Res.* **2014**, *47*, 1935–1949.

(2) Martinez-Cuezva, A.; Saura-Sanmartin, A.; Alajarin, M.; Berna, J. Mechanically Interlocked Catalysts for Asymmetric Synthesis. *ACS Catalysis* **2020**, *10*, 7719–7733.

(3) Hart, L. F.; Hertzog, J. E.; Rauscher, P. M.; Rawe, B. W.; Tranquilli, M. M.; Rowan, S. J. Material Properties and Applications of Mechanically Interlocked Polymers. *Nat. Rev. Mater.* **2021**, *6*, 508–530.

(4) Aprahamian, I. The Future of Molecular Machines. *ACS Cent. Sci.* **2020**, *6*, 347–358.

(5) Thomas, S.; Sarathchandran, C.; Ilangovan, S. A.; Moreno-Pirajan, J. C. *Handbook of Carbon-Based Nanomaterials*. (Elsevier 2021)

(6) Jasti, R.; Bhattacharjee, J.; Neaton, J. B.; Bertozzi, C. R. Synthesis, Characterization, and Theory of [9]-, [12]-, and [18]Cycloparaphenylene: Carbon Nanohoop Structures. *J. Am. Chem. Soc.* **2008**, *130*, 17646–17647.

(7) Xu, Y.; Kaur, R.; Wang, B.; Minameyer, M. B.; Gsä, S.; Meyer, B.; Drewello, T.; Guldi, D. M.; Von Delius, M. Concave−Convex π−π Template Approach Enables the Synthesis of [10]Cycloparaphenylene−Fullerene [2]Rotaxanes. *J. Am. Chem. Soc.* **2018**, *140*, 13413–13420.

(8) Fan, Y. Y.; Chen, D.; Huang, Z. A.; Zhu, J.; Tung, C. H.; Wu, L. Z.; Cong, H. An Isolable Catenane Consisting of Two Möbius Conjugated Nanohoops. *Nat. Commun.* **2018**, *9*, 3037.

(9) Van Raden, J. M.; White, B. M.; Zakharov, L. N.; Jasti, R. Nanohoop Rotaxanes from Active Metal Template Syntheses and Their Potential in Sensing Applications. *Angew. Chem. Int. Ed.* **2019**, *58*, 7341–7345.

(10) Van Raden, J. M.; Jarenwattananon, N. N.; Zakharov, L. N.; Jasti, R. Active Metal Template Synthesis and Characterization of a Nanohoop [C2]Daisy Chain Rotaxane. *Chem. Eur. J.* **2020**, *26*, 10205–10209.

(11) Segawa, Y.; Kuwayama, M.; Hijikata, Y.; Fushimi, M.; Nishihara, T.; Pirillo, J.; Shirasaki, J.; Kubota, N.; Itami, K. Topological Molecular Nanocarbons: All-Benzene Catenane and Trefoil Knot. *Science* **2019**, *365*, 272–276.

(12) Segawa, Y.; Kuwayama, M.; Itami, K. Synthesis and Structure of [9]Cycloparaphenylene Catenane: An All-Benzene Catenane Consisting of Small Rings. *Org. Lett.* **2020**, *22,* 1067–1070.

(13) Bu, A.; Zhao, Y.; Xiao, H.; Tung, C. H.; Wu, L. Z.; Cong, H. A Conjugated Covalent Template Strategy for All-Benzene Catenane Synthesis. *Angew. Chem. Int. Ed.* **2022**, *61*, e202209449.

(14) May, J. H.; Van Raden, J. M.; Maust, R. L.; Zakharov, L. N.; Jasti, R. Active Template Strategy for the Preparation of π-Conjugated Interlocked Nanocarbons. *Nat. Chem.* **2023**, *15*, 170–176.

(15) Otteson, C. E.; Levinn, C. M.; Van Raden, J. M.; Pluth, M. D.; Jasti, R. Nanohoop Rotaxane Design to Enhance the Selectivity of Reaction-Based Probes: A Proof-of-Principle Study. *Org. Lett.* **2021**, *23*, 4612–4612.

(16) Patrick, C. W.; Woods, J. F.; Gawel, P.; Otteson, C. E.; Thompson, A. L.; Claridge, T. D. W.; Jasti, R.; Anderson, H. L. Polyyne [3]Rotaxanes: Synthesis via Dicobalt Carbonyl Complexes and Enhanced Stability. *Angew. Chem. Int. Ed.* **2022**, *61*, e202116897.

(17) Steudel, F. M.; Ubasart, E.; Leanza, L.; Pujals, M.; Parella, T.; Pavan, G. M.; Ribas, X.; von Delius, M.; Steudel, F. M.; von Delius, M.; Ribas, X.; Leanza, L.; Pavan, G. M. Synthesis of C60/[10]CPP-Catenanes by Regioselective, Nanocapsule-Templated Bingel Bis-Addition. *Angew. Chem. Int. Ed.* **2023**, *62*, e202309393.

(18) Ishibashi, H.; Rondelli, M.; Shudo, H.; Maekawa, T.; Ito, H.; Mizukami, K.; Kimizuka, N.; Yagi, A.; Itami, K. Noncovalent Modification of Cycloparaphenylene by Catenane Formation Using an Active Metal Template Strategy. *Angew. Chem. Int. Ed.* **2023**, *62*, e202310613.

(19) Wasserman, E. The Preparation of Interlocking Rings: A Catenane. *J. Am. Chem. Soc.* **1960**, *82*, 4433–4434.

(20) Baluna, A. S.; Galan, A.; Leigh, D. A.; Smith, G. D.; Spence, J. T. J.; Tetlow, D. J.; Vitorica-Yrezabal, I. J.; Zhang, M. In Search of Wasserman's Catenane. *J. Am. Chem. Soc.* **2023**, *145*, 9825–9833.

(21) Harrison, I. T.; Harrison, S. The Synthesis of a Stable Complex of a Macrocycle and a Threaded Chain. *J. Am. Chem. Soc.* **1967**, *89*, 5723–5724.

(22) Schill, G.; Lüttringhaus, A. The Preparation of Catena Compounds by Directed Synthesis. *Angew. Chem. Int. Ed.* **1964**, *3*, 546–547.

(23) Dietrich-Buchecker, C. O.; Sauvage, J. P.; Kintzinger, J. P. Une Nouvelle Famille de Molecules: Les Metallo-Catenanes. *Tetrahedron Lett.* **1983**, *24*, 5095–5098.

(24) Beves, J. E.; Blight, B. A.; Campbell, C. J.; Leigh, D. A.; McBurney, R. T. Strategies and Tactics for the Metal-Directed Synthesis of Rotaxanes, Knots, Catenanes, and Higher Order Links. *Angew. Chem. Int. Ed.* **2011**, *50*, 9260–9327.

(25) Aucagne, V.; Hänni, K. D.; Leigh, D. A.; Lusby, P. J.; Walker, D. B. Catalytic "Click" Rotaxanes: A Substoichiometric Metal-Template Pathway to Mechanically Interlocked Architectures. *J. Am. Chem. Soc.* **2006**, *128*, 2186–2187.

(26) Denis, M.; Goldup, S. M. The Active Template Approach to Interlocked Molecules. *Nat. Rev. Chem*. **2017**, 1, 0061.

(27) Amabilino, D. B.; Stoddart, J. F. Interlocked and Intertwined Structures and Superstructures. *Chem. Rev.* **1995**, *95*, 2725–2828.

(28) Allwood, B. L.; Spencer, N.; Shahriari-Zavareh, H.; Stoddart, J. F.; Williamsa, D. J. Complexation of Paraquat by a Bisparaphenylene-34-Crown-10 Derivative. *J. Chem. Soc., Chem. Commun.*, **1987**, 1064 –1066.

(29) Ashton, P. R.; Goodnow, T. T.; Kaifer, A. E.; Reddington, M. V.; Slawin, A. M. Z.; Spencer, N.; Stoddart, J. F.; Vicent, C.; Williams, D. J. A [2] Catenane Made to Order. *Angew. Chem. Int. Ed. Engl.* **1989**, *28*, 1396–1399.

(30) Lewis, S. E. Cycloparaphenylenes and Related Nanohoops. *Chem. Soc. Rev.* **2015**, *44*, 2221–2304.

(31) Friederich, R.; Nieger, M.; Vögtle, F. Auf Dem Weg Zu Makrocyclischen Para-Phenylenen. *Chem. Ber.* **1993**, *126*, 1723–1732.

(32) Jasti, R.; Bhattacharjee, J.; Neaton, J. B.; Bertozzi, C. R. Synthesis, Characterization, and Theory of [9]-, [12]-, and [18]Cycloparaphenylene: Carbon Nanohoop Structures. *J. Am. Chem. Soc.* **2008**, *130*, 17646–17647.

(33) Kayahara, E.; Patel, V. K.; Xia, J.; Jasti, R.; Yamago, S. Selective and Gram-Scale Synthesis of [6]Cycloparaphenylene. *Synlett* **2015**, *26*, 1615–1619.

(34) Sisto, T. J.; Golder, M. R.; Hirst, E. S.; Jasti, R. Selective Synthesis of Strained [7]Cycloparaphenylene: An Orange-Emitting Fluorophore. *J. Am. Chem. Soc.* **2011**, *133*, XXXX–YYYY.

(35) Darzi, E. R.; Sisto, T. J.; Jasti, R. Selective Syntheses of [7]-[12]Cycloparaphenylenes Using Orthogonal Suzuki-Miyaura Cross-Coupling Reactions. *J. Org. Chem.* **2012**, *77*, 6624–6628.

(36) Evans, P. J.; Darzi, E. R.; Jasti, R. Efficient Room Temperature Synthesis of a Highly Strained Carbon Nanohoop Fragment of Buckminsterfullerene. *Nat. Chem.* **2014**, *6*, 404–408.

(37) Takaba, H.; Omachi, H.; Yamamoto, Y.; Bouffard, J.; Itami, K.; Takaba, H.; Omachi, H.; Yamamoto, Y.; Bouffard, J.; Itami, K. Selective Synthesis of [12]Cycloparaphenylene. *Angew. Chem. Int. Ed.* **2009**, *48*, 6112–6116.

(38) Yamago, S.; Watanabe, Y.; Iwamoto, T.; Yamago, S.; Watanabe, Y.; Iwamoto, T. Synthesis of [8]Cycloparaphenylene from a Square-Shaped Tetranuclear Platinum Complex. *Angew. Chem. Int. Ed.* **2010**, *49*, 757–759.

(39) Tsuchido, Y.; Abe, R.; Ide, T.; Osakada, K. A Macrocyclic Gold(I)–Biphenylene Complex: Triangular Molecular Structure with Twisted Au_2(Diphosphine) Corners and Reductive Elimination of [6]Cycloparaphenylene. *Angew. Chem. Int. Ed.* **2020**, *59*, 22928–22932.

(40) Darzi, E. R.; Jasti, R. The Dynamic, Size-Dependent Properties of [5]-[12]Cycloparaphenylenes. *Chem. Soc. Rev* **2015**, *44*, 6401–6410.

(41) Wong, B. M. Optoelectronic Properties of Carbon Nanorings: Excitonic Effects from Time-Dependent Density Functional Theory. *J. Phys. Chem. C* **2009**, *113*, 21921–21927.

(42) Kayahara, E.; Kouyama, T.; Kato, T.; Takaya, H.; Yasuda, N.; Yamago, S. Isolation and Characterization of the Cycloparaphenylene Radical Cation and Dication. *Angew. Chem. Int. Ed.* **2013**, *52*, 13722–13726.

(43) Lin, J. B.; Darzi, E. R.; Jasti, R.; Yavuz, I.; Houk, K. N. Solid-State Order and Charge Mobility in [5]- to [12]Cycloparaphenylenes. *J. Am. Chem. Soc.* **2018**, *141*, 952–960.

(44) Kayahara, E.; Sun, L.; Onishi, H.; Suzuki, K.; Fukushima, T.; Sawada, A.; Kaji, H.; Yamago, S. Gram-Scale Syntheses and Conductivities of [10]Cycloparaphenylene and Its Tetraalkoxy Derivatives. *J. Am. Chem. Soc.* **2017**, *139*, 18480–18483.

(45) Mun, J.; Kang, J.; Zheng, Y.; Luo, S.; Wu, H.-C.; Matsuhisa, N.; Xu, J.; Nathan Wang, G.-J.; Yun, Y.; Xue, G.; B-H Tok, J.; Bao, Z.; Mun, J.; Kang, J.; Wu, H.; Matsuhisa, N.; Xu, J.; Yun, Y.; B-H Tok, J.; Bao, Z.; Zheng, Y.; Wang, G. N.; Luo, S.; Xue, G. Conjugated Carbon Cyclic Nanorings as Additives for Intrinsically Stretchable Semiconducting Polymers. *Adv. Mater.* **2019**, *31*, 1903912.

(46) Iwamoto, T.; Watanabe, Y.; Sadahiro, T.; Haino, T.; Yamago, S. Size-Selective Encapsulation of C_{60} by [10]Cycloparaphenylene: Formation of the Shortest Fullerene-Peapod. *Angew. Chem. Int. Ed.* **2011**, *50*, 8342–8344.

(47) Xia, J.; Bacon, J. W.; Jasti, R. Gram-Scale Synthesis and Crystal Structures of [8]- and [10]CPP, and the Solid-State Structure of C_{60}@[10]CPP. *Chem. Sci.* **2012**, *3*, 3018–3021.

(48) Povie, G.; Segawa, Y.; Nishihara, T.; Miyauchi, Y.; Itami, K. Synthesis of a Carbon Nanobelt. *Science* **2017**, *356*, 172–175.

(49) Cheung, K. Y.; Gui, S.; Deng, C.; Liang, H.; Xia, Z.; Liu, Z.; Chi, L.; Miao, Q. Synthesis of Armchair and Chiral Carbon Nanobelts. *Chem* **2019**, *5*, 838–847.

(50) Cheung, K. Y.; Watanabe, K.; Segawa, Y.; Itami, K. Synthesis of a Zigzag Carbon Nanobelt. *Nat. Chem.* **2021**, *13*, 255–259.

(51) Lovell, T. C.; Colwell, C. E.; Zakharov, L. N.; Jasti, R. Symmetry Breaking and the Turn-on Fluorescence of Small, Highly Strained Carbon Nanohoops. *Chem. Sci.* **2019**, *10*, 3786–3790.

(52) Hermann, M.; Wassy, D.; Esser, B. Conjugated Nanohoops Incorporating Donor, Acceptor, Hetero- or Polycyclic Aromatics. *Angew. Chem. Int. Ed.* a**2021**, *60*, 15743–15766.

(53) Leonhardt, E. J.; Jasti, R. Emerging Applications of Carbon Nanohoops. *Nat. Rev. Chem*. **2019**, *3*, 672–686.

(54) White, B. M.; Zhao, Y.; Kawashima, T. E.; Branchaud, B. P.; Pluth, M. D.; Jasti, R. Expanding the Chemical Space of Biocompatible Fluorophores: Nanohoops in Cells. *ACS Cent. Sci.* **2018**, *4*, 1173–1178.

(55) Lovell, T. C.; Bolton, S. G.; Kenison, J. P.; Shangguan, J.; Otteson, C. E.; Civitci, F.; Nan, X.; Pluth, M. D.; Jasti, R. Subcellular Targeted Nanohoop for One- And Two-Photon Live Cell Imaging. *ACS Nano* **2021**, *15*, 15285-15293

(56) Peters, G. M.; Grover, G.; Maust, R. L.; Colwell, C. E.; Bates, H.; Edgell, W. A.; Jasti, R.; Kertesz, M.; Tovar, J. D. Linear and Radial Conjugation in Extended π-Electron Systems. *J. Am. Chem. Soc.* **2020**, *142*, 2293–2300.

(57) Huang, Q.; Zhuang, G.; Zhang, M.; Wang, J.; Wang, S.; Wu, Y.; Yang, S.; Du, P. A Long π-Conjugated Poly(Para-Phenylene)-Based Polymeric Segment of Single-Walled Carbon Nanotubes. *J. Am. Chem. Soc.* **2019**, *141*, 18938–18943.

(58) Aucagne, V.; Hänni, K. D.; Leigh, D. A.; Lusby, P. J.; Walker, D. B. Catalytic "Click" Rotaxanes: A Substoichiometric Metal-Template Pathway to Mechanically Interlocked Architectures. *J. Am. Chem. Soc.* **2006**, *128*, 2186–2187.

(59) Barin, G.; Coskun, A.; Fouda, M. M. G.; Stoddart, J. F. Mechanically Interlocked Molecules Assembled by π-π Recognition. *ChemPlusChem*. **2012**, *14*, 159–185.

(60) Kubota, N.; Segawa, Y.; Itami, K. H6-Cycloparaphenylene Transition Metal Complexes: Synthesis, Structure, Photophysical Properties, and Application to the Selective Monofunctionalization of Cycloparaphenylenes. *J. Am. Chem. Soc.* **2015**, *137*, 1356–1361.

(61) Van Raden, J. M.; Louie, S.; Zakharov, L. N.; Jasti, R. 2,2′-Bipyridyl-Embedded Cycloparaphenylenes as a General Strategy To Investigate Nanohoop-Based Coordination Complexes. *J. Am. Chem. Soc.* **2017**, *139*, 2936–2939.

(62) Berná, J.; Goldup, S. M.; Lee, A. L.; Leigh, D. A.; Symes, M. D.; Teobaldi, G.; Zerbetto, F. Cadiot-Chodkiewicz Active Template Synthesis of Rotaxanes and Switchable Molecular Shuttles with Weak Intercomponent Interactions. *Angew. Chem. Int. Ed.* **2008**, *47*, 4392–4396.

(63) Movsisyan, L. D.; Franz, M.; Hampel, F.; Thompson, A. L.; Tykwinski, R. R.; Anderson, H. L. Polyyne Rotaxanes: Stabilization by Encapsulation. *J. Am. Chem. Soc.* **2016**, *138*, 1366–1376.

(64) Hashimoto, S.; Kayahara, E.; Mizuhata, Y.; Tokitoh, N.; Takeuchi, K.; Ozawa, F.; Yamago, S. Synthesis and Physical Properties of Polyfluorinated Cycloparaphenylenes. *Org. Lett.* **2018**, *20*, 5973–5976.

(65) Coropceanu, V.; Cornil, J.; da Silva Filho, D. A.; Olivier, Y.; Silbey, R.; Brédas, J. L. Charge Transport in Organic Semiconductors. *Chem. Rev*. **2007**, *107*, 926–952.

(66) Slater, A. G.; Cooper, A. I. Function-Led Design of New Porous Materials. *Science* **2015**, *348*, aaa8075.

(67) Xia, J.; Bacon, J. W.; Jasti, R. Gram-Scale Synthesis and Crystal Structures of [8]- and [10]CPP, and the Solid-State Structure of C 60[10]CPP. *Chem. Sci.* **2012**, *3*, 3018–3021.

(68) White, N. G.; Costa, P. J.; Carvalho, S.; Félix, V.; Beer, P. D. Increased Halide Recognition Strength by Enhanced Intercomponent Preorganisation in Triazolium Containing [2]Rotaxanes. *Chem. Eur. J.* **2013**, *19*, 17751–17765.

(69) Leanza, L.; Perego, C.; Pesce, L.; Salvalaglio, M.; von Delius, M.; Pavan, G. M. Into the Dynamics of Rotaxanes at Atomistic Resolution. *Chem. Sci.***2023**, *14*, 6716–6729.

(70) Ishibashi, H.; Rondelli, M.; Shudo, H.; Maekawa, T.; Ito, H.; Mizukami, K.; Kimizuka, N.; Yagi, A.; Itami, K. Noncovalent Modification of Cycloparaphenylene by Catenane Formation Using an Active Metal Template Strategy. *Angew. Chem. Int. Ed.* **2023**, *62*, e202310613.

(71) Campbell, C. J.; Leigh, D. A.; Vitorica-Yrezabal, I. J.; Woltering, S. L. A Simple and Highly Effective Ligand System for the Copper I-Mediated Assembly of Rotaxanes. *Angew. Chem. Int. Ed.* **2014**, *53*, 13771–13774.

(72) Lahlali, H.; Jobe, K.; Watkinson, M.; Goldup, S. M.; Lahlali, H; Jobe, K.; Watkinson, M.; Goldup, S. M. Macrocycle Size Matters: "Small" Functionalized Rotaxanes in Excellent Yield Using the CuAAC Active Template Approach. *Angew. Chem. Int. Ed.* **2011**, *50*, 4151–4155.

(73) Lewis, J. E. M.; Modicom, F.; Goldup, S. M. Efficient Multicomponent Active Template Synthesis of Catenanes. *J. Am. Chem. Soc.* **2018**, *140*, 4787–4791.

(74) Lewis, J. E. M.; Winn, J.; Cera, L.; Goldup, S. M. Iterative Synthesis of Oligo[n]Rotaxanes in Excellent Yield. *J. Am. Chem. Soc.* **2016**, *138*, 16329–16336.

(75) Van Raden, J. M.; Louie, S.; Zakharov, L. N.; Jasti, R. 2,2′-Bipyridyl-Embedded Cycloparaphenylenes as a General Strategy to Investigate Nanohoop-Based Coordination Complexes. *J. Am. Chem. Soc.* **2017**, *139*, 2936–2939.

(76) Winn, J.; Pinczewska, A.; Goldup, S. M. Synthesis of a Rotaxane CuI Triazolide under Aqueous Conditions. *J. Am. Chem. Soc.* **2013**, *135*, 13318–13321.